APPL1 INHIBITS CELL MIGRATION BY MODULATING INTEGRIN TRAFFICKING AND RAC SIGNALING

By

Nicole Lee Diggins

Dissertation

Submitted to the Faculty of the

Graduate School of Vanderbilt University

In partial fulfillment of the requirements

For the degree of

DOCTOR OF PHILOSOPHY

in

Biological Sciences

February 28, 2018

Nashville, Tennessee

Approved:

Todd Graham, Ph.D.

Andrea Page-McCaw, Ph.D.

Charles Singleton, Ph.D.

Katherine Friedman, Ph.D.

To my parents, Brian and Christi, for their love and unwavering support.

ACKNOWLEDGMENTS

My pursuit of a Ph.D. has been a long and challenging road, filled with many ups and downs, excitements and frustrations. I would not have made it this far without the help and support from many people that I need to thank.

First, I would like to express my gratitude to my research advisors, Dr. Donna Webb and Dr. Katherine Friedman. I will always be appreciative of Donna for accepting me into her lab, helping with the early development of my project, encouraging me to apply for outside funding, and supporting my travel to several conferences and workshops. She was taken away from science too soon. I cannot express enough how thankful I am to Kathy for agreeing to continue as my advisor after Donna passed away and supporting me as I completed revisions on my first author paper and wrote this dissertation. I would also like to thank my committee, Dr. Todd Graham (Chair), Dr. Andrea Page-McCaw, Dr. Charles Singleton, and Dr. Katherine Friedman, for their continued support and guidance throughout my graduate studies. In addition, I am sincerely grateful to Dr. Alissa Weaver for guiding me through the review process of my paper.

I would like to thank all of the members of the Webb lab, past and present, for their friendship, valued feedback, and lively discussions. I owe special thanks to Begüm Erdoğan-Utz, Mikin Patel, Cristina Robinson, and Jessica Abner for commiserating with me and providing emotional support during the difficult year surrounding the passing of our advisor and the closing of the Webb lab. My work would not have been possible without funding from the National Institutes of Health, most notably a Ruth L. Kirschstein National Service Award (NRSA) CA189710 awarded to me. I would also like to thank the administrative staff in the Department of Biological Sciences, especially Carol Wiley and Alicia Goostree, for always being available to answer my questions and offer their support.

The stress of graduate school was greatly lessened by my support system in Nashville. Thanks to my Zumba friends, Rachel, Jennifer, Claire, Laura, Christina, Alice, and Cecilia, for dancing with me! My Nashville family, Daniel, Alex, Jennifer, Beverly, Mike, Betsy, and Hagie, have treated me as one of their own; they make home feel not so far away.

From the bottom of my heart, thanks to my family for always knowing that I would accomplish my dreams, even when I didn't. Thanks to my parents, for the phone calls on my way from lab, whether it was about accomplishments or struggles. My sisters, Angela, Bridgett, and Kelly, have always believed in me, and have been calling me Dr. Diggins since well before graduate school! My nephews, Joey and Lewis, remind me that being a scientist is cool, and put my love of science into perspective. The Winrich family deserves my thanks- Christine is one of my longest lasting friends, and it warms my heart to see pictures of the adorable Freya and Finn.

I owe deep gratitude to two of my closest friends, Gwynne and Amanda, for their friendship. Since I met them during the first week of IGP, they have shared in my triumphs and troubles. They were always around for coffee/snack breaks during long days in the lab, craft nights, long runs, hiking/camping adventures, and retrieving tennis balls I hit over the fence to get out my frustrations. Long live the 5-6-7 crew!

My years in Nashville have been some of the best of my life thanks to my awesome boyfriend, Steve. He always finds a way to make me laugh, even when science gets me down. I'm looking forward to our next adventure as I relocate us to Oregon for my postdoc. Finally, thanks to my kitties for cuddles and emotional support.

TABLE OF CONTENTS

LIST OF TABLES

Table Page

LIST OF FIGURES

LIST OF ABBREVIATIONS

1D	One-dimensional
2D	Two-dimensional
3D	Three-Dimensional
ACAP1	ArfGAP with Coiled-Coil, Ankyrin repeat and PH domain 1
AdipoR1	Adiponectin receptor 1
AMPK	5’ adenosine monophosphate-activated protein kinase
ANOVA	Analysis of Variance
AP-1/2	Activating protein 1/2
APPL	The adaptor protein containing a pleckstrin homology domain, phosphotyrosine binding domain, and leucine zipper motif
APPL1-AAA	APPL1 with three point mutations, R146A/K152A/K154A
APPL1-N308D	APPL1 with point mutation at residue 308, asparagine to aspartic acid
APPL1-ΔPTB-GFP	APPL1 PTB domain deletion mutant
AR	Androgen Receptor
ARAP2	ArfGAP with RhoGAP domain, Ankyrin repeat and PH domain 2
Arf	ADP ribosylation factor
Arp2/3	Actin related protein 2/3
A.U.	Arbitrary Units
BAR	Bin-Amphiphysin-Rvs
BCA	bicinchoninic acid
BRAG2	brefeldin A-resistant ARF-GEF2
CA-PAK	Constitutively Active PAK

Cas9	CRISPR-assocaited protein-9 nuclease
Cdc42	Cell division control protein 42 homolog
ColI	Collagen I
CRISPR	Clustered Regularly Interspaced Short Palindromic Repeats
DCC	Deleted in colorectal cancer
DMEM	Dulbeco's Modified Eagles Medium
DNA	Deoxyribonucleic acid
Dvl2	Dishevelled 2
ECM	Extracellular Matrix
EEA1	Early endosome antigen 1
EGFR	Epidermal growth factor receptor
EHD	Eps15 homology domain
ESCRT	Endosomal sorting complex required for transport
FA	Focal adhesion
F-actin	Filamentous actin
FAK	Focal Adhesion Kinase
FBS	Fetal Bovine Serum
FL-paxillin	GFP-paxillin with full-length CMV promoter
FL-vinculin	GFP-vinculin with full-length CMV promoter
FN	Fibronectin
FSHR	Follicle stimulating hormone receptor
GAP	GTPase activating protein
GDI	Guanine nucleotide dissociation factors

GDP	Guanosine diphosphate
GEF	Guanine nucleotide exchange factor
GFP	Green Fluorescent Protein
GIT1	G-protein-coupled receptor kinase-interacting protein 1
GIPC1	GAIP-interacting protein C terminus, member 1
gRNA	guide RNA
GSK3-β	Glycogen synthase-3β
GST	Glutathione-S-transferase
GTP	Guanosine triphosphate
HDAC	Histone deacetylase
HGF	Hepatocyte growth factor
hr	Hour
I	Fluorescence Intensity
I_0	Initial Fluorsecence Intensity
ID numbers	Identificaiton numbers
IgG	Immunoglobulin G
INDEL	insertion/deletion
IR	Insulin receptor
IRS1/2	Insulin receptor substrate 1 and 2
kDa	Kilodalton
LPA	Lysophosphatidic acid
LPA_1	Lysophosphatidic acid receptor 1
m	slope

MAPK	Mitogen-activated protein kinase
MEF	Murine embryonic fibroblast
MET	Mesynchymal to Epithelial Transition, Hepatocyte Growth Factor Receptor
min	minute
µl	microliter
µm	micrometer
µM	micromolar
MSD	Mean Square Displacement
m/v	Mass/Volume
Myo6	Myosin VI
NA	Numerical Aperture
NHS	N-hydroxysuccinimide esters
NMDA	N-methyl-D-aspartate
Nrp1	Neuorpilin-1
n.s.	not significant
NT	Non-targetting
OCRL	Oculocerebrorenal syndrome of Lowe
$p21^{CIP1}$	Cyclin-dependent kinase inhibitor 1
PAASTA	Platform for the automated analysis segmentation and tracking of adhesions
PAK	p21-activated kinase
PBD	p21 binding domain
PBS	Phosphate buffered saline
PIX	Pak-interacting exchange factor

PDZ	PSD-95/Discs-large/ZO-1
PH	Pleckstrin homology
PI3K	Phosphatidylinositol-4,5-bisphosphate 3-kinase
pPAK	phosphorylated PAK
$pPAK^{Thr423}$	PAK phosphorylated at reside Threonine 423
PTB	Phosphotyrosine binding
PtdIns	Phosphatidylinositol
Rab	Ras-associated binding
Rab5-L38R	Rab5 point mutation at residue 38, leucine to arginine
Rac	Ras-related C3 botulinum toxin substrate 1
Rho	Ras homology
RGD	Arginine-glycine-aspartic acid
RGE	Arginine-glycine-glutamic acid
RNA	Ribonucleic acid
ROCK	Rho-associated protein kinase
ROI	Region of interest
SDS	Sodium dodecyl sulfate
SDS-PAGE	SDS-polyacrylamide gel electrophoresis
sec	second
S.E.M or s.e.m	standard error of the mean
siRNA	small interfering RNA
Spec-paxillin	GFP-paxillin with truncated (speckled) CMV promoter
Spec-vinculin	GFP-vinculin with truncated (speckled) CMV promoter

Src	Sarcoma
$t_{1/2}$	Half life
TBS-T	Tris-buffered saline, 0.1% (v/v) Tween 20
TIRF	Total internal reflection fluorescence
Tfn	Trasnferrin
TfnR	Transferrin Receptor
TrkA	Tropomyosin receptor kinase A
TSC2	Tuberous sclerosis complex 2
VASP	Vasodilator-stimulated phosphoprotein
v/v	Volume/Volume
WASP	Wiskott-Aldrich syndrome protein
WAVE	WASP-family verprolin-homologous protein
WB	Western blot
WDFY2	WD repeat and FYVE containing 2

CHAPTER I

INTRODUCTION

Portions of this chapter were published as Diggins and Webb (2017). APPL1 is a multifunctional endosomal signaling adaptor protein. *Biochem Soc Trans*. 45, 771-779.

Cell Migration

Cell migration, or the movement of cells from one location to another, is a fundamental process to many life forms, ranging from the search for food by unicellular bacteria and amoebae to the development and maintenance of complex multicellular organisms (Artemenko et al., 2014; Harshey, 2003; Reig et al., 2014; Vicente-Manzanares et al., 2005). In multicellular organisms, cell migration is essential to processes such as embryonic development, the inflammatory response, and wound healing (Chi and Trinkaus-Randall, 2013; Nakamura et al., 2013; Pick et al., 2013). However, misregulated cell migration often leads to pathological states, including atherosclerosis and cancer metastasis (Bradbury et al., 2012; Finney et al., 2017).

Cancer metastasis is associated with poor prognosis and is a leading cause of morbidity and mortality in patients. Metastasis is responsible for approximately 90% of cancer-related deaths (Seyfried and Huysentruyt, 2013). The metastatic cascade is initiated when cancer cells escape from the primary tumor, usually by breaking through the basement membrane, and invade into surrounding tissue. Cells may then enter the bloodstream or lymphatic system, and eventually disseminate to distant organs to form secondary, or metastatic, tumor sites (Friedl and Alexander, 2011). Understanding the molecular mechanisms underlying cell migration not only contributes to our knowledge of basic cell biology, and is also key to gaining insight into cancer progression and therapeutics.

Cell Migration- 2D vs. 3D

Traditionally, migration and adhesion studies have been performed on two-dimensional (2D) cell culture dishes. 2D cell culture systems are an appropriate system for certain types of cell migration, such as wound healing. However, over the past decade or so, studies on three-dimensional (3D) cell migration and adhesion have provided evidence that 2D cell culture systems are not always the best representation of cell migration *in vivo* (Beningo et al., 2004; Cukierman et al., 2001; Doyle and Yamada, 2016; Grinnell, 2003). As such, there are now multiple systems in use to study 3D migration.

One method of generating 3D matrices is by polymerizing gels of various ECM components (usually collagen I or Matrigel®) with cells either plated on top and allowed to migrate into the gel or embedded during the polymerization and allowed to adhere (Doyle, 2016; Kramer et al., 2013). Another method is to generate cell-derived matrices by culturing fibroblasts at high density over several days. Cancer cells can be plated and immediately used for 2D migration analysis or allowed to permeate the matrix over 24 hours and then assessed for 3D migration (Erdogan et al., 2017; Kutys et al., 2013). Factors such as ECM components, concentration, or even polymerizing temperature can result in a variety of matrix architectures (Doyle, 2016; Hakkinen et al., 2011), complicating the interpretation of experiments of 3D migration.

2D cell culture conditions consist of rigid surfaces that support cells with a spread morphology and a large, fan-like lamellipodium (Meyer et al., 2012). In these conditions, migration is fastest on an intermediate amount of ECM substrate. The presence of too little or too much substrate slows cell migration speeds (Huttenlocher et al., 1996). Cells in 3D, however, tend to have long, thin protrusions, a round cell body forming the rear of the cell, and a spindle-

like morphology (Doyle et al., 2013; Hakkinen et al., 2011), due to the constraint of having to push the nucleus through the ECM (Petrie et al., 2017; Petrie et al., 2014; Petrie and Yamada, 2016). 3D migration is influenced by additional confounding factors, such as matrix porosity, rigidity, and matrix stiffness (both global stiffness as well as local stiffness at cell-matrix adhesions) (Baker and Chen, 2012; Doyle et al., 2015; Doyle et al., 2013). 3D migration is more similar to 1D migration than 2D migration, as cells form thin protrusions and tend to migrate on ECM 'tracks' (Doyle et al., 2009). While the same proteins are involved in 2D and 3D cell-matrix adhesion formation and migration, the mechanisms can be different (Cukierman et al., 2001; Geiger and Yamada, 2011; Harunaga and Yamada, 2011; Jacquemet et al., 2013b; Kutys and Yamada, 2014). However, there are similarities between 2D and 3D migration; 2D protrusion is a good indicator of 3D cell migration speed (Meyer et al., 2012). Given the difficulty in performing biochemical assays in 3D cell culture, many studies employ 2D cell culture systems to tease apart molecular mechanisms, and confirm and compare these results in 3D cell culture systems (Caswell et al., 2008; Dozynkiewicz et al., 2012; Jacquemet et al., 2013b; Jean et al., 2013; Jean et al., 2014; Meyer et al., 2012).

The Cell Migration Cycle

Cell migration is a multistep process that requires the integration and temporal coordination of different processes, such as actin reorganization, adhesion turnover, and the establishment of polarity, that occur in spatially distinct locations within the cell (Beningo et al., 2001; Borisy and Svitkina, 2000; Ridley, 2011). The migrating cell exhibits front-back polarity, with a leading edge (protrusion) and trailing edge (cell rear) (Broussard et al., 2008; Ridley, 2011; Ridley et al., 2003). Cell migration is viewed as a cyclic process, defined by four key steps (Figure 1.1) (Abercrombie et al., 1970; Abercrombie et al., 1971; Ridley et al., 2003). Migration

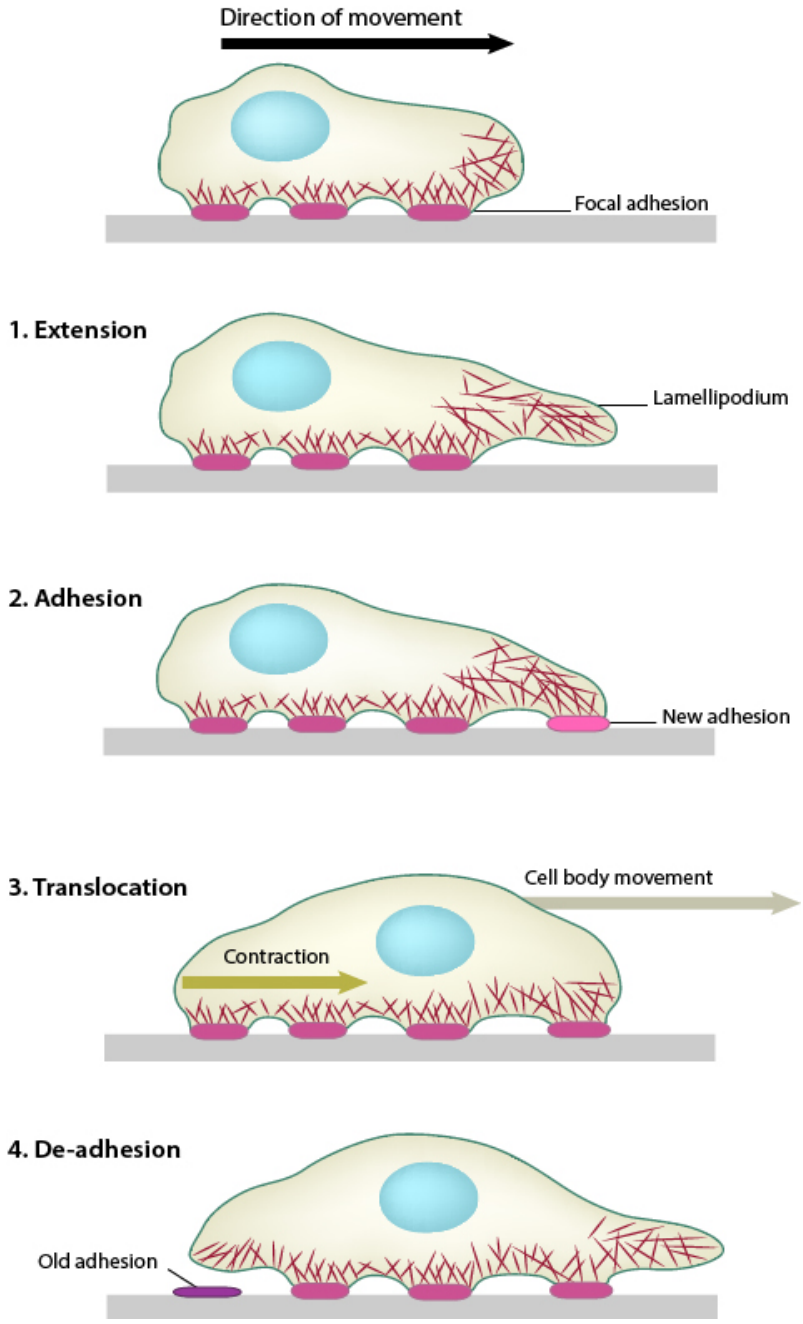

Figure 1.1. The cell migration cycle. 1) Actin polymerization at the leading edge forms a protrusion that begins forward movement of the cell. 2) Adhesions stabilize the protrusion and act as traction points for cellular movement. 3) Actomyosin contractility transmits forces to pull the cell body forward in the direction of movement. 4) Adhesions at the cell rear disassemble and the trailing edge retracts.

Used with permission from MBInfo contributors. Conserved steps in cell spreading and movement. http://mbinfo.mbi.nus.edu.sg/figure/1384242961310/

begins with the extension of a protrusion, or lamellipodium, which is driven by actin polymerization (Higgs and Pollard, 2001; Pollard and Borisy, 2003; Urban et al., 2010). This protrusion is stabilized by the formation of adhesions that link the extracellular matrix (ECM) to the cellular cytoskeleton, and these cell-matrix adhesions serve as traction points for the generation of forces needed for cellular movement (Beningo et al., 2001; Geiger and Yamada, 2011; Parsons et al., 2010). These adhesions must continually assemble and disassemble, in a process termed adhesion turnover, for efficient migration to occur (Vicente-Manzanares and Horwitz, 2011; Webb et al., 2002; Wehrle-Haller, 2012). Translocation of the cell body and deadhesion of the cell rear are the last two steps of the cell migration cycle, and these steps are dependent on the intracellular forces generated by adhesions (Burridge and Chrzanowska-Wodnicka, 1996). Actomyosin contractility, driven by nonmuscle myosin II, provides the forces necessary for adhesion maturation in the lamellipodium, translocation of the nucleus and the cell body, and adhesion disassembly at the trailing edge of the cell; adhesion disassembly completes the forward movement of the cell and the process can begin again (Sanz-Moreno et al., 2011; Vicente-Manzanares et al., 2009).

Cell-Matrix Adhesions- Formation and Composition

Migrating cells must interact with the ECM to transduce the forces necessary for cellular movement. Cell-matrix adhesions are mediated by a few groups of adhesion receptors (cadherins, Ig superfamily, integrins, selectins) (Juliano, 2002) and co-receptors (syndecans) (Beauvais and Rapraeger, 2004). This dissertation will focus on integrin-based adhesions.

Integrin-based adhesions vary in size and location within the cell. Nascent adhesions are less than 0.25 μm and form cooperatively with actin polymerization in the lamellipodium (Alexandrova et al., 2008; Choi et al., 2008). While the exact mechanisms and timing of the

formation of nascent adhesions are still largely unknown, recent evidence suggests that integrins associate with kindlins and α-actinin to promote clustering of integrins and link to the actin cytoskeleton (Bachir et al., 2014). Following myosin II activity in the lamellipodium, talin then binds to integrins to begin recruiting other adhesion proteins, such as vinculin (Bachir et al., 2014; Sun et al., 2014). Most nascent adhesions turn over rapidly as they reach regions of actin disassembly at the rear of the lamellipodium (Vicente-Manzanares and Horwitz, 2011). However, a subset of nascent adhesions is pulled centripetally from the lamellipodium in the direction of actin retrograde flow to the lamella, a region of more stable, bundled actin. These adhesions grow and mature into larger focal complexes (0.5 μm) and further into focal adhesions (FAs; 1-5 μm) (Choi et al., 2008). As the most well characterized adhesions involved in cell migration, FAs are composed of hundreds of proteins serving a variety of roles—structural, scaffolding, adaptor, force transduction, and receptors—to link the cell to the ECM (Figure 1.2) (Kanchanawong et al., 2010; Parsons et al., 2010).

Recent efforts in the field of cell-matrix adhesions have strived to determine the complete composition of adhesions, termed the 'adhesome'. These efforts have yielded varied results, due to multiple experimental methods used, differences between adhesions of various cell lines, as well as the heterogeneity of adhesion size and dynamic nature of adhesion composition within a single cell. The first attempt to define the adhesome analyzed published experimental data on adhesion proteins and interactions, and reported a network of 156 adhesion components with 690 links (either activation, inhibition, or direct interaction) (Zaidel-Bar et al., 2007a). With the development of protocols for the isolation of integrin-associated protein complexes (Humphries et al., 2009; Jones et al., 2015), several studies utilized proteomics approaches to analyze these isolated adhesions and refine the adhesome. These studies have revealed core networks of

adhesion proteins that are involved in adhesion formation and maturation (Byron et al., 2015; Byron et al., 2011; Kuo et al., 2011; Schiller et al., 2011; Schiller et al., 2013). Combining these studies on the adhesome has currently provided a consensus of 232 proteins and over 6,000 interactions (either activating, inhibiting, or direct binding interactions) (Winograd-Katz et al., 2014). The exact composition of the adhesome is still being refined with the addition of new data and analysis. There is now a vast literature on the key players and protein-protein interactions involved in adhesion formation, maturation, and turnover; however, there are some broad groups of proteins and protein functions that are crucial to FAs, which are discussed below (Figure 1.2).

Integrins are transmembrane adhesion receptors that link the ECM to actin cytoskeleton (Huttenlocher and Horwitz, 2011). They link the inside of the cell to the extracellular environment by binding multiple structural and signaling adhesion proteins via a cytoplasmic tail, and matrix components via an extracellular domain (Wegener and Campbell, 2008). Although the cytoplasmic tails of integrins are short, there are a multiple interacting proteins, serving a variety of functions. These interacting proteins include adaptors such as talin and paxillin and signaling proteins such as focal adhesion kinase (FAK) (Lock et al., 2008).

Talin directly binds the NPxY motifs in the β integrin tail, and may be important for integrin activation (Anthis et al., 2009; Kim et al., 2011; Tanentzapf and Brown, 2006; Wegener et al., 2007; Ye et al., 2011), and the combined binding of talin and kindlin-3 to integrin tails further activates integrins (Lefort et al., 2012). Furthermore, talin directly binds actin and vinculin, a mechanosensing protein that is involved in protrusion and force transduction (Calderwood, 2004; Moser et al., 2009). Vinculin in turn binds a number of proteins involved in actin polymerization: the Arp2/3 complex (important for actin nucleation), the actin crosslinker α-actinin, the actin regulator vasodilator-stimulated phosphoprotein (VASP), and actin itself

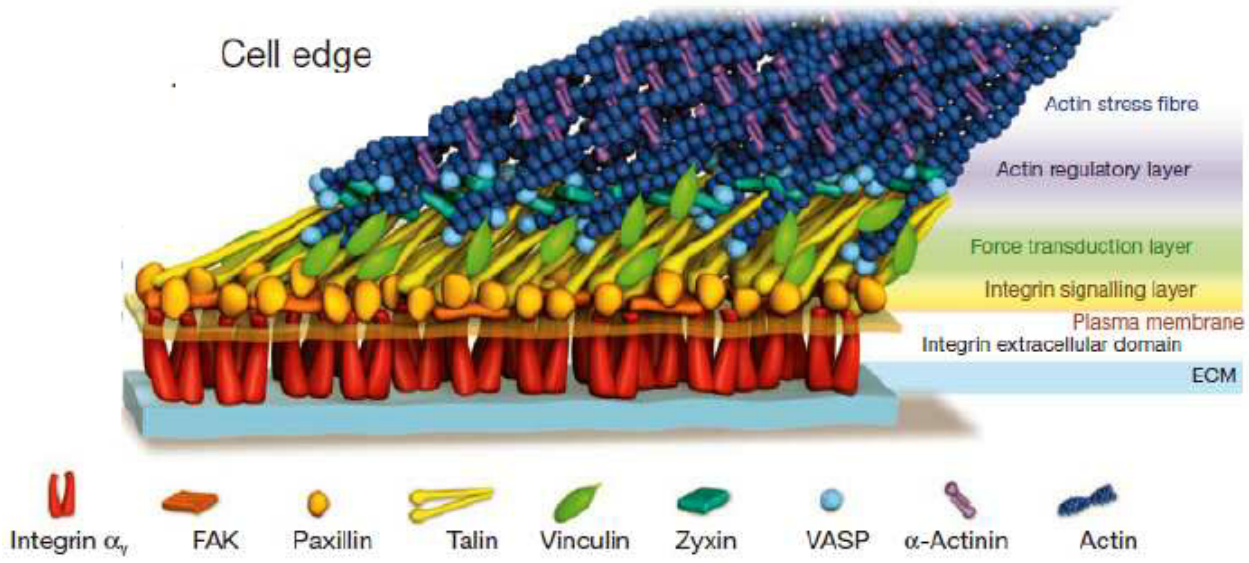

Figure 1.2. Schematic of focal adhesion composition. FAs are composed of hundreds of proteins that link the ECM to actin stress fibers. Integrins bind ECM through the extracellular domain, and singlaling proteins via its intracellular domain. Further inside the cell membrane are proteins that transduce forces generated by the adhesion. Other proteins important for adhesion are those that bind actin to attach the adhesion to the actin cytoskeleton. Light blue, ECM; Red, integrin extracellular domain; yellow, integrin intracellular domain and associated signaling proteins; green, force transduction proteins; blue and purple, actin binding proteins; dark blue, actin fibers.

Figure reprinted from (Kanchanawong et al., 2010).

(Bays and DeMali, 2017). In addition to its roles in actin regulation, vinculin is necessary for traction force generation within the adhesion. Paxillin recruits vinculin to adhesions in a myosin II-dependent manner (Pasapera et al., 2010). Moreover, forces exerted on adhesions stretches talin to reveal cryptic binding sites for vinculin, thereby increasing the strength of the adhesion (Bays and DeMali, 2017; del Rio et al., 2009).

One function of paxillin is to bind the actin-binding proteins vinculin and actopaxin to anchor actin and strengthen the adhesion (LaLonde et al., 2006; Lopez-Colome et al., 2017). Perhaps more importantly, paxillin acts as a docking site for kinases, guanine nucleotide exchange factors (GEFs), other adaptor proteins, and actin binding proteins to localize and initiate various signaling cascades (Lopez-Colome et al., 2017; Schaller, 2001). p21-activated kinase (PAK) is crucial for the recruitment of G-protein-coupled receptor kinase-interacting protein 1 (GIT1) and promotes the GIT1-PIX-PAK signaling axis to promote activation of the GTPase Rac (a critical regulator of actin polymerization and cell migration) (Nayal et al., 2006). Paxillin also localizes the kinases FAK and Src, both of which are important for adhesion turnover (Brown et al., 2005; Webb et al., 2004).

Adhesion Turnover

Adhesions, both at the leading and trailing edges of the cell, must continuously assemble and disassemble, in a process termed adhesion turnover, for migration to occur (Broussard et al., 2008; Webb et al., 2002; Wehrle-Haller, 2012). Most nascent adhesions at the cell front turn over rapidly, which is important for protrusion dynamics (Bershadsky et al., 2003). The leading edge is a site of branched actin polymerization, and promotes the formation of nascent adhesions (Borisy and Svitkina, 2000). The lamellipodium-lamellum border, however, is a site where actin depolymerization and adhesion disassembly occurs, regulated by proteins such as the actin

severing protein cofilin (Delorme et al., 2007; Pollard and Borisy, 2003). Actin depolymerization destabilizes nascent adhesions, resulting in their turnover (Wehrle-Haller, 2012). A subset of nascent adhesions are pulled inward from the leading edge and mature into FAs, where they undergo dynamic turnover (Wehrle-Haller, 2012). Bundling of actin, in part by α-actinin, into stress fibers supports maturation of nascent adhesions and focal complexes into FAs (Choi et al., 2008; Roca-Cusachs et al., 2013). Myosin II also aids in actin bundling, and regulates FA maturation and disassembly through force generation. Loss of tension is associated with adhesion disassembly (Vicente-Manzanares et al., 2009). Trailing adhesions at the cell rear are required for maintenance of cell polarization, but must also turn over to allow for the translocation of the cell body (Broussard et al., 2008). Signaling from adhesion proteins largely regulates these processes, although recent evidence has given support to the role of other cellular processes such as vesicular trafficking.

Paxillin has multiple Ser/Thr and Tyr phosphorylation sites that modulate its localization and downstream signaling to regulate adhesion turnover. Recruitment of paxillin to adhesion sites regulates adhesion assembly (Deakin and Turner, 2008). Serine phosphorylation of paxillin by PAK stimulates Rac activation in a positive feedback loop (PAK is a Rac effector) and promotes adhesion turnover (Lopez-Colome et al., 2017; Nayal et al., 2006). FAK and Src phosphorylate paxillin at residues Tyr31 and Tyr118, and both phosphorylation sites are required for adhesion disassembly and cell migration (Lopez-Colome et al., 2017; Mitra et al., 2005; Turner, 2000). FAK associates with tyrosine-phosphorylated paxillin (Cai et al., 2006), and paxillin acts as a scaffold to recruit proteins downstream of FAK-Src signaling to FAs (Zaidel-Bar et al., 2007b).

FAK is also a critical regulator of adhesion turnover, and is required for adhesion maturation and disassembly. FAK promotes adhesion maturation by phosphorylating and inhibiting α-actinin binding to actin. An optimal level of α-actinin phosphorylation is required to allow for adhesion maturation; too much phosphorylation inhibits actin crosslinking into stress fibers in FAs, whereas too little phosphorylation prevents the linkage of integrins to actin in nascent adhesions (Izaguirre et al., 2001; Mitra et al., 2005; Roca-Cusachs et al., 2013; von Wichert et al., 2003). However, FAK likely plays a bigger role in adhesion disassembly, as fibroblasts from FAK null mice have decreased migration rates and increased size and number of adhesions (Ilic et al., 1995; Webb et al., 2004; Webb et al., 2002). FAK associates with activators and inhibitors of several small GTPases involved in adhesion dynamics. FAK phosphorylation and activation of Src promotes phosphorylation of the GTPase activating protein (GAP) p190RhoGAP and recruitment of the Rac GEF Pak-interacting exchange factor (PIX), ultimately decreasing myosin force generation to promote FA disassembly (Schober et al., 2007). Moreover, FAK phosphorylated at Tyr397 recruits dynamin to FAs through the adaptor protein Grb2. Localization of dynamin promotes microtubule-dependent integrin endocytosis, and FAK is subsequently dephosphorylated at residue Tyr397 (Ezratty et al., 2005; Nagano et al., 2012).

Microtubule dynamics have been implicated in FAs disassembly through multiple mechanisms (Broussard et al., 2008). First, microtubules localize the tyrosine kinase Arg, which inhibits the GTPase Rho, thereby releasing tension locally at the site of adhesion (Peacock et al., 2007). Additionally, proteolysis of talin by calpain promotes destabilization of the adhesion leading to adhesion disassembly (Franco et al., 2004), and this process is microtubule-driven (Bhatt et al., 2002). The microtubule motor kinesin-1 has been implicated in FA disassembly

through recruitment of dynamin, supporting a model where microtubules induce FA disassembly through vesicular transport. Intriguingly, endocytosis (Ezratty et al., 2005), subsequent endocytic trafficking (Caswell et al., 2009), and exocytosis (Stehbens et al., 2014) have also been implicated in FA turnover, and require microtubules (Soldati and Schliwa, 2006). There are multiple studies implicating endocytosis in FA destabilization and disassembly, and this process seems to require FAK activity (Ezratty et al., 2009; Mendoza et al., 2013). Our understanding of the regulation of adhesion turnover is still incomplete. It will be intriguing to discover if any additional cellular processes are involved in adhesion turnover.

Integrins

Integrins are transmembrane adhesion receptors that link the extracellular matrix to the actin cytoskeleton (Bouvard et al., 2001), and are the major structural components of adhesions (Berrier and Yamada, 2007; Huttenlocher and Horwitz, 2011; Hynes, 2002). Integrins are important for cell survival, differentiation and migration, and are essential to multicellular organisms (Ganguly et al., 2013; Haack and Hynes, 2001). Loss of almost any integrin subunits is embryonically lethal in mice (Bouvard et al., 2001; Johnson et al., 2009). There are 18 α subunits and 8 β subunits, each encoded from a different gene, that form 24 distinct heterodimers (Figure 1.3 A); each heterodimer binds specific extracellular matrix substrate(s), including (FN), Laminin, Vitronectin, and Collagen (Humphries et al., 2006). Many integrins can bind more than one ligand; for example, FN, Vitronectin, and Osteopontin are all substates for αVβ3 integrin (Zheng et al., 2000). Moreover, multiple integrins can bind the same ECM substrate, as is the case for α5β1 and αVβ3 integrins, which can both bind FN, suggesting some redundancy in integrin receptors (Hynes, 2002; Legate et al., 2009; Margadant et al., 2011).

Each integrin subunit is composed of a large extracellular domain, a transmembrane

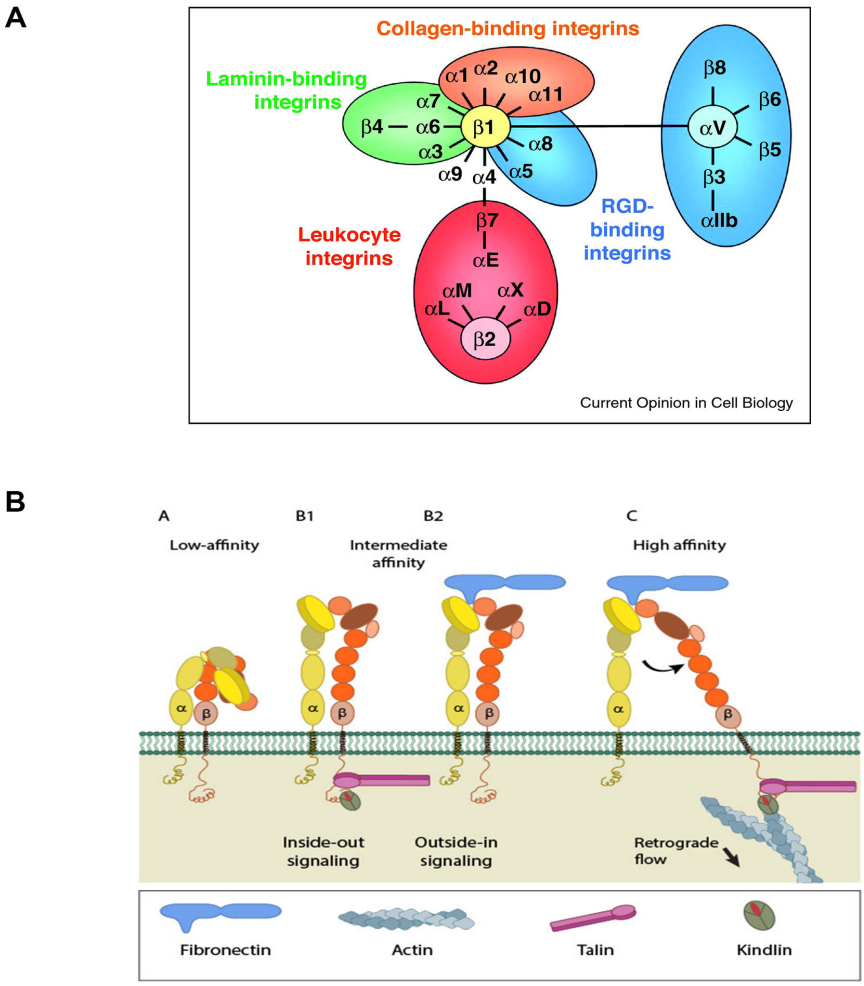

Figure 1.3. Integrin heterodimer substrates and activation. (A) Integrins are composed of one α and one β subunit, forming a heterodimer. There are 18 α and 8 β integrin subunits. The combination of different α and β subunits dictates affinity for various ECM substrates, such as Collagen, Laminin, and RGD-containing proteins (i.e. Fibronectin and Vitronectin). (B) Integrins exist in multiple conformations, which result in different activation states, or affinities for ECM substrate. In the bent conformation, integrins have low affinity for substrate, and are considered inactive. Intermediate activation occurs as a result of outside-in or inside-out signaling; the integrin is in an extended conformation, but not fully open. Separation of the cytoplasmic tails of the two subunits leads to a fully open and extended, active conformation.

(A) Reprinted from (Margadant et al., 2011). (B) Used with permission from MBInfo contributors. Integrin Activation. https://www.mechanobio.info/figure/1384245207230/

domain, and a short cytoplasmic tail. One α and one β subunit are non-covalently bound to form an integrin heterodimer. Integrins exist in different conformations (Figure 1.3 B), which represent various activation states (ligand affinity). In the bent and closed conformation, the integrin is considered inactive, with low ligand affinity (Fu et al., 2012). The integrin can also be 'primed' in the extended conformation with a closed headpiece, exhibiting an intermediate ligand affinity. The transmembrane and cytoplasmic domains of the α and β subunits are in closer association when the integrin is in the low and intermediate affinity states (Anthis and Campbell, 2011; Anthis et al., 2009; Calderwood, 2004; Wegener and Campbell, 2008). The integrin has the highest ligand affinity in the extended conformation with an open headpiece (Arnaout et al., 2005). The switching of these receptors between different activation states allows for bidirectional signaling (Hu and Luo, 2013). Although integrins are not initially expressed in an activated/high affinity state on the cell surface, ligand binding can lead to stabilization of the high affinity state and eventually to integrin clustering, so that integrins are activated and then transmit signals to the interior of the cell ('outside-in' signaling) (Kim et al., 2003). However, when a signal within the cell causes proteins, such as talin or kindlin, to bind to the cytoplasmic tail of integrins, a conformational change occurs to activate the integrin and increase ligand affinity ('inside-out' signaling) (Lefort et al., 2012; Margadant et al., 2012; Moser et al., 2009).

Once integrins are activated, clustering of multiple heterodimers occurs within the adhesion, contributing the strength of the adhesion, or avidity (Carman and Springer, 2003). The cytoplasmic tails of activated integrins bind to multiple adhesion proteins, including paxillin, talin, kindlin, α-actinin, and Src; these protein-protein interactions contribute to the structural role of integrins in adhesions (Lad et al., 2007; Liu et al., 2000). Integrins act as mechanotransducers in the adhesion, where forces pulling on the integrin can lead to its

activation and exposure of binding sites for downstream proteins (Ross et al., 2013). Integrins themselves do not have enzymatic activity, but function in signaling in many ways, including recruitment of the non-receptor tyrosine kinase FAK (Anthis and Campbell, 2011), the Rho GTPases Rac, Rho, and Cdc42 (involved in actin dynamics) (Jaffe and Hall, 2005), and by influencing signaling through receptors, such as epidermal growth factor receptor (EGFR) (Caswell et al., 2008).

Integrin Trafficking

Cell surface expression regulates the functions of integrins by attenuating cell-matrix adhesions and integrin signaling (Ivaska, 2012; Rossier et al., 2012). Changes in cell surface expression are largely accomplished through endocytic-exocytic cycles of integrins, where trafficking of these receptors is spatially and temporally regulated to target integrins to specific sites, namely adhesions (Pellinen and Ivaska, 2006; Sczekan and Juliano, 1990). Integrins are constitutively endocytosed and recycled to the cell surface; very little integrin is degraded in lysosomes (Bottcher et al., 2012; Bretscher, 1989; Bretscher, 1992; Dozynkiewicz et al., 2012; Lobert et al., 2010; Tiwari et al., 2011). Besides targeting to adhesions, integrin trafficking also functions to clear ligand from activated integrins and deliver active receptors back to the plasma membrane (Dozynkiewicz et al., 2012; Ng et al., 1999). Ligand binding of integrins in adhesions can promote integrin endocytosis (Dalton et al., 1995; Huttenlocher and Horwitz, 2011).

Integrin trafficking controls adhesion turnover as well as tumor cell migration, invasion, and metastasis (Huttenlocher and Horwitz, 2011; Kawauchi, 2012; Scales et al., 2013; Valdembri and Serini, 2012). Internalization of integrins not only serves to clear bound ligand and act as a checkpoint for damaged integrins that need to be degraded (Dozynkiewicz et al., 2012; Memmo and McKeown-Longo, 1998; Paul et al., 2015b), but endocytosis of integrins can also regulate

adhesion turnover. Integrin internalization can destabilize the adhesion leading to its disassembly (Mendoza et al., 2013). However, endocytosis of integrins also generates an internal pool of integrins which, when recycled, can lead to the formation of new adhesions (Paul et al., 2015b; Valdembri and Serini, 2012). Moreover, integrin recycling has also been linked to cell adhesion and migration. One purpose for integrin recycling is ensuring the proper localization of integrins to adhesions. It is largely believed that integrin recycling is polarized to the leading edge of the cell to promote the formation of new adhesions, although recycling from the trailing to leading edge of migrating cells has not been directly observed (Caswell and Norman, 2006; Paul et al., 2015b). It is also possible that integrin recycling contributes to sliding adhesions at the trailing edge of the cell to promote retraction of the cell rear (Ballestrem et al., 2001; Valdembri and Serini, 2012).

Various members of the Rab and Arf families of GTPases, which have known roles in vesicular trafficking, are key regulators of integrin trafficking (Paul et al., 2015b). Rabs recruit effector proteins that perform a variety of functions, including cargo sorting, motor protein binding, and tethering, docking, and fusion of vesicles (Hutagalung and Novick, 2011). Rab5, an important regulator of vesicle formation and formation of early endosomes, has been linked to integrin endocytosis, early endosome trafficking, and adhesion turnover (Mendoza et al., 2014; Mendoza et al., 2013; Sandri et al., 2012; Torres and Stupack, 2011), as has Rab21 (Pellinen et al., 2006), which is in the Rab5 subfamily (Pereira-Leal and Seabra, 2000; Pereira-Leal and Seabra, 2001). Additionally, Rab4 and Rab11 control different routes of integrin recycling (Caswell and Norman, 2006; Caswell et al., 2009; Paul et al., 2015b; Pellinen and Ivaska, 2006). Interestingly, Rab11 recycling compartments also contain Arf6 (Powelka et al., 2004). Arf proteins recruit coating proteins that function in vesicle budding, linking to motor proteins, and

regulating phospholipid signaling (Casalou et al., 2016). Arf5 promotes endocytosis of α5β1 integrin through the GEF brefeldin A-resistant ARF-GEF2 (BRAG2), which binds directly to clathrin and AP-2 (Dunphy et al., 2006; Moravec et al., 2012). Arf6 has been reported to increase both internalization and recycling of α5β1 integrin (Morgan et al., 2013; Powelka et al., 2004; Sakurai et al., 2010). Indeed, the Arf6 GAP "ArfGAP with RhoGAP Domain, Ankyrin Repeat and PH Domain 2" (ARAP2) is required for β1 integrin internalization and disassembly of adhesions (Chen et al., 2014), and Arf6-dependent recycling of α5β1 integrin also leads to adhesion disassembly (Morgan et al., 2013), indicating that the mechanisms underlying Arf6 integrin trafficking are quite complex.

While there are some aspects of integrin trafficking that resemble canonical trafficking pathways of membrane proteins (Caswell and Norman, 2006), integrins also have unique trafficking cycles (Figure 1.4). These trafficking pathways are dependent on the activation state of the integrin, the specific heterodimer, and the type of adhesion (Bretscher, 1992; Caswell et al., 2009; Paul et al., 2015b; Sandri et al., 2012; Valdembri et al., 2011). For instance, while αvβ3 integrin traffics through 'short-loop' recycling pathways and is dependent on Rab4 (Christoforides et al., 2012), α5β1 integrin traffics through the 'long-loop' pathway and is dependent on Rab11 (see Figure 1.4 for description of these pathways) (Caswell and Norman, 2006). In addition, Rab25 can rescue active integrins from degradation by recycling them from late endosomes to the plasma membrane, as opposed to lysosomes (Dozynkiewicz et al., 2012). Adding to the complexity of these trafficking routes, specific trafficking proteins can be utilized in markedly different mechanisms to traffic either active or inactive integrins. Dab2 associates with Eps15 homology domain (EHD) proteins to internalize inactive β1 integrins (Teckchandani et al., 2012; Teckchandani et al., 2009). However, Dab2 also interacts with AP-2 to internalize

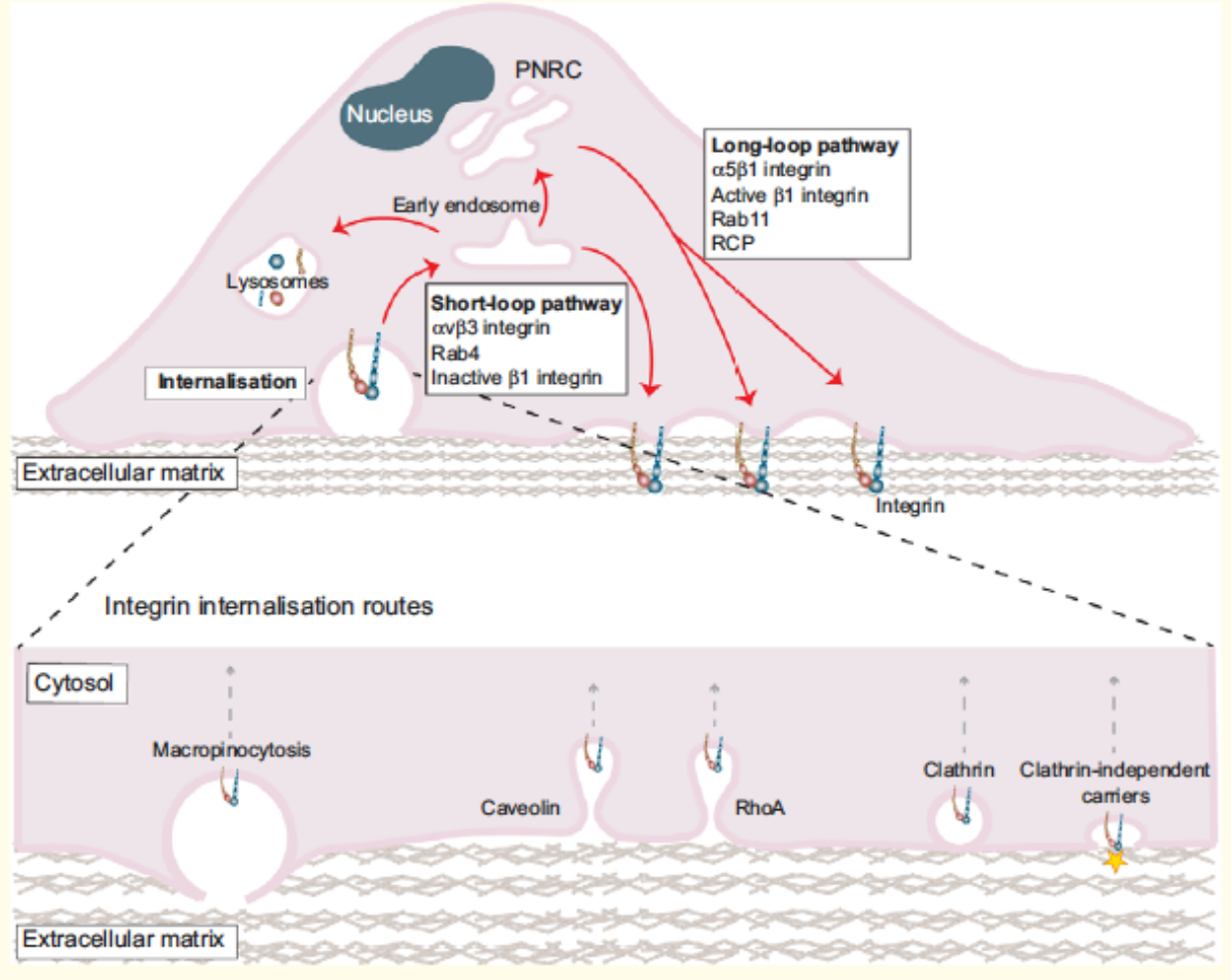

Figure 1.4. Integrin trafficking. Integrins undergo different trafficking pathways from other receptors. Integrins are endocytosed through clathrin-dependent and –independent mechanisms, and are trafficked into early endosomes (EE). Most integrins are recycled, with very little degradation in the lysosome. αvβ3 integrins are recycled directly from EEs ('short-loop' recycling), dependent on Rab4. α5β1 integrins go through 'long loop' recycling pathways, where integrins are sorted through recycling endosomes (RE) before being trafficked to the plasma membrane (dependent on Rab11). Active integrins can also undergo more complex recycling pathways from late endosomes, driven by Rab25.

Figure reprinted from (De Franceschi et al., 2015).

active β1 integrins (Chao et al., 2010; Ezratty et al., 2009). Moreover, distinct mechanisms of integrin internalization exist for integrins within different adhesion types and locations within the cell (Paul et al., 2015b). For instance, Dab2-dependent internalization of β1 integrins occurs at larger FAs located more central to the cell (Nishimura and Kaibuchi, 2007), whereas Numb is responsible for internalization of β1 integrins from focal complexes at the leading edge of the cell (Teckchandani et al., 2009).

Many studies have investigated trafficking of α5β1 integrin, the major fibronectin receptor. α5β1 integrin is internalized by clathrin-dependent and –independent mechanisms in a process that requires Rab5. Also, α5β1 integrin undergoes 'long loop' recycling, where it is trafficked to the perinuclear recycling center before being returned to the plasma membrane in an Arf6-dependent manner (Li et al., 2005). Endocytosis of active α5β1 integrin from adhesions has been shown to occur through a complex involving neuropilin-1 (Nrp1) and GAIP c-terminus interacting protein 1 (GIPC1). This complex is necessary to mediate adhesion of endothelial cells on fibronectin (Valdembri et al., 2009). Nrp1 associates with the extracellular domain of α5 integrin, and both of these receptors are endocytosed into Rab5 positive vesicles through binding of GIPC1 to both Nrp1 and α5 integrin (Katoh, 2013; Tani and Mercurio, 2001; Valdembri et al., 2009). This complex is then trafficked along actin filaments by myosin VI (Myo 6), which binds to the C-terminal domain of GIPC1 (Aschenbrenner et al., 2003; Frank et al., 2004).

Besides regulation of adhesions, integrin trafficking also governs cell migration by directly influencing RhoGTPase signaling (White et al., 2007). There is a fine balance between Rac and RhoA signaling in cell migration (discussed in more detail in the GTPases and Cell Migration section), and disruption of this balance can alter cell migration modes (Evers et al., 2000; Ridley et al., 2003; Schwartz, 2004). Likewise, there is a balance between trafficking of

αvβ3 and α5β1 integrins, which has direct consequences for Rho GTPase signaling (Christoforides et al., 2012; Danen et al., 2005). αvβ3 trafficking suppresses α5β1 trafficking, and vice versa. When αvβ3 trafficking is predominant, the balance in GTPase signaling favors Rac-driven directional migration (Jacquemet et al., 2013c; Pankov et al., 2005). Suppression of αvβ3 trafficking enhances α5β1 endocytic-exocytic cycle, promoting RhoA activity and random migration (Caswell et al., 2009; Jacquemet et al., 2013a; Paul et al., 2015a). While many of the mechanisms underlying integrin trafficking are now understood, the complexity of these processes and the consequences for cell adhesion, adhesion turnover, and cell migration are still under intense study.

Rho GTPases and Cell Migration

GTPases act as molecular switches, cycling between an inactive (GDP-bound) and active (GTP-bound) state (Jaffe and Hall, 2005), and play crucial roles in cell biology (Machacek et al., 2009). The GDP-GTP exchange of these proteins is largely regulated by GEFs and GAPs. GEFs promote the release of GDP, allowing for GTP binding; GAPs increase the intrinsic GTPase activity, leading to hydrolysis of GTP to GDP to inactivate the GTPase (Schmidt and Hall, 2002). Some GTPases have C-terminal farnesyl or geranylgeranyl posttranslational modification for insertion into membranes, and binding of guanine dissociation factors (GDIs) to the C-terminus of the GTPase sequesters GTPases to the cytosol and negatively regulates signaling (Cherfils and Zeghouf, 2013). GEFs, GAPs, and GDIs are regulated by upstream signals, and the summed activities of these proteins determine the relative activation state of GTPases (Sadok and Marshall, 2014; Schwartz, 2004). Active GTPases associate with their effectors to elicit downstream signaling pathways involved in many processes, including migration, adhesion, and cytokinesis (Szczepanowska, 2009).

A number of GTPases are involved in cell migration. While the Rab and Arf GTPase families (involved in vesicular trafficking), are becoming more appreciated for their roles in adhesion turnover and cell migration (Caswell and Norman, 2006; Caswell et al., 2009; Paul et al., 2015b), the Rho (Ras-homology) family of small GTPases has been most studied for its roles in cell migration. Within the Ras superfamily, the Rho GTPase family contains 22 proteins (Lawson and Ridley, 2017). Rac, Cdc42, and RhoA have been extensively studied, and are the most relevant Rho GTPases to cell migration. These Rho GTPases are crucial for regulating actin dynamics in polarized, migrating cells (Nobes and Hall, 1995; Ridley, 2015).

Polymerization of branched actin networks and formation of lamellipodia requires Rac. Rac has many downstream effectors that promote the formation and maintenance of lamellipodia. For example, WASP/WAVE proteins are Rac effectors that activate the Arp2/3 complex to form branched actin (Law et al., 2013; Michael et al., 2010; Ridley, 2015). Cdc42 stimulates the formation of filopodia through the formation of unbranched actin networks. Interestingly, Cdc42 can also activate the Arp2/3 complex (which forms branched actin), but crosslinks these actin filaments through actin-bundling proteins (Jaffe and Hall, 2005; Svitkina et al., 2003; Vignjevic et al., 2003). RhoA is associated with cell rear detachment through the formation of large, contractile actin bundles, called stress fibers (Cox and Huttenlocher, 1998; Nobes and Hall, 1995; Ridley, 2001). However, RhoA is active in the lamellipodia as well, and is necessary for lamellipodia extension, possibly by regulating turnover of focal complexes (Heasman et al., 2010; Lawson and Burridge, 2014; Machacek et al., 2009; Ridley, 2015). RhoA acts through the effector protein mDia1, a formin that allows for the processive elongation of actin filaments (Isogai et al., 2015; Jaffe and Hall, 2005; Zaoui et al., 2008).

While it was originally thought that Rac is at the leading edge and RhoA is located at the cell rear (Nobes and Hall, 1995), it is now clear that Rac can be activated at the cell rear and RhoA is required in the lamellipodia (Gardiner et al., 2002; Heasman et al., 2010; Machacek et al., 2009). The activities of Rac and RhoA are mutually antagonistic (Sander et al., 1999); The RhoA effector Rho-associated protein kinase (ROCK) activates the Rac GAP ARHGAP22 (Sanz-Moreno et al., 2008), and Rac activates the RhoA GAP p190RhoGAP through a WAVE-dependent mechanism (Wennerberg et al., 2003). The balance between Rac and RhoA activation in different parts of the cell is crucial to cell polarization and migration. Rac may be primarily activated at the cell front, yet still be necessary to antagonize RhoA at the cell rear. Likewise, the majority of RhoA activation may occur at the cell rear, but the pool of active RhoA at the cell front seems crucial for lamellipodia extension (Evers et al., 2000; Lawson and Burridge, 2014; Sackmann, 2015). Elegant FRET live imaging studies revealed that RhoA is activated at the edge of the cell front, whereas Rac and Cdc42 are activated 2 μm from the cell edge, approximately 40 sec after RhoA activation (Machacek et al., 2009). This suggests a complex spatiotemporal regulation of the antagonistic interplay between Rac and RhoA activation during cell migration.

Rab5 Regulates Integrin Trafficking and Rac Signaling

Rab proteins are key regulators of membrane trafficking. They are the largest family of GTPases within the Ras superfamily, with over 60 proteins in this family identified to date (Zerial and McBride, 2001). Rabs associate with the membranes of a donor compartment in the GDP-bound state, and upon GTP binding are recruited to a budding vesicle. Once this vesicle reaches the acceptor compartment, GTP is hydrolyzed (with the aid of a Rab-GAP), and thereby stimulates vesicle fusion (Hutagalung and Novick, 2011). Various Rabs localize to different vesicular structures within the endocytic-exocytic pathway, and so regulate different processes. Rab5 is a

well-characterized Rab protein involved in endocytosis and trafficking into early endosomes (van der Bliek, 2005). Rab5 has been shown to be an important in cell migration (Lanzetti and Di Fiore, 2008), and overexpression of Rab5 has been shown to promote the invasiveness of cancer cell lines (Torres and Stupack, 2011). Recent evidence points to Rab5-dependent regulation of integrin trafficking and Rac activation.

Besides its roles in endocytic trafficking, Rab5 has also been identified as a signaling GTPase (Lanzetti et al., 2004). Rab5-dependent endocytosis, downstream of Caveolin-1, has recently been shown to activate Rac on endosomes through the Rac-GEF Tiam1 (Diaz et al., 2014a; Lanzetti et al., 2004; Palamidessi et al., 2008). Caveolin-1 binds to and sequesters the Rab5 GAP, p85α, thereby allowing for Rab5 activation (Diaz et al., 2014a; Diaz et al., 2014b). It is believed that Rac brings together Rac and its GEF, Tiam1, and subsequent recycling of Rac to the leading edge promotes lamellipodia formation (Mendoza et al., 2014). In agreement with this hypothesis, Rab5 activation promotes lamellipodia formation and migration in wound healing assays, and inhibition of Rab5-mediated Rac activation decreases cancer cell migration and invasion (Diaz et al., 2014a; Hagiwara et al., 2009; Mendoza et al., 2013).

Rab5 has also been linked to integrin trafficking. Like many other receptors, endocytosis and trafficking of integrins to early endosomes requires Rab5 (Yuan et al., 2010). Interestingly, Rab5 associates with α and β integrin subunits (Mendoza et al., 2013; Pellinen et al., 2006; Torres et al., 2010). Furthermore, Rab5 localizes to focal adhesions and associates in a complex with vinculin and paxillin. Live cell imaging studies revealed that a subset of Rab5 vesicles is localized to the leading edge of the cell, and when one of these vesicles touches a FA, focal adhesion disassembly quickly follows (Mendoza et al., 2013). Moreover, Rab5 activation integrates integrin trafficking and Rac activation. R-Ras associates with adhesions, and, when

activated, associates with the Rab5 GEF RIN2. This association converts RIN2 from a GEF to an adaptor protein that preferentially binds Rab5-GTP. This binding induces Rab5-mediated endocytosis of active β1 integrins and translocation of R-Ras into early endosomes, where Rac activation occurs (Sandri et al., 2012). This evidence suggests that endocytic trafficking through Rab5 is important for regulation of cell migration.

APPL1 is a Multifunctional Endosomal Adaptor Protein

Signaling endosomes are believed to function as platforms for integrating distinct communication pathways within cells (Palfy et al., 2012). Endosome-associated adaptor proteins are critical in mediating this crosstalk between signaling pathways because of their ability to interact with multiple proteins (Palfy et al., 2012). APPL1, also known as DIP13α, is a 709-amino acid adaptor protein that is receiving increasing attention because it can facilitate signaling pathway crosstalk on endosomal surfaces. For example, APPL1 has been proposed to mediate crosstalk between Wnt and insulin signaling pathways by bringing together proteins involved in these pathways on endosomes (Palfy et al., 2012; Schenck et al., 2008). APPL1 acts as a signaling adaptor protein to coordinate signaling and trafficking events and regulate cellular processes, including cell migration and adhesion.

APPL1 integrates signaling crosstalk via multiple domains that mediate protein and lipid interactions (Miaczynska et al., 2004; Mitsuuchi et al., 1999). The N-terminal Bin-Amphiphysin-Rvs (BAR) domain is implicated in sensing or inducing membrane curvature (Habermann, 2004; Takei et al., 1999), while both the central pleckstrin homology (PH) and C-terminal phosphotyrosine (PTB) domains have been shown to bind to phospholipids (Li et al., 2007). Indeed, multiple studies have demonstrated the ability of APPL1 to bind phosphoinositides, including PtdIns(3)P, PtdIns(4)P, PtdIns(5)P, PtdIns(3,4)P_2 and PtdIns(3,5)P_2, and

PtdIns(3,4,5)P_3 (Chial et al., 2008; Li et al., 2007). Through its BAR domain, APPL1 can oligomerize to form homodimers (APPL1-APPL1) or heterodimers with APPL2 (APPL1-APPL2) (Chial et al., 2008). APPL1 is unique from other BAR domain-containing proteins, in that the BAR and PH domains of APPL1 together form a functional domain that binds the small GTPase Rab5 (Figure 1.5). Mutagenesis studies have revealed that Rab5 binds to both the BAR and PH domains of APPL1, as Rab5 could not interact with APPL1 lacking either one of them (Zhu et al., 2007). The BAR-PH domain of APPL1 also binds Rab21 (Zhu et al., 2007), which is similar in structure to Rab5 (Pereira-Leal and Seabra, 2001). The PTB domain enables interaction of APPL1 with a number of receptor proteins, including EGFR (Miaczynska et al., 2004), tropomyosin receptor kinase A (TrkA) (Lin et al., 2006), deleted in colorectal cancer (DCC) (Liu et al., 2002), adiponectin receptor (AdipoR1) (Mao et al., 2006), insulin receptor (IR) (Ryu et al., 2014), follicle stimulating hormone receptor (FSHR) (Nechamen et al., 2004), androgen receptor (AR) (Yang et al., 2003), and N-methyl-D-aspartate (NMDA) receptors (Husi et al., 2000), to regulate signaling (Li et al., 2007). At its C-terminus, APPL1 binds the PSD-95/Discs-large/ZO-1 (PDZ) domain of the adaptor protein GIPC1 (Varsano et al., 2012), a protein involved in loading cargoes onto vesicles through its interaction with the actin motor protein myosin VI (Katoh, 2013) (Figure 1.5).

Moreover, APPL1 associates with at least thirty-three unique proteins (Table 1), and possibly many more, as indicated by numerous studies (data deposited in BioGrid dataset: https://thebiogrid.org/117522/summary/homo-sapiens/appl1.html) (Stark et al., 2006b). It is highly implausible that APPL1 interacts with all of these proteins simultaneously. More likely, APPL1 binds a subset of these proteins in a cell type dependent manner to regulate specific signaling pathways. Furthermore, interactions between APPL1 and some of the listed proteins

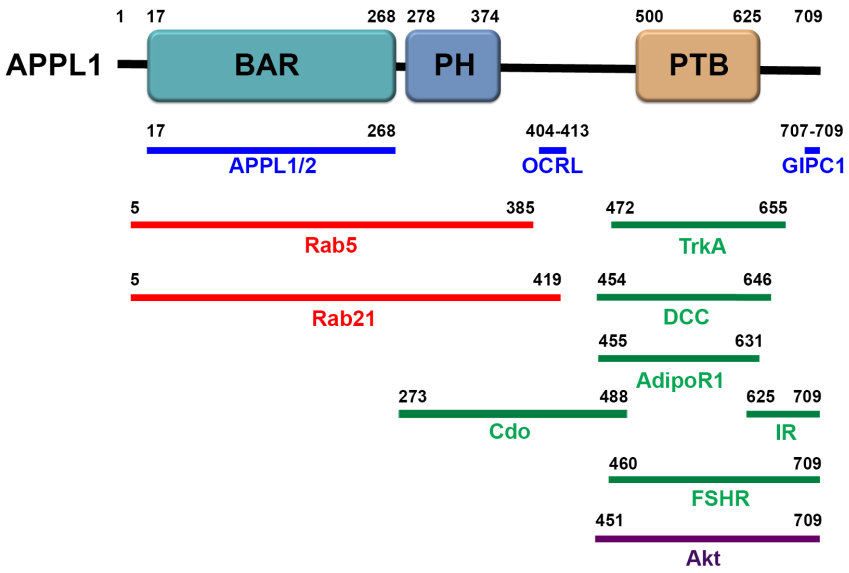

Figure 1.5. Domain structure and interacting protein binding sites of APPL1. Numbers correspond with amino acid residues. Numbering of APPL1 domains is based on Li et al. (2007). Interacting proteins are labeled as follows: red, trafficking proteins; purple, signaling proteins; blue, proteins involved in both signaling and trafficking; green, receptors.

Table 1.1. List of APPL1 interactions identified through the BioGRID database and literature searches. At least 33 proteins interact with APPL1. Protein interactions identified by BioGRID through high throughput methods have been excluded. For full list, see https://thebiogrid.org/117522/summary/homo-sapiens/appl1/html (Stark et al., 2006a).

ID	Experimental Method	References
ADIPOR1/2	Affinity Capture-Western, Protein Fragmentation Complementation Assay, Two-Hybrid, Reconstituted Complex	(Aouida et al., 2013; Mao et al., 2006)
AKT1/2	Affinity Capture-Western, Reconstituted Complex, Two-Hybrid	(Mitsuuchi et al., 1999; Nechamen et al., 2007; Yang et al., 2003)
APPL1	Co-crystal Structure, Reconstituted Complex	(Zhu et al., 2007)
APPL2	Affinity Capture-Western	(Nechamen et al., 2007)
AR	Affinity Capture-Western	(Yang et al., 2003)
CDON	Affinity Capture-Western, Two-Hybrid	(Bae et al., 2010)
DCC	Affinity Capture-Western, Two-Hybrid	(Liu et al., 2002)
DVL2	Affinity Capture-Western	(Banach-Orlowska et al., 2015)
EGFR	Co-Localization	(Lee et al., 2011; Miaczynska et al., 2004)
FSHR	Affinity Capture-Western, Two-Hybrid	(Cohen et al., 2004; Nechamen et al., 2004)
GIPC1	Affinity Capture-Western	(Lin et al., 2006; Varsano et al., 2006; Varsano et al., 2012)
HDAC1-3	Affinity Capture-Western, Reconstituted Complex	(Banach-Orlowska et al., 2009; Joshi et al., 2013)
INPP5B	Affinity Capture-Western	(Erdmann et al., 2007)
INSR	Affinity Capture-Western	(Ryu et al., 2014)
IRS1/2	Affinity Capture-Western	(Ryu et al., 2014)
MTA 2	Affinity Capture-Western, Reconstituted Complex	(Banach-Orlowska et al., 2009; Miaczynska et al., 2004)
NTRK1	Affinity Capture-Western	(Lin et al., 2006)
OCRL	Affinity Capture-Western	(Erdmann et al., 2007)
PIKCA	Affinity Capture-Western	(Mitsuuchi et al., 1999)
PIK3R1	Affinity Capture-Western	(Yang et al., 2003)
PRKCZ	Affinity Capture-Western, Reconstituted Complex	(Song et al., 2015)
RAB5A	Affinity Capture-Western, Reconstituted Complex	(Mao et al., 2006; Miaczynska et al., 2004; Zhu et al., 2007)
RAB21	Reconstituted Complex	(Zhu et al., 2007)
RBBP4/7	Affinity Capture-Western Reconstituted Complex	(Banach-Orlowska et al., 2009) (Miaczynska et al., 2004)
RUVBL2	Affinity Capture-Western, Reconstituted Complex	(Rashid et al., 2009)
TGFBR1	Affinity Capture-Western, Co-localization, Reconstituted Complex	(Song et al., 2015)
TRAF6	Affinity Capture-Western	(Cheng et al., 2013)
TUBB3	Affinity Capture-Western	(Song et al., 2015)

may not be direct since they were found by immunoprecipitation assays. Thus, more reconstitution studies should be performed to define proteins that directly interact with APPL1. Nevertheless, the number of putative interactors of APPL1 suggests its great potential to regulate a variety of processes.

APPL1 and APPL2: Similarities and Contrasts

APPL2 is a 669-amino acid protein that shares 54% identity with APPL1 (Miaczynska et al., 2004). APPL1 and APPL2 share similar BAR, PH, and PTB domains, as well as a C-terminal SEA motif for binding PDZ domains (Liu et al., 2002). APPL1 and APPL2 share some similar roles. For instance, APPL1 and APPL2 both contribute to cell survival, but their roles occur through distinct signaling pathways (Pyrzynska et al., 2013; Schenck et al., 2008). APPL1 regulates Akt signaling to mediate cell survival, requiring its endosomal localization (Schenck et al., 2008). On the other hand, APPL2 decreases gene expression of apoptosis-related genes, and this effect on cell survival is independent of its endosomal localization (Pyrzynska et al., 2013). Furthermore, the two proteins may have some redundant roles, as evidenced by the APPL1 knockout mouse, which is viable, with no obvious phenotypes. MEFs from the APPL1 knockout mouse exhibit impaired Akt signaling in response to HGF stimulation, and this effect is aggravated by APPL2 depletion (Tan et al., 2010). The additive effect of APPL1 and APPL2 on migration has recently been confirmed with a double knockout mouse for APPL1/2; APPL1 knockout results in defects in HGF-induced migration, and double knockout of APPL1/2 enhances this effect (Tan et al., 2016). However, APPL1 and APPL2 are not fully redundant, as the two proteins display some differences in binding partners. For instance, both APPL1 and APPL2 interact with Rab5 (Zhu et al., 2007), but APPL2 cannot bind Rab21; conversely, Rab22a, Rab24, and Rab31 can bind APPL2, but not APPL1 (King et al., 2012). APPL1 and

APPL2 also exhibit some opposing functions; for example, APPL1 is a positive regulator of AdipoR1 signaling, whereas APPL2 is a negative regulator (Wang et al., 2009). APPL2 has not been as well studied as APPL1, and further studies on APPL2 will be important to reveal redundant and/or unique novel functions of APPL2.

APPL1 in Trafficking

APPL1, which localizes to early endosomes via interaction with Rab5 as well as lipid binding (Zhu et al., 2007), may mark a transient and very early compartment in the endocytic pathway (Zoncu et al., 2009). In support of this idea, highly motile tubulovesicular transport carriers that traffic receptors and fuse to early endosomes were shown to contain APPL1 (Gan et al., 2013). APPL1-positive vesicles may serve as a precursor for more mature, early endosome antigen (EEA1)-positive, endosomes (Urbanska et al., 2011; Zoncu et al., 2009). Indeed, little to no colocalization occurs between APPL1 and EEA1, although both are Rab5 effectors (Miaczynska et al., 2004). Furthermore, EEA1 competes with APPL1 for Rab5 binding on endosomes, and upon a phosphoinositide switch, APPL1 is lost and EEA1 is gained, giving more evidence to a model where APPL1 endosomes mature into EEA1 endosomes (Zoncu et al., 2009). Interestingly, another Rab5 effector, WD Repeat and FYVE Domain Containing 2 (WDFY2), partially colocalizes with both APPL1 and EEA1(Zoncu et al., 2009). After APPL1 was lost from WDFY2 compartments, these compartments then fused to form larger endosomes, which then acquired EEA1 and lost WDFY2 (Zoncu et al., 2009).

However, recent evidence suggests that a subset of APPL1 endosomes make up a distinct early endosome compartment that can be very stable (Kalaidzidis et al., 2015). Mathematical modeling argues against the hypothesis of APPL1 endosome maturation into EEA1-positive ones as an obligatory mechanism along the endocytic route (Kalaidzidis et al., 2015). Moreover,

APPL1 compartments can act as sites of cargo sorting, which enable recycling of cargo back to the plasma membrane (Kalaidzidis et al., 2015). In support of this model, the endosomal sorting complex required for transport (ESCRT)-0 was recently shown to mark an APPL1-independent route for trafficking to EEA1-positive endosomes, indicating that there are alternative ways of endosome maturation (Flores-Rodriguez et al., 2015). A subset of APPL1 endosomes most likely mature into and/or bidirectionally exchange cargo with EEA1 endosomes, whereas another subset directly sort cargo for recycling (Kalaidzidis et al., 2015).

APPL1 has also been implicated in the regulation of trafficking, which is crucial for modulating signals from receptors. For instance, APPL1 is linked to EGFR trafficking by modulating Rab5 activation (Lee et al., 2011). EGFR is quickly internalized after activation by EGF, in a Rab5-dependent manner. Then it is trafficked to early endosomes for sorting into recycling endosomes or lysosomes for degradation. Overexpression of APPL1 decreases Rab5 activation and subsequently inhibits internalization of EGFR, which reduces degradation of the receptor. Conversely, APPL1 depletion increases Rab5 activation, resulting in increased internalization and trafficking of EGFR to lysosomes to regulate EGFR protein levels and signaling (Lee et al., 2011). Thus, APPL1 is an important regulator of endocytic trafficking, and further studies will be needed to reveal the mechanisms by which APPL1 regulates the trafficking of a variety of receptors.

APPL1 in Signaling

In addition to its roles in endocytic trafficking, APPL1 also regulates signaling events by interacting with receptors and other signaling proteins. APPL1 binds various signaling proteins, including the serine/threonine kinase Akt (Mitsuuchi et al., 1999), p110α and p85 subunits of phosphatidylinositol-4,5-bisphosphate 3-kinase (PI3K) (Yang et al., 2003), insulin receptor

substrate proteins 1 and 2 (IRS1/2) (Ryu et al., 2014), and the Rab5 effector oculocerebrorenal syndrome of Lowe (OCRL) (Erdmann et al., 2007) (Figure 1.5). As a signaling adaptor protein, APPL1 is important for mediating signaling specificity (Palfy et al., 2012). For example, APPL1 regulates phosphorylation of glycogen synthase-3 beta (GSK3-β) by Akt, playing a role in cell survival. However, APPL1 is not required for Akt-mediated activation of tuberous sclerosis complex 2 (TSC2), which plays a role in growth control (Palfy et al., 2012; Schenck et al., 2008).

APPL1-mediated signaling is largely coordinated through its PTB domain, located near the C-terminus. This domain allows APPL1 to couple trafficking and signaling, as lipid binding and Rab5 interaction (accomplished through the BAR and PH domains located near the N-terminus of the protein) would not interfere with APPL1 interaction with signaling proteins (Palfy et al., 2012). The PTB domain of APPL1 is similar to that of another adaptor protein Shc, which recognizes the NPXpY consensus sequence in its interacting proteins (Deepa and Dong, 2009). However, the binding of most PTB domains is independent of tyrosine phosphorylation (Schlessinger and Lemmon, 2003), and this seems to be the case for APPL1 (Deepa and Dong, 2009; Lin et al., 2006; Ryu et al., 2014). Indeed, APPL1 has been shown to interact exclusively with the inactive (unphosphorylated) form of Akt2 (Mitsuuchi et al., 1999). Similarly, binding between the PTB domain of APPL1 and TrkA or AdipoR1 does not depend on the presence of phosphotyrosine (Lin et al., 2006; Mao et al., 2006). Mutation of all tyrosine residues in AdipoR1 had no effect on APPL1 binding (Mao et al., 2006). Thus, it is likely that APPL1 mediates its signaling interactions through a novel mechanism, independent of tyrosine phosphorylation, and understanding this mechanism will require further studies to elucidate.

APPL1 allows the signaling events to occur after internalization of receptors into compartments termed signaling endosomes (Palfy et al., 2012). During endocytosis, signaling endosomes can be trafficked to specific locations within the cell to mediate certain signaling cascades. One example can be regulation of lysophosphatidic acid (LPA)-induced signaling by APPL1 and its interacting partner GIPC1 (Varsano et al., 2012). Depletion of GIPC1 sustains lysophosphatidic acid receptor 1 (LPA_1)-mediated Akt signaling on APPL1 endosomes. At the same time, trafficking of the receptor into EEA1-positive early endosomes that attenuates signaling is restricted. When LPA_1 is in the APPL1 compartment, Akt signaling continues, while trafficking to EEA1 attenuates LPA_1-mediated signaling (Varsano et al., 2012). Therefore, APPL1 may represent an important mode of regulation of signaling events through endosomes.

APPL1-regulated signaling is not limited to signaling endosomes. APPL1 couples the trafficking of receptors into early endosomes with the transmission of signals to the nucleus, through the interaction of APPL1 with Rab5. Upon GTP hydrolysis of Rab5, APPL1 is lost from endosomes and translocates to the nucleus, where it stimulates changes in chromatin remodeling and transcription (Miaczynska et al., 2004). In support of this model, APPL1 interacts with and modulates the functions of histone deacetylases (HDAC)1-3 (Banach-Orlowska et al., 2009; Joshi et al., 2013) to influence the expression of cyclin-dependent kinase inhibitor 1 ($p21^{CIP1}$) (Banach-Orlowska et al., 2009). APPL1 also forms a complex with the tumor repressor Reptin in complex with HDAC1 to relieve translational repression and promote transcription of Wnt-signaling target genes (Rashid et al., 2009). Moreover, APPL1 binds Dishevelled 2 (Dvl2) and enhances its ability to promote non-canonical Wnt signaling through the transcription factor activating protein 1 (AP-1). This function is dependent on the endosomal localization of APPL1

(Banach-Orlowska et al., 2015). As such, APPL1 seems to regulate post-internalization signaling by coupling signaling and transcription to endocytic trafficking.

In addition to regulating signaling specificity, APPL1 facilitates crosstalk between multiple signaling pathways; one example is the synergism between the adiponectin and insulin signaling pathways. APPL1 associates with AdipoR1 upon stimulation with adiponectin, leading to downstream phosphorylation of 5' adenosine monophosphate-activated protein kinase (AMPK) and p38 mitogen-activated protein kinase (MAPK) (Deepa and Dong, 2009). Co-treatment with adiponectin and insulin usually results in Akt phosphorylation, but not in cells depleted of APPL1 (Deepa and Dong, 2009). Furthermore, APPL1 mediates sensitization of insulin signaling through adiponectin. Treatment of C2C12 cells with adiponectin leads to phosphorylation of APPL1 at Ser401. Co-treatment with insulin mediates the association of phosphorylated APPL1, IR, and IRS1/2 to allow for insulin signaling (Ryu et al., 2014). Together, this evidence highlights an important role for APPL1 as a signaling adaptor that mediates signaling pathways coupled to endosomal trafficking.

APPL1 in Cancer

APPL1 has been implicated in cell survival, growth, and proliferation (Lin et al., 2006; Liu et al., 2002; Schenck et al., 2008). As these processes have been implicated in cancer progression, it is therefore possible that APPL1 could play a role in cancer. It has been proposed that APPL1 is a tumor suppressor, as deletion of the region of the chromosome containing APPL1 or the gene itself has been demonstrated in a variety of cancers (Kok et al., 1997; Mitsuuchi et al., 1999). APPL1 also interacts with the tumor suppressor DCC, where depletion of APPL1 blocks DCC-mediated apoptosis (Liu et al., 2002). A recent study identified a micro RNA with oncogenic functions in colorectal cancer, acting by repressing APPL1 expression and promoting cell

survival (Saleh et al., 2016). However, while APPL1 seems to be downregulated in some cancers (Cerami et al., 2012; Mitsuuchi et al., 1999; Saleh et al., 2016), it is upregulated in others (Bidkhori et al., 2013; Johnson et al., 2014; Song et al., 2015; Zhai et al., 2016). In many of these studies, overexpression of APPL1 corresponded with overexpression of Rab5, a master regulator of endocytic events that has been well established in promoting tumorigenesis (Fukui et al., 2007). Another study implicating APPL1 in glioma involved its interaction with the adaptor protein GIPC1. GIPC1 was shown to promote glioma cell invasion, and knockdown of GIPC1 led to a decrease in APPL1 expression and decreased downstream signaling (Zhang et al., 2016). Much like APPL1, GIPC1 is upregulated or downregulated in various cancers (Katoh, 2013). This may be due to the complexity of adaptor proteins to modulate signaling and trafficking processes, and how these processes relate to cancer could be cell-type specific.

APPL1 as a Regulator of Cell Migration

While the functions of APPL1 in trafficking and signaling have been studied, the role of APPL1 in regulating cell migration is still poorly understood. This role was initially explored in a study using murine embryonic fibroblasts (MEFs) from the APPL1 knockout mouse. Although APPL1 is dispensable for development, fibroblasts require APPL1 for proper Akt signaling during hepatocyte growth factor (HGF)-mediated survival and cell migration (Tan et al., 2010).

The importance of APPL1 in the regulation of cell migration has also been documented in cancer cell line models. A study by Broussard et al. (2012) showed that cell lines exhibiting lower migratory rates express higher levels of APPL1 in comparison to highly motile cancer cell lines. It is therefore hypothesized that alterations in APPL1 expression levels affect cell migration. In support of this hypothesis, expression of APPL1-GFP in HT1080 fibrosarcoma cells leads to a decrease in cell migration speeds, which is dependent on endosomal localization

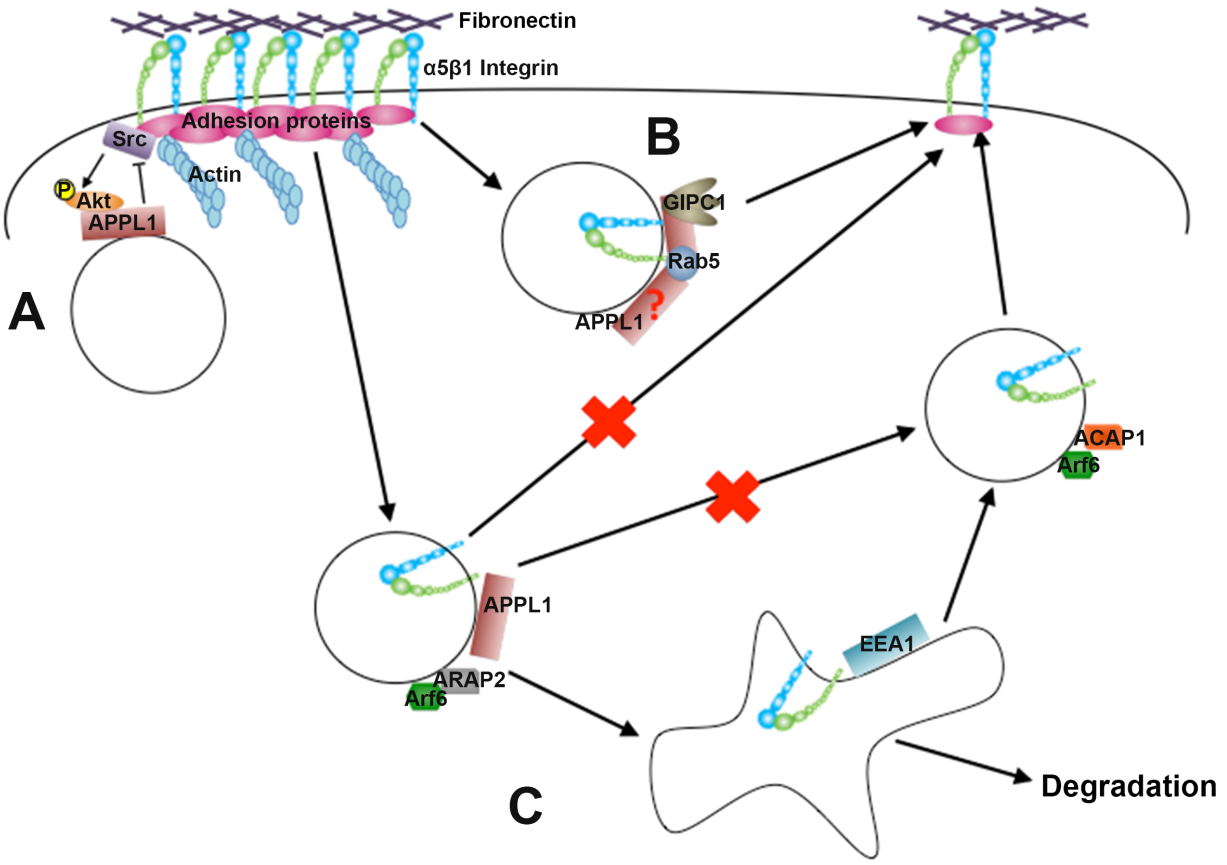

Figure 1.6. Function of APPL1 in cell migration and adhesion. (A) APPL1 decreases migration speeds by inhibiting Akt tyrosine phosphorylation by Src within adhesions. This process requires endosomal localization of APPL1. Circle represents APPL1-positive early endosomes. (B) Rab5 and GIPC1 promote internalization of active α5β1 integrin from adhesions, which is subsequently recycled to newly forming adhesions. APPL1 may be involved in this process. Circle represents Rab5-positive early endosomes that may contain APPL1. (C) APPL1 colocalizes with the Arf6 compartment containing the GAP ARAP2, which promotes transition of integrins from APPL1-endosomes to EEA1-endosomes, and may block transition of integrins to recycling endosomes. Arf6 compartments containing ACAP1, however, promote recycling of integrins. Circles represent Arf6 compartments marked by either ARAP2/APPL1 or ACAP1. Irregular shaped compartment represents EEA1-positive early endosomes.

of APPL1 and its ability to coordinate signaling. Mechanistically, APPL1 inhibits Akt activity within adhesions and downstream of the tyrosine kinase Src (Figure 1.6 A). Indeed, APPL1 decreases Src-mediated tyrosine phosphorylation of Akt, and this Akt activation is necessary for migration. As a result, APPL1-GFP-expressing cells exhibit slower migration due to impaired turnover of leading edge adhesions (Figure 1.7) (Broussard et al., 2012).

Several studies suggest that APPL1 is involved in integrin trafficking, which is critical for cell adhesion and migration. In endothelial cells, GIPC1 interaction with the glycoprotein Nrp1 was shown to promote internalization of active α5β1 integrin into Rab5-positive vesicles, which is then recycled to the cell surface near adhesion sites (Valdembri et al., 2009) (Figure 1.6 B). This is crucial for cell adhesion to the extracellular matrix protein fibronectin as well as fibronectin fibrillogenesis. Because APPL1 interacts with both GIPC1 and Rab5, Valdembri et al. suggest that APPL1 is involved in this pathway (Figure 1.6 B) (Valdembri et al., 2009). Future studies are needed to determine the importance of APPL1-dependent regulation of integrin internalization for cell migration.

More recently, APPL1 was implicated in the regulation of integrin trafficking in Arf6-mediated adhesion and migration. Arf6 has been paradoxically shown to both increase and decrease cell adhesion by accelerating integrin recycling and by increasing integrin internalization, respectively. Chen et al. (2014) demonstrated that these opposite effects on integrin trafficking and focal adhesion size are accomplished by spatially separating two Arf6 GAPs, namely ARAP2 and ArfGAP with Coiled-Coil, Ankyrin Repeat and PH Domains 1 (ACAP1) (Chen et al., 2014). ACAP1 was shown to promote recycling of integrins, while ARAP2 instead decreases integrin recycling (Figure 1.6 C). ARAP2 colocalizes with Arf6 and APPL1 in distinct structures that are separate from ACAP1/Arf6 recycling endosomes.

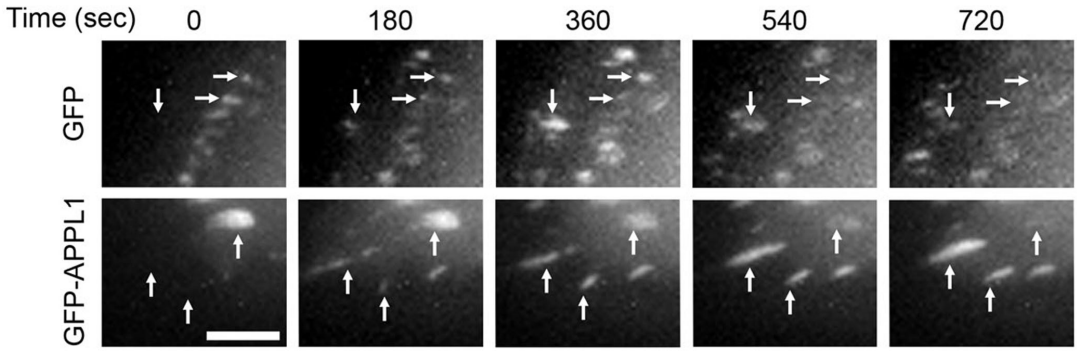

Figure 1.7. APPL1 impairs adhesion turnover at the leading edge of cells. HT1080 cells were cotransfected with mCherry-paxillin and either GFP or GFP-APPL1 and imaged using time-lapse microscopy. In GFP-APPL1–expressing cells, the leading edge adhesions assemble and disassemble more slowly than those in control cells expressing GFP (arrows). Scale bar, 5 μm.

Figure reprinted from (Broussard et al., 2012).

Knockdown of ARAP2 enhances trafficking of β1 integrin, and reduces β1 integrin transit from APPL1 to EEA1 vesicles (Figure 1.6 C), whereas overexpression of ARAP2 leads to an increase in adhesion size. The former phenotype has been also reported for cells overexpressing APPL1 (Chen et al., 2014). It is plausible that impaired trafficking of integrins by ARAP2 would favor adhesions that turn over more slowly. Since APPL1 has been shown to reduce adhesion turnover (Broussard et al., 2012), it is tempting to speculate that APPL1 and ARAP2 are both involved in this process. On the other hand, ACAP1, which promotes integrin recycling, localizes to an APPL1-negative Arf6 compartment that has a different effect on Arf6-mediated cell adhesion. Interestingly, an inhibition of Akt prevents ACAP1-mediated integrin recycling (Li et al., 2005). As APPL1 downregulates Akt activation during cell migration, this could mean that APPL1 promotes ARAP2 activity by inhibiting ACAP1.

Studies focusing on APPL1 in the context of cell migration are only beginning to emerge, and thus, much remains to be learned. However, multiple proteins that interact with APPL1 have been implicated in cell migration, and could represent feasible mechanisms for APPL1-mediated cell migration. For instance, Rab5, in addition to its roles in regulating early endosome dynamics, is known to promote cell migration in a number of ways (Torres and Stupack, 2011). Rab5 localizes to the leading edge of migrating cells and promotes lamellipodia formation (Palamidessi et al., 2008; Torres and Stupack, 2011). Mechanistically, Rab5, downstream of Caveolin-1, promotes activation of the GTPase Rac by recruiting the GEF Tiam1 (Diaz et al., 2014a; Lanzetti et al., 2004; Palamidessi et al., 2008). APPL1 signaling endosomes could therefore be important for coordinating the signals leading to Rac activation. Moreover, Rab5 localizes to focal adhesions (Torres et al., 2010), associates in a complex with focal adhesion proteins vinculin and paxillin, and also promotes focal adhesion disassembly (Mendoza et al.,

2013). There is already evidence for the role of APPL1 in focal adhesion turnover (Broussard et al., 2012); therefore, the interaction between APPL1 and Rab5 might be important for focal adhesion dynamics. APPL1 also interacts with Rab21, a poorly studied Rab protein involved in the endocytic pathway. Rab21 associates with and controls trafficking of integrins to regulate cell migration (Pellinen et al., 2006). Since APPL1 has already been shown to bind to Rab5 and Rab21 (Chen et al., 2014; Torres and Stupack, 2011; Zhu et al., 2007), APPL1 may also be involved in Rab21-mediated integrin trafficking.

Future directions for APPL1

APPL1 is an important adaptor protein for coordinating both signaling and trafficking events within cells in order to regulate processes such as cell migration and adhesion. Although the role of APPL1 in signaling and trafficking has been well characterized, future studies are needed to understand the complexity of APPL1 endosome formation and exchange and/or maturation with other Rab5-positive endosomes, and how this affects signaling on endosomes. A number of intriguing questions still remain. What is the importance of the ability of APPL1 to bind to unphosphorylated tyrosine residues? Is it to prevent signaling until the bound protein is released from the APPL1 compartment? Are there other receptors or signaling proteins that interact with APPL1? How does APPL1 mediate signaling specificity to coordinate multiple signaling pathways?

Studies focusing on APPL1 in the context of cell migration are only beginning to emerge, and thus, much remains to be learned. However, multiple proteins that interact with APPL1 have been implicated in cell migration, and could represent feasible mechanisms for APPL1-mediated cell migration. For instance, Rab5, in addition to its roles in regulating early endosome dynamics, is known to promote cell migration in a number of ways (Torres and Stupack, 2011).

Rab5 localizes to the leading edge of migrating cells and promotes lamellipodia formation (Palamidessi et al., 2008; Torres and Stupack, 2011). Mechanistically, Rab5, downstream of Caveolin1, promotes activation of the GTPase Rac by recruiting the guanine nucleotide exchange factor (GEF) Tiam1 (Diaz et al., 2014a; Lanzetti et al., 2004; Palamidessi et al., 2008). APPL1 signaling endosomes could therefore be important for coordinating the signals leading to Rac activation. Moreover, Rab5 localizes to focal adhesions (Torres et al., 2010), associates in a complex with focal adhesion proteins vinculin and paxillin, and also promotes focal adhesion disassembly (Mendoza et al., 2013). There is already evidence for the role of APPL1 in focal adhesion turnover (Broussard et al., 2012); therefore, the interaction between APPL1 and Rab5 might be important for focal adhesion dynamics. APPL1 also interacts with Rab21, a poorly studied Rab protein involved in the endocytic pathway. Rab21 associates with and controls trafficking of integrins to regulate cell migration (Pellinen et al., 2006). Since APPL1 has already been shown to bind to Rab5 and Rab21 (Chen et al., 2014; Torres and Stupack, 2011; Zhu et al., 2007), APPL1 may also be involved in Rab21-mediated integrin trafficking.

The integration of signaling and trafficking through adaptor proteins, such as APPL1, is an intriguing area of research that is still not well understood. Signaling specificity and crosstalk between multiple signaling pathways are complex, and studying APPL1 may provide a greater understanding into how signaling is controlled. Further studies into APPL1 will lend insight in the molecular mechanisms underlying trafficking and signaling, as well as cell migration and adhesion.

Hypothesis

Cell migration is spatiotemporally regulated and requires the coordination of many molecular components. Adaptor proteins serve as integrators of various cellular events and thus

are being increasingly studied as regulators of cell migration. This thesis explores the role of the adaptor protein APPL1 in regulating signaling and trafficking events during cell migration. APPL1 interacts with multiple proteins with various functions in cell migration, such as Rab5, GIPC1, and Akt. However, the role of APPL1 in cell migration is still poorly understood. Rab5 is a critical regulator of cell migration through integrin trafficking and Rac signaling. As a signaling adaptor protein, APPL1 mediates crosstalk between multiple cellular pathways. In this thesis, I test the hypothesis that APPL1 regulates cell migration by coordinating signaling and trafficking pathways, namely Rac activation and integrin trafficking, through its interaction with Rab5.

CHAPTER II

α5β1 INTEGRIN TRAFFICKING AND RAC ACTIVATION ARE REGULATED BY APPL1 IN A RAB-5 DEPENDENT MANNER TO INHIBIT CELL MIGRATION

Nicole L. Diggins[1*], Hakmook Kang[2], Alissa Weaver[3,4,5], and Donna J. Webb[1,5,6#]

[1]Department of Biological Sciences, Vanderbilt University, Nashville, TN 37232
[2]Department of Biostatistics, Vanderbilt University School of Medicine, Nashville, TN 37232
[3]Department of Cell and Developmental Biology, Vanderbilt University School of Medicine, Nashville, TN 37232
[4]Department of Pathology, Microbiology, and Immunology, Vanderbilt University Medical Center, Nashville, TN 37232
[5]Department of Cancer Biology, Vanderbilt University School of Medicine, Nashville, TN 37232
[6]Vanderbilt Kennedy Center, Vanderbilt University Medical Center, Nashville, TN 37232

[*]Correspondence to Nicole L. Diggins: email: nicole.l.diggins@gmail.com; mailing address: VU station B, Box 35-1634, Nashville, TN 37235; phone: 615-343-9031; fax: 615-343-6707

[#]deceased

This article has been accepted for publication under the same title in the *Journal of Cell Science*. Accepted for publication January 9, 2018.

Summary

Coordination of signaling and trafficking pathways is critical for cell migration. Here, we show that the endosomal adaptor protein APPL1 regulates α5β1 integrin and Rac activity through the GTPase Rab5.

Abstract

Cell migration is a tightly coordinated process that requires the spatiotemporal regulation of many molecular components. Because adaptor proteins can serve as integrators of cellular events, they are being increasingly studied as regulators of cell migration. The adaptor protein containing a pleckstrin-homology (PH) domain, phosphotyrosine binding (PTB) domain, and leucine zipper motif 1 (APPL1) is a 709-amino acid endosomal protein that plays a role in cell proliferation and survival as well as endosomal trafficking and signaling. However, its function in regulating cell migration is poorly understood. Here, we show that APPL1 hinders cell migration by modulating both trafficking and signaling events controlled by Rab5 in cancer cells. APPL1 decreases internalization and increases recycling of α5β1 integrin, leading to higher surface levels of α5β1 integrin that hinder adhesion dynamics. Furthermore, APPL1 decreases the activity of the GTPase Rac and its effector PAK, which in turn regulate cell migration. Thus, we demonstrate a novel role for the interaction between APPL1 and Rab5 in governing crosstalk between signaling and trafficking pathways on endosomes to affect cancer cell migration.

Introduction

The establishment of cell polarity requires vesicular trafficking of proteins to distinct cellular locations, which is critical for cell migration (Jacquemet et al., 2013b; Maritzen et al., 2015). Cell migration is marked by four key steps: [1] extension of an actin-rich protrusion, [2]

establishment of cell-matrix adhesions, [3] translocation of the cell body, and [4] retraction of the cell rear (Borisy and Svitkina, 2000; Ridley, 2011; Ridley et al., 2003). Each step requires spatiotemporal regulation of protein transport. For example, adhesions, which link the ECM to the actin cytoskeleton, must continuously assemble and disassemble—a process termed adhesion turnover— for cells to migrate efficiently (Broussard et al., 2008; Lock et al., 2008; Vicente-Manzanares and Horwitz, 2011; Wehrle-Haller, 2012). Trafficking of key adhesion proteins, particularly integrins, through the early endocytic pathway is emerging as an important mechanism for regulating adhesion dynamics (Paul et al., 2015b).

Integrins are constitutively endocytosed and recycled back to the cell surface of migrating cells (Bretscher, 1989; Bretscher, 1992; Caswell and Norman, 2006; Lawson and Maxfield, 1995). Integrin trafficking is spatiotemporally regulated to target integrins to adhesions (Caswell and Norman, 2006) and regulate adhesion turnover (Chen et al., 2014; Mendoza et al., 2013; Pellinen et al., 2006). The internalization and recycling of integrins through the endocytic pathway have been intensely studied (Caswell et al., 2007; Dozynkiewicz et al., 2012; Lobert et al., 2010; Tiwari et al., 2011; White et al., 2007), yet there are still questions remaining as to which endocytic proteins are involved in this process. Rab5 is considered to be a master regulator of early endocytic events, controlling cargo recruitment, fusion, and motility of early endosomes (van der Bliek, 2005). In addition, Rab5 promotes cell migration by regulating vesicular trafficking and localization of proteins involved in migration (Mendoza et al., 2014; Torres and Stupack, 2011). Intriguingly, Rab5 associates with focal adhesion proteins and α and β integrins and promotes the disassembly of adhesions, potentially by promoting the internalization of integrins (Mendoza et al., 2013; Pellinen et al., 2006). Moreover, Rab5-mediated trafficking regulates signaling events, as Rab5-dependent endocytosis has been shown

to activate the small GTPase Rac on endosomes through the GEF Tiam1 (Diaz et al., 2014a; Palamidessi et al., 2008; Torres et al., 2010). Active Rac associates with effectors, including PAK, to promote actin polymerization (Szczepanowska, 2009). Re-localization of active Rac to the leading edge by Rab5 induces the forward protrusion of the membrane necessary for migration (Palamidessi et al., 2008). Through its regulation of trafficking events, Rab5 promotes tumor cell invasion and metastasis (Christoforides et al., 2012; Kawauchi, 2012; Mendoza et al., 2014; Torres and Stupack, 2011), further suggesting that endocytic trafficking through Rab5 is important for regulating cell migration.

While Rab5 is known to induce cell migration through endocytic trafficking, the effectors in this process are not well understood. The adaptor protein containing a pleckstrin-homology (PH) domain, phosphotyrosine binding (PTB) domain, and leucine zipper motif 1 (APPL1) is a 709-amino acid protein that localizes to early endosomes (Li et al., 2007) and interacts with Rab5 (Zhu et al., 2007). APPL1 is composed of several domains. The N-terminal Bin-Amphiphysin-Rvs (BAR) domain allows APPL1 to form homodimers or heterodimers with APPL2 (Chial et al., 2010; Zhu et al., 2007). The central pleckstrin homology (PH) domain binds phosphoinositol lipids and may be partially responsible for association of APPL1 with endosomal membranes (Li et al., 2007; Zhu et al., 2007). The BAR and PH domains interact to form a functional BAR-PH domain that mediates the binding of Rab5 (Zhu et al., 2007). The C-terminal phosphotyrosine-binding (PTB) domain binds signaling proteins including Akt (Mitsuuchi et al., 1999; Schenck et al., 2008) and a variety of receptors (Deepa and Dong, 2009; Lin et al., 2006; Liu et al., 2002; Varsano et al., 2012). The SEA motif on the C-terminus of APPL1 binds to GIPC1 (Lin et al., 2006), a protein involved in loading cargoes onto vesicles (Aschenbrenner et al., 2003), suggesting a role for APPL1 in cellular trafficking.

APPL1 mediates cellular functions including cell survival, cell growth, and proliferation (Miaczynska et al., 2004; Schenck et al., 2008; Tan et al., 2010). Interestingly, APPL1 has also been implicated in cell migration (Diggins and Webb, 2017). Our group has previously shown that APPL1 expression hinders cell migration by reducing Akt activation, thereby impairing adhesion turnover (Broussard et al., 2012). In addition, studies employing a genetic approach show that both APPL1 and APPL2 are necessary for hepatocyte growth factor (HGF)-induced migration of murine embryonic fibroblasts (MEFs) (Tan et al., 2016; Tan et al., 2010). A recent study demonstrated that a subset of Arf6 compartments that co-localizes with APPL1 mediates recycling of β1 integrins, suggesting that APPL1 may be involved in integrin trafficking (Chen et al., 2014). Whether APPL1 is directly involved in the regulation of integrin trafficking or merely present on compartments containing integrins is currently unknown.

In this study, we demonstrate that APPL1 decreases the rate of α5β1 integrin internalization and increases the rate of recycling to promote higher surface levels of integrin. In addition, APPL1 decreases activation of Rac and its effector PAK in a Rab5-dependent manner. Therefore, we have identified a new mechanism by which APPL1 modulates migration via α5β1 integrin trafficking and Rac signaling, mediated by Rab5.

Materials and Methods

Plasmids

APPL1-GFP was prepared by cloning full-length APPL1 cDNA into pEGFP-C3 and mCherry-C3 vector as previously described (Broussard et al., 2012). APPL1-N308D-GFP and APPL1-N308D-mCherry were generated via site-directed mutagenesis of full-length APPL1-GFP and APPL1-mCherry, respectively, by the QuickChange II kit (Agilent Technologies, Santa Clara, CA) using the following primers to mutate residue N308 to aspartic acid: 5’-

ACTTCACGCAGGGTGGAGATTTAATGAGTCAGGCC-3' and 5'-GGCCTGACTCATTAAATCTCCACCCTGCGTGAAGT-3'. APPL1-AAA-GFP and APPL1-ΔPTB-GFP were prepared as previously described (Broussard et al., 2012). Rab5-mCherry was a kind gift from Jim Goldenring (Vanderbilt University, Nashville, TN). Rab5-L38R-mCherry was made by site-directed mutagenesis of full-length Rab5-mCherry using the following primers to mutate residue L38 to arginine: 5'-GGCCTTTCACAAAACGACGCACTAGGCTTGATTTG-3' and 5'-CAAATCAAGCCTAGTGCGTCGTTTTGTGAAAGGCC-3'. Constitutively active PAK (PAK1-T423E) was generously provided by Jonathon Chernoff (Fox Chase Cancer Center, Philadelphia, PA). mCherry-paxillin was kindly provided by Steve Hanks (Vanderbilt University, Nashville, TN.) α5-PA-GFP was a kind gift from Jim Norman (Beatson Institute for Cancer Research, Glasgow, Scotland, UK). TfnR-PA-mCherry was a gift from Vladislav Verkhusha (Addgene plasmid #31948). siGENOME siRNA SMARTpool for APPL2 (M-016272-01-0005) and non-targeting control (D-001206-14-05) were ordered from Dharmacon (Horizon Discovery). Clustered regularly interspaced short palindromic repeats (CRISPR) plasmids were obtained from ALSTEM (Richmond, CA). Three different guide RNAs were designed to target exon 2 of APPL1 and were inserted into PX459 vector. The guide RNA sequences are as follows:

gRNA1, 5'-GCATCGGATTTATGATGCACAGG-3'

gRNA2, 5'- GATGCATAGCTTGATACAACTGG-3'

gRNA3, 5'- AGTTGTATCAAGCTATGCATCGG-3'

A non-targeting guide RNA (5'-GTGGATTTGGTAATGCAGA-3') in the PX459 vector was used as a control.

Antibodies and reagents

Primary antibodies used were as follows: mouse anti-β actin (clone AC15, Sigma-Aldrich, St. Louis, MO, 1:5000 for WB), rabbit anti-APPL1 (21st Century Biochemicals, Malbaro, MA), mouse anti-APPL2 (clone F-2, Santa Cruz Biotechnology, Dallas, TX), mouse anti-integrin α5 (clone SNAKA51, EMD Millipore, Billerica, MA), mouse anti-integrin α5 (clone 6F4, a kind gift from Rick Horwitz, Allen Institute for Cell Science, Seattle, WA), mouse anti-active integrin β1 (clone 12G10, Abcam, Cambridge, UK), mouse anti-integrin β1 (clone P5D2, Abcam), rabbit anti-integrin β1 (AB1952, MilliporeSigma), rabbit anit-integrin β3 (ERP17507, Abcam), mouse anti-FLAG (clone M2, Sigma-Aldrich, 1:500 for WB), rabbit anti-phospho-T423-PAK (#2601, Cell Signaling Technology, Danvers, MA), rabbit anti-phospho-S199-PAK (#2605, Cell Signaling Technology), rabbit anti-PAK1/2/3 (#2604, Cell Signaling Technology), rabbit anti-Rab5 (#3547, Cell Signaling Technology). Primary antibodies were diluted 1:500 for IF and 1:1000 for WB, unless noted otherwise. For function blocking experiments, mouse anti-integrin α5 (clone P1D6, Millipore) and mouse anti-integrin αV (clone 272-17E6, Abcam) were used. Mouse IgG (#0107-01) was purchased from Southern Biotech (Birmingham, AL) and was used as a control in these experiments. For IF staining, Alexa Fluor® 488 goat anti-mouse, 488 donkey anti-rabbit, 555 goat anti-rabbit, 555 donkey anti-mouse, 647 goat anti-rabbit, and 647 goat anti-mouse secondary antibodies were used at 1:1000 dilution (Thermo Fisher Scientific, Waltham, MA). For WB, Alexa Fluor® 680 donkey anti-mouse or goat anti-rabbit (Thermo Fisher Scientific) and IRDye800® donkey anti-mouse or goat anti-rabbit (Rockland, Inc., Limerick, PA), anti–mouse HRP-conjugated IgG (Rockland Immunochemicals) and anti–rabbit HRP-conjugated IgG (Promega) secondary antibodies were used. Fibronectin (FN; #F0895), puromycin (#P7255), and primaquine bisphosphate (#160393) were purchased from Sigma-

Aldrich. Rat-tail type I Collagen I (ColI) was purchased from BD Biosciences (San Jose, CA). RGD and RGE peptides were from Bachem (Bubendorf, Switzerland).

Cell Culture and Transfection

HT1080 cells were maintained in Dulbecco's Modified Eagle's Medium (DMEM; Life Technology, Carlsbad, CA) supplemented with 10% fetal bovine serum (FBS) and penicillin–streptomycin. MDA-MB-231 cells were maintained in Roswell Park Memorial Institute medium (RPMI) 1640 with 10% FBS and penicillin–streptomycin. Cells were transfected with Lipofectamine® 2000 (Thermo Fisher Scientific) per the manufacturer's instructions. For APPL2 knockdown, 50 nM of either APPL2 or non-targeting siRNA pool was transfected into HT1080 cells using DharmaFECT 1 transfection reagent (Horizon Discovery), following the manufacturers' protocols. For migration assays and imaging experiments, GFP-postive (or mCherry-positive) cells were chosen for analysis. For bulk biochemical assays, all cells were used.

3D Cell Culture

Rat-tail ColI was mixed to a final concentration of 1.5mg/ml in PBS and neutralized with NaOH (23µl x volume of ColI solution) on ice. Cells were trypsinized and resuspended in DMEM (200,000 cells/ml). 500µl of collagen solution was mixed with 500µl of cell suspension and plated in 6-well cell culture dishes. Gels were allowed to solidify for 30 minutes at 37°C, and then 2ml DMEM was added to the gels. Subsequently, gels were incubated at 37°C for 24 hours to allow cells to attach and extend protrusions. 3D gels with embedded cells were used in migration assays.

Microscopy

A Quorum WaveFX spinning disk confocal system equipped with a Nikon Eclipse Ti microscope and a Hamamatsu ImagEM-CCD camera was used for imaging of IF-stained coverslips, photoactivation experiments, and 3D migration assays. An Apo TIRF 60x objective (NA 1.49) was used for imaging photoactivation experiments and IF-stained coverslips. A Nikon 10X Ph1 ADL objective (NA 0.25) was used to image 3D cell migration assays. DAPI, Alexa Fluor® 488, Alexa Fluor® 555, and Alexa Fluor® 647 were excited by the laser lines at 405 nm, 491 nm, 561 nm, and 642 nm, respectively (Semrock, Rochester, NY). Emission filters for these fluorophores were 460/50, 525/50, 593/40 or 620/60, and 700/75, respectively (Semrock). TIRF microscopy and 2D migration assays were performed using an inverted Olympus IX71 microscope (Melville, NY) with a Retiga EXi CCD camera (QImaging, Surrey, BC). An Olympus UPlanFl N 10X objective (NA 0.30) was employed for cell migration assays. TIRF images were taken using an Olympus PlanApo 60X OTIRFM objective (NA 1.45) with a 543-nm laser line from a HeNe laser (Prairie Technologies, Middleton, WI). Images were acquired and analyzed using MetaMorph software (Molecular Devices, Sunnyvale, CA). Images from TIRF and photoactivation experiments were run through a 3 x 3 median filter using MetaMorph software to remove background.

Migration Assays

Cell culture dishes were coated with either 2.5μg/ml FN or 5μg/ml rat tail ColI in PBS for 1 hour at 37°C, after which cells were plated and permitted to adhere for 1 hour at 37°C in cell culture media. Cells were kept at 37°C in SFM4MAb^{TM} media (HyClone, Logan, UT) supplemented with 2% FBS at pH 7.4 (imaging media) during imaging using phase contrast microscopy. Images were acquired at 5-minute intervals for 6 hours, using MetaMorph software. For 3D

migration assays, the media was changed to imaging media after 24 hours and cells were imaged. Migration was assessed for cells at least 100μm deep into the gel to ensure that cells were in a 3D environment. For both 2D and 3D migration assays, cell movement was tracked from time-lapse images using MetaMorph, and migration speed was calculated by dividing the total distance moved in microns by the time. Persistence and directionality was quantified using an Excel Macro described by Gorelik and Gautreau (2014). Wind-Rose plots were generated by transposing *x*, *y* coordinates of cell tracks to a common origin.

Immunofluorescence

For most experiments, cells were plated onto glass coverslips coated with 2.5μg/ml FN or 5μg/ml rat tail ColI and allowed to adhere for one hour at 37°C. Cells were fixed using 4% paraformaldehyde supplemented with 0.12M sucrose in PBS for 15 minutes at room temperature. Following fixation, cells were permeabilized with 0.2% (v/v) Triton X-100 for 3 minutes. Blocking was performed using 20% goat serum in PBS. Primary and secondary antibodies were diluted in 5% goat serum with 0.2% (v/v) Triton X-100 and were incubated with the cells at 4°C overnight or 45 minutes at room temperature, respectively. Following each antibody step, coverslips were washed with PBS extensively. Alexa Fluor® 647 phalloidin (#A22287, Thermo Fisher Scientific) co-stains were performed along with secondary antibodies. Coverslips were mounted on glass slides using Aqua Poly/Mount (Polysciences, Inc., Warrington, PA). For TIRF experiments, cells were plated on FN-coated glass bottom dishes, stained as described above, and kept submerged in PBS instead of mounted slides with Aqua Poly/Mount.

The average fluorescence intensity was quantified by dividing the background-corrected, integrated fluorescence intensity of individual cells by the cell unit area using MetaMorph software. For colocalization analysis, images were background subtracted, a 3 x 3 median filter

was applied, and colocalization was measured as the percent overlap between the two channels.

Photoactivation

Cells were co-transfected with α5-PA-GFP and either mCherry or APPL1-mCherry (or TfnR-PA-mCherry and either GFP or APPL1-GFP), plated on FN-coated, glass bottom dishes, and maintained in imaging media. A circular region of interest (ROI) at the edge of the cell was subjected to photoactivation using a 405-nm diode laser for a 500-millisecond pulse with 100% laser power. For some experiments, APPL1 gRNA#3 or NT gRNA cells were transfected with mCherry-paxillin, and adhesions were chosen as ROIs. Following photoactivation, images were taken every 10 seconds for 6 minutes using MetaMorph software. Images were taken before photoactivation to provide reference images. To analyze the kinetics of signal loss in the ROI, the average fluorescence intensity of the ROI was quantified for each time point and normalized to the average fluorescence intensity of the ROI from the first image post-photoactivation.

Antibody Internalization and Recycling Assays

Internalization assay: Cells were plated on FN-coated coverslips and allowed to adhere for 1 hour at 37°C. The cell surface was labeled by incubating with the appropriate antibody diluted 1:500 in PBS at 4°C for 45 minutes. Cells were washed with PBS, cell culture media was added, and cells were returned to 37°C for 0-60 minutes to allow internalization. Cell surface labeling was removed by a wash with acetic acid, pH 2.5, on ice, for 5 minutes. Cells were fixed and stained with secondary antibodies as described above. The average fluorescence intensity for each time point was expressed as a percent of the maximum intensity measured per experiment (set to 100%), and the initial value was set to zero by subtracting the average fluorescence intensity at the 0 minute time point from each value. In some experiments, cells were treated with 0.6μM primaquine, a recycling inhibitor.

For visualizing internal levels of Transferrin Receptor (TfnR), cells were allowed to adhere for 1 hr, and then 25μl/ml pHrodo® Red Transferrin conjugate (Thermo Fisher Scientific) was added to cell culture media for the indicated time points. Coverslips were fixed and mounted as described for immunofluorescence.

Recycling assay: Cells were initially treated as described above for the internalization assay. Internalization was allowed to proceed for 30 minutes at 37°C in the presence of primaquine and cells were acid washed as described above. Cells were returned to 37°C in cell culture media (without primaquine) for 0-20 minutes, acid washed, and immunostained as described above. Recycling was quantified as a percent of the original internal pool remaining at each time point, subtracted from the signal observed immediately following the first acid wash (where neither internalization nor recycling has occurred). The original internal pool was defined as the average fluorescence intensity at the 0-minute time point (where internalization, but not recycling has occurred).

Western blot

The cells were lysed using RIPA buffer (25mM Tris-HCl, pH 7.6, 150mM NaCl, 1% NP-40, 1% sodium deoxycholate, 0.1% SDS) with protease inhibitor cocktail (Sigma-Aldrich). Protein concentration in the cell lysates was measured by the bicinchoninic acid (BCA) assay (BioRad Laboratories, Hercules, CA). 40 μg of each cell lysate was run in an SDS-PAGE gel and transferred to a nitrocellulose membrane. The membrane was incubated with the primary antibody diluted in 5% (m/v) non-fat dry milk in Tris-buffered saline, 0.1% (v/v) Tween 20 (TBS-T) at 4°C overnight, then incubated with the secondary antibody for 45 minutes at room temperature. Membranes were imaged using the Odyssey CLx imaging system (LI-COR Biosciences, Lincoln, NE). For phosphorylated PAK WB, cell lysates were then prepared with

addition of PhosSTOP phosphatase inhibitor cocktail (MilliporeSigma) to the lysis buffer. HRP-conjugated secondary antibodies were used and detected with SuperSignal West Femto maximum sensitivity substrate kit (Thermo Fisher Scientific) via an Amersham Imager 600 (GE Healthcare). Band intensities were measured using Image Studio Lite Software version 4 (LI-COR Biosciences) and normalized to a β -actin loading control.

Biotinylation Internalization and Recycling Assay

Internalization assay: HT1080 cells were transfected in with the indicated constructs and after six hours, the media was changed to serum-free DMEM overnight. Per condition, $2.5x10^5$ cells were plated in each well of a 6-well plate, grown to approximately 80% confluency, and then transfected with the indicated constructs. Cells were cooled with PBS for 45 minutes on ice to stop internalization. The cell surface was labeled with NHS-SS-Biotin (Thermo Fisher Scientific) at 4°C for 30 minutes. The biotinylation reaction was terminated by two five-minute washes with 0.1M glycine in PBS. For internalization, cells were washed PBS, cell culture media with 0.6μM primaquine was added, and cells were returned to 37°C for 0-60 minutes to allow internalization. Cell surface biotin was removed (except for total surface level condition) by two washes with 50 mM TCEP (Thermo Fisher Scientific) in NT buffer (150 mM NaCl, 1.0 mM EDTA, 0.2% BSA, 20 mM Tris, pH 8.6). Cells were lysed as described above and lysates were incubated with streptavidin agaorse beads (Thermo Fisher Scientific) at 4°C overnight. Beads were washed with RIPA buffer three times and protein was eluted with 5x sample buffer for 30 minutes, followed by Western Blot analysis.

Recycling assay: Cells were initially treated as described above for the internalization assay. One well in a 6-well plate was used for each condition. Internalization was allowed to proceed for 60 minutes at 37°C in the presence of primaquine and cells were washed with 50 mM TCEP as

described above. Cells were returned to 37°C in cell culture media (without primaquine) for 0-10 minutes, cell surface biotin was removed with 50 mM TCEP, and biotin was pulled down as described above. Recycling was quantified as a percent of the original internal pool (the 0-minute time point, where internalization, but not recycling has occurred) remaining at each time point.

Active Rac Pulldown Assay

Cells plated on cell culture dishes coated with 2.5μg/ml FN or 5μg/ml rat tail ColI were transfected with FLAG-Rac1 and indicated constructs. After 24h, cells were lysed and assayed for active Rac as previously described (Bristow et al., 2009; Ren et al., 1999). In brief, lysates were incubated with glutathione sepharose beads coated with GST-tagged p21 binding domain (PBD) from the Rac effector PAK to facilitate specific pull down of the active form of Rac. Whole cell lysates (total Rac) and pulldown samples (active Rac) were loaded on the same gel and immunoblotted for FLAG and β-actin.

Data analysis and statistics

Statistical analysis was performed using SPSS software version 24. p-values were determined using either a Student's t-test (if comparing two means), or a one-way ANOVA followed by Tukey's post hoc test (if comparing more than two means), unless otherwise noted. In figures, *, $p<0.05$, **, $p<0.005$, and ***, $p<0.0005$, as indicated (unless otherwise noted), and these were designated as statistically significant. Bar graphs were generated using Microsoft Excel and presented as the mean ± s.e.m. of at least three independent experiments. Box and whisker plots were generated using GraphPad Prism version 7.02 (GraphPad Software, La Jolla, CA). The box ranges from 25-75th percentile, the line indicates the median, and whiskers indicate the minimum and maximum values.

Results

The endosomal protein APPL1 is a negative regulator of cell migration

To begin investigating the role of APPL1 in cell migration, HT1080 fibrosarcoma cells were transfected with constructs expressing either APPL1-GFP or GFP, plated on fibronectin (FN)-coated cell culture dishes, and migration assays were performed. APPL1-GFP was overexpressed approximately 2.8-fold over endogenous (Figure 2.1 A). We observed that APPL1-GFP-expressing cells migrated significantly shorter distances, compared to control (Figure 2.1 B), suggesting that APPL1 inhibits cell migration. Quantification of the migration speed showed a 1.4-fold decrease in APPL1-GFP-expressing cells compared to control (Figure 2.1 C). Notably, analysis of mean squared displacement (MSD) showed that APPL1-GFP-expressing cells explored significantly less area than GFP-expressing cells (Figure 2.1 D). This difference in MSD is likely due to the decrease in migration speed, as cells expressing APPL1-GFP showed no difference in persistence, quantified as the distance traveled divided by the total path travelled (Figure 2.1 E). Additionally, direction autocorrelation was calculated as an unbiased measure of directionality by compensating for differences in speed (Gorelik and Gautreau, 2014), and showed no difference between APPL1-GFP- and GFP-expressing cells (Figure 2.1 F). To determine whether this effect is specific to HT1080 cells or represents a more general mechanism, we also performed migration assays with MDA-MB-231 cells. As with HT1080 cells, expression of APPL1-GFP in MDA-MB-231 cells led to significantly shorter migration distances (Figure 2.2 A) and a 2.7-fold decrease in speed compared to control (Figure 2.2 B). Moreover, MDA-MB-231 cells expressing APPL1-GFP had decreased MSD (Figure 2.2 C), but no change in persistence (Figure 2.2 D) or directionality (Figure 2.2 E), compared to control. To examine the effects of APPL1 on migration in a more *in vivo*-like environment, we performed

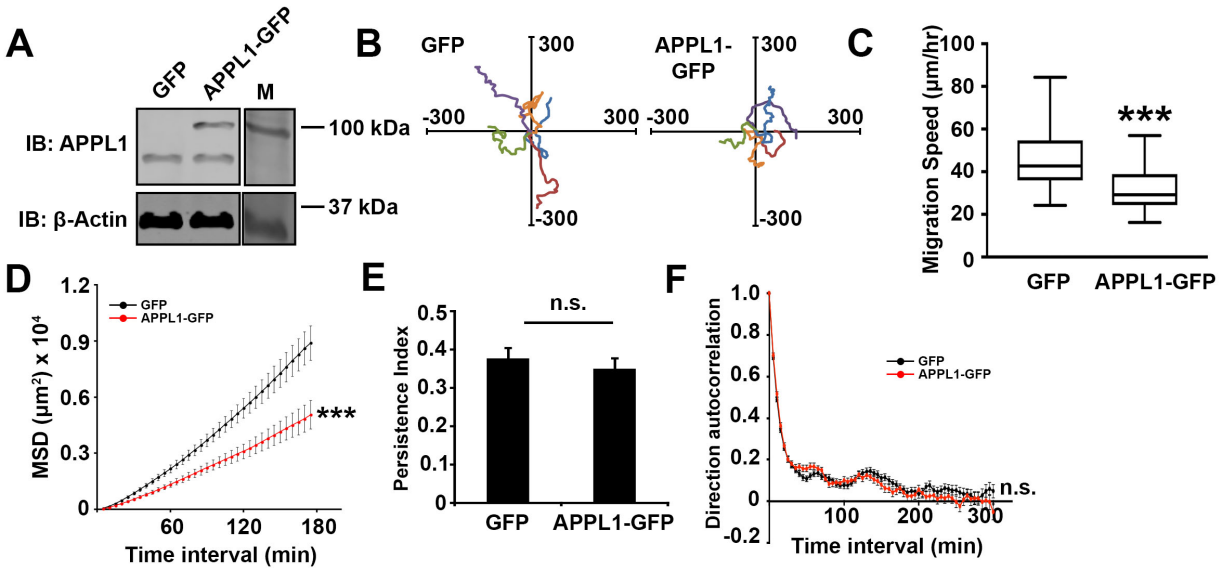

Figure 2.1. APPL1 overexpression decreases cell migration. (A) Lysates derived from cells expressing GFP or APPL1-GFP were subjected to immunoblot analysis for levels of APPL1 and β-Actin (loading control). A representative image is shown. M, molecular weight marker; kDa, Kilodaltons. (B) Migration was quantified for individual cells expressing either GFP or APPL1-GFP. Rose plots show individual tracks of representative cells from each condition. (C) Box plot showing migration speeds for GFP- and APPL1-GFP-expressing cells. 59-66 cells total were analyzed from each condition from at least three experiments. (D-F) MSD (D) persistence index (E) and directional autocorrelation analysis (F) of HT1080 cells expressing GFP or APPL1-GFP. Error bars represent s.e.m. from 44-46 cells total from each condition from at least three separate experiments. (***, $p<0.0001$, comparing slopes of the lines using a likelihood ratio test (D), n.s., not significant, $p=0.48$, determined by Student's t-test (E), $p=0.353$, determined by mixed effects model to compare the curves, with controlling false discovery rate (FDR) at 0.1 (F)). All box plots range from the 25-75th percentile, the line indicates the median, and whiskers show the minimum and maximum.

migration assays in 3D collagen I (ColI) gels. HT1080 cells expressing APPL1-GFP or GFP were embedded in ColI gels supplemented with FN and allowed to adhere overnight. Similar to 2D migration, APPL1-GFP-expressing cells migrated approximately 1.5-fold slower than cells expressing GFP in 3D matrices (Figure 2.2 F), and exhibited decreased MSD (Figure 2.2 G). However, there was no change in persistence (Figure 2.2 H) or directionality (Figure 2.2 I) between GFP and APPL1-GFP-expressing cells in 3D matrices. Together, these data indicate a role for APPL1 in modulating cell migration.

To explore further the role of APPL1 in regulating cell migration, we used the CRISPR/Cas9 system to generate frame shift mutations in APPL1. HT1080 cells were transfected with plasmids expressing Cas9 and one of three different guide RNAs (gRNA) or a non-targeting (NT) gRNA as a control. Cells containing the plasmid were selected by puromycin resistance, which resulted in a mixed population of cells with various insertions/deletions (INDELs) in the APPL1 gene. As anticipated, cells expressing each gRNA (APPL1 gRNA#1-3) showed an ~85-90% reduction in APPL1 expression, compared to NT gRNA-expressing cells, indicating that the CRISPR/Cas9 system was effective for greatly diminishing APPL1 expression (Figure 2.3 A,B). Migration assays were performed using APPL1 gRNA-expressing cells or control cells. APPL1 gRNA-expressing cells had longer migration paths compared to control cells (Figure 2.3 C). APPL1 gRNA#1 led to approximately 1.3-fold increase in migration speed, while APPL1 gRNA#2 and APPL1 gRNA#3 led to approximately 1.4-fold increase in migration speed, compared to control cells (Figure 2.3 D). Expression of all three guide RNAs resulted in an increased MSD compared to the non-targeting control (Figure 2.3E), but no difference in persistence (Figure 2.3 F) or directionality (Figure 2.3 G). Since all three gRNAs had similar effects on APPL1 expression and cell migration (Figure 2.3 C,D), APPL1 gRNA#3 cells were

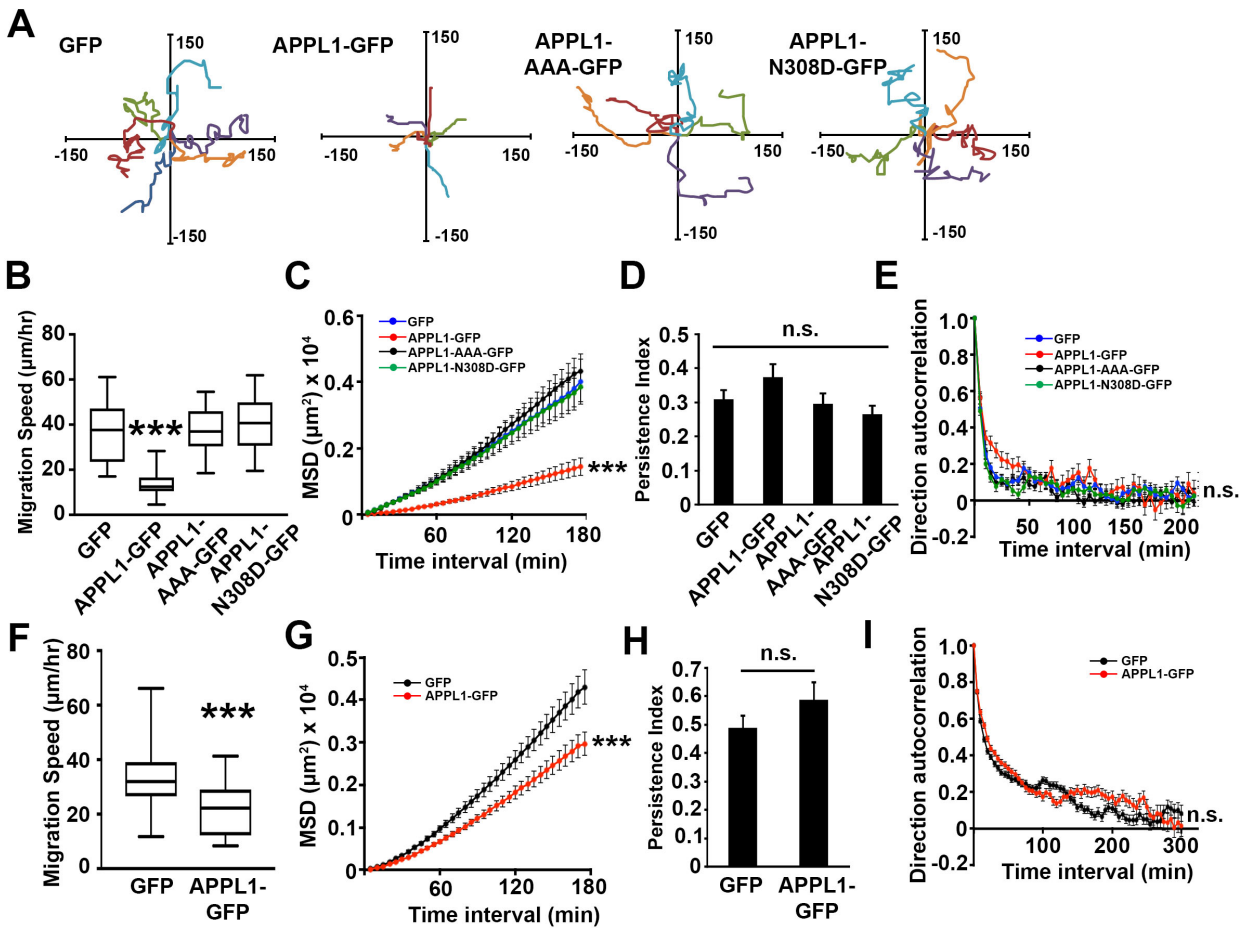

Figure 2.2. APPL1 regulates 2D and 3D cell migration. (A) Migration of MDA-MB-231 cells expressing GFP, APPL1-GFP, APPL1-AAA-GFP, or APPL1-N308D-GFP was quantified. Rose plots show individual tracks of representative cells from each condition. (B) Box plot showing migration speeds for GFP-, APPL1-GFP-, APPL1-AAA-GFP-, and APPL1-N308D-GFP-expressing cells. 25-35 cells total were analyzed from each condition from at least three experiments (*, $p<0.05$, ***, $p<0.0001$, determined by one-way ANOVA followed by Tukey's post hoc test). (C) MSD of MDA-MB-231 cells expressing GFP, APPL1-GFP, APPL1-AAA-GFP, or APPL1-N308D-GFP. Error bars represent s.e.m. from 25-35 cells total from each condition from at least three separate experiments ($p<0.0001$, comparing slopes of the lines using a likelihood ratio test). (D) Persistence index of MDA-MB-231 cells expressing GFP, APPL1-GFP, APPL1-AAA-GFP, or APPL1-N308D-GFP. Error bars represent s.e.m. from 25-35 cells total from each condition from at least three separate experiments (n.s., not significant, $p=0.1$, determined by one-way ANOVA). (E) Directional autocorrelation analysis of MDA-MB-231 cells expressing GFP, APPL1-GFP, APPL1-AAA-GFP, or APPL1-N308D-GFP. Error bars represent s.e.m. from 25-35 cells total from each condition from at least three separate experiments ($p=0.992$, 0.784, and 0.18, GFP compared to APPL1-GFP, APPL1-AAA-GFP, and APPL1-N308D-GFP, respectively, determined by determined by mixed effects model to compare the curves, with controlling FDR at 0.1). (F) HT1080 cells were embedded in 1.5 mg/ml ColI matrices supplemented with 30μg/ml FN. Cells were allowed to adhere to matrices

for 24 hours at 37°C, imaged with time-lapse microscopy, and migration speed was quantified for individual cells. Box plots show migration speed for cells expressing GFP or APPL1-GFP in 3D matrices. 24-31 cells total were analyzed from each condition from at least three experiments (***, p=0.0002, determined by Student's t-test). (G) MSD of HT1080 cells expressing GFP or APPL1-GFP in 3D matrices. Error bars represent s.e.m. from 61-63 cells total from each condition from at least three separate experiments ($p<0.0001$, comparing slopes of the lines using a likelihood ratio test). (H) Persistence index of HT1080 cells expressing GFP or APPL1-GFP in 3D matrices. Error bars represent s.e.m. from 61-63 cells total from each condition from at least three separate experiments (n.s., not significant, p=0.17, determined by Student's t-test). (I) Directional autocorrelation analysis of HT1080 cells expressing GFP or APPL1-GFP in 3D matrices. Error bars represent s.e.m. from 61-63 cells total from each condition from at least three separate experiments (p=0.974, determined by determined by mixed effects model to compare the curves, with controlling false discovery rate (FDR) at 0.1).

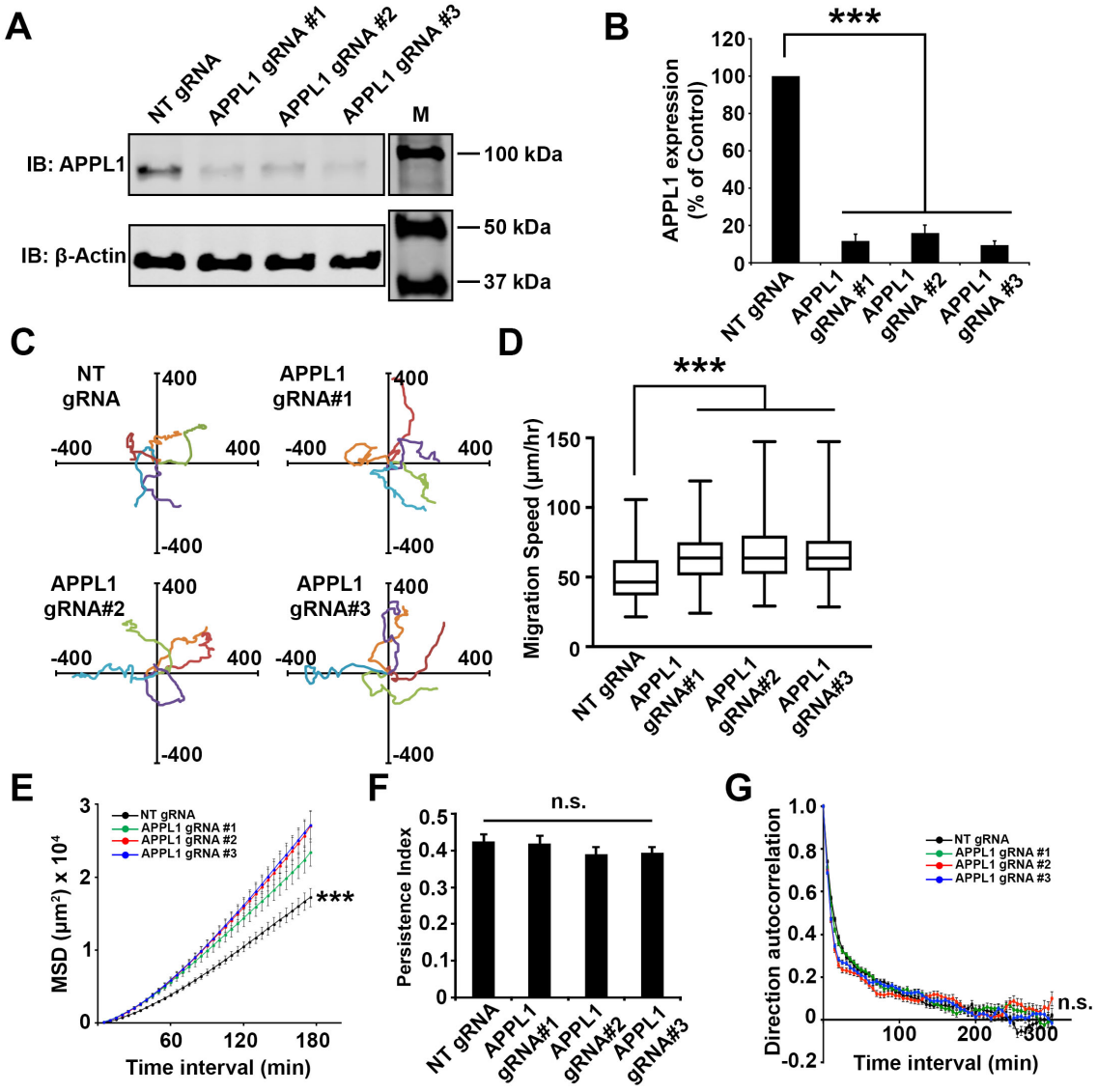

Figure 2.3. APPL1 knockout increases migration speeds. (A) Lysates derived from cells expressing one of three different CRISPR plasmids targeting APPL1 (APPL1 gRNA#1-3) or non-targeting guide RNA (NT gRNA) were subjected to immunoblot analysis for endogenous levels of APPL1 and β-Actin (loading control). A representative image is shown. M, molecular weight marker; kDa, Kilodaltons. (B) Quantification of the endogenous levels of APPL1 in the blots described in (A), normalized to β-Actin. Error bars represent the s.e.m. from three separate experiments (***, $p<0.0001$, determined by one-way ANOVA). (C) Rose plots from migration assays show the individual track paths for APPL1 gRNA cell lines or control cells. (D) Box plot showing migration speed for the indicated cell lines. >60 cells total were analyzed for each condition from at least three experiments (*** $p<0.0001$, determined by one-way ANOVA). (E-G) MSD (E), persistence index (F), and directional autocorrelation analysis (G) of HT1080 cells expressing APPL1 gRNA#1-3 or NT gRNA. Error bars represent s.e.m. from >60 cells total from each condition from at least three separate experiments (***, $p<0.0001$, comparing slopes

of the lines using a likelihood ratio test (E), n.s., not significant, p=0.48, determined by one-way ANOVA (F), p=0.115, 0.404, and 0.044, NT gRNA compared to gRNA #1, gRNA #2, and gRNA #3, respectively, determined by determined by mixed effects model to compare the curves, with controlling FDR at 0.1 (G)).

utilized for all subsequent experiments. In order to test whether APPL2 also plays a role in cell migration, APPL1 gRNA#3 or NT gRNA cells were transfected with a siRNA pool targeted against APPL2, resulting in a 50% decrease in APPL2 expression (Figure 2.4 A,B). No difference in migration speed was observed in cells depleted of APPL2 alone or in combination with depletion of APPL1 (Figure 2.4 C). Overall, these results suggest that APPL1 is an important regulator of cell migration.

Regulation of cell migration by APPL1 depends on α5 integrin

Our previous work has shown that some regulators of cell migration act in an ECM-specific manner (Bristow et al., 2009; Jean et al., 2014). Since APPL1 regulates 3D migration (Figure 2.2 F), a situation in which cells are in the presence of both ColI and FN, we wanted to test whether APPL1-mediated migration is ECM-dependent. Migration assays were performed with HT1080 cells expressing APPL1-GFP or GFP and plated on either FN or ColI. While APPL1-GFP-expressing cells showed decreased migration speed on FN, APPL1 had no effect on migration speed on ColI (Figure 2.5 A). Likewise, APPL1 gRNA#3 cells increased migration when plated on FN, but not ColI (Figure 2.5 B), suggesting that APPL1 may regulate migration in a manner dependent on α5β1, a major FN-binding integrin. 3D migration assays were performed in the presence of the synthetic peptide RGD (10μM) to block integrin-ligand interactions or an equal concentration of RGE peptide as a control. Treatment with RGD did not disrupt attachment of GFP- or APPL1-GFP-expressing cells in the ColI gels (Figure 2.5 C). Consistent with our previous results, APPL1-GFP-expressing cells migrated more slowly than control cells in the presence of RGE (control) peptide, whereas the presence of RGD abrogated the effect of APPL1 on cell migration (Figure 2.5 D). The RGD peptide blocks the function of multiple integrins, not just α5β1. To verify specificity, we evaluated migration speeds in 3D migration assays while

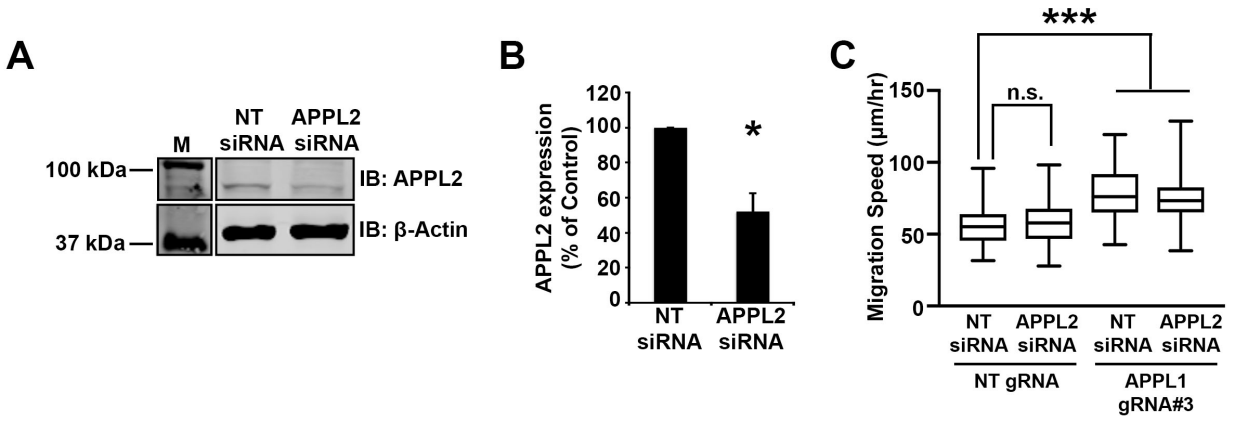

Figure 2.4. APPL2 has no effect on cell migration. (A) Lysates derived from cells expressing APPL2 siRNA or non-targeting siRNA (control) were subjected to immunoblot analysis for levels of APPL2 and β-Actin (loading control). A representative image is shown. M, molecular weight marker; kDa, Kilodaltons. (B) Quantification of the endogenous levels of APPL2 in the blots described in (A), normalized to β-Actin. Error bars represent s.e.m. from three separate experiments (*$p<0.05$, determined by Student's t-test). (C) Box plots showing migration speed on FN for HT1080 cells expressing APPL1 gRNA#3 or NT gRNA and either APPL2 siRNA or NT siRNA. 71-81 cells total were analyzed from each condition from three separate experiments (***$p<0.0001$, n.s., not significant, $p>0.99$, determined by one-way ANOVA).

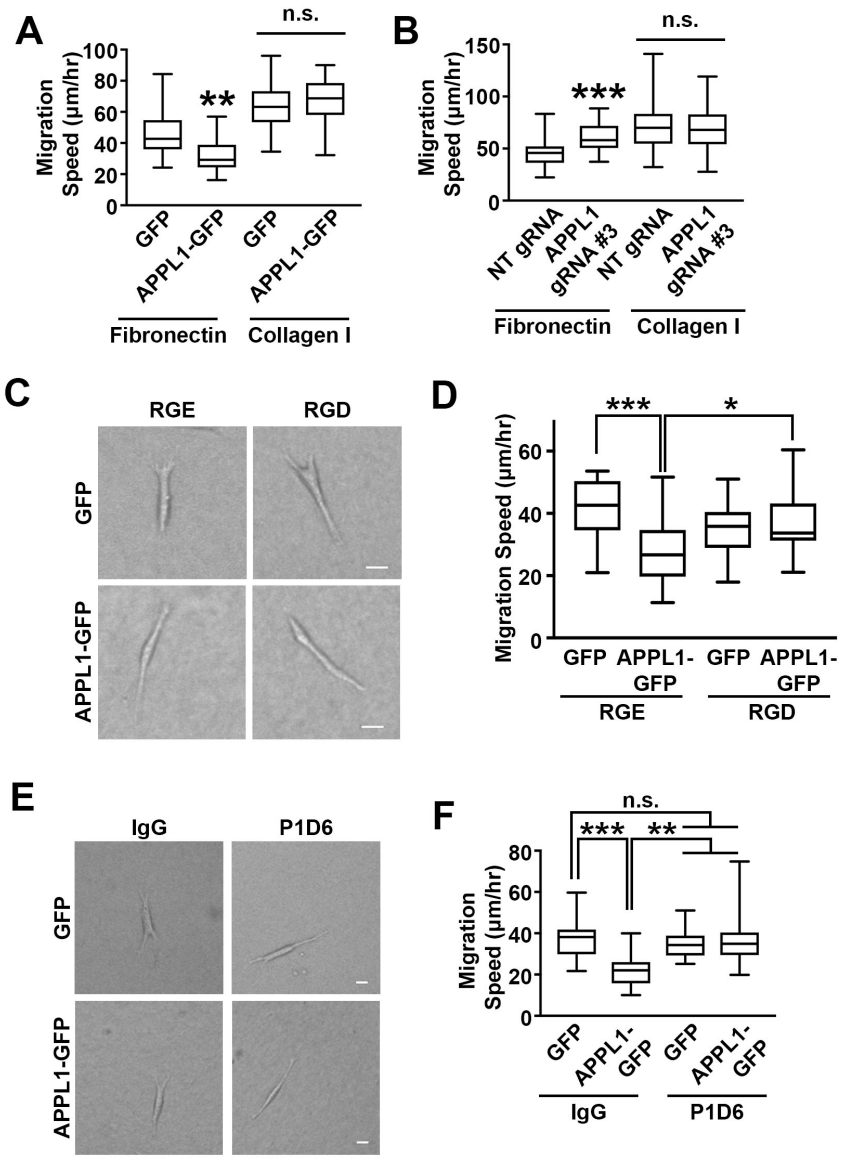

Figure 2.5. APPL1 regulates migration dependent on α5 integrin. (A, B) Box plot showing migration speed for GFP- or APPL1-GFP-expressing cells (A) or cells expressing APPL1 gRNA#3 or NT gRNA (B) plated on either FN or ColI substrate. At least 25 cells (A) or at least 55 cells (B) total were analyzed from each condition from at least three separate experiments (**, $p<0.005$, ***, $p<0.0001$, n.s., not significant, $p=0.41$ and 0.57 from (A) and (B), respectively, determined by Student's t-test). (C) Images of cells transfected with GFP or APPL1-GFP and treated with RGD peptide or RGE (control) show that this treatment did not affect cell attachment. Scale bar = 20 μm. (D) Box plots showing migration speed for cells expressing GFP or APPL1-GFP and embedded in 3D matrices in the presence of RGD or RGE peptide (control). 12-18 cells total were analyzed from each condition from at least three experiments (***, $p<0.0001$, n.s., not significant, $p=0.60$, determined by Student's t-test). (E) Images of cells transfected with GFP or APPL1-GFP and treated with α5 integrin function blocking antibody (P1D6) or control (IgG) show that this treatment did not affect cell attachment. Scale bar = 20

μm. (F) Box plot show migration speed for GFP- or APPL1-expressing cells in 3D migration assays treated with α5 integrin function-blocking antibody (P1D6) or control antibody (IgG). 18-31 cells total were analyzed from each condition from three separate experiments (**, $p<0.005$, ***, $p<0.0001$, n.s., not significant, $p=0.79$ and >0.99, comparing GFP control to GFP and APPL1-GFP treated with P1D6, respectively, determined by one-way ANOVA followed by Tukey's post hoc test).

treating with an anti-α5 integrin function-blocking antibody (clone P1D6) or control IgG antibody. Treatment with P1D6 had no effect on attachment of GFP- or APPL1-GFP-expressing cells in the 3D ColI gel (Figure 2.5 E). As expected, APPL1-GFP-expressing cells migrated significantly more slowly in the presence of the control antibody, but no difference in migration speed was observed when APPL1-GFP-expressing cells were treated with P1D6 antibody (Figure 2.5 F). These results suggest that the effect of APPL1 on cell migration is dependent on α5β1 integrin.

We hypothesized that APPL1 could affect surface level expression of α5β1 integrin to mediate cell migration. To address this possibility, APPL1-GFP or GFP-expressing cells were surface labeled with biotin, and labeled proteins were pulled down using streptavidin agarose beads and subjected to Western Blot analysis. Whole cell lysates from GFP and APPL1-GFP-expressing cells showed no difference in total expression levels of α5, β1, or β3 integrin (Figure 2.6 A,B). However, APPL1-GFP expression led to increased surface levels of both α5 and β1 integrin, but not β3 integrin (Figure 2.6 A,C). Conversely, APPL1 gRNA#3 cells had levels of total α5, β1, and β3 integrin similar to NT gRNA cells (Figure 2.6 D,E), yet had decreased surface levels of α5 and β1 (but not β3) integrin (Figure 2.6 D,F). To confirm these results, HT1080 cells expressing APPL1-GFP or GFP were immunostained for both total and active α5 integrin (clones 6F4 and SNAKA51, respectively). Cell surface integrins were visualized by total internal reflection (TIRF) microscopy. Cells expressing APPL1-GFP exhibited higher levels of both total (Figure 2.7 A,B) and active (Figure 2.7 C,D) α5 integrin, compared to GFP-expressing cells. Conversely, decreasing endogenous APPL1 expression through expression of APPL1 gRNA#3 reduced surface levels of both total (Figure 2.7 E,F) and active (Figure 2.7 G,H) α5 integrin, suggesting that APPL1 promotes higher cell surface levels of α5β1 integrin to inhibit

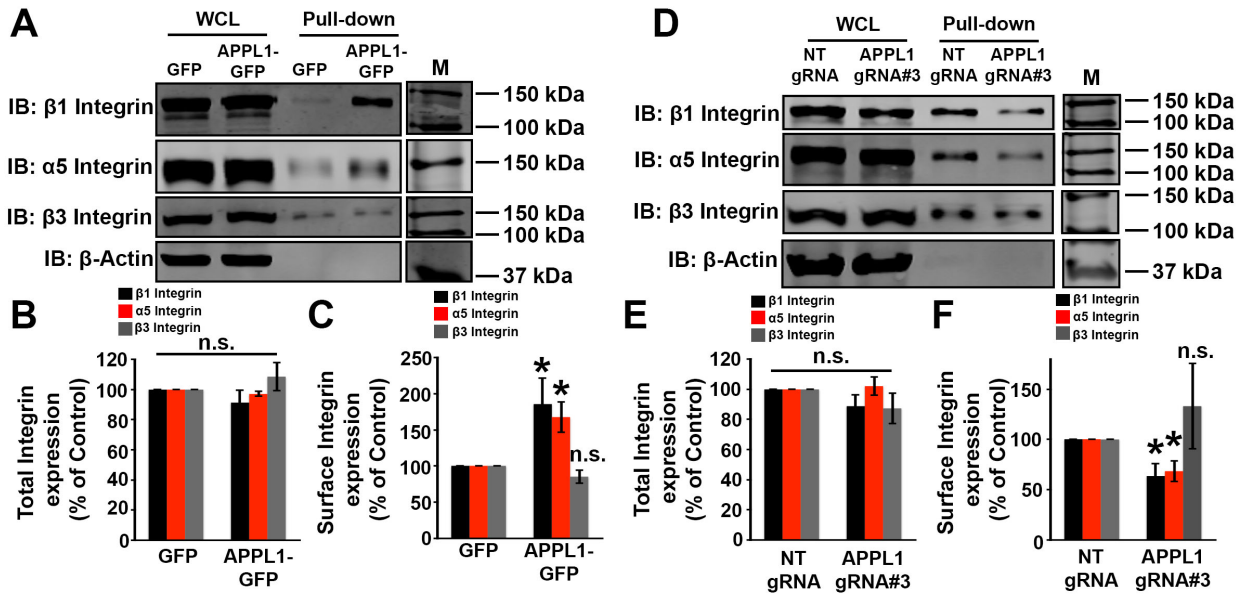

Figure 2.6. APPL1 increases surface levels of α5β1 integrin. (A, D) HT1080 cells expressing GFP or APPL1-GFP (A) or NT gRNA or APPL1 gRNA#3 (D) were surface labeled with NHS-SS-Biotin and pulled down with streptavidin. Surface (pulldown) and total (whole cell lysate, WCL) samples were immunoblotted for α5, β1, or β3 integrin and β-actin. A representative image is shown. M, molecular weight marker; kDa, Kilodaltons. (E, F, H, I) Quantifcation of total (B, E) or surface (C, F) α5, β1, or β3 integrin from (A, D), respectively, shown as a percent of control. Error bars represent s.e.m. from at least three separate experiments (*, $p<0.05$, n.s., not significant, p=0.35, 0.36, and 0.32 (B), p=0.56 (C), p=0.24, 0.83, and 0.46 (E), and p=0.26 (F)).

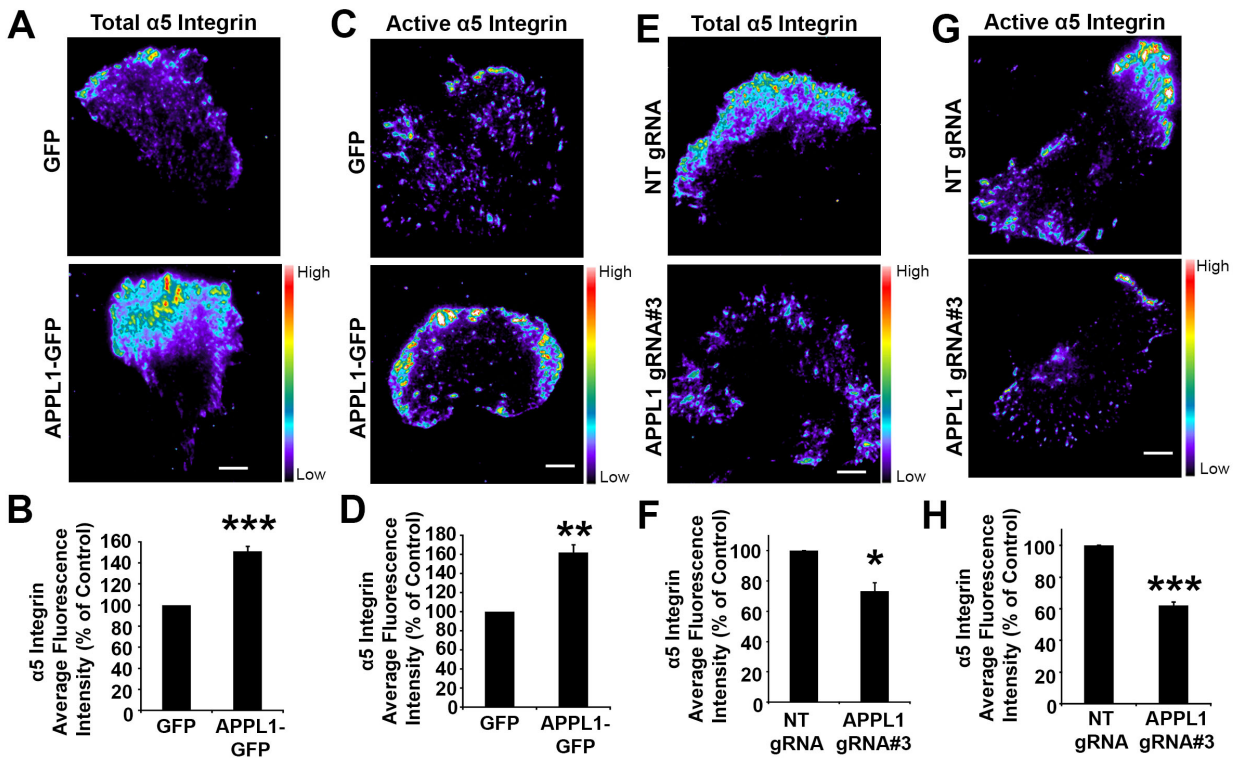

Figure 2.7. APPL1 increases surface levels of active and total α5 integrin. (A, C, E, G) HT1080 cells expressing GFP or APPL1-GFP (A, C) or APPL1 gRNA#3 or non-targeting (NT) gRNA (E, G) were immunostained for total α5 integrin (clone 6F4) (A, E) or active α5 integrin (clone SNAKA51) (C, G). TIRF microscopy was performed to visualize surface level expression. Representative images are pseudocolored for intensity, where warm colors represent higher intensity and cool colors represent lower intensity. Scale bar = 20 μm. (B, D, F, H) Quantification of α5 integrin levels from (A, C, E, G), respectively, shown as percent of control. Error bars represent the s.e.m. from 55-66 cells total from three separate experiments (*, $p<0.05$, **, $p<0.005$, ***, $p<0.0005$, determined by Student's t-test).

cell migration.

We further investigated the relationship between APPL1 and α5 integrin by assessing α5 integrin dynamics. HT1080 cells were co-transfected with a photoactivatable GFP-tagged α5 integrin (α5-PA-GFP) and either APPL1-mCherry or mCherry (control). Live cell imaging experiments were performed in which a region of interest (ROI) was selected at the edge of an mCherry positive cell, and then the fluorescence of α5-PA-GFP was activated by a 500 millisecond pulse of 405nm light. Following photoactivation, fluorescence in control cells quickly dissipated, demonstrating rapid movement of α5 integrin away from the edge of the cell, either through lateral movement or internalization. However, APPL1-mCherry-expressing cells retained significantly higher levels of fluorescence in the ROI over time, indicating that α5 integrin has slower dynamics as a result of increased APPL1 expression (Figure 2.8 A,B). APPL1 has been shown to regulate adhesion dynamics (Broussard et al., 2012), so we next assessed whether α5 integrin dynamics were altered in adhesions. Similar experiments were performed with NT gRNA or APPL1 gRNA#3 cells transfected with α5-PA-GFP and mCherry-paxillin, an adhesion marker. ROIs were chosen at sites of adhesions, where APPL1 gRNA#3 cells showed faster α5 integrin dynamics, compared to NT gRNA cells (Figure 2.8 C,D). It is possible that APPL1 could alter the dynamics of receptors other than just α5 integrin; therefore, Transferrin Receptor (TfnR) was tested. Unlike our results with α5 integrin, cells expressing APPL1-GFP showed no difference in TfnR dynamics compared to control cells (Figure 2.9). Taken together, these results suggest that APPL1 inhibits cell migration by diminishing α5 integrin movement away from adhesions.

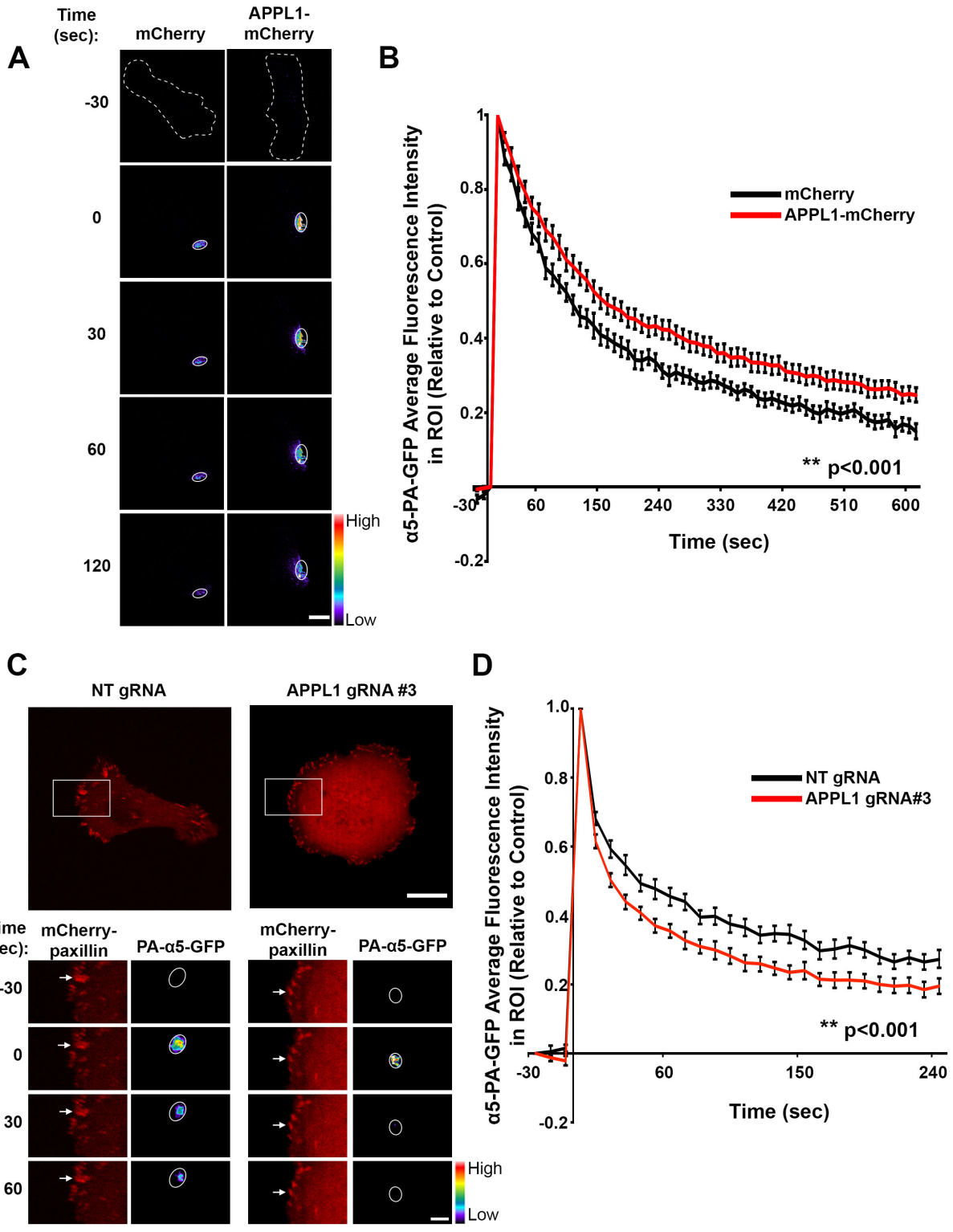

Figure 2.8. APPL1 alters α5 integrin dynamics. (A) HT1080 cells expressing α5-PA-GFP and either mCherry or APPL1-mCherry were subjected to live-cell photoactivation experiments as

described in Methods. Images from selected time points are shown and are pseudocolored for intensity. Circle demarcates ROI used for photoactivation and subsequent average fluorescence intensity measurements. Dotted lines indicate the boundaries of the cell. Scale bar = 15 μm. (B) Quantification of experiments from (A) as average fluorescence intensity, normalized to the amount of signal within the ROI at time=0. (C) HT1080 cells expressing APPL1 gRNA#3 or NT gRNA were transfected with α5-PA-GFP and mCherry-paxillin and subjected to live-cell photoactivation experiments. White boxes in top images indicate regions shown at higher magnification in bottom panels. Bottom left, zoomed images from top panel showing mCherry-paxillin. Arrows indicate adhesions chosen as ROI for photoactivaiton. Bottom right, images showing α5-PA-GFP fluorescence from selected time points, pseudocolored for intensity. White circles represent ROI used for quantification. Top, scale bar = 15 μm; bottom, scale bar = 5 μm. (D) Quantification of photoactivation experiments from (C). Error bars represent the s.e.m. from 14-15 cells (B) or 27-28 cells (D) total from each condition from three separate experiments. A nonparametric regression analysis was used to fit the curves (using natural cubic splines with three knots) and then compared the difference in the curves between two groups using the likelihood ratio test (**, $p<0.001$).

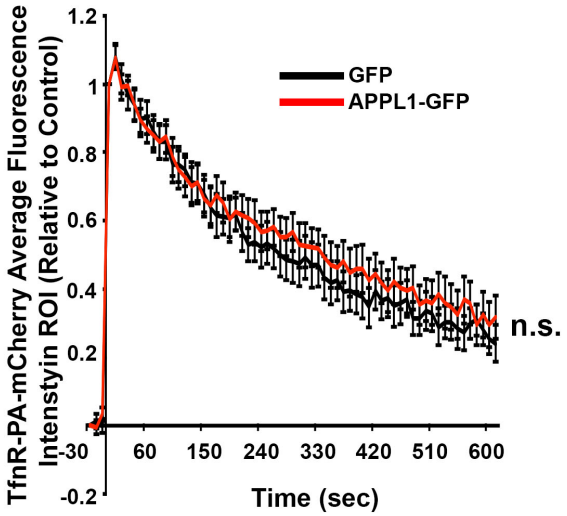

Figure 2.9. APPL1 does not alter Transferrin Receptor dynamics. HT1080 cells expressing TfnR-PA-mCherry and either GFP or APPL1-mCherry were subjected to live-cell photoactivation experiments. TfnR-PA-mCherry fluorescence was activated by stimulation with 405nm light within a ROI near the cell edge. Cells were imaged every 10 seconds for 30 seconds prior to photoactivation and for 6 minutes after photoactivation. Quantification of photoactivation experiments is shown as average fluorescence intensity, normalized to the amount of signal within the ROI at time=0. Error bars represent the s.e.m. 18 cells total were analyzed from each condition from three separate experiments. A nonparametric regression analysis was used to fit the curves (using natural cubic splines with three knots) and then compared the difference in the curves between two groups using the likelihood ratio test (not significant, p=0.026).

APPL1 regulates α5β1 integrin trafficking

Because APPL1 hindered the dynamics of α5 integrin at the cell edge and APPL1 is involved in vesicular trafficking, we hypothesized that APPL1 affects α5β1 integrin trafficking. We performed biotinylation internalization assays, where HT1080 cells expressing APPL1-GFP or GFP were surface labeled with NHS-SS-biotin and internalization was allowed to occur for 0-60 minutes. Surface-associated biotin was removed by TCEP, a reducing agent, biotinylated (internal) proteins were pulled down with streptavidin, and western blots were performed for α5 and β1 integrin. At all time points, APPL1-GFP-expressing cells showed a decrease in internal levels of both β1 (Figure 2.10 A,B) and α5 integrin (Figure 2.10 A,C). We confirmed these results using an immunofluorescence-based method, labeling the cell surface with a β1 integrin antibody (clone P5D2, detailed in Methods). Similar to the biotinylation-based method, antibody internalization assays showed decreased internal levels of β1 integrin in APPL1-GFP-expressing cells, compared to control (Figure 2.10 D,E). Internalization assays using an antibody specific to active β1 integrin (clone 12G10) revealed that excess APPL1 expression also decreased internal levels of active β1 integrin (Figure 2.10 F,G).

To test the effect of APPL1 depletion on integrin internalization, we performed antibody internalization assays with APPL1 gRNA#3 or control cells. APPL1 depletion led to increased levels of internal β1 integrin (Figure 2.11 A,B). Next, we tested the ability of APPL1-GFP, or mutants of APPL1-GFP, to rescue the integrin internalization effects in APPL1 depleted cells. HT1080 cells expressing NT gRNA or APPL1 gRNA#3 were transfected with GFP, APPL1-GFP, APPL1-N308D-GFP, a mutant that cannot bind Rab5 (Zhu et al., 2007), or APPL1 missing the PTB domain (APPL1-ΔPTB-GFP), and biotinylation internalization assays were performed. APPL1 gRNA#3 cells exhibited increased internalization of β1 (Figure 2.11 C,D) and α5 integrin

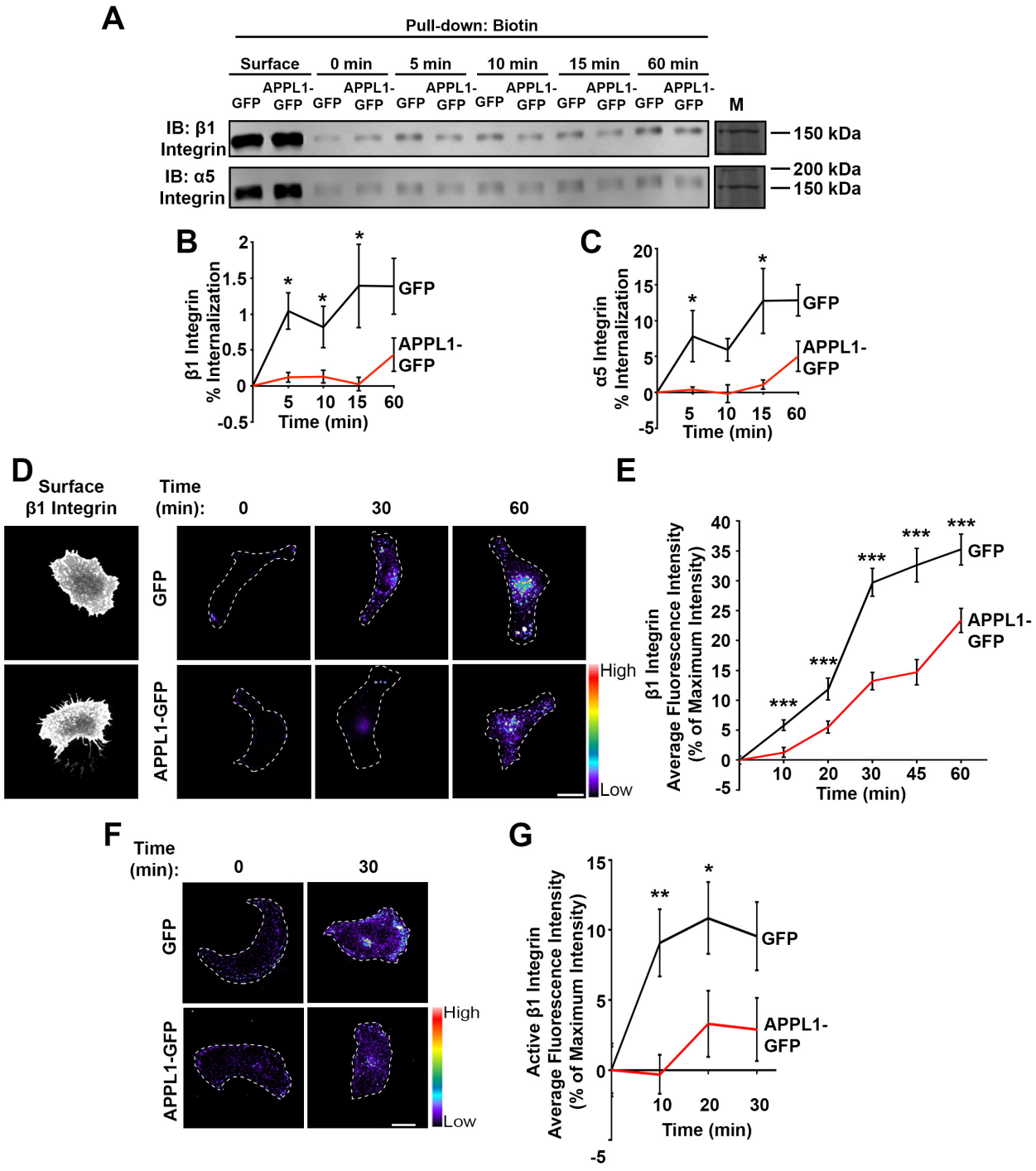

Figure 2.10. APPL1 regulates α5β1 integrin internalization. (A) HT1080 cells expressing GFP or APPL1-GFP were surface labeled with NHS-SS-Biotin for 30 minutes at 4°C and biotinylation internalization assays were performed as described in Methods. Surface and internalized α5 and β1 integrin were assessed by Western blot analysis. A representative image is shown. M, molecular weight marker; kDa, Kilodaltons. (B, C) Quantification of β1 integrin (B) or α5 integrin (C) internalization from (A), shown as a percent of surface integrin. Error bars

represent s.e.m. from at least three separate experiments (*, $p<0.05$, determined by Student's t-test). (D, F) HT1080 cells expressing GFP or APPL1-GFP were surface labeled with a total β1 integrin antibody (clone P5D2) (D) or active β1 integrin antibody (clone 12G10) (F) at 4°C. Antibody internalization assays were performed as described in Methods. 0 minutes indicates cells that were surface labeled and acid washed, but not allowed to internalize integrin. Representative images are shown, pseudocolored to show intensity, where warm colors represent higher intensity and cool colors represent lower intensity. Dotted lines indicate cell boundaries. Scale bar = 15μm. (E, G) Quantification of β1 integrin internalization assay from (D, F), respectively. At least 58 cells (D,E) or 40-60 cells (F,G) total were analyzed from each condition from three separate experiments (*, $p<0.05$, **, $p<0.005$, ***, $p<0.0005$, determined by Student's t-test).

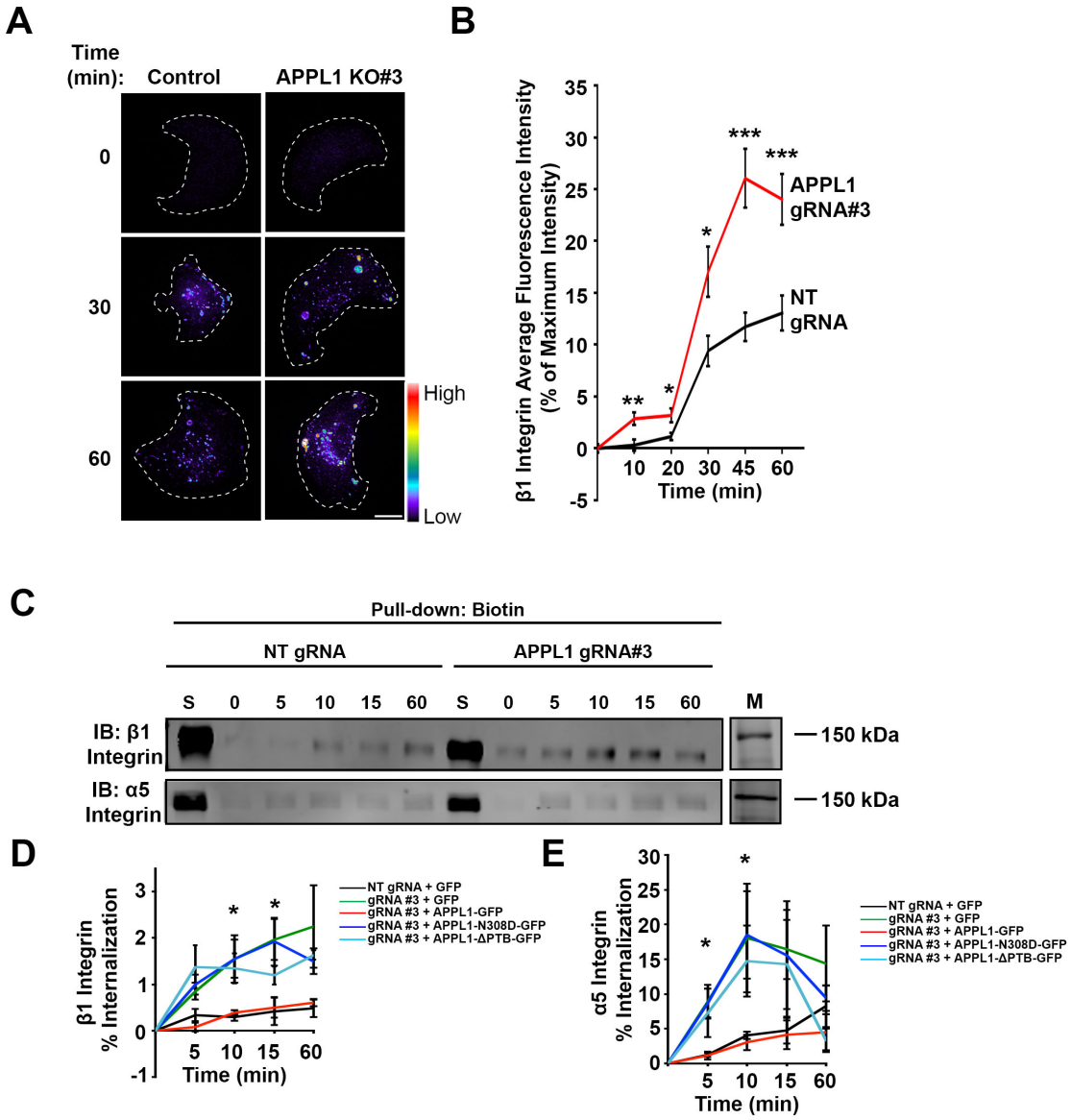

Figure 2.11. APPL1 regulates α5β1 integrin internalization. (A) HT1080 cells expressing APPL1 gRNA#3 or NT gRNA were surface labeled with a total β1 integrin antibody (clone P5D2) at 4°C. Antibody internalization assays were performed as described in Methods. 0 minutes indicates cells that were surface labeled and acid washed, but not allowed to internalize integrin. Representative images are shown, pseudocolored to show intensity, where warm colors represent higher intensity and cool colors represent lower intensity. Dotted lines indicate cell boundaries. Scale bar = 15μm. (B) Quantification of β1 integrin internalization assay from (A). 44-60 cells total were analyzed from each condition from three separate experiments (*, $p<0.05$, **, $p<0.005$, ***, $p<0.0005$, determined by Student's t-test). (C) HT1080 cells expressing APPL1 gRNA#3 or non-targeting (NT) gRNA were transfected with GFP, APPL1-GFP, APPL1-N308D-GFP, or APPL1-ΔPTB-GFP and then were surface labeled with NHS-SS-Biotin and internalization assays were performed. A representative image is shown. S, surface; M, molecular weight marker; kDa, Kilodaltons. (D, E) Quantification of β1 integrin (D) or α5

integrin (E) internalization from (C) is shown as a percent of surface integrin. Error bars represent s.e.m. from three separate experiments (*, $p<0.05$, determined by one-way ANOVA, comparing NTgRNA + GFP to gRNA3 + GFP).

(Figure 2.11 C,E), compared to control cells. However, rescue with APPL1-GFP, but not APPL1-N308D-GFP or APPL1-ΔPTB-GFP, in APPL1 gRNA#3 cells resulted in internal integrin levels similar to NT gRNA cells (Figure 2.11 D,E), suggesting that APPL1 expression can modulate integrin internalization, dependent on its interaction with Rab5 and its PTB domain.

To ensure that APPL1 was not grossly affecting trafficking, internalization assays were performed to assess Transferrin Receptor (TfnR) trafficking. Transferrin (Tfn) conjugated to a pH sensitive dye pHrodo® Red (Tfn-pHrodo Red), was added to cell culture media of GFP- or APPL1-GFP-expressing HT1080 cells. Since pHrodo® Red dye is non-fluorescent at neutral pH but fluoresces brightly in acidic environments like endosomes, fluorescence is proportional to the amount of internalized TfnR-Tfn complex. No difference in internal TfnR levels between GFP- or APPL1-GFP-expressing cells was observed, suggesting that APPL1 does not alter TfnR trafficking (Figure 2.12 A,B). Overall, these results suggest that APPL1 decreases internal levels of β1 integrin, but not TfnR.

Lower internal integrin levels could result from a decreased rate of internalization or from an increased rate of recycling. Therefore, we performed antibody internalization assays in the presence of primaquine, a recycling inhibitor. In the presence of primaquine, APPL1-GFP-expressing cells still exhibited lower internal levels compared to control, suggesting that APPL1 decreases β1 integrin internalization (Figure 2.13 A). Next, we directly assessed the ability of APPL1 to modulate integrin recycling. Antibody recycling assays were performed in which cells were treated with primaquine during the internalization step to prevent recycling, surface antibody was removed by acid wash, and then internal integrin was chased back to the cell surface by returning cells to 37°C for 0-20 minutes in the absence of primaquine, followed by a

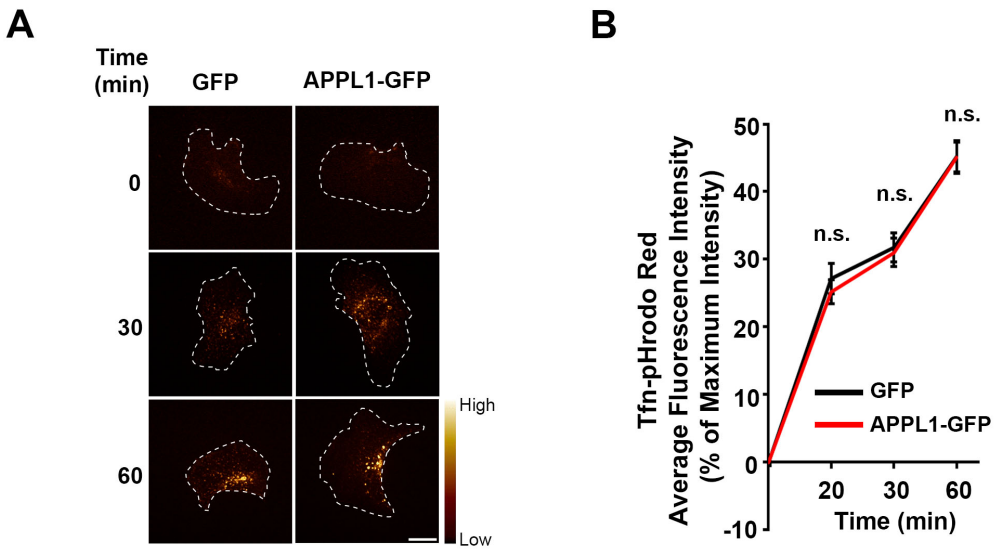

Figure 2.12. APPL1 does not alter Transferrin Receptor trafficking. (A) HT1080 cells expressing GFP or APPL1-GFP were plated on FN-coated coverslips and incubated with 25µl/ml Tfn-pHrodo Red at 37°C for 0-60 minutes. Cells were fixed and imaged to show internal levels of Tfn. Representative images are pseudocolored for intensity as indicated. Dotted lines demarcate the boundaries of the cell. Scale bar = 15µm. (B) Quantification of Tfn internalization assay from (A). Average fluorescence intensity is shown as a percent of the cell with the maximum intensity from each experiment. 58-60 cells total were analyzed from each condition from three separate experiments (n.s., not significant, p=0.70, 0.99, and 0.81 for the 20, 30, and 60 minute time points, respectively; determined by Student's t-test).

second acid wash to remove antibody recycled to the cell surface. Intriguingly, APPL1-GFP-expressing cells recycled β1 integrin significantly faster compared to GFP-expressing cells (Figure 2.13 B,C). We confirmed these results biochemically, and observed similar results to the immunofluorescence method used to probe integrin recycling (Figure 2.13 D-F). Collectively, these data demonstrate that APPL1 both decreases integrin internalization and promotes integrin recycling, leading to lower internal levels of β1 integrin.

APPL1 inhibits cell migration in a Rab5-dependent manner

APPL1 was previously shown to interact with the GTPase Rab5 on early endosomes (Zhu et al., 2007), and our results indicate that APPL1 affects integrin trafficking. We hypothesized that endosomal localization of APPL1 is important its effect on cell migration. Migration assays were performed using an APPL1 variant [APPL1-R146A/K152A/K154A (APPL1-AAA-GFP)] that has three point mutations in the BAR domain that abolish endosomal localization (Broussard et al., 2012; Schenck et al., 2008). Whereas APPL1-GFP localized to punctate endosomal structures, APPL1-AAA-GFP showed diffuse localization (Figure 2.14 A), consistent with previous findings (Broussard et al., 2012). While APPL1-GFP expression hindered cell migration in HT1080 cells, APPL1-AAA-GFP-expressing cells migrated similar distances (Figure 2.14 C) and speeds (Figure 2.14 D) compared to control. Analogous results were obtained in MDA-MBA-231 cells expressing APPL1-AAA-GFP (Figure 2.2 A,B), as well as in 3D migration assays (Figure 2.14 E). Additionally, MDA-MB-231 cells expressing of APPL1-AAA-GFP had similar MSD, persistence, and directionality, compared to control (Figure 2.2 C-E). Thus, APPL1 endosomal localization is important for its effect on cell migration.

Rab5 promotes cell migration and invasion, as well as integrin trafficking and adhesion turnover (Lanzetti and Di Fiore, 2008; Torres and Stupack, 2011; Valdembri et al., 2009). Since

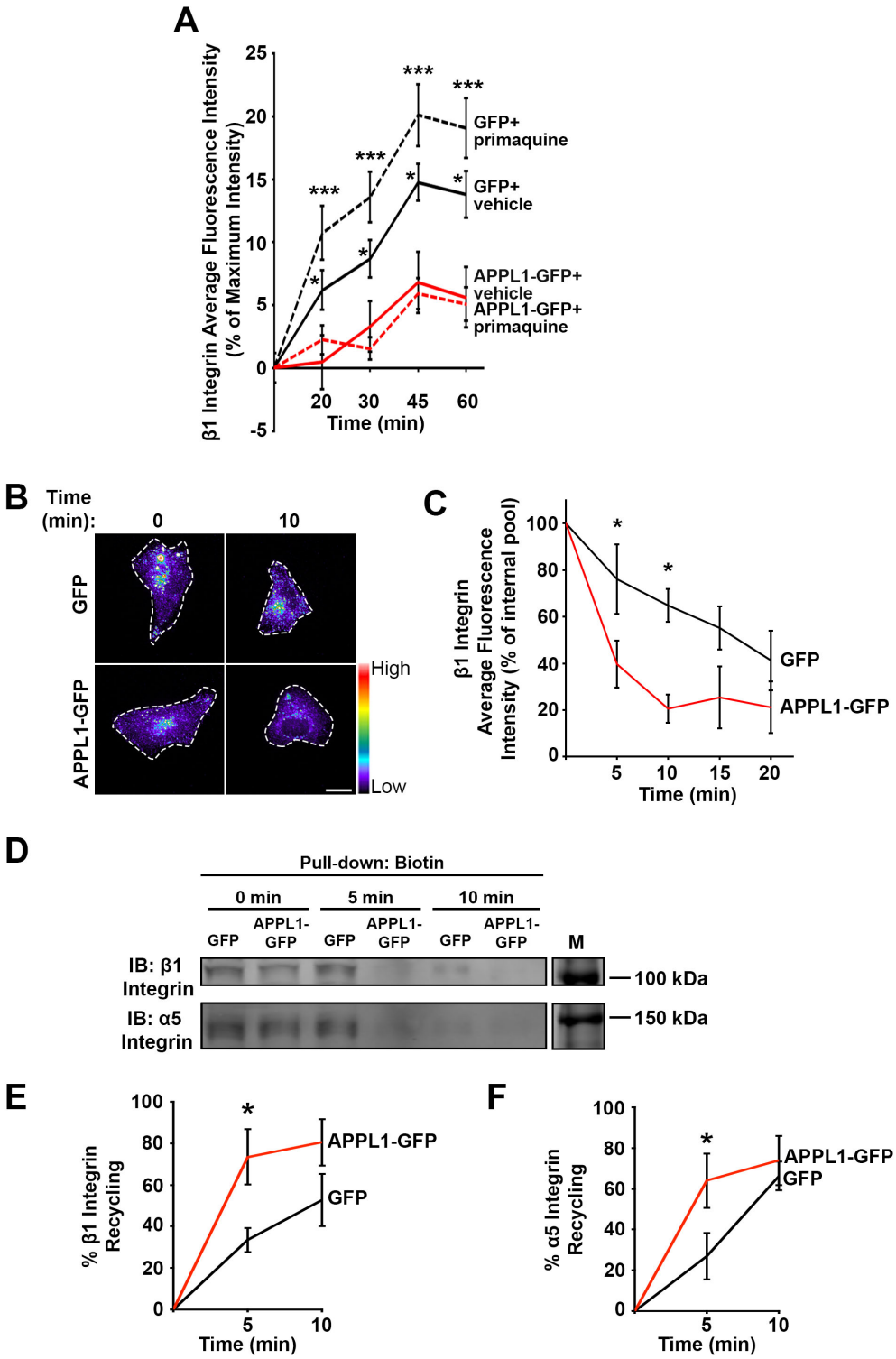

Figure 2.13. APPL1 regulates α5β1 integrin internalization and recycling. (A) HT1080 cells expressing either APPL1-GFP or GFP were used in β1 integrin internalization assays in the presence of primaquine or vehicle. Quantification of the average fluorescence intensity is shown

as a percent normalized to the cell with the maximum intensity from each experiment. At least 46 cells total were analyzed from each condition from at least three separate experiments (*, $p<0.05$ compared to APPL1-GFP + Vehicle, ***, $p<0.0001$ compared to APPL1-GFP + Vehicle, determined by one-way ANOVA followed by Tukey's post hoc test). (B) HT1080 cells expressing either APPL1-GFP or GFP were subjected to antibody recycling assays as described in Methods. (C) Quantification of the average fluorescence intensity from (B) is shown as a percent of the internal pool of integrin at time=0. 51-71 cells total were analyzed from each condition from three separate experiments (*, $p<0.05$, determined by Student's t-test). (D) HT1080 cells expressing GFP or APPL1-GFP were surface labeled with NHS-SS-Biotin for 30 minutes at 4°C and biotinylation recycling assays were performed as described in Methods. Western blot analysis was used to assess the remaining internal pool of α5β1 integrin. A representative image is shown. M, molecular weight marker; kDa, Kilodaltons. (E,F) Quantification of β1 integrin (D) or α5 integrin (F) recycling from (D) is shown as a percent recycled (0% recycled at time=0). Error bars represent s.e.m. from three separate experiments (*, $p<0.05$, determined by Student's t-test).

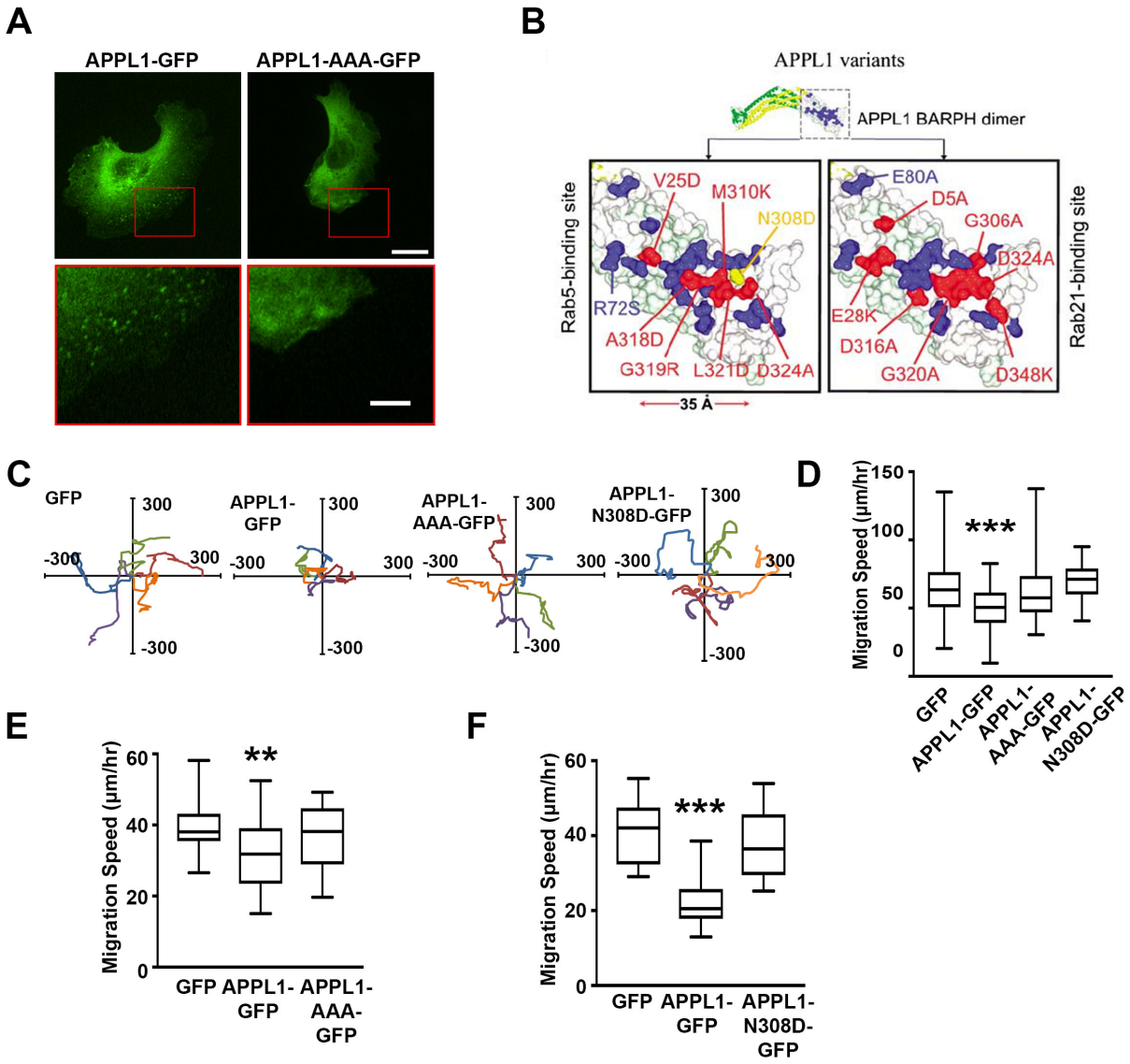

Figure 2.14. APPL1 requires endosomal localization and Rab5 interaction to regulate cell migration. (A) Top panels, GFP fluorescence in HT1080 cells expressing APPL1-GFP or APPL1-AAA-GFP. Scale bar = 15μm. Bottom panels, zoomed images of boxed regions from the top panels. Scale bar = 5μm. (B) Interaction sites between Rab5 (left) and Rab21 (right) on APPL1. APPL1-N308D mutant is used in subsequent experiments to diminish Rab5-binding. (C) HT1080 cells expressing GFP, APPL1-GFP, APPL1-AAA-GFP, or APPL1-N308D-GFP were plated on FN and migration assays were performed. Rose plots show individual track paths of representative cells from each condition. (D) Box plots showing quantification of migration speed from (C). At least 50 cells total were analyzed from each condition from three separate experiments (***, $p<0.0001$, determined by one-way ANOVA followed by Tukey's post hoc test). (E) Box plots showing migration speeds for cells expressing GFP, APPL1-GFP, or APPL1-AAA-GFP in 3D matrices. 16-31 cells total were analyzed from each condition from at least three experiments (**, $p=0.0055$, determined by one-way ANOVA followed by Tukey's post

hoc test). (F) Box plots showing migration speeds for cells expressing GFP, APPL1-GFP, or APPL1-N308D-GFP in 3D matrices. 15-23 cells total were analyzed from each condition from at least three experiments (***, $p<0.0001$, determined by one-way ANOVA followed by Tukey's post hoc test).

(B) Reprinted from (Zhu et al., 2007).

our results show that endosomal localization is important for APPL1-mediated migration, and APPL1 (but not an APPL1 mutant that cannot bind Rab5) affects integrin trafficking (Figure 2.11 D,E), we postulated that APPL1 affects cell migration through its interaction with Rab5. We generated a point mutation in the PH domain of APPL1 that reduces the interaction of APPL1 with Rab5 (N308D) (Figure 2.14 B)(Zhu et al., 2007). The migration speed of cells expressing APPL1-N308D-GFP was not significantly different from cells expressing GFP in 2D (Figure 2.14 C,D) and 3D (Figure 2.14 F). Furthermore, APPL1-N308D-GFP expression in MDA-MB-231 cells had no effect on migration, whereas APPL1-GFP decreased migration speed and MSD, compared to GFP expression (Figure 2.2 A-C), suggesting that APPL1-mediated migration is dependent on its interaction with Rab5.

Next, we tested the ability of APPL1-GFP and/or point mutants of APPL1 to rescue the migration phenotype APPL1 depleted cells. HT1080 cells expressing NT gRNA or APPL1 gRNA#3 were transfected with GFP, APPL1-GFP, APPL1-AAA-GFP, or APPL1-N308D-GFP, and migration assays were performed. As previously observed, APPL1 gRNA#3 cells increased migration speeds. However, expression of APPL1-GFP, but not APPL1-AAA-GFP or APPL1-N308D-GFP, in APPL1 gRNA#3 cells resulted in migration speeds similar to NT gRNA cells (Figure 2.15 A), suggesting that APPL1 expression can modulate migration, dependent on endosomal localization and interaction with Rab5.

To probe further the relationship between APPL1 and Rab5 in cell migration, APPL1-GFP and Rab5-mCherry and/or point mutants of each protein were co-expressed in HT1080 cells, and migration was assessed. Similar to our previous results, cells co-expressing APPL1-GFP and mCherry (but not APPL1-N308D-GFP and mCherry) showed decreased migration speed compared to control (GFP and mCherry) (Figure 2.15 B). Cells expressing GFP and Rab5-

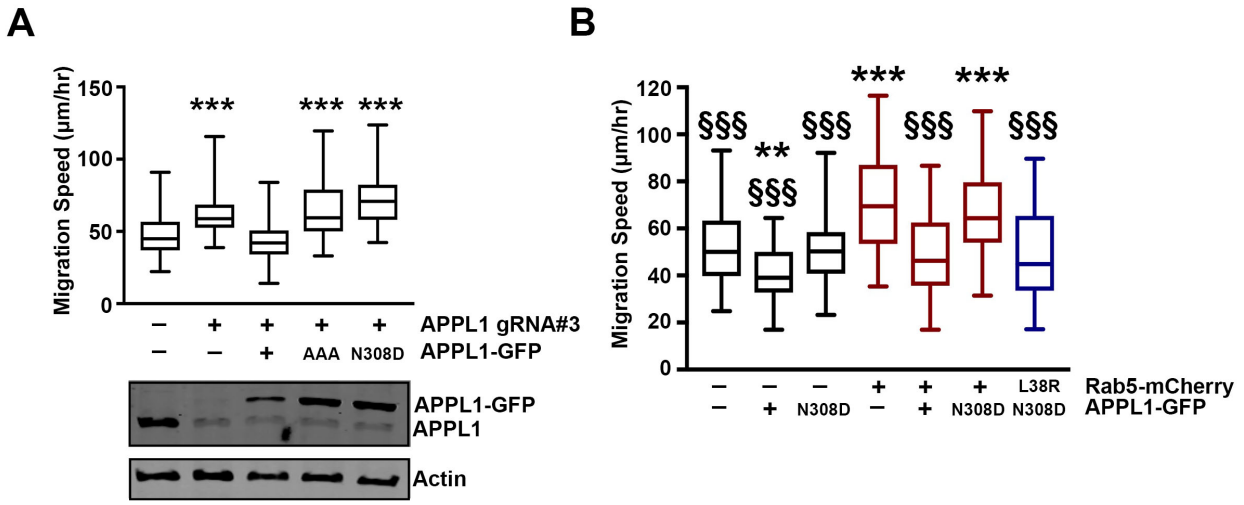

Figure 2.15. APPL1 mediates migration through interaction with Rab5. (A) HT1080 cells expressing APPL1 gRNA#3 or NT gRNA were transfected with GFP, APPL1-GFP, APPL1-AAA-GFP, or APPL1-N308D-GFP, and migration assays were performed. Western blot shows APPL1 expression levels from each condition, with β-actin as a loading control. Box plot shows migration speeds from each condition. At least 35 cells total were analyzed from each condition from at least three separate experiments (***, $p<0.0001$, compared to NT gRNA + GFP, determined by one-way ANOVA followed by Tukey's post hoc test). (B) Box plot shows migration speeds for HT1080 cells that were co-transfected with GFP, APPL1-GFP, or APPL1-N308D-GFP (N308D) and either mCherry, Rab5-mCherry, or Rab5-L38R-mCherry (L38R) and used in migration assays. – indicates expression of the tag only (GFP or mCherry); + indicates expression of APPL1-GFP or Rab5-mCherry. At least 44 cells total were analyzed from each condition from at least three separate experiments (**, $p=0.001$ compared to GFP + mCherry, ***, $p<0.0001$ compared to GFP + mCherry, §§§, $p<0.0001$ compared to GFP + Rab5-mCherry, determined by one-way ANOVA followed by Tukey's post hoc test).

mCherry exhibited increased migration speed, consistent with previous findings that Rab5 promotes migration (Torres and Stupack, 2011). Interestingly, co-expression of APPL1-GFP and Rab5-mCherry led to decreased migration compared to Rab5 alone, indicating that APPL1-GFP expression suppresses Rab5-induced migration. Co-expression of APPL1-N308D-GFP with Rab5-mCherry did not abrogate Rab5-promoted migration, consistent with the reduced interaction of APPL1-N308D with Rab5. We generated a compensatory mutation in Rab5 described by Zhu et al. (2007) (L38R) that, when co-expressed with APPL1-N308D, re-establishes the interaction between APPL1 and Rab5. When APPL1-N308D-GFP and Rab5-L38R-mCherry were co-expressed, migration speeds were reduced to near control levels (Figure 2.15 B), suggesting that APPL1 reduces migration by antagonizing the ability of Rab5 to promote migration.

Next, we tested whether the interaction between APPL1 and Rab5 is important for the regulation of α5 integrin dynamics. Photoactivation of α5-PA-GFP at the leading edge of cells revealed that co-expressing either mCherry or APPL1-N308D-mCherry-resulted in a more rapid loss of fluorescence than APPL1-mCherry, suggesting that the interaction of APPL1 with Rab5 is important for APPL1-mediated α5 integrin dynamics (Figure 2.16 A,B). In addition, we observed that APPL1 colocalizes with a subset of β1 integrin and Rab5 puncta (Figure 2.17 A). Since our results suggest that APPL1 inhibits α5 integrin dynamics (Figure 2.16 A,B) and α5β1 internalization in a Rab5-dependent manner (Figure 2.11 D,E), we hypothesized that APPL1 may inhibit the association between Rab5 and β1 integrin, thus slowing its trafficking and inhibiting migration. Indeed, overexpression of APPL1 reduces colocalization of Rab5 with β1 integrin (Figure 2.17 B,C), while APPL1 knockout increases colocalization between Rab5 and β1 integrin (Figure 2.17 D,E). Together, these results illustrate an important role for the

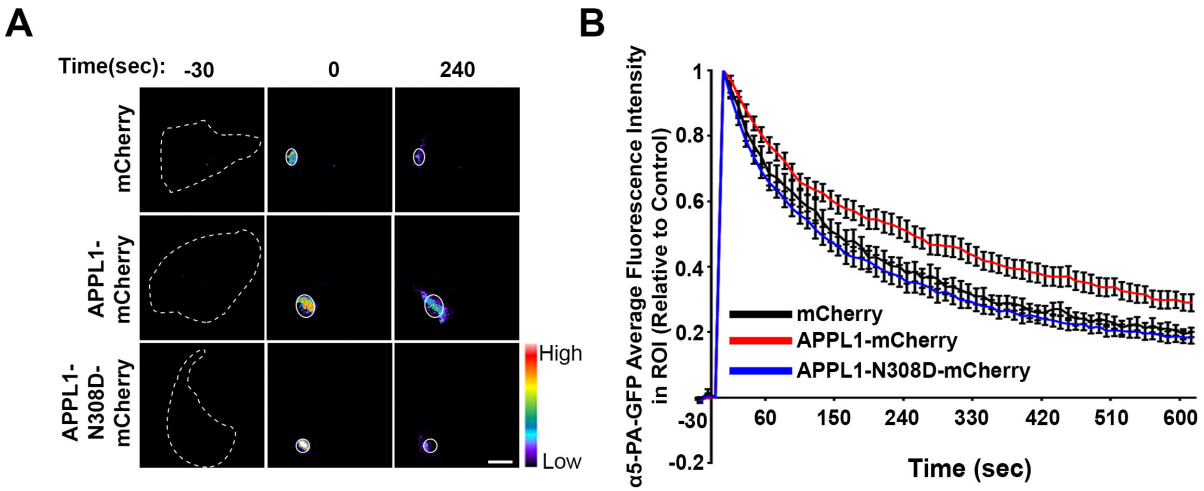

Figure 2.16. APPL1 regulation of α5 integrin dynamics is Rab5-dependent. (A) HT1080 cells expressing α5-PA-GFP and either mCherry, APPL1-mCherry, or APPL1-N308D-mCherry were subjected to live-cell photoactivation experiments, as described in the legend to Figure 2.8. Images from selected time points are shown, pseudocolored to show intensity. Circle demarcates ROI used for photoactivation and subsequent average fluorescence intensity measurements. Dotted lines indicate the boundaries of the cell. Scale bar = 15 μm. (B) Quantification of photoactivation experiments as average fluorescence intensity, normalized to the amount of signal within the ROI in mCherry-expressing cells at time=0. Error bars represent the s.e.m. at each time point. 25-34 cells total were analyzed from each condition from three separate experiments. A nonparametric regression analysis was used to fit the curves (using natural cubic splines with three knots) and then compared the difference in the curves between three groups using the likelihood ratio test ($p<0.001$).

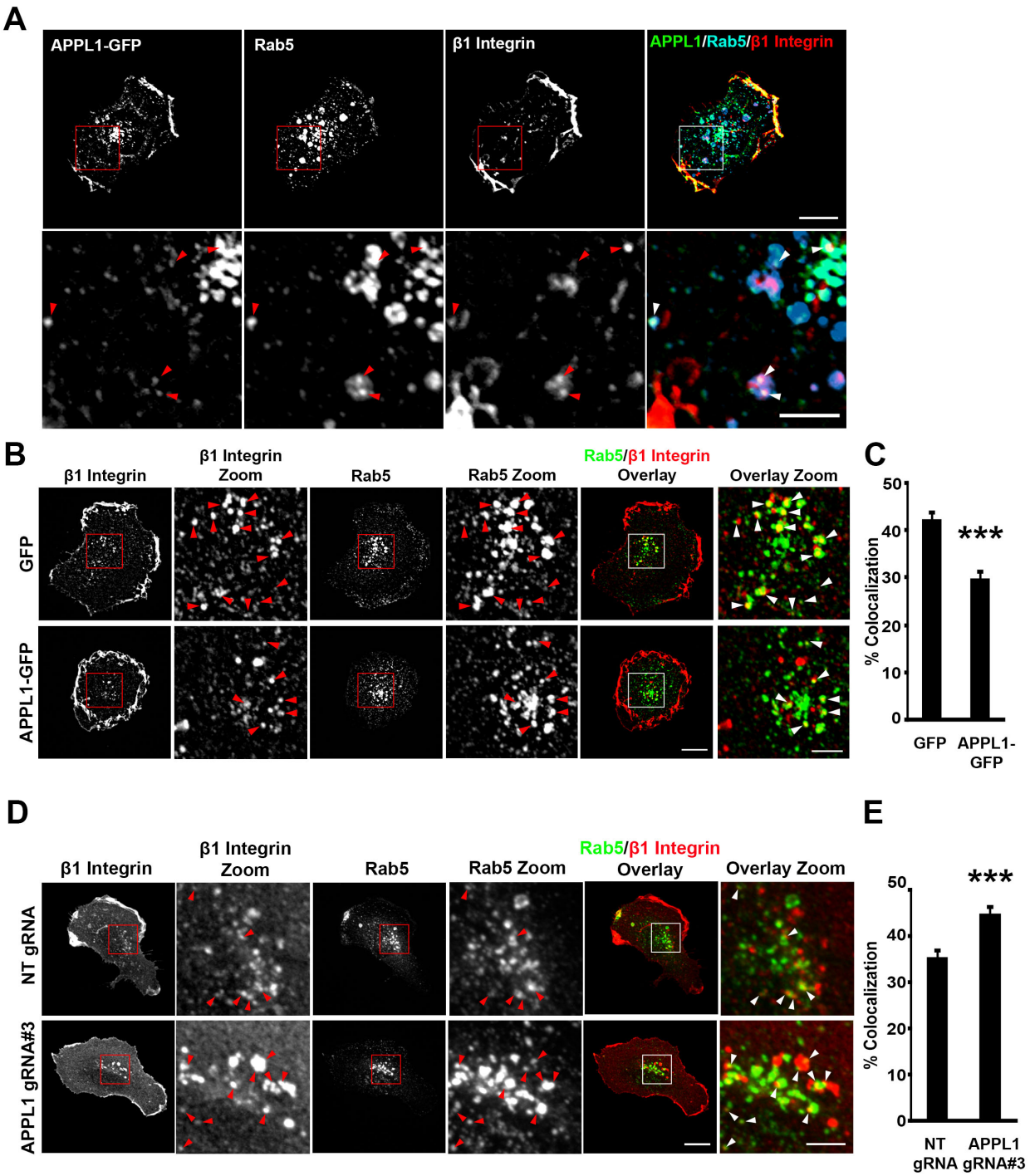

Figure 2.17. APPL1 inhibits association between Rab5 and β1 integrin. (A) HT1080 cells expressing APPL1-GFP were immunostained for Rab5 and β1 integrin. Representative images are shown. Red/white boxes (single color/overlay, upper panels) indicate regions shown at higher magnification in bottom panels. Red/white arrowheads (single color/overlay) indicate colocalization between APPL1, Rab5, and β1 integrin. Scale bar = 15 μm (top panel) and 5 μm (bottom panel). (B) HT1080 cells expressing GFP or APPL1-GFP were immunostained for Rab5

and β1 integrin. Representative images are shown. Red/white boxes (single color/overlay) indicate regions shown at higher magnification. Red/white arrowheads (single color/overlay) indicate colocalization between Rab5 and β1 integrin. Scale bar = 15 μm (overlay) and 5 μm (overlay zoomed images). (C) Quantification of % Rab5 colocalized with β1 integrin from (B). Error bars represent s.e.m. from 57 cells from each condition from at least three separate experiments (***, $p<0.0001$, determined by Student's t-test). (D) HT1080 cells expressing APPL1 gRNA#3 or NT gRNA were immunostained for Rab5 and β1 integrin. Representative images are shown. Red/white boxes (single color/overlay) indicate regions shown at higher magnification. Red/white arrowheads (single color/overlay) indicate colocalization between Rab5 and β1 integrin. Scale bar = 15 μm (overlay) and 5 μm (overlay zoomed images). (E) Quantification of % Rab5 colocalized with β1 integrin from (D). Error bars represent s.e.m. from 75 cells from each condition from at least three separate experiments (***, $p<0.0001$, determined by Student's t-test).

interaction between APPL1 and Rab5 in regulating α5β1 integrin and cell migration.

APPL1 reduces the amount of active Rac in cells

Rab5 has been shown to promote Rac activation and thereby migration (Palamidessi et al., 2008). Since our results indicate that APPL1 negatively regulates the ability of Rab5 to promote migration, we hypothesized that APPL1 would inhibit Rac activity. To test this hypothesis, we examined the effect of APPL1 on cellular levels of activated Rac. HT1080 cells were plated on either FN or ColI and transfected with FLAG-Rac and either APPL1-GFP or GFP, and active Rac pulldown assays were performed. When APPL1-GFP-expressing cells were plated on FN, a 67% reduction in active Rac was observed, compared to cells expressing GFP (Figure 2.18 A,B). However, when cells were plated on ColI, no difference in the levels of active Rac was observed between cells expressing APPL1-GFP or GFP (Figure 2.18 C,D), which is consistent with our observations on APPL1-mediated migration. Rac activity was also assessed in APPL1 depleted cells. APPL1 gRNA#3 or NT gRNA cells were transfected with FLAG-Rac, and active Rac pulldown assays were performed. APPL1 gRNA#3 cells had increased levels of active Rac (~65%), compared to NT gRNA cells (Figure 2.18 E,F). Additionally, whereas expression of APPL1-GFP led to decreased Rac activity, APPL1-N308D-GFP had no effect on active Rac levels, compared to GFP-expressing cells (Figure 2.18 G,H). From these results, we conclude that APPL1 diminishes Rac activity in a Rab5-dependent manner.

APPL1 decreases activation of the Rac effector PAK

Since APPL1 decreased levels of activated Rac (Figure 2.18), we hypothesized that APPL1 would also negatively regulate activity of the Rac effector PAK. Phosphorylation of PAK at residue Thr423 is critical for its activation (Zenke et al., 1999); therefore, the phosphorylation state of PAK can be used to assess PAK activity. We immunostained cells expressing APPL1-

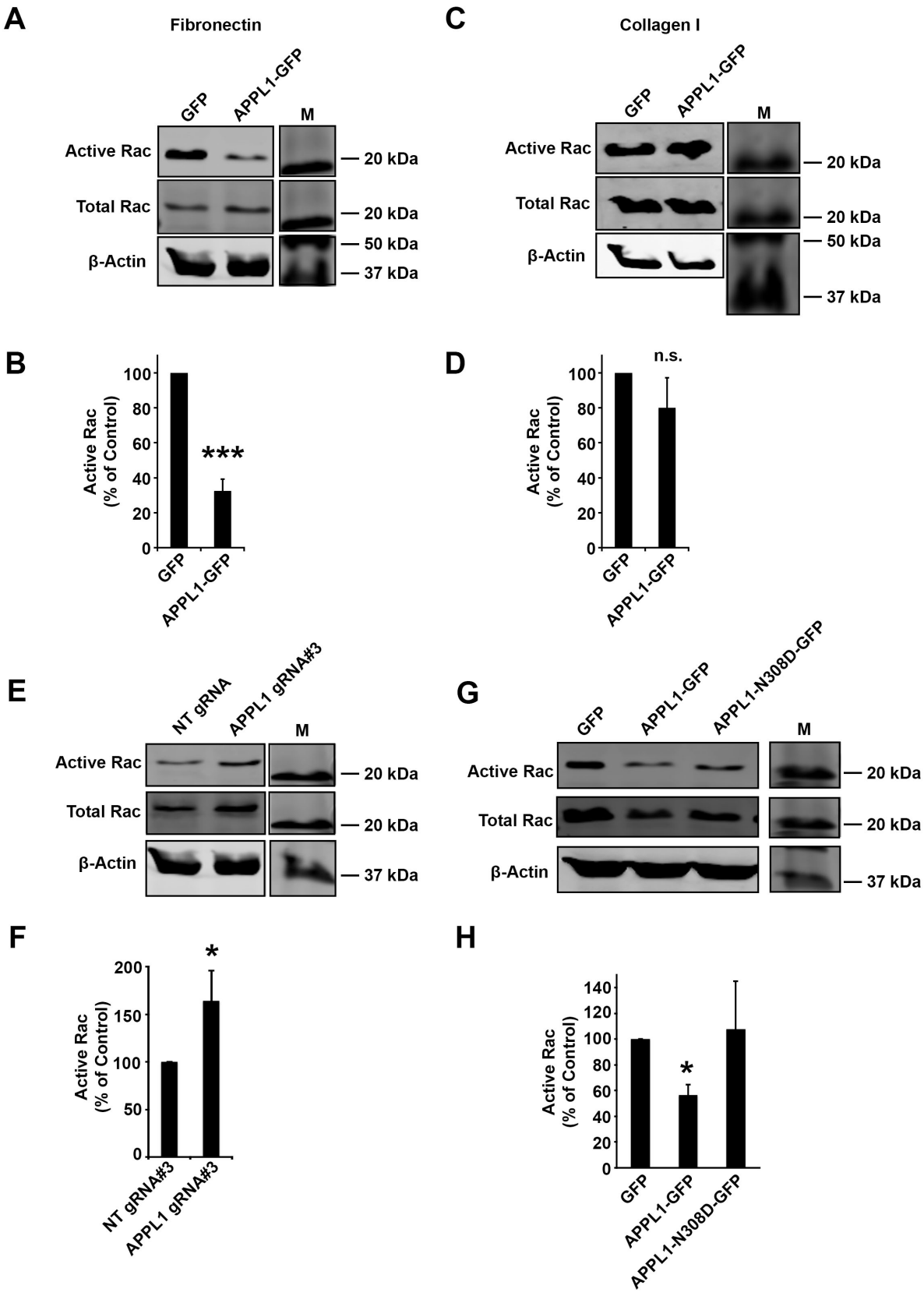
A
Fibronectin
GFP
APPL1-GFP
M
Active Rac
Total Rac
β-Actin
20 kDa
20 kDa
50 kDa
37 kDa
C
Collagen I
GFP
APPL1-GFP
M
Active Rac
Total Rac
β-Actin
20 kDa
20 kDa
50 kDa
37 kDa
B
Active Rac (% of Control)
100
80
60
40
20
0
***
GFP
APPL1-GFP
D
n.s.
Active Rac (% of Control)
100
80
60
40
20
0
GFP
APPL1-GFP
E
NT gRNA
APPL1 gRNA#3
M
Active Rac
Total Rac
β-Actin
20 kDa
20 kDa
37 kDa
G
GFP
APPL1-GFP
APPL1-N308D-GFP
M
Active Rac
Total Rac
β-Actin
20 kDa
20 kDa
37 kDa
F
*
Active Rac (% of Control)
200
150
100
50
0
NT gRNA#3
APPL1 gRNA#3
H
Active Rac (% of Control)
140
120
100
80
60
40
20
0
*
GFP
APPL1-GFP
APPL1-N308D-GFP

Figure 2.18. APPL1 decreases Rac activity. (A, C, E, G) HT1080 cells plated on either FN (A, E, G) or ColI substrate (C) were expressing GFP or APPL1-GFP (A, C), APPL1 gRNA#3 or NT gRNA (E), or GFP, APPL1-GFP, or APPL1-N308D-GFP (G) and transfected with FLAG-Rac1. GTP-bound (active) Rac was pulled down from lysates as described in Methods, and western blots were performed. Representative images are shown. Total Rac and β-actin are shown as loading controls. (B, D, F, H) Quantification of active Rac levels from (A, C, E, G), respectively. Error bars represent the s.e.m. from at least three separate experiments (*, $p<0.05$, ***, $p<0.0001$, n.s., not significant, $p=0.35$, determined by Student's t-test (B, D, F) or one-way ANOVA followed by Tukey's post hoc test(H)).

GFP or GFP with an antibody that recognizes PAK phosphorylated at Thr423 (pPAK^{Thr423}). When cells were plated on FN, the amount of pPAKThr^{423} (active PAK) was lower in cells expressing APPL1-GFP, compared to control (Figure 2.19 A,B). However, when cells were plated on ColI, APPL1-GFP expression had no effect on the levels of active PAK (Figure 2.19 D,E). APPL1-GFP expression had no effect on total PAK levels when plated either on either FN (Figure 2.19 A,C) or ColI (Figure 2.19 D,F). Consistent with our hypothesis, depletion of APPL1 resulted in a 1.4-fold increase in active PAK levels (Figure 2.19 G,H), but had no significant effect on total PAK levels (Figure 2.19 G,I). We confirmed our results biochemically, where APPL1 gRNA#3 cells led to a two-fold increase in pPAK (Figure 2.19 J,K), but did not alter total PAK expression (Figure 2.19 J,L), compare to NT gRNA cells. Together, these results implicate APPL1 in negatively regulating PAK activity.

If APPL1 acts upstream to negatively regulate PAK activation, then expression of a constitutively active form of PAK is predicted to abolish APPL1 regulation. To test this hypothesis, APPL1-GFP or GFP was co-expressed with a constitutively active variant of PAK [PAK-T423E (CA-PAK)] or control vector, and migration assays were performed. While APPL1-GFP-expressing cells migrated significantly slower than GFP-expressing cells when co-transfected with control vector, there was no significant difference in migration speed when APPL1-GFP was co-transfected with CA-PAK, compared to cells expressing GFP and CA-PAK (Figure 2.20 A), suggesting that CA-PAK abrogates the effect of APPL1 on cell migration. Similar results were observed for cells co-expressing APPL1-GFP and CA-PAK in 3D migration assays (Figure 2.20 B). These results support the hypothesis that APPL1 regulates migration by antagonizing PAK activity.

Because our results show that APPL1 mediates migration through its interaction with

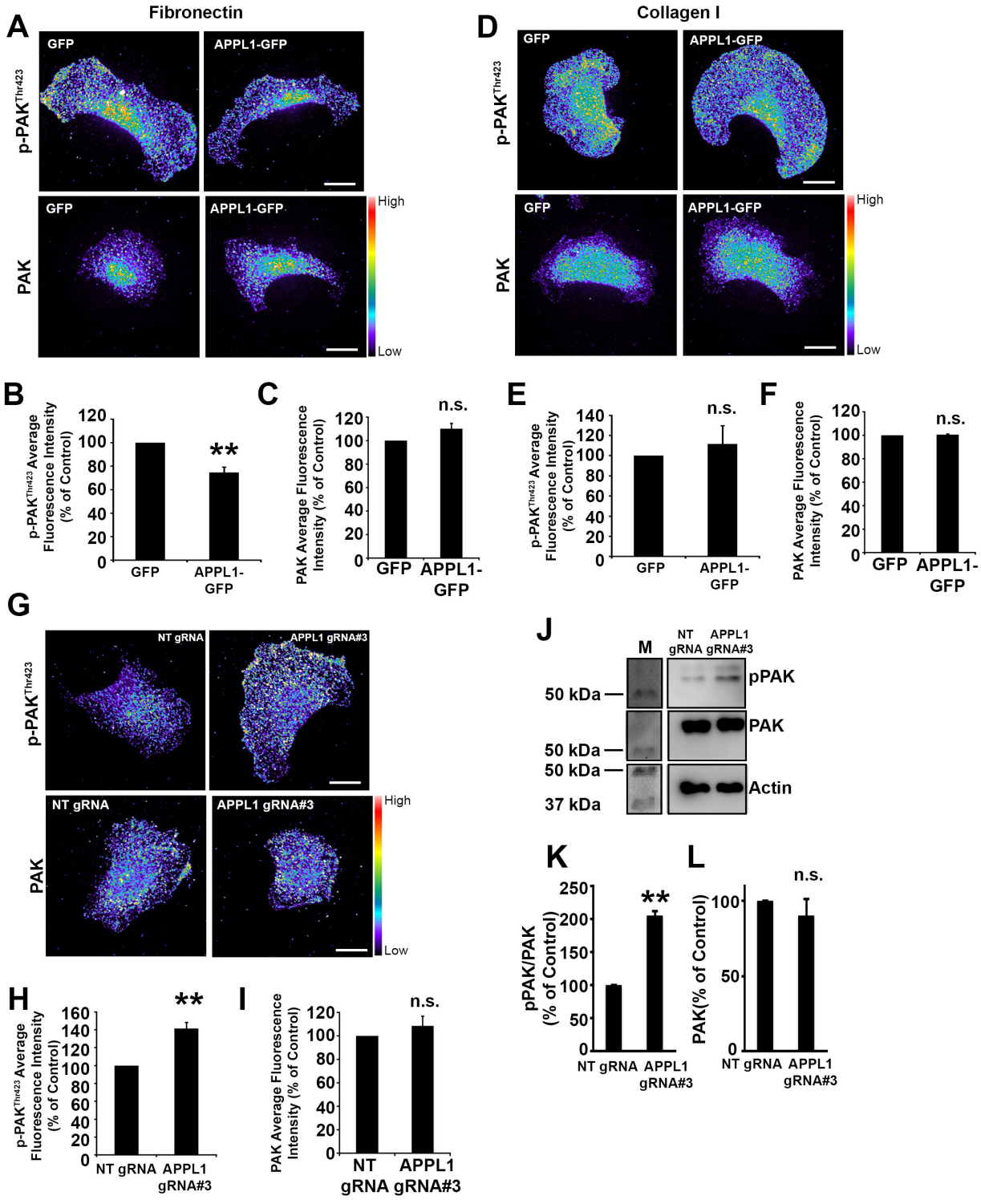

Figure 2.19. APPL1 decreases PAK activity in HT1080 cells. (A, D, G) HT1080 cells expressing GFP or APPL1-GFP (A, D) or APPL1 gRNA#3 or NT gRNA control cells (G) were plated on FN (A, G) or ColI (D) and immunostained for PAK phosphorylated at threonine 423

(p-PAK^{Thr423}) or total PAK. Representative images are pseudocolored for intensity. Scale bar = 15 μm. (B, E, H) Quantification of p-PAK^{Thr423} levels from (A, D, G), respectively, is shown as percent of control. Error bars represent the s.e.m. from at least 58 cells total from each condition from three separate experiments (*, $p<0.05$, **, $p\leq0.007$, n.s, not significant, $p=0.81$, determined by Student's t-test). (C, F, I) Quantification of total PAK levels from (A, D, G), respectively, shown as percent of control cells. Error bars represent the s.e.m. from >60 cells total from each condition from three separate experiments (n.s., not significant, $p=0.10$, 0.81, 0.09, respectively, determined by Student's t-test). (G) HT1080 cells expressing APPL1 gRNA#3 or NT gRNA (control) were lysed and western blots were performed for phosphorylated PAK (pPAK), total PAK, or β-actin (loading control). A representative image is shown. M, molecular weight marker; kDa, Kilodaltons.

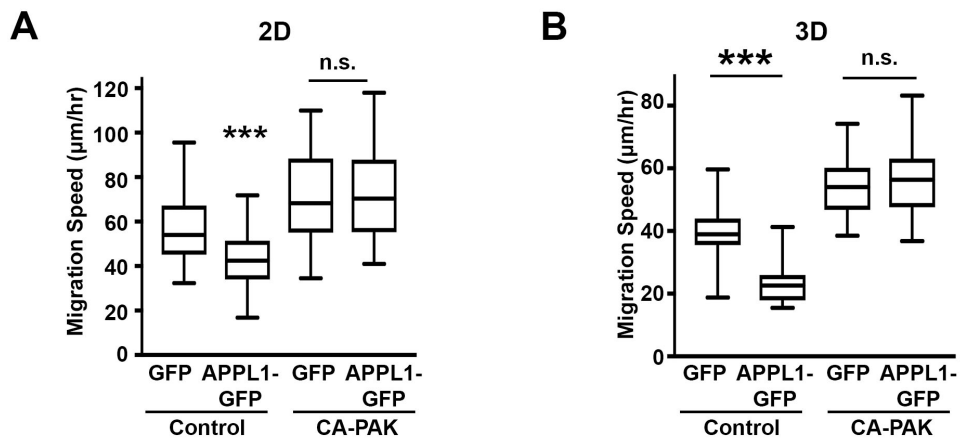

Figure 2.20. CA-PAK abrogates APPL1 inhibition of migration. (A) Box plot for 2D migration assays performed for cells co-transfected with APPL1-GFP or GFP and either constitutively active PAK (CA-PAK) or vector control. At least 25 cells total were analyzed from each condition from three separate experiments (***, $p<0.0001$, n.s., not significant, $p=0.63$, determined by Student's t-test). (B) Box plots showing migration speeds for cells in 3D matrices co-expressing either GFP or APPL1-GFP and either CA-PAK or control vector. 16-29 cells total were analyzed from each condition from at least three experiments (***, $p<0.0001$, n.s., not significant, $p=0.65$, determined by Student's t-test).

Rab5, a regulator of Rac activity, and APPL1 decreased Rac activity, we postulated that the negative effect of APPL1 on PAK would require Rab5 and endosomal localization. In both HT1080 (Figure 2.21) and MDA-MB-231 cells (Figure 2.22), APPL1-GFP, but not APPL1-AAA-GFP or APPL1-N308D-GFP, decreased the amount of active PAK (Figures 2.21 A,B,D,E and 2.22 A,B). Neither APPL1-GFP, nor mutants of APPL1-GFP, had any effect on total PAK levels in HT1080 (Figure 2.21 A,C,D,F) or MDA-MB-231 cells (Figure 2.22 A,C). These data point to a role for APPL1 in negatively regulating PAK activity through its interaction with Rab5.

PAK regulates cytoskeletal remodeling and focal adhesion dynamics at the leading edge of cells (Bokoch, 2003; Dharmawardhane et al., 1997); thus, we tested whether there were differences in PAK activity at the cell front in cells expressing APPL1-GFP. APPL1-GFP- and GFP-expressing cells were immunostained for p-PAK^{Thr423} and phalloidin. As shown in Figure 2.23 A, we observed lower levels of active PAK at the leading edge of the cell when APPL1-GFP was expressed. When we quantified PAK activity as a function of distance from the leading edge of cells (as determined by phalloidin staining), APPL1-GFP expression led to significantly lower levels of active PAK at the leading edge, and this difference was most pronounced at the very edge of the cell (Figure 2.23 B). Collectively, these results indicate that APPL1 diminishes PAK activity at the leading edge of migrating cells to impair cell migration.

Discussion

Vesicular trafficking is known to contribute to cell migration processes, but the mechanisms are poorly understood. Here, we show that the endocytic adaptor protein APPL1 modulates migration on FN by altering α5β1 trafficking and Rac and PAK signaling through the interaction of APPL1 with Rab5 (see model in Figure 2.24). Using a structure-function approach, we

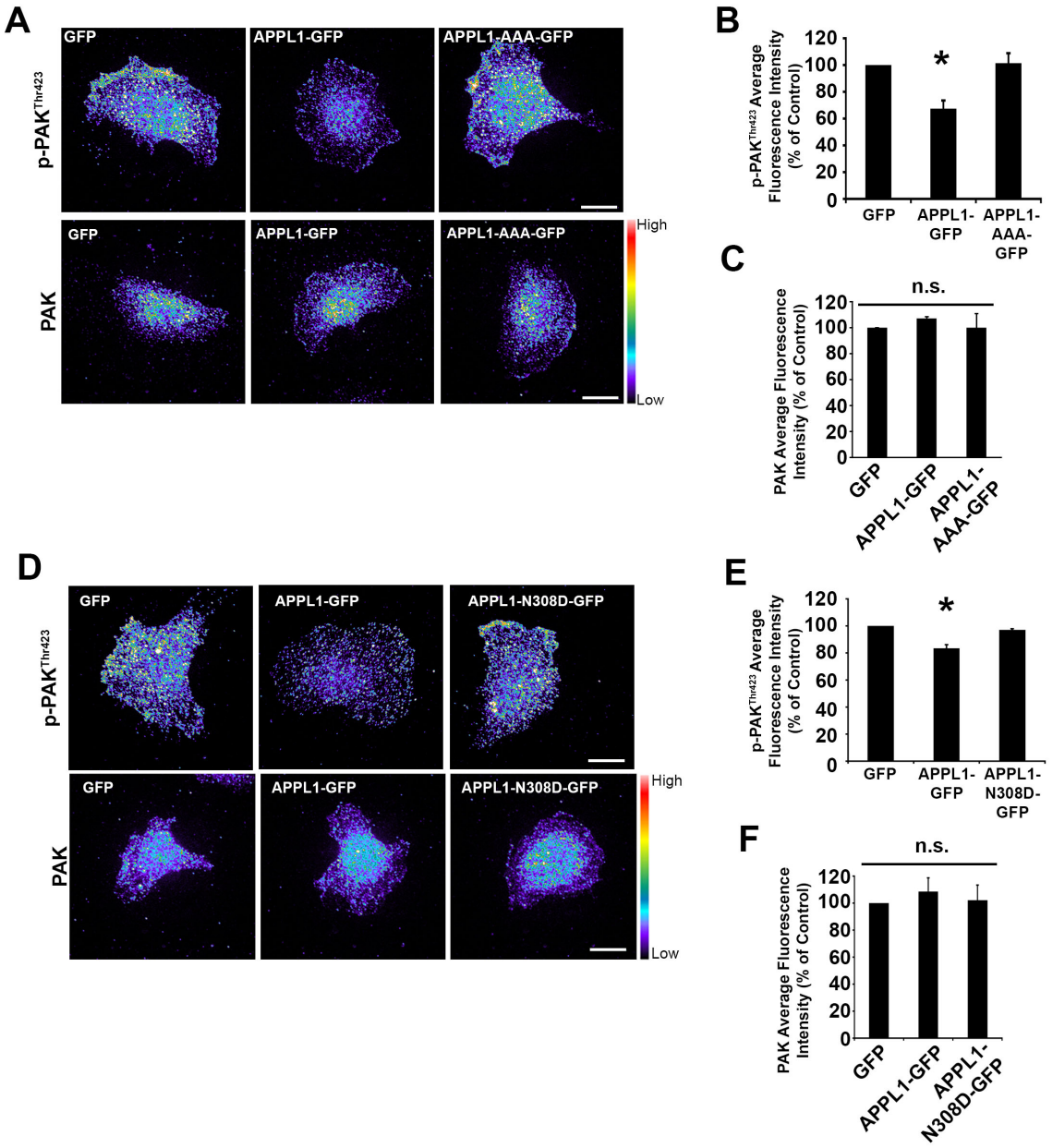

Figure 2.21. APPL1 decreases PAK activity, dependent on its endosomal localization and interaction with Rab5. (A, D) HT1080 cells expressing GFP, APPL1-GFP, and APPL1-AAA-GFP (A) or APPL1-N308D-GFP (D) were plated on FN and immunostained for PAK phosphorylated at threonine 423 (p-PAK^{Thr423}) or total PAK. Representative images are pseudocolored for intensity. Scale bar = 15 μm. (B, E) Quantification of p-PAK^{Thr423} levels from (A, D), respectively, is shown as percent of control. Error bars represent the s.e.m. from at least 58 cells total from each condition from three separate experiments (*, $p<0.05$, **, $p\leq0.007$determined by one-way ANOVA followed by Tukey's post hoc test). (C, F) Quantification of total PAK levels from (A, D), respectively, shown as percent of control cells (GFP). Error bars represent the s.e.m. from 60-70 cells total from each condition from at least

three separate experiments (n.s., not significant, p=0.77 and 0.84 from (C, F), respectively, determined by one-way ANOVA).

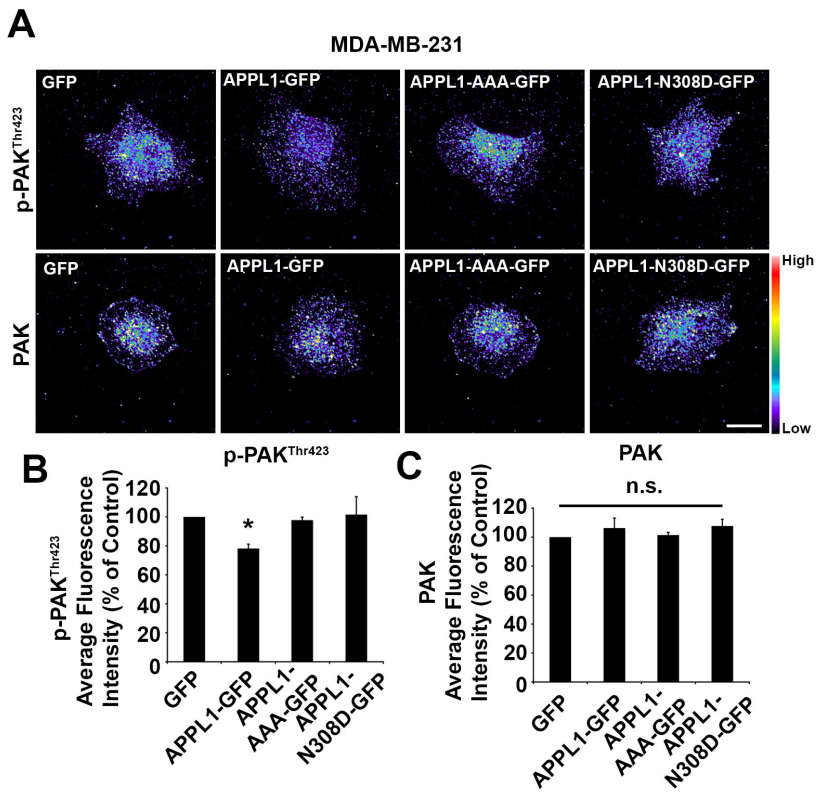

Figure 2.22. APPL1 decreases PAK activity in MDA-MB-231 cells. (A) MDA-MB-231 cells expressing GFP, APPL1-GFP, APPL1-AAA-GFP, or APPL1-N308D-GFP were immunostained for p-PAK^{Thr423} or total PAK. Images are pseudocolored for intensity. Scale bar = 15 μm. (B) Quantification p-PAK^{Thr423} levels from (A), shown as percent of control cells (GFP). Error bars represent the s.e.m. from 60-61 cells total from each condition from three separate experiments (**, p=0.002 determined by one-way ANOVA followed by Tukey's post hoc test). (C) Quantification of total PAK levels from (A), shown as percent of control cells (GFP). Error bars represent the s.e.m. from 78-80 cells total from each condition from at least three separate experiments (n.s., not significant, p=0.64, determined by one-way ANOVA).

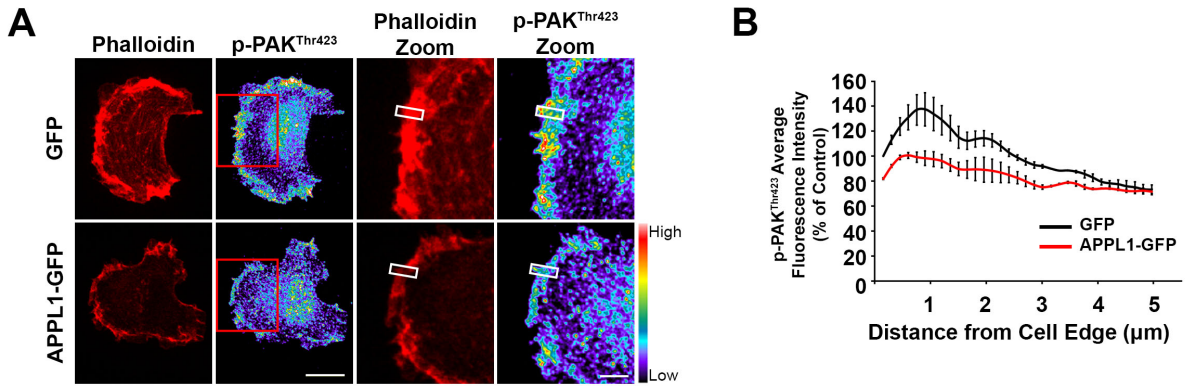

Figure 2.23. APPL1 inhibits PAK activity at the leading edge of migrating cells. (A) Cells expressing APPL1-GFP or GFP were immunostained for F-actin (phalloidin, red) and p-PAK^{Thr423} (pseudocolored for intensity). Red boxes in the second set of panels indicate regions shown at higher magnification in the third and fourth sets of panels. White boxes represent a 5μm region corresponding to the leading edge of the cell used for linescan analysis in this example. Left, scale bar = 15μm. Right, scale bar = 5μm. (B) Linescan analysis was performed at the leading edge of cells (identified by intense phalloidin staining) expressing APPL1-GFP or GFP. Quantification of the average fluorescence intensity is represented as a percent of control (GFP at 0μm). Error bars represent the s.e.m. from 45-50 cells total from each condition from three separate experiments ($Z=-5.012$, $p<0.0001$, determined by Wilcoxon signed rank test).

demonstrate that APPL1 interacts with Rab5 to inhibit Rab5-promoted migration. This inhibition results in higher surface levels of α5β1 integrin, due to decreased integrin endocytosis and increased integrin recycling. Furthermore, APPL1 decreases Rac activity, which, in turn, decreases PAK activity, particularly where PAK levels are most important at the leading edge. As a result, cell migration is impaired due to altered actin and adhesion dynamics.

APPL1 can act as the regulator for multiple pathways through its ability to engage in many protein-protein interactions and control trafficking. There is already evidence that APPL1 regulates crosstalk between multiple signaling pathways (Deepa and Dong, 2009; Rashid et al., 2009; Ryu et al., 2014). APPL1 mediates Akt signaling during cell migration, and our results point to a role for APPL1 in modulating Rac signaling as well. Both Akt and Rac signaling are critical for migration (Ridley, 2015; Xue and Hemmings, 2013) and have been implicated in integrin trafficking (Jacquemet et al., 2013a; Jacquemet et al., 2013b). Our data indicate that most APPL1 functions in migration require APPL1 to bind to Rab5, including α5β1 internalization, Rac activation, and PAK activation. These data suggest a feedback cycle between integrin trafficking and cellular signaling that depends on trafficking through Rab5 compartments and is controlled by APPL1 (Figure 2.24). We note that APPL1 also interacts with Rab21, which is similar in structure to Rab5. Rab21 has been implicated in regulating integrin trafficking to promote cell migration (Pellinen et al., 2006). Therefore, we cannot rule out the possibility that the interaction between APPL1 and Rab21 contributes to APPL1-mediated effects on cell migration.

Our results here together with our previous work (Broussard et al., 2012) indicate that APPL1 can be a negative regulator of cell migration, depending on the ECM substrate and the integrin repertoire (Figures 2.1, 2.3, and 2.5-2.6). By contrast, other studies have reported that

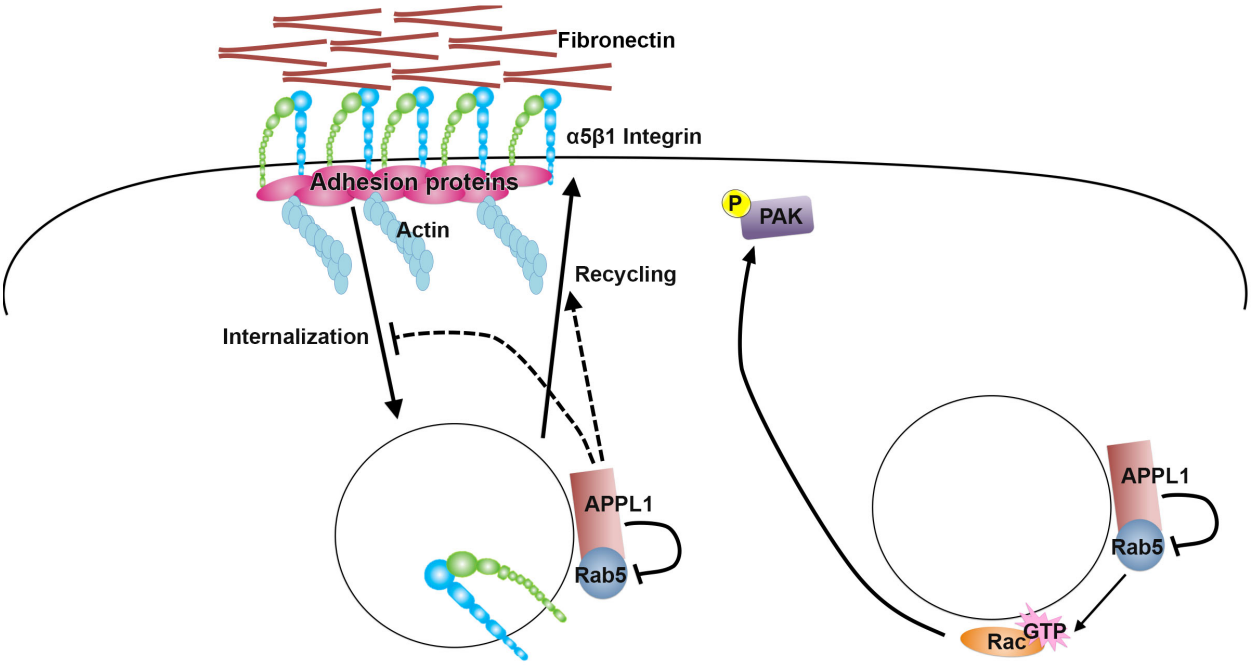

Figure 2.24. Model for APPL1 regulation of α5β1 integrin trafficking and Rac activation in migrating cells. Dynamic recycling of α5β1 integrin through Rab5-positive endosomes (circle) promotes adhesion dynamics and cellular migration. In the presence of FN, APPL1 modulates α5β1 integrin internalization and recycling (left), and Rac/PAK activation (right) through negative interactions with Rab5. Recycling of activated Rac (Palamidessi et al., 2008) to the plasma membrane may promote cellular migration, potentially by activating PAK at the leading edge.

APPL1 is a positive regulator of migration (Tan et al., 2016; Tan et al., 2010). There are some key differences between these studies that may explain the contradictory results, including the use of embryonic mouse cells (Tan et al., 2010) versus human cancer cells (Figures 2.1-2.4) (Broussard et al., 2012). Perhaps more importantly, the experiments performed by Tan et al. (2010) did not report the use of any ECM substrate coatings and instead induced migration with HGF. We did not explore the contribution of HGF to our phenotype. Based on the context-dependence of our finding (e.g. APPL1 regulates migration of cancer cells on FN but not ColI), we speculate that APPL1 might cause different phenotypes due to altered internalization of different migration-regulating receptors. Thus, whereas decreased internalization of α5β1 integrin leads to slower migration on FN, perhaps APPL1 also alters trafficking of the HGF receptor MET, which could lead to an increase in HGF-induced migration (Menard et al., 2014; Muller et al., 2013). Tan et al. (2016) also implicated APPL2 in cell migration, acting redundantly with APPL1. However, although APPL2 is expressed in HT1080 cells, a 50% knockdown of APPL2 alone, or in APPL1-depleted cells, showed no effect on migration speed on FN (Figure 2.4 C). More studies should be performed in the future to reconcile these differences.

Our findings indicate that APPL1 regulates both integrin internalization and recycling. It is likely that APPL1 blocks internalization by inhibiting Rab5 from internalizing integrin, as expression of APPL1-N308D-GFP was unable to rescue the internalization phenotype in APPL1 gRNA#3 cells (Figure 2.11 D,E). Indeed, our results indicate that APPL1 affects colocalization of Rab5 with β1 integrin (Figure 2.17 B,C). Previous reports have implicated Rab5 and GIPC1 in promoting α5β1 integrin endocytosis from adhesion sites in endothelial cells, and it was suggested that APPL1 could act as a positive regulator in this process (Valdembri et al., 2009).

In contrast, our results suggest that APPL1 is a negative regulator of integrin internalization, and this is dependent on its interaction with Rab5. Intriguingly, deletion of the PTB domain in APPL1 also failed to rescue control levels of integrin internalization in rescue experiments (Figure 2.11 D,E), consistent with the previously reported requirement for this domain to regulate cell migration and adhesion turnover (Broussard et al., 2012). As GIPC1 interacts with the C-terminus of the APPL1 PTB domain (Lin et al., 2006) and also binds α5 integrin (Tani and Mercurio, 2001), and APPL1 also interacts with Rab5, this is an interesting potential pathway for APPL1-mediated integrin trafficking. In addition, PTB domains of various proteins are known to bind NPxY motifs (Schlessinger and Lemmon, 2003) and β1 integrin has two NPxY motifs that regulate internalization and recycling (Bottcher et al., 2012; Margadant et al., 2012; Steinberg et al., 2012). Further study is required to determine if APPL1 acts through any of these mechanisms.

APPL1 has also been implicated in sorting proteins for recycling (Kalaidzidis et al., 2015), consistent with our observation that APPL1 promotes recycling of α5β1 integrin (Figure 2.13 B-F). APPL1 colocalizes with some Arf6 compartments that contain the GAP "ArfGAP with RhoGAP Domain, Ankyrin Repeat and PH Domain 2" (ARAP2). ARAP2 regulates transit of α5β1 integrin from APPL1 to EEA1 compartments, and overexpression of ARAP2 promotes the formation of large adhesions (Chen et al., 2014), a phenotype similar to that of cells overexpressing APPL1 (Broussard et al., 2012). A future study should test whether the APPL1-dependent effects on integrin recycling are sensitive to ARAP2 levels.

Rab5 has been shown to promote Rac activation on endosomes (Diaz et al., 2014a; Hagiwara et al., 2009; Palamidessi et al., 2008; Sandri et al., 2012; Torres et al., 2010). We found that APPL1 negatively regulates Rac (Figure 2.18) and its effector, PAK (Figures 2.19-

2.23), depending on the interaction of APPL1 with Rab5. The regulation of Rac activation is linked to integrin trafficking (Sandri et al., 2012), as APPL1 decreased active Rac levels only when cells were plated on FN, and not on ColI (Figure 2.18 A-D). Since α5β1 integrin is internalized through caveolar-dependent endocytosis (Caswell and Norman, 2006; Shi and Sottile, 2008) and Rab5 and is required for caveolin-dependent Rac activation (Diaz et al., 2014a; Hagiwara et al., 2009), this could be a potential mechanism for APPL1-regulation of both Rac activity and integrin trafficking.

Interestingly, overexpression of APPL1 specifically decreases PAK activation at the leading edge of cells (Figure 2.23 A,B) where PAK activity is most important for cell migration (Broussard et al., 2008; Mayor and Etienne-Manneville, 2016; Nayal et al., 2006). It is currently unclear how PAK at the leading edge is regulated by APPL1-mediated changes in endosomal sorting. One possibility is that PAK is activated in Rab5-positive endosomes by Rac and recycled back to the cell surface; APPL1 might inhibit both the activation and the recycling. Alternatively, PAK could be activated *in situ* at the leading edge by recycled Rac (Palamidessi et al., 2008). As PAK is a key regulator of adhesion turnover (Delorme-Walker et al., 2011; Kiosses et al., 2002; Santiago-Medina et al., 2013; Webb et al., 2002), dynamic regulation through trafficking may ensure that it is present in the appropriate spatiotemporal manner (Disanza et al., 2009).

APPL1 is either deleted or mutated in multiple cancers (Cerami et al., 2012; Gao et al., 2013; Saleh et al., 2016), an observation consistent with our data suggesting that APPL1 is a negative regulator of cancer cell migration. In other cancers, APPL1 overexpression accompanied by an increase in Rab5 expression (Bidkhori et al., 2013; Johnson et al., 2014; Zhai et al., 2016), implying that the ratio of these interacting proteins may be important for the cancer

phenotype. In summary, our study supports a model where APPL1, in a FN-dependent manner, acts as a negative regulator of cancer cell migration through inhibition of Rab5-dependent processes, namely α5β1 integrin trafficking and Rac/PAK activation.

CHAPTER III

CONCLUSIONS AND FUTURE DIRECTIONS

Cancer cell migration is one of the initial steps in metastasis, which is a leading cause of death in cancer patients. The regulation of cell migration is complex and tightly coordinated. A multitude of signaling pathways contribute to cell migration, and crosstalk between these pathways is essential to the establishment and maintenance of cell polarization and movement. Additionally, increasing evidence suggests that vesicular trafficking can spatially restrict key proteins involved in cell migration. The integration of signaling and trafficking is coordinated through adaptor proteins, such as APPL1, is an intriguing area of research that is still not well understood.

APPL1 plays a critical role in vesicular trafficking and signaling on endosomes (Kalaidzidis et al., 2015; Schenck et al., 2008). However little is known about how APPL1 regulates these events during cell migration. In this thesis, my colleagues and I aimed to elucidate the mechanisms by which APPL1-mediated signaling and endosomal trafficking suppresses cancer cell migration. Results presented here support a novel model wherein APPL1 inhibits migration by interfering with integrin trafficking and Rac signaling through a Rab5-dependant mechanism.

APPL1 overexpression decreases migration speeds in HT1080 (Figure 2.1) and MDA-MB-231 cells (Figure 2.2). Given that these cells are derived from human cancers of different origins, fibrosarcoma and breast adenocarcinoma, respectively, this similar behavior suggests that the effects of APPL1 represent a general mechanism for the regulation of cancer cell migration. There is disagreement on whether APPL1 is a positive or negative regulator of cell

migration. For example, the work in this thesis shows that APPL1 negatively regulates cell migration on FN (but not ColI) (Figure 2.5), while studies from APPL1 knockout mice showed impaired migration after stimulation with HGF, suggesting a stimulatory role for APPL1 (Tan et al., 2016; Tan et al., 2010). Furthermore, while studies from the knockout mouse found a redundant role for APPL2 in cell migration, I observed that knockdown of APPL2 expression had no effect on migration (Figure 2.4), suggesting that APPL2 either has no role in cell migration or its effect is cell type or context-specific. However, complete knockdown was not achieved, and so it is possible that small amounts of APPL2 may affect cell migration. I hypothesize that APPL1 regulates migration in a context-dependent manner, depending on the trafficking of different receptors. Increased integrin recycling by APPL1 (Figure 2.13) leads to higher surface levels of integrin (Figures 2.6, 2.7) and slower migration (Figure 2.1). However, recycling of the HGF receptor, c-MET, is necessary for sustained Rac activation (Fan et al., 2016; Xiang et al., 2017); if APPL1 increases recycling of MET, the result could be increased migration speeds. Further studies are needed to fully understand the mechanisms underlying APPL regulation of cell migration.

Exploring 3D cell migration has become more appreciated in the past decade, as there is increasing evidence that regulation of cell migration in 2D conditions is not always representative of how cell migration is regulated *in vivo* (Beningo et al., 2004; Cukierman et al., 2001; Doyle and Yamada, 2016; Grinnell, 2003). However, APPL1 had the same effect on migration in 3D environments as on 2D substrates (Figure 2.2). APPL1 has been previously shown to inhibit adhesion turnover on 2D substrates (Broussard et al., 2012). It would be interesting to use the platform, PAASTA, developed to analyze adhesions in 3D (discussed in Appendix A) to probe the role of APPL1 in 3D adhesion turnover (Broussard et al., 2015).

Interestingly, changes in APPL1 expression only affected cell speed, and did not alter directionality or persistence of migrating cancer cells in 2D (Figures 2.1,2.3) or 3D (Figure 2.2). Rho GTPases have been linked to directional persistent migration; Rac activity drives directional migration, while RhoA is associated with random motility (Bergert et al., 2012; Jacquemet et al., 2013a; Pankov et al., 2005; Petrie et al., 2009). The unaltered directionality in APPL1 overexpressing cells is consistent with our unpublished data showing no difference in RhoA activity in APPL1-GFP-expressing cells. However, given that APPL decreases Rac activation (Figure 2.18), it is surprising that APPL1 has no affect on directionality. The cell migration assays performed used cells that demonstrate primarily random patterns of migration. Moreover, these migration assays did not employ any chemotactic (chemical gradient) or haptotactic (ECM gradient) stimuli. Perhaps experiments directly testing directional migration, such as wound closure or boyden chamber assays would reveal whether APPL1 plays any role in persistent migration (Justus et al., 2014).

We show for the first time that the effect of APPL1 on migration is dependent on α5β1 integrin. Ectopic expression of APPL1 decreased migration speed when cells were plated on Fn, an ECM substrate that binds α5β1 integrin, but not on ColI, a substrate lacking α5β1 interaction (Figure 2.5 A,B). Interfering specifically with α5 integrin function also abrogated APPL1-mediated effects on migration (Figure 2.5 D). Together, these results make it unlikely that APPL1 affects migration through ColI-binding integrins. αVβ3 integrin also binds to Fn (Morgan et al., 2009), raising the possibility that αVβ3 integrin contributes to APPL1-mediated migration. However, blocking α5 integrin abrogates the APPL1-mediated effects on migration, suggesting that αVβ3 is insufficient to mediate these outcomes. Moreover, surface levels of β3

integrin were unaffected by APPL1 overexpression or depletion (Figure 2.6). Therefore, we conclude that the APPL1-mediated effect on migration is dependent on α5β1 integrin.

Broussard et al. (2012) demonstrated that cells overexpressing APPL1 form large FAs that take longer to assemble and disassemble than in control cells, thereby decreasing adhesion turnover. This observation is consistent with our results showing increased surface levels of active and total α5β1 integrin in APPL1-GFP-expressing cells (Figures 2.6, 2.7). I hypothesize that the increased amount of integrin on the cell surface makes the cells 'sticky.' Rapid adhesion turnover is crucial for cell migration (Broussard et al., 2008; Webb et al., 2002), and so an imbalance of integrins on the cell surface may slow cell migration. Photoactivation data presented here (Figure 2.8) is also in agreement with the effects of APPL1 on adhesion turnover. In cells with increased APPL1 expression, α5 integrin remains in adhesions for longer periods of time, explaining how APPL1 increases integrin surface level expression and suggesting that these adhesions are not turning over efficiently.

Excess APPL1 drives lower levels of internal α5 and β1 integrin (Figure 2.10); conversely, depletion of APPL1 increases α5β1 integrin internalization (Figure 2.11). It is unlikely that APPL1 affects αVβ3 integrin trafficking, as APPL1 had no effect on αVβ3 integrin surface levels (Figure 2.6). Additionally, αVβ3 and α5β1 integrins usually traffic through distinct pathways (Caswell and Norman, 2006; Caswell et al., 2009; Margadant et al., 2011; Paul et al., 2015b; Pellinen and Ivaska, 2006; Valdembri and Serini, 2012). Surprisingly, APPL1 decreases internalization of both active and total α5β1 integrin (Figure 2.10). This dual effect is unusual, given that active and inactive integrins tend to be internalized through different mechanisms (Paul et al., 2015b), although we have not explored the possibility that APPL1 mediates internalization of active and inactive integrin through different mechanisms. Moreover, our data

only specifically addresses the recycling of total α5β1 integrin (Figure 2.13). We have not explicitly shown that APPL1 increases recycling of both active and inactive α5β1 integrin.

Integrin endocytosis generates a pool of internal integrins that can be readily recycled to form new adhesions or destabilize adhesions. APPL1 decreases integrin internalization (Figure 2.10), which could explain why APPL1 overexpression decreases adhesion assembly and disassembly (Broussard et al., 2012). Interestingly, the FAK-Src complex recruits microtubules to FAs through interaction between FAK and dynamin, a GTPase involved in clathrin-dependent endocytosis. These interactions promote β1 integrin internalization and FA disassembly (Ezratty et al., 2005; Nagano et al., 2012; Nagano et al., 2010). Broussard et al. (2012) showed that APPL1 inhibits adhesion turnover in a Src-dependent mechanism. This observation, in combination with our results implicating APPL1 as a negative regulator of integrin endocytosis, could represent a potential mechanism that includes Src, FAK, dynamin, and APPL1.

The PTB domain of APPL1 is important for regulating adhesion turnover (Broussard et al., 2012). Additionally, our results have shown that APPL1 also requires its PTB domain to inhibit integrin internalization (Figure 2.11 D,E). APPL1 binds multiple proteins through its PTB domain, and so there are multiple protein-protein interactions that could contribute to integrin trafficking by APPL1. An intriguing possibility is that APPL1 could interact with the cytoplasmic tail of β1 integrin, although there is no direct evidence for this yet. APPL1 colocalizes with a subset of β1 integrin and requires its PTB domain to regulate integrin internalization. PTB domains of various proteins bind NPxY motifs (Calderwood et al., 2003), and there are two of these motifs in β1 integrin that are crucial to regulation of its trafficking by interaction with talin and kindlin (Margadant et al., 2012). Both NPxY motifs are required for internalization of β1 integrin, and one of these motifs is required for integrin recycling

(Margadant et al., 2012). Similarly, Dab2, Eps8, and Numb also bind NPxY motifs of the β1 integrin cytoplasmic domain to regulate clathrin-dependent endocytosis (Calderwood et al., 2003; Dulabon et al., 2000; Paul et al., 2015b). Competitive binding of APPL1 with β1 integrin to block any of these proteins (although this would not directly require Rab5) would be a potential mechanism to explain how APPL1 inhibits β1 integrin endocytosis or stimulate integrin recycling.

APPL1 also requires interaction with Rab5 to decrease integrin internalization. Expression of an APPL1 point mutant that cannot interact with Rab5, APPL1-N308D, has no effect on α5 integrin dynamics or integrin endocytosis (Figure 2.11 D,E). Our migration data is in agreement with these results, as APPL1 inhibits Rab5-induced migration (Figure 2.15 B). Likewise, APPL1 expression affects the association of Rab5 with β1 integrin. Overexpression of APPL1 decreases colocalization between Rab5 and β1 integrin (Figure 2.17 B,C), and APPL1 knockout increases this association (Figure 2.17 D,E). Rab5 interacts with β1 integrin, either directly or indirectly (Mendoza et al., 2013; Pellinen et al., 2006; Torres et al., 2010), and also associates with paxillin and vinculin in adhesions. Rab5 promotes adhesion disassembly, potentially through endocytosis of integrins. This was shown by elegant live cell studies, which showed that Rab5-positive endosomes localized to adhesions sites, and adhesion disassembly quickly followed (Mendoza et al., 2013). I hypothesize that APPL1 impairs adhesion turnover and decreases cell migration by blocking the Rab5/β1 interaction through one or more of the following mechanisms: impeding integrin endocytosis, increased integrin recycling, or sequestering of Rab5 from compartments that traffic β1 integrin.

Recycling assays revealed that APPL1 increases α5β1 integrin recycling (Figure 2.13 B-F). Increased integrin recycling cannot entirely explain the lower internal levels of α5β1 integrin,

as lower internal levels of integrin are observed even in the presence of primaquine, a recycling inhibitor, indicating that APPL1 both decreases internalization and increases recycling (Figure 2.13 A). This result begs the question of how APPL1 affects both internalization and recycling of α5β1 integrin. There are multiple possible mechanisms that require further study, and are discussed in detail below.

APPL1 is localized to an Arf6 compartment containing the GAP ARAP2, which has been shown to regulate β1 integrin trafficking. ARAP2 promotes internalization and inhibits recycling of β1 integrin, which is the opposite phenotype from our results with APPL1. ARAP2 impedes recycling by inhibiting another Arf6 GAP, ACAP1, and blocking transport to ACAP1/Arf6 positive recycling endosomes. β1 integrin is instead rerouted to from Arf6/ARAP2/APPL1 compartments to EEA1 endosomes, thus delaying recycling (Chen et al., 2014). ARAP2 has the opposite effect on integrin trafficking from our results on APPL1. Since APPL1 has is involved in sorting and recycling (Gan et al., 2013; Kalaidzidis et al., 2015), it is feasible that while ARAP2 inhibits, APPL1 may promote Arf6-mediated integrin recycling. Interestingly, Akt activates ACAP1 (Li et al., 2005) Since APPL1 has also been shown to inhibit Akt activity during cell migration (Broussard et al., 2012) and to associate with ARAP2 (Chen et al., 2014), these interactions may suggest a complex interplay between APPL1, Arf6, and Arf GAPs to regulate both integrin trafficking.

APPL1 interacts not only with Rab5, but also Rab21, which is similar in structure to Rab5 (Zhu et al., 2007). Rab21 has been implicated in regulating integrin recycling to promote cell migration (Pellinen et al., 2006). Therefore, we cannot rule out the possibility that the interaction between APPL1 and Rab21 contributes to APPL1-mediated effects on cell migration. In addition, the role of Rab5 in integrin recycling was not directly tested. Perhaps APPL1 hinders

Rab5-mediated integrin endocytosis and promotes Rab21-mediated integrin recycling. The binding sites for Rab5 and Rab21 with APPL1 have been well characterized (Zhu et al., 2007), and so a structure-function approach could be employed to test this hypothesis. Specifically, mutation of APPL1 residue 318 from Alanine to Aspartic Acid was shown to inhibit APPL1 interaction with Rab21, but not Rab5 (Zhu et al., 2007). The effects of Rab5 and Rab21 interaction with APPL1 regulation of integrin trafficking, adhesion turnover, and cell migration could be determined by utilizing this mutant in combination with the APPL1-N308D point mutant.

Our results strongly suggest that APPL1 regulates cell migration through its interaction with Rab5 (Figures 2.14, 2.15). Both the endosomal localization of APPL1 and its interaction with Rab5 are required for APPL1 to inhibit cell migration (Figure 2.14). Expression of APPL1-GFP in APPL1-depleted cells can rescue the migration phenotype; APPL1-AAA-GFP (endosomal localization mutant) and APPL1-N308D-GFP (Rab5 binding mutant) cannot (Figure 2.15). Consistent with previous studies, our results demonstrate that Rab5 is a positive regulator of migration (Diaz et al., 2014a; Mendoza et al., 2014; Torres et al., 2010; Torres and Stupack, 2011). When APPL1 is co-expressed with Rab5, APPL1 inhibits the Rab5-mediated increase in migration speed. However, when Rab5 is co-expressed with APPL1-N308D-GFP, which cannot interact with Rab5, Rab5 retains its ability to increase migration, indicating that APPL1 requires interaction with Rab5 to inhibit Rab5-mediated migration. This effect is rescued by co-expressing a Rab5 mutant, Rab5-L38R-mCherry, that reestablishes the interaction with APPL1-N308D-GFP (Figure 2.15). We conclude that APPL1 inhibits Rab5-mediated migration through direct interaction of the two proteins.

The question remains as to how APPL1 inhibits Rab5 function. It is unlikely that APPL1

inhibits Rab5 by recruiting a GAP, as APPL1 only binds Rab5-GTP (Zhu et al., 2007) and my unpublished data show that APPL1 is still able to decrease migration speeds of HT1080 cells when co-expressed with CA-Rab5 (Rab5-Q79L), which is deficient in GTP hydrolysis (Figure 3.1). Interestingly, APPL1 is either deleted or mutated in multiple cancers (Cerami et al., 2012; Gao et al., 2013; Saleh et al., 2016), an observation consistent with our data suggesting that APPL1 is a negative regulator of cancer cell migration. In other cancers, APPL1 overexpression is accompanied by an increase in Rab5 expression (Bidkhori et al., 2013; Johnson et al., 2014; Zhai et al., 2016), implying that the ratio of these interacting proteins may be important for the cancer phenotype. One plausible explanation is that APPL1 sequesters Rab5 from other Rab5 effectors that would promote migration. APPL1 binds to both of the switch regions of Rab5; Rabaptin5 also binds the switch II region, and can compete for binding with APPL1 (Zhu et al., 2007). Moreover, the binding sites for other Rab5 effectors have not been well characterized. Therefore, it is possible that APPL1 competes with other effectors for Rab5 binding, which could inhibit Rab5-mediated cell migration. I hypothesize that APPL1 helps to 'put on the brakes' and prevent Rab5-induced cell migration. Since cell migration is a tightly regulated process, APPL1 could prevent Rab5 from stimulating migration under inappropriate circumstances. Misregulation of APPL1 and Rab5 would therefore lead to increased cell migration, which would be detrimental in cancer.

Rab5 has been identified as a signaling GTPase, and is required for Rac activation on endosomes (Diaz et al., 2014b; Lanzetti et al., 2004; Mendoza et al., 2014; Palamidessi et al., 2008; Torres and Stupack, 2011). Expression of APPL1-N308D had no effect on Rac activation (Figure 2.18 G,H), indicating that APPL1 decreases Rac activity in a Rab5-dependent manner. This result is in agreement with our migration assays that suggest APPL1 inhibits Rab5-induced

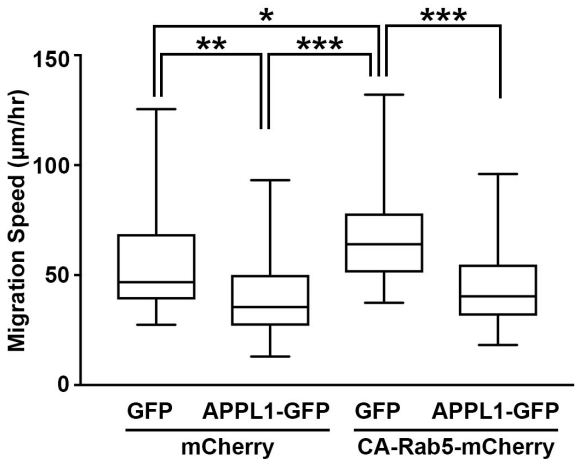

Figure 3.1. APPL1 inhibits active Rab5-induced migration. Box plot shows migration speeds for HT1080 cells that were co-transfected with GFP or APPL1-GFP and either mCherry or CA-Rab5-mCherry and used in migration assays. At least 20 cells total were analyzed from each condition from at least three separate experiments (*, $p<0.05$, **, $p<0.005$, ***, $p<0.0001$, determined by one-way ANOVA followed by Tukey's post hoc test).

migration (Figure 2.15). Additionally, APPL1 only affected Rac activation when cells were plated on FN (Figure 2.18 A-D). This result is particularly interesting, given that integrin trafficking has also been implicated in regulating Rho GTPase signaling (Del Pozo et al., 2002; Grande-Garcia et al., 2005). A Ras/RIN2/Rab5 signaling module has been described that promotes the endocytosis of active β1 integrins and subsequently recruits the GEF Tiam1 to early endosomes to activate Rac (Sandri et al., 2012). APPL1 inhibits both β1 integrin endocytosis and Rac activation, suggesting that APPL1 is a negative regulator of Ras/RIN2/Rab5-induced integrin trafficking and Rac activation.

Rab5 promotes Rac activation through recruitment of the Rac-GEF Tiam1 (Palamidessi et al., 2008). Although it is not currently known whether Rab5 directly or indirectly binds Tiam1, it is possible that competition by APPL1 could inhibit Tiam1 interaction with Rab5 or a complex containing Rab5. Downstream of Rac in this pathway is its effector, PAK. APPL1 decreased active PAK levels dependent on endosomal localization (Figure 2.21 A,B), Rab5 interaction (Figure 2.21 D,E), and in an ECM-dependent manner (Figure 2.19). Co-expression of APPL1 with CA-PAK, in both 2D and 3D conditions, abolished the APPL1-mediated decrease in migration (Figure 2.20). Because Rab5-induced Rac activation leads to trafficking of Rac to the leading edge of the cell (Palamidessi et al., 2008), it is likely that APPL1 affects Rac and PAK activity in adhesions. Rac and PAK are regulators of adhesion turnover through multiple mechanisms. PAK is part of the GIT1-PIX-PAK signaling module that phosphorylates and activates paxillin, which promotes adhesion turnover. This signaling axis also leads to downstream activation of Rac, creating a positive-feedback loop (Nayal et al., 2006). Furthermore, Rac activates PAK, which phosphorylates inactivates stathmin, a microtubule binding that prevents microtubule polymerization leading to microtubule catastrophe.

Consequently, PAK promotes microtubule growth and FA disassembly by preventing microtubule catastrophe at the leading edge of cells (Bokoch, 2003; Daub et al., 2001; Szczepanowska, 2009; Wittmann et al., 2003). The positive effects of Rac and PAK on adhesion turnover can explain our results in downstream effects of APPL1 on cell migration. Overexpression of APPL1 specifically decreases PAK activation at the leading edge of cells (Figure 2.23), where Rac and PAK activity are most important for cell migration.

Our work has investigated the role of APPL1 in endocytic trafficking and signaling processes important to cell migration. However, little is known about APPL1 regulation itself, and what role such regulation might play in cell migration. Thirteen phosphorylation sites have been identified in APPL1 by mass spectrometry. Four of these phosphorylation sites are located in important functional domains, including one in the BAR domain (Ser97/98), two at the edge of the PH domain (Ser374 and Tyr378), and one in the PTB domain (Tyr604) (Gant-Branum et al., 2010). Whether these phosphorylation sites are physiologically important to APPL1 has yet to be discerned. Based on the location of these phosphorylation sites, they could affect APPL1 dimerization, interaction with Rab5, Akt signaling, or interaction of PTB domain-binding proteins. Only one study has investigated the functional consequences of APPL1 phosphorylation, and showed that phosphorylation of APPL1 at Ser430 is important for regulating insulin signaling (Liu et al., 2012). Mutagenesis studies could provide insight into the importance of APPL1 phosphorylation, and whether regulated phosphorylation has any effect on cell migration.

In summary, our work reveals a novel mechanism by which APPL1-mediated signaling and endosomal trafficking suppress cancer cell migration. Because our results show that APPL1 requires its trafficking functions to regulate migration and previous work as well as our work has

shown that APPL1 signaling is important for its ability to regulate migration, I propose that APPL1 serves as a crucial link between signaling and trafficking pathways that are important to cell migration. While our work has provided insight into some of the cellular processes regulated by APPL1, there is still much that remains to be explored. Further studies into APPL1 will lead to insights in the molecular mechanisms underlying cell migration.

APPENDIX A

AUTOMATED ANALYSIS OF CELL-MATRIX ADHESIONS IN 2D AND 3D ENVIRONMENTS

Joshua A. Broussard[1,‡], Nicole L. Diggins[1,‡], Stephen Hummel[2] , Walter Georgescu[2,3,4], Vito Quaranta[2,3,5], and Donna J Webb[1,3,5]

[1]Department of Biological Sciences and Vanderbilt Kennedy Center for Research on Human Development
[2]Center for Cancer Systems Biology at Vanderbilt
[3]Vanderbilt Institute for Integrative Biosystems Research and Education (VIBRE)
[4]Department of Biomedical Engineering
[5]Department of Cancer Biology, Vanderbilt University, Nashville, Tennessee 37235.

‡These authors have contributed to an equal extent.

N.L.D. analyzed the data for 3D adhesions, contributed to Figures A.7-A.9, performed all statistical analysis, and wrote the paper. J.A.B. prepared biological materials, analyzed data for 2D adhesions, contributed to Figures A.3-A.6, and edited and revised the paper. S.H. and W.G. generated the platform for the automated analysis, segmentation, and tracking of adhesions (PAASTA) and contributed to Figures A.1-A.2.

This article has been published under the same title in *Scientific Reports*. 2015 January 29; 5, 8124.

Abstract

Cell-matrix adhesions are of great interest because of their contribution to numerous biological processes, including cell migration, differentiation, proliferation, survival, tissue morphogenesis, wound healing, and tumorigenesis. Adhesions are dynamic structures that are classically defined on two-dimensional (2D) substrates, though the need to analyze adhesions in more physiologic three-dimensional (3D) environments is being increasingly recognized. However, progress has been greatly hampered by the lack of available tools to analyze adhesions in 3D environments. To address this need, we have developed a platform for the automated analysis, segmentation, and tracking of adhesions (PAASTA) based on an open source MATLAB framework, CellAnimation. PAASTA enables the rapid analysis of adhesion dynamics and many other adhesion characteristics, such as lifetime, size, and location, in 3D environments and on traditional 2D substrates. We manually validate PAASTA and utilize it to quantify rate constants for adhesion assembly and disassembly as well as adhesion lifetime and size in 3D matrices. PAASTA will be a valuable tool for characterizing adhesions and for deciphering the molecular mechanisms that regulate adhesion dynamics in 3D environments.

Introduction

Cell-matrix adhesions are sites of contact between a cell and the ECM that physically link the ECM to the cytoskeleton and function to transmit extracellular signals to the interior of cells (Burridge and Chrzanowska-Wodnicka, 1996; Hynes, 2002; Kanchanawong et al., 2010). They are critical to many biological processes including cell migration, survival, proliferation, differentiation, tissue morphogenesis, tissue homeostasis, wound repair, and tumorigenesis (Berrier and Yamada, 2007; Dubash et al., 2009; Geiger et al., 2001; Reddig and Juliano, 2005;

Wolfenson et al., 2013). In many of these processes, adhesions are dynamic structures that are constantly changing and remodeling. For example, adhesions must continuously assemble and disassemble, in a process termed adhesion turnover, in order for cells to migrate efficiently (Vicente-Manzanares and Horwitz, 2011; Webb et al., 2004; Wehrle-Haller, 2012). Adhesions are composed of a number of different proteins, including integrin transmembrane receptors, which bind to the ECM, and intracellular signaling and structural proteins, such as paxillin, vinculin, talin, and FAK, that link integrins to the actin cytoskeleton (Burridge et al., 1988; Geiger and Yamada, 2011; Miyamoto et al., 1995; Zaidel-Bar et al., 2003). Many of the studies characterizing adhesions have focused on cells plated on planar 2D substrates (Dubash et al., 2009; Hanein and Horwitz, 2012). These studies have proven to be very beneficial for identifying key adhesion proteins as well as regulatory mechanisms. However, recent work has highlighted the importance of examining adhesions in more physiologic 3D environments (Cukierman et al., 2001; Deakin and Turner, 2011; Geraldo et al., 2012; Harunaga and Yamada, 2011; Kubow and Horwitz, 2011; Petroll and Ma, 2003).

Although the characterization of adhesions in 3D matrices is in its infancy, available data indicate that adhesions in 2D and 3D environments can differ, at least in some aspects (Cukierman et al., 2002; Harunaga and Yamada, 2011). For example, when fibroblasts were plated on 2D substrates or in 3D cell- or tissue-derived matrices, FAK was differentially phosphorylated in 2D and 3D adhesions (Cukierman et al., 2001). Other studies have also shown differences in adhesion signaling, morphology, and composition between 2D and 3D (Hakkinen et al., 2011; Harunaga and Yamada, 2011; Li et al., 2003). These differences point to the need to better characterize adhesions in 3D environments. Some key proteins, such as integrins, paxillin, talin, and FAK, have been observed in adhesions in various 3D matrices (Cukierman et al., 2001;

Deakin and Turner, 2011; Hakkinen et al., 2011; Li et al., 2003; Tamariz and Grinnell, 2002), which will provide useful markers for studying adhesion structure and dynamics in 3D environments.

While our current knowledge regarding adhesion dynamics in 3D environments is limited, adhesions have been shown to assemble, mature, and disassemble in cells migrating in 3D type I collagen matrices (Kubow and Horwitz, 2011). In these live-cell imaging experiments, adhesions formed along collagen fibers at the leading edge of protrusions and traveled rearward as they matured, causing fiber deformation (Kubow and Horwitz, 2011). Adhesion maturation in 3D environments has been linked to myosin II contractility and the structure of the microenvironment surrounding the adhesion (Doyle et al., 2012; Kubow et al., 2013). Photorecovery of adhesion proteins also demonstrates that adhesions assemble and disassemble in cells migrating on one-dimensional (1D) patterned fibril-like structures, which were used as a model system for oriented 3D fibrillar matrices (Doyle et al., 2012; Doyle et al., 2009). However, little mechanistic data for the regulation of adhesion assembly, maturation, and disassembly in 3D matrices is currently available. Progress in this rapidly emerging field has been greatly hampered by the lack of available tools to analyze adhesion dynamics in 3D environments.

To address this need, we have created an automated platform, PAASTA, for analyzing adhesion dynamics in cells migrating on both 2D substrates and in 3D environments, that is based on an open source MATLAB framework, CellAnimation (Georgescu et al., 2012). We manually validate our platform using an established adhesion analysis method (Webb et al., 2004) and use PAASTA to quantify adhesion dynamics in 3D matrices.

Materials and Methods

Cell culture and transfection

HT1080 and U2OS cells were maintained in Dulbeco's Modified Eagles Medium (DMEM) (Invitrogen, Carlsbad, CA) that was supplemented with 10% fetal bovine serum (FBS) (HyClone, Logan, UT) and 1% penicillin/streptomycin (Invitrogen). Both HT1080 and U2OS cells were transiently transfected with Lipofectamine™ 2000 (Invitrogen) according to the manufacturer's instructions.

Imaging adhesions on 2D substrates

Cells transfected with either GFP-paxillin, GFP-vinculin, Spec-paxillin, or Spec-vinculin were plated on glass-bottomed dishes, which were precoated with 2.5 μg/mL fibronectin (Sigma, St. Louis, MO), and permitted to adhere for 1 h at 37^{o}C. While imaging, cells were maintained in SFM4MAb™ media (Hyclone) supplemented with 2% FBS, pH 7.4. Cells were imaged on an inverted Olympus IX71 microscope (Melville, NY), which was equipped with a Retiga EXi CCD camera (QImaging, Surrey, BC) and an Olympus PlanApo 60X OTIRFM objective (NA 1.45), using MetaMorph software (Molecular Devices, Sunnyvale, CA). TIRF images were acquired by exciting with a 488 nm laser line from an Argon-Ion laser (Prairie Technologies, Middleton, WI). For TIRF imaging, a z488/543 rpc filter was used (Chroma, Brattleboro, VT). GFP-vinculin was a kind gift from Susan Craig (Johns Hopkins University, Baltimore, MD). Spec-paxillin and Spec-vinculin were generously provided by Rick Horwitz (University of Virginia, Charlottesville, VA).

Imaging adhesions in 3D matrices

Rat-tail type I collagen (BD Biosciences, Bedford, MA) was mixed with sterile 10x DMEM (Invitrogen), sterile dH_2O, FBS, and 1N NaOH to a final concentration of 2 mg/mL type I

collagen, 10% FBS and 1x DMEM. NaOH was used for neutralization at 0.023 mL x the volume of type I collagen solution. U2OS cells transfected with either Spec-paxillin or Spec-vinculin were seeded (~1.5 x 10^5 cells) into 300 μL of type I collagen solution and pipetted into the bottom of glass-bottomed dishes. The type I collagen solution with embedded cells was allowed to polymerize for at least 30 min at 37 °C in a cell culture incubator with 5% CO_2. Subsequently, 2 mL of culture medium was gently added to each dish, and cells were incubated for approximately 18 h at 37 °C in a cell culture incubator with 5% CO_2. Prior to imaging, the culture medium was replaced with SFM4MAb™ medium supplemented with 10% FBS, pH 7.4.

Z-series were acquired using a Quorum WaveFX-X1 spinning disk confocal system with a Yokogawa CSU-X1 spinning disk (Yokogawa Electric Corporation, Newnan, GA) modified with a Borealis upgrade (Guelph, Canada) and a Nikon Eclipse Ti microscope that was equipped with an EM-CCD camera (Hamamatsu, Hamamatsu City, Japan) and a Plan Fluor 40X objective (N.A. 1.3). Z-series were collected using MetaMorph software at time intervals of 45 sec - 1 min with a z-interval of 0.5 μm. GFP was excited with a 491 nm laser line and imaged with a 525/50 emission filter (Semrock, Rochester, NY). Only cells that were completely embedded within the 3D collagen matrix (at least 100 μm from the coverslips) were imaged.

Manual adhesion analysis

All manual image analysis was performed using MetaMorph software. Individual adhesions were identified, and a region was created with the trace region tool that completely outlined the adhesion at the timepoint in which the adhesion had the greatest area. The integrated intensity for the fluorescently-tagged adhesion marker (paxillin or vinculin) in this region was recorded over time. An exact duplicate region was positioned within an area adjacent to the tracked adhesion, which was inside the cell and did not contain an adhesion at any timepoint. The

integrated fluroescence intensity of this region was then used as background and was subtracted from each timepoint from the region containing the adhesion. These background-corrected data were then used in further processing steps to calculate adhesion kinetics.

Adhesion analysis with PAASTA

For adhesion analysis, a Gaussian smoothing module was applied to the raw images to reduce noise and then corrected for uneven background illumination by dividing each smoothed image with a low pass filtered version of itself. A local thresholding module was used to compare the intensity of each pixel with the mean value of the local neighborhood of the pixel in order to detect adhesions. Cell outlines were detected by thresholding the background-corrected images using a global intensity threshold module. Adhesions were selected by combining the binary mask of the cell with the binary image of the adhesions. Kernel sizes and thresholds were user designated because images can vary due to experimental conditions. Individual adhesions, which were assigned ID numbers, were tracked over time using a nearest neighbor algorithm. Adhesions that split into two adhesions during imaging were tracked as separate adhesions; the adhesion that remained closest to the previous image was tracked with the same ID number whereas the other adhesion was assigned a new ID number. Adhesion ID numbers, individual adhesion integrated intensities, and area information at every time point were exported to comma-separated text files for further analysis. A set of images showing the detected adhesion outlines, with or without ID numbers, were overlaid on the original images for manual validation of the automated quantification. Adhesions were imaged with a temporal resolution ($\leq$ 1 min) that was sufficient to obtain numerous data points for adhesion analysis. Furthermore, because the temporal resolution was high, the number of adhesions did not vary greatly between subsequent images, which allowed the user to adjust any ID numbers due to splitting and

merging adhesions. The vast majority of adhesions in cells were correctly identified and tracked using PAASTA, indicating that the adhesion density was amenable to tracking with the nearest neighbor algorithm. A modified nearest neighbor algorithm or binary integer programming can be added to PAASTA if the adhesion density increases dramatically and the nearest neighbor algorithm is no longer sufficient for adhesion tracking.

Calculating rate constants for adhesion assembly and disassembly

The background-corrected integrated fluorescence intensities in individual adhesions were determined manually or with PAASTA. Semilogarithmic plots of the background-subtracted fluorescence intensities over time were then generated as follows: $ln\ [I_0/I]$ vs. time for adhesion disassembly and $ln\ [I/I_0]$ vs. time for adhesion assembly, where $[I]$ is the intensity of the adhesion at a given timepoint and $[I_0]$ is the initial intensity of the adhesion. Data were then fitted with a linear trendline, and rate constants were determined from the slopes. Rate constants were used to calculate half-life values for adhesion assembly and disassembly using the equation: $t_{1/2} = ln(2)/k$, where k is the rate constant.

Results

An automated platform, PAASTA, for adhesion analysis

In order to perform automated detection and quantification of adhesions over time, we begin with raw images, which are acquired with time-lapse microscopy, of cells with fluorescently-labeled adhesions (Figure A.1). Initially, a Gaussian smoothing module is applied to the raw images to reduce noise and then corrected for uneven background illumination by dividing each smoothed image with a low pass filtered version of itself. To detect adhesions, we employ a local thresholding module that compares the intensity of each pixel with the mean value of the

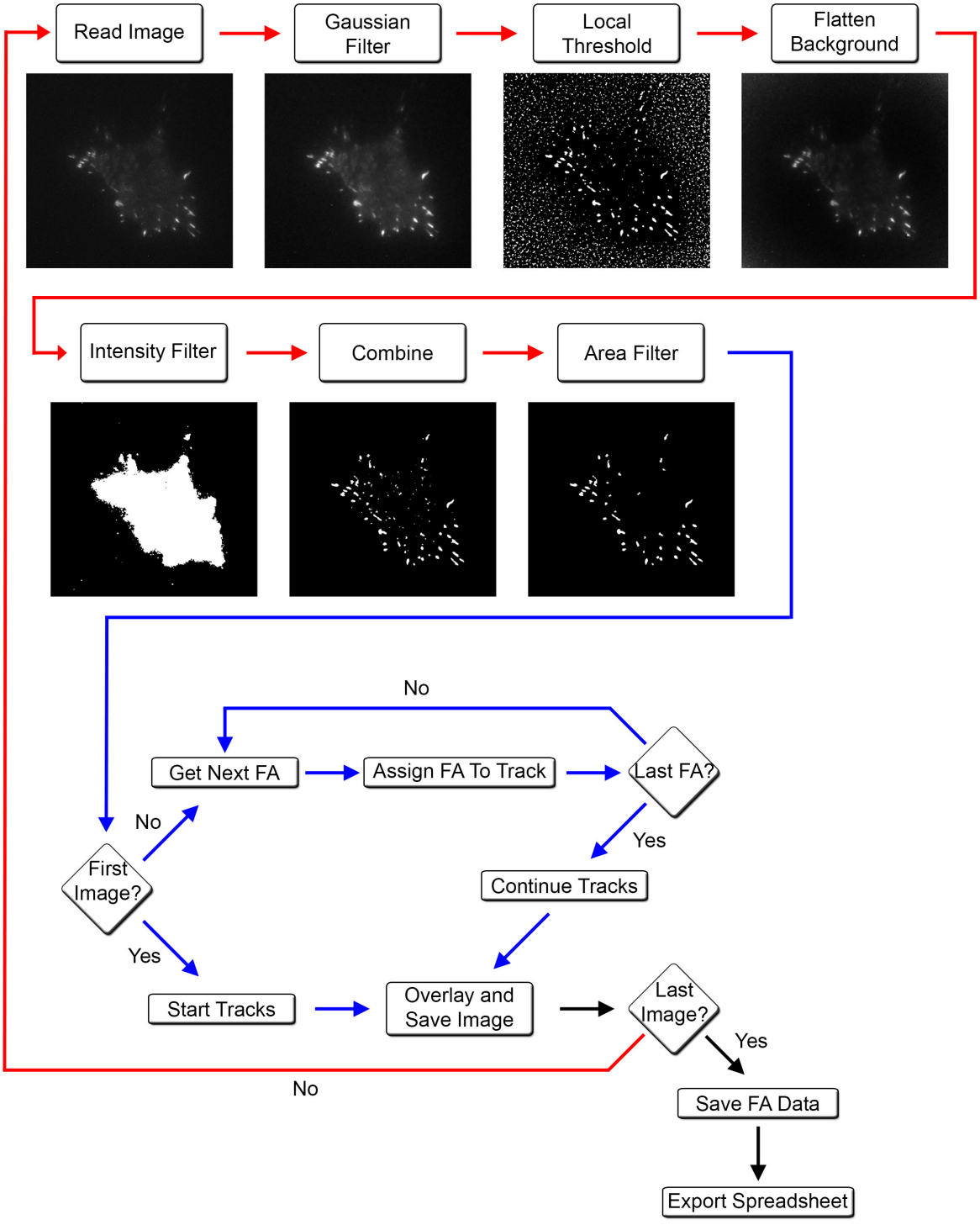

Figure A.1. An automated platform, PAASTA, for tracking and analyzing adhesions. This platform subjects raw images to a series of steps to identify adhesions. A flow chart detailing

each step with a corresponding output image is shown. A segmentation pipeline (red lines), where images are processed in order to segment adhesions, is followed by a tracking pipeline (blue lines) that identifies and tracks adhesions through a series of time-lapse images. Upon completion of the track assignment process for a particular frame, an overlay image is generated which displays the ID numbers for each adhesion in the frame. These images may be used for visual inspection of the automated tracking assignments. Intensity values are calculated for all tracked adhesions at every time point using the background-corrected intensity image. When the tracking assignment is completed for all the frames, the final adhesion ID numbers along with centroid locations and intensity values are exported to comma-separated text files for further analysis.

local neighborhood of the pixel. If the value of the pixel is higher than the local average, it is classified as an adhesion pixel; otherwise, it is assigned to the background pixel class. Objects less than 1 μm^2 are excluded to ensure that background noise is eliminated from the analysis. Cell outlines are detected by thresholding the background-corrected images using a global intensity threshold module. Adhesions are selected by combining the binary mask of the cell with the binary image of the adhesions. Individual adhesions, which are assigned identification (ID) numbers, are tracked over time using a nearest neighbor algorithm. Adhesion ID numbers, individual adhesion integrated intensities, and area information at every time point are exported to comma-separated text files for further analysis. Sets of images showing the detected adhesion outlines, with or without ID numbers, are overlaid on the original images for manual validation of the automated quantification (Figure A.2).

Manual validation of PAASTA

We manually validated the automated tracking data received from PAASTA from time-series of cells expressing the fluorescently-tagged adhesion proteins, paxillin or vinculin. In these experiments, GFP-paxillin transfected HT1080 cells were plated on glass bottom dishes, which were coated with the ECM protein fibronectin (2D substrate), and imaged using total internal reflection fluorescence (TIRF) microscopy. From these images, we manually tracked individual adhesions, measured fluorescence intensities in these adhesions, and quantified the kinetics of adhesion assembly and disassembly as previously described (Webb et al., 2004). We next compared this manual adhesion data to the output generated by PAASTA using the same raw images. The relative changes in fluorescence intensities obtained from PAASTA for assembling adhesions was similar to that measured manually (Figure A.3 A,B). To calculate apparent rate constants for adhesion assembly, we generated semilogarithmic plots of fluorescence intensities

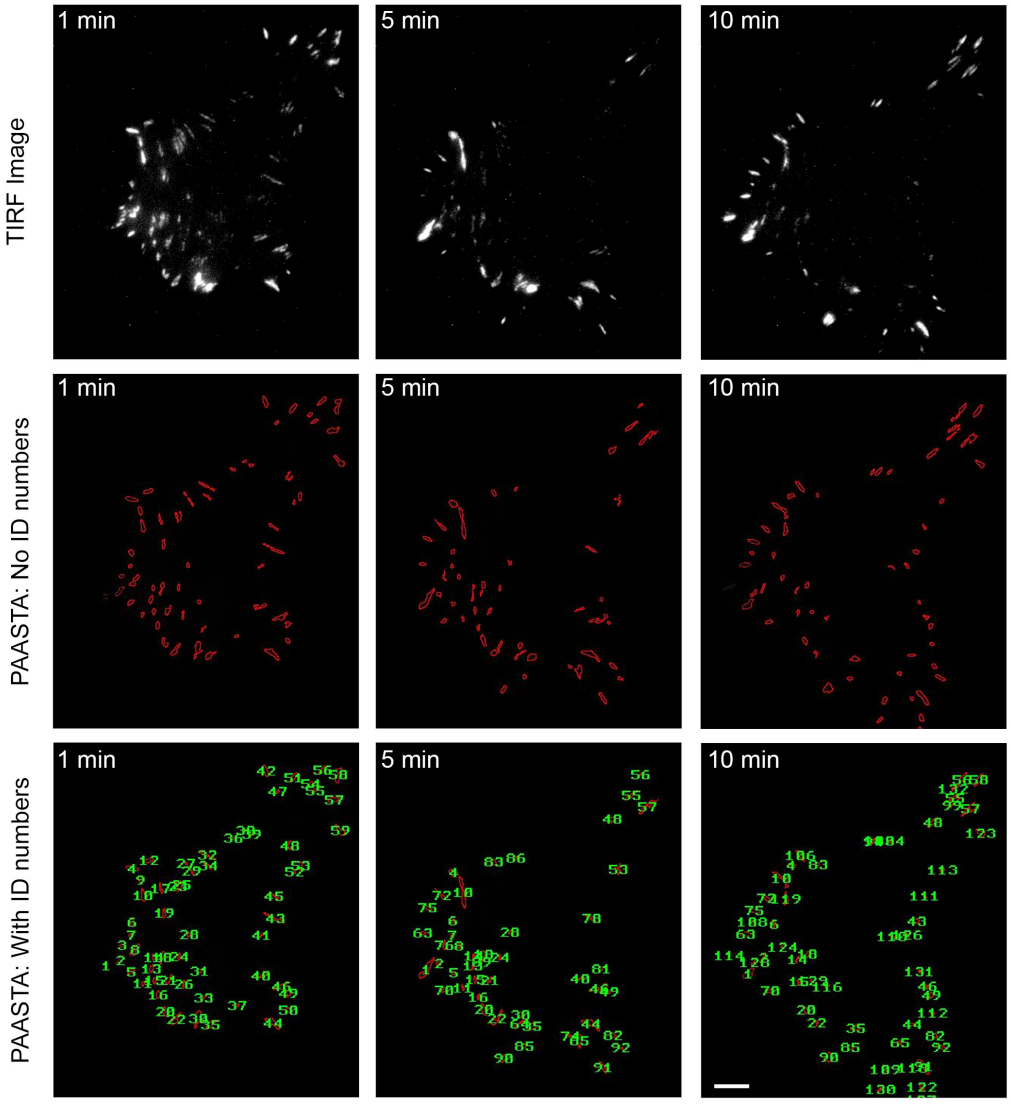

Figure A.2. Adhesion identification and tracking using PAASTA. Raw time-lapse TIRF images of an HT1080 cell expressing GFP-paxillin are shown (upper panels). These images were then processed with PAASTA to generate individual adhesion tracks that are shown in the lower panels both without labeling (No ID numbers) and with ID numbers labeling each adhesion (With ID numbers). Bar, 5 μm.

of individual adhesions as a function of time. The slopes of these graphs, which correspond to the apparent rate constant for adhesion assembly, were similar for the manually generated data and the data from PAASTA (Figure A.3 C). In addition, for disassembling adhesions, the fluorescence intensity profiles attained manually and from PAASTA were similar (Figure A.3 D,E), and the rate constants for adhesion disassembly were comparable for data obtained manually and with PAASTA (Figure A.3 F). Indeed, the rate constants for adhesion assembly and disassembly, which we express as $t_{1/2}$ values, that were obtained from manually tracking GFP-paxillin adhesions were very similar to those attained with PAASTA (Figure A.3 G). An individual value plot shows the range of $t_{1/2}$ values for adhesion assembly and disassembly (Figure A.4). Moreover, in HT1080 cells expressing GFP-vinculin, another adhesion protein, the $t_{1/2}$ values for adhesion assembly and disassembly were comparable for manual adhesion tracking and PAASTA (Figure A.3 H). When we extended these observations to U2OS cells, we obtained very similar results for adhesion assembly (Figure A.5 A-C) and adhesion disassembly (Figure A.5 D-F). Thus, these results indicate that PAASTA accurately tracks and analyzes adhesion dynamics.

Applications of PAASTA to adhesion dynamics

To further demonstrate the capabilities of PAASTA, we compared adhesions in HT1080 and U2OS cells (Figure A.6 A). In these time-series, PAASTA tracked a total of 46 adhesions in the HT1080 cell and 50 adhesions in the U2OS cell. The average adhesion lifetime, defined as the total time an adhesion was observed during the time course, was 6.7 ± 0.7 min and 9.9 ± 1.0 min for the HT1080 and U2OS cell, respectively. The U2OS cell had more adhesions with a lifetime of greater than 19 min compared to the HT1080 cell (Figure A.6 B). The average adhesion size for the HT1080 and U2OS cell was 5.4 ± 0.4 μm^2 and 5.8 ± 0.6 μm^2, respectively.

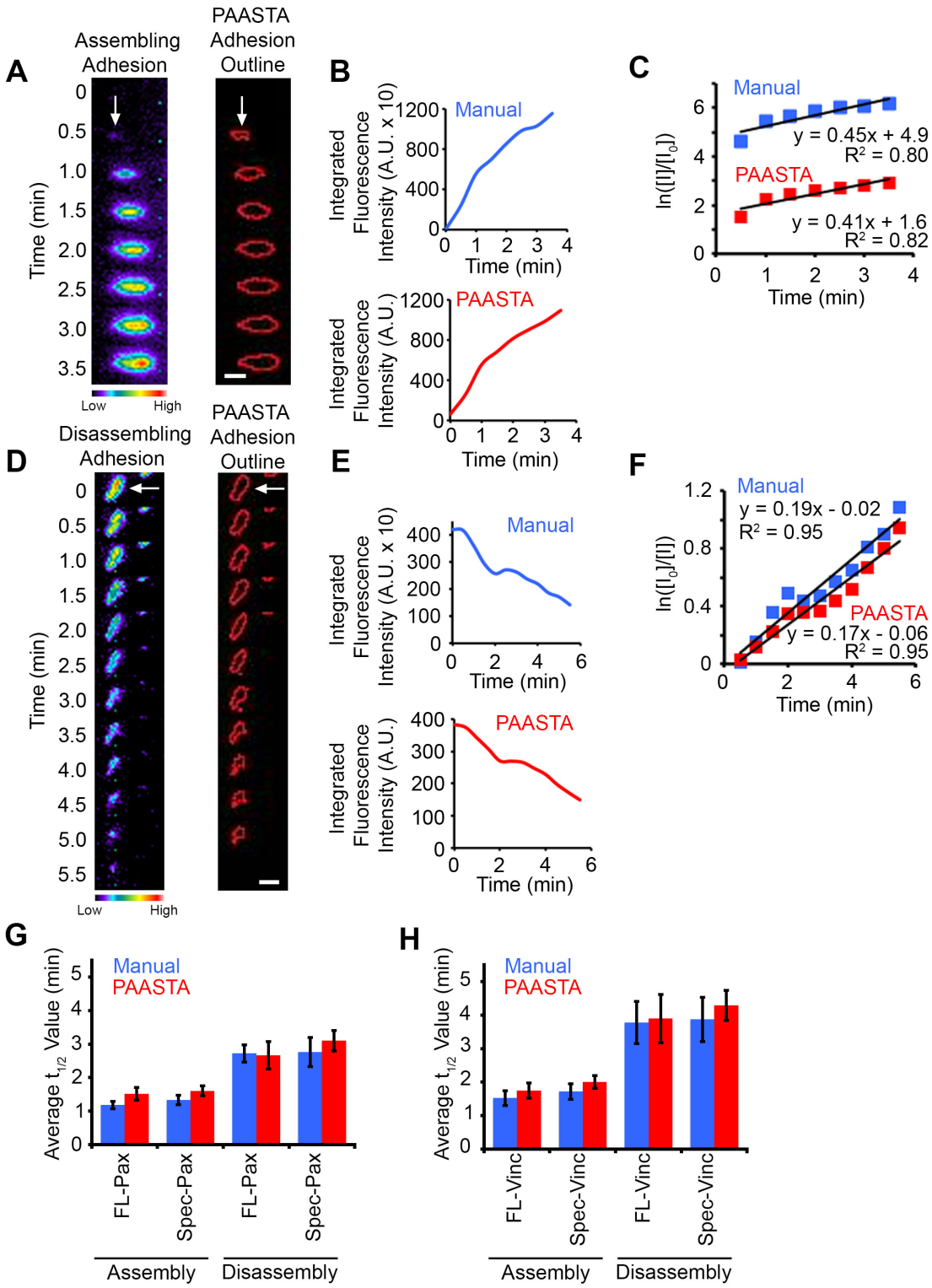

Figure A.3. Manual validation of PAASTA with HT1080 cells. (A) Left, A montage of time-lapse TIRF images for an assembling adhesion (white arrow) in an HT1080 cell expressing GFP-

paxillin is shown in pseudo-color coding. Warm colors correspond to higher fluorescence intensity values whereas cool colors represent lower fluorescence intensity values. Right, An outline of the assembling adhesion as segmented by PAASTA. (B) A graph of the fluorescence intensities, which were obtained manually (Manual) or with PAASTA, as a function of time for the assembling adhesion is shown. (C) A plot of the natural log of the fluorescence intensity of the adhesion at a given time point (I) over the initial fluorescence intensity (I_0) is shown. A trendline with the corresponding equation ($y = mx + b$) and R^2 values are shown for fluorescence intensities attained manually (Manual) and with PAASTA. The slope of this graph (m) is the apparent rate constant for adhesion assembly. (D) Left, A montage of TIRF time-lapse images for a disassembling adhesion (white arrow) in an HT1080 cell expressing GFP-paxillin is shown in pseudo-color coding. Right, An outline of the disassembling adhesion as segmented by PAASTA. (E) A graph of fluorescence intensities of the disassembling adhesion over time is shown for both Manual and PAASTA tracking. (F) A plot of the natural log of the initial fluorescence intensity (I_0) over the fluorescence intensity at a given time point (I) is shown. A trendline with the corresponding equation ($y = mx + b$) and R^2 values are shown for both Manual and PAASTA adhesion tracking. The slope of this graph (m) is the rate constant for adhesion disassembly. (G) The average $t_{1/2}$ values for adhesion assembly and disassembly for HT1080 cells expressing GFP-paxillin (FL-Pax) or GFP-paxillin with a truncated CMV promoter (Spec-Pax) are shown for Manual and PAASTA adhesion tracking. S.E.M. was calculated from: 22 adhesions (12 assembly, 10 disassembly) for Manual FL-Pax and 21 adhesions (11 assembly, 10 disassembly) for PAASTA FL-Pax; 24 adhesions (14 assembly, 10 disassembly) for Manual Spec-Pax and 22 adhesions (12 assembly, 10 disassembly) for PAASTA Spec-Pax. A total of 14 cells were analyzed for adhesion assembly and disassembly. (H) The average $t_{1/2}$ values for adhesion assembly and disassembly for HT1080 cells expressing GFP-vinculin (FL-Vinc) or GFP-vinculin with a truncated CMV promoter (Spec-Vinc) are shown for manually generated data (Manual) and PAASTA. S.E.M. was calculated from: 21 adhesions (11 assembly, 10 disassembly) for Manual FL-Vinc and 21 adhesions (11 assembly, 10 disassembly) for PAASTA FL-Vinc; 20 adhesions (10 assembly, 10 disassembly) for Manual Spec-Vinc and 20 adhesions (10 assembly, 10 disassembly) for PAASTA Spec-Vinc. A total of 13 cells were analyzed for adhesion assembly and disassembly. A Wilcoxon rank sum test showed no statistically significant difference between Manual and PAASTA adhesion tracking for FL-Pax assembly (*$Z = -1.689$, $p = 0.091$*), disassembly (*$Z = -0.153$, $p = 0.878$*); Spec-Pax assembly (*$Z = -0.941$, $p = 0.347$*), disassembly (*$Z = -1.580$, $p = 0.114$*); FL-Vinc assembly (*$Z = -0.561$, $p = 0.575$*), disassembly (*$Z = -0.255$, $p = 0.799$*); or Spec-Vinc assembly (*$Z = -1.122$, $p = 0.262$*), disassembly (*$Z = -1.172$, $p = 0.241$*). For panels A and D, Bar, 1 μm.

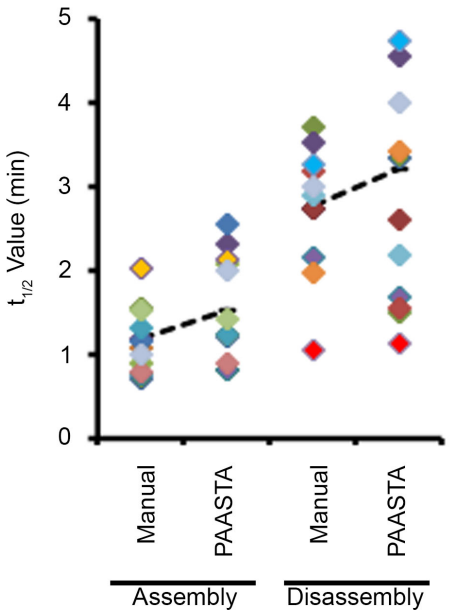

Figure A.4. An individual value plot of $t_{1/2}$ values for adhesion assembly and disassembly. Individual $t_{1/2}$ values were obtained from TIRF imaging of HT1080 cells expressing GFP-paxillin with a truncated CMV promoter (Spec-Pax) with both manual and PAASTA tracking. Matching colors correspond to the same adhesion, and the dashed lines correspond to the average of each category.

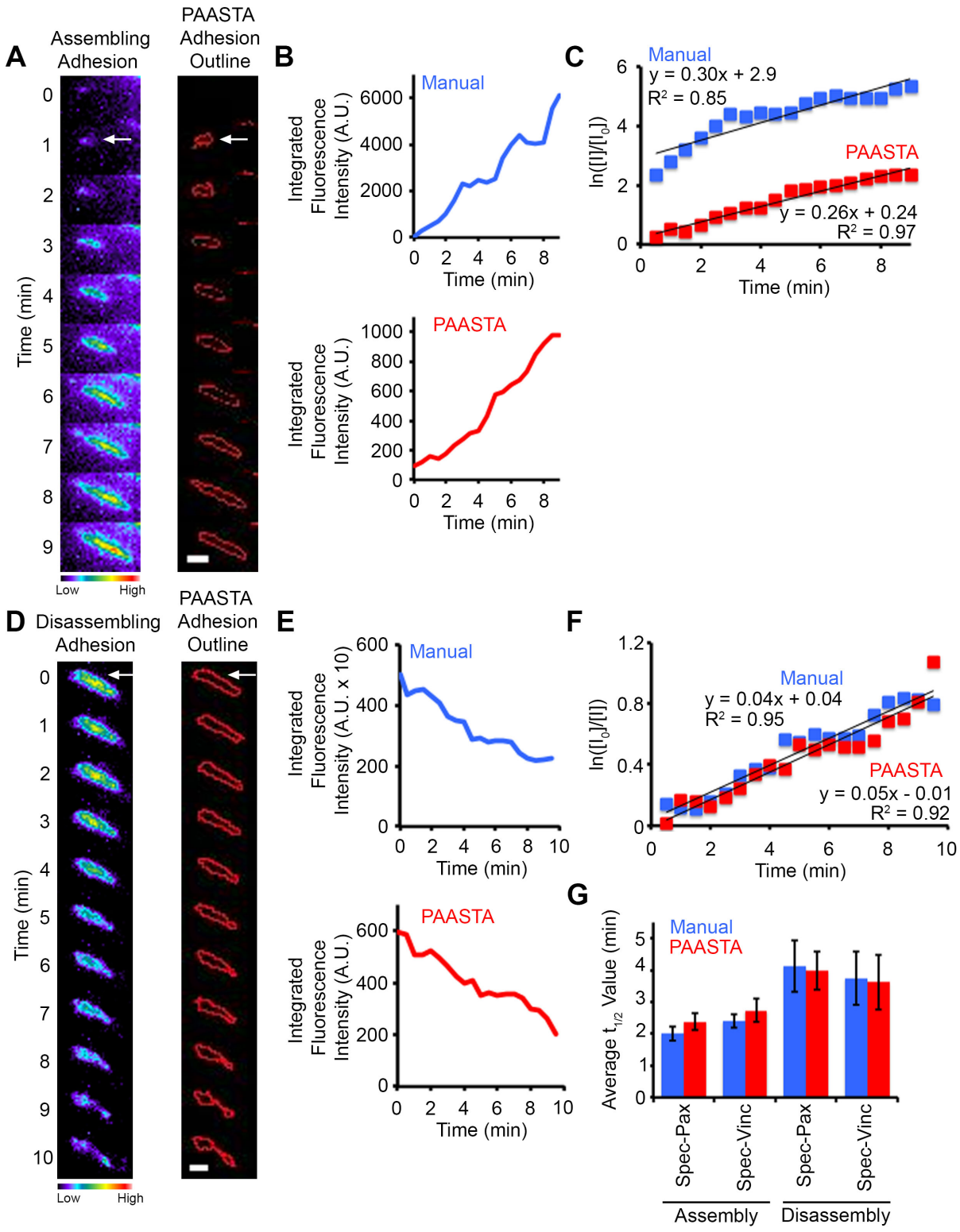

Figure A.5. Manual and PAASTA analysis of adhesion assembly and disassembly in U2OS cells. (A) Left, A montage of time-lapse TIRF images for an assembling adhesion (white arrow) in a U2OS cell expressing GFP-paxillin is shown in pseudo-color coding, which indicates the

range of fluorescence intensities. Cool colors correspond to lower intensity values and warm colors correspond to higher intensity values. Right, An outline of the assembling adhesion as segmented by PAASTA. (B) A graph of the fluorescence intensities of the assembling adhesion is shown for both Manual and PAASTA tracking. (C) A plot of the natural log of the fluorescence intensity of the adhesion at a given time point (I) over the initial fluorescence intensity (I_0) is shown. A trendline with the corresponding equation ($y = mx + b$) and R^2 values are shown for fluorescence intensities that were obtained manually (Manual) and with PAASTA. The slope of this graph (m) is the apparent rate constant for adhesion assembly. (D) Left, A montage of time-lapse TIRF images for a disassembling adhesion (white arrow) in a U2OS cell expressing GFP-paxillin is shown in pseudo-color coding. Right, An outline of the disassembling adhesion as segmented by PAASTA. (E) A graph of fluorescence intensities as a function of time is shown for the disassembling adhesion for both Manual and PAASTA tracking. (F) A plot of the natural log of the initial fluorescence intensity (I_0) over the fluorescence intensity at a given time point (I) is shown. A trendline with the corresponding equation ($y = mx + b$) and R^2 values are shown for both Manual and PAASTA adhesion tracking. The slope of this graph (m) is the rate constant for adhesion disassembly. **(**G**)** The average $t_{1/2}$ values for adhesion assembly and disassembly for U2OS cells expressing Spec-Pax or Spec-Vinc are shown for Manual and PAASTA adhesion tracking. S.E.M. was calculated from: 20 adhesions (10 assembly, 10 disassembly) for Manual Spec-Pax and 20 adhesions (10 assembly, 10 disassembly) for PAASTA Spec-Pax; 21 adhesions (11 assembly, 10 disassembly) for Manual Spec-Vinc and 21 adhesions (11 assembly, 10 disassembly) for PAASTA Spec-Vinc. A total of 14 cells were analyzed for adhesion assembly and disassembly. A Wilcoxon rank sum test showed no statistically significant difference between Manual and PAASTA adhesion tracking for Spec-Pax assembly (*Z= -1.682, p = 0.093*), disassembly (*Z= -0.153, p = 0.878*); or Spec-Vinc assembly (*Z= -1.112, p = 0.266*), disassembly (*Z= -0.255, p = 0.799*). For panels A and D, Bar, 1 μm.

Interestingly, even though the average size was comparable between the two cells, the U2OS cell had more small and large adhesions, while the HT1080 cell had a majority of moderately sized adhesions (Figure A.6 C). Furthermore, the two cells showed very similar trends when comparing adhesion lifetime to adhesion size (Figure A.6 D).

Analysis of adhesion dynamics in a 3D environment with PAASTA

An attractive feature of PAASTA is that it is designed to analyze adhesion dynamics in 3D environments. *Kubow et al.* (2011) recently showed that very low expression of GFP-tagged adhesion proteins under the control of a truncated CMV promoter is ideal for imaging adhesions in 3D matrices. Hence, we employed this approach to generate time-lapse images for analysis of adhesions with PAASTA. In initial experiments, we expressed GFP-paxillin and GFP-vinculin cDNAs with the truncated CMV promoter (Spec-paxillin and Spec-vinculin) in both HT1080 and U2OS cells. We subsequently imaged these cells using time-lapse microscopy and quantified the $t_{1/2}$ values for adhesion assembly and disassembly both manually and with PAASTA. The average $t_{1/2}$ values obtained with these truncation constructs were quite similar to those attained in HT1080 cells with GFP-paxillin and GFP-vinculin with the full-length CMV promoter (FL-paxillin and FL-vinculin) (Figure A.3 G,H). Moreover, we observed comparable $t_{1/2}$ values with these truncation constructs in U2OS cells (Figure A.5 G). We therefore proceeded to use these constructs to analyze adhesion assembly and disassembly in U2OS cells embedded in 3D type I collagen matrices.

We generated multidimensional time-lapse images (with a z-interval of 0.5 μm) for U2OS cells expressing either Spec-paxillin or Spec-vinculin. Only cells that were at least 100 μm from the coverslips were imaged to ensure they were embedded in the 3D matrices. Adhesions were identified in each z-plane and tracked as a function of time through the z-stack

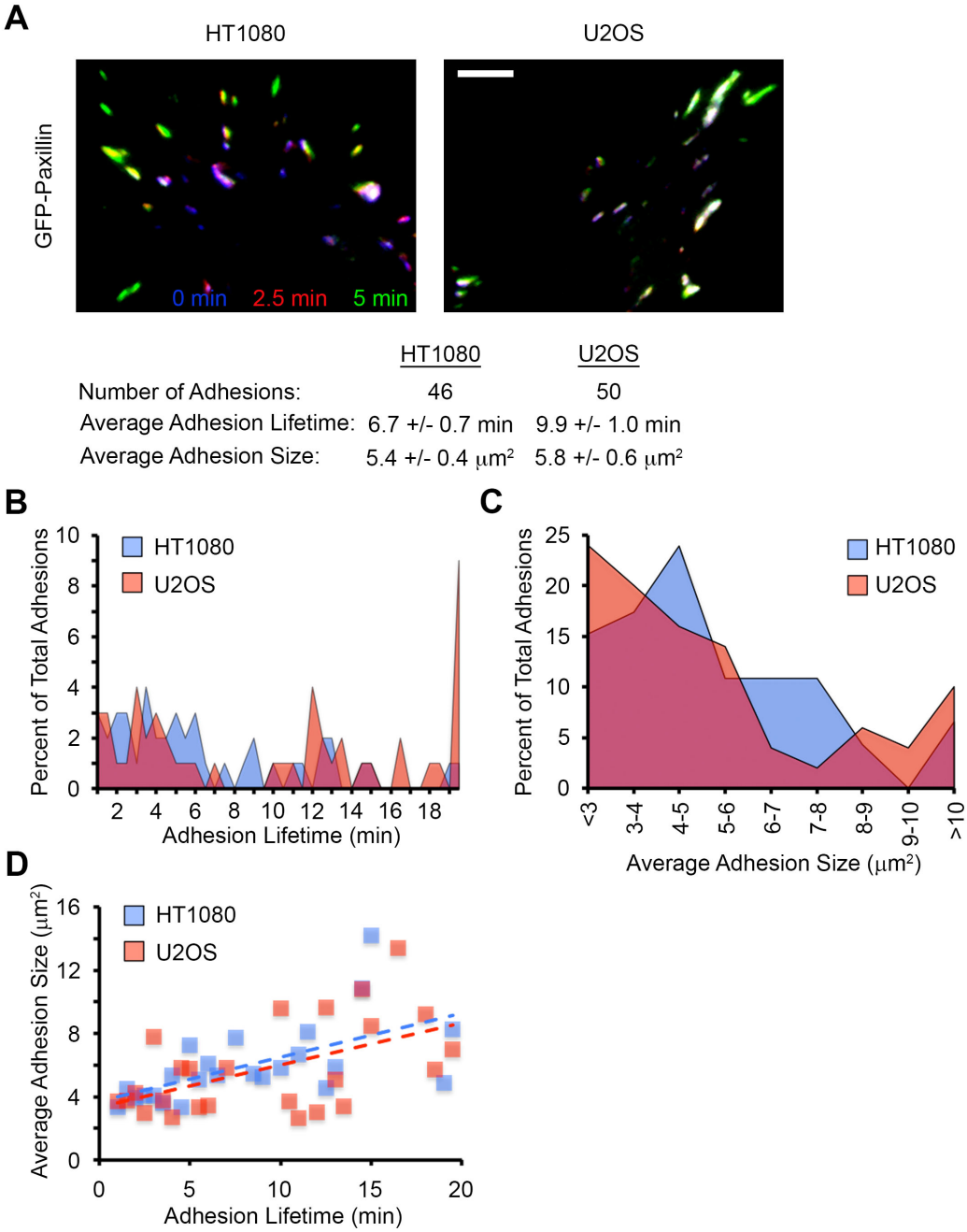

Figure A.6. Capabilities of PAASTA for adhesion analysis. (A) A three-color temporal overlay is shown for an HT1080 and U2OS cell expressing GFP-paxillin. In general, blue and purple adhesions correspond to disassembly, green and yellow adhesions indicate assembly, and white adhesions are stable. The total number of adhesions, average adhesion lifetime, and average adhesion size calculated for these cells using PAASTA is shown below. Bar, 5 μm. (B) The percent of total adhesions with a given lifetime is shown for both cells in panel A. (C) The

percent of total adhesions of a given size are shown for both cells in panel A. (D) The average adhesion size is plotted as a function of their lifetime for cells in panel A. Dashed lines represent the trendline for the indicated cell.

using the nearest neighbor algorithm. This approach allows adhesions that are moving through different focal planes to be tracked over time. Adhesion ID numbers were exported along with the average integrated fluorescence intensities from the z-planes in which the adhesions were present. A profile of the fluorescent intensities obtained from PAASTA showed an adhesion assembling and disassembling in 3D type I collagen matrices (Figure A.7 A). Changes in fluorescence intensities for an assembling (Figure A.8 A,B) and disassembling (Figure A.8 E,F) adhesion are also shown along with semilogarithmic plots of fluorescence intensities over time (Figure A.8 C,G). The average R^2 values for the adhesion assembly and disassembly plots are 0.89 ± 0.01 (S.E.M. from 43 adhesions) and 0.88 ± 0.01 (S.E.M. from 48 adhesions), respectively. From these plots, $t_{1/2}$ values were calculated for assembly and disassembly of adhesions tracked through PAASTA (Figure A.8 I). An individual value plot shows the range of the $t_{1/2}$ values for adhesion assembly and disassembly (Figure A.7 B). Distribution plots revealed that most paxillin and vinculin-containing adhesions have $t_{1/2}$ values of less than 10 min for assembly and disassembly in 3D type I collagen matrices (Figure A.8 D,H). Moreover, the average adhesion lifetime was 13.4 ± 1.0 min, and the average adhesion size was 6.1 ± 0.4 μm^2 for U2O2 cells in 3D type I collagen matrices (Figure A.9 A,B). However, these plots show some variability with some adhesions having $t_{1/2}$ values of greater than 20 min, lifetimes of 30 min, and average sizes larger than 10 μm^2. Others have similarly reported variability in adhesion parameters, including their size, distribution, shape, and location (Chien et al., 2011; Welf et al., 2011; Welf et al., 2009). Interestingly, the average adhesion size correlated with the adhesion lifetime (Figure A.9 C), suggesting that smaller adhesions have a shorter lifetime than the larger adhesions. Taken together, our data demonstrate that PAASTA is a useful platform for rapidly analyzing multiple adhesion parameters in 3D environments over time.

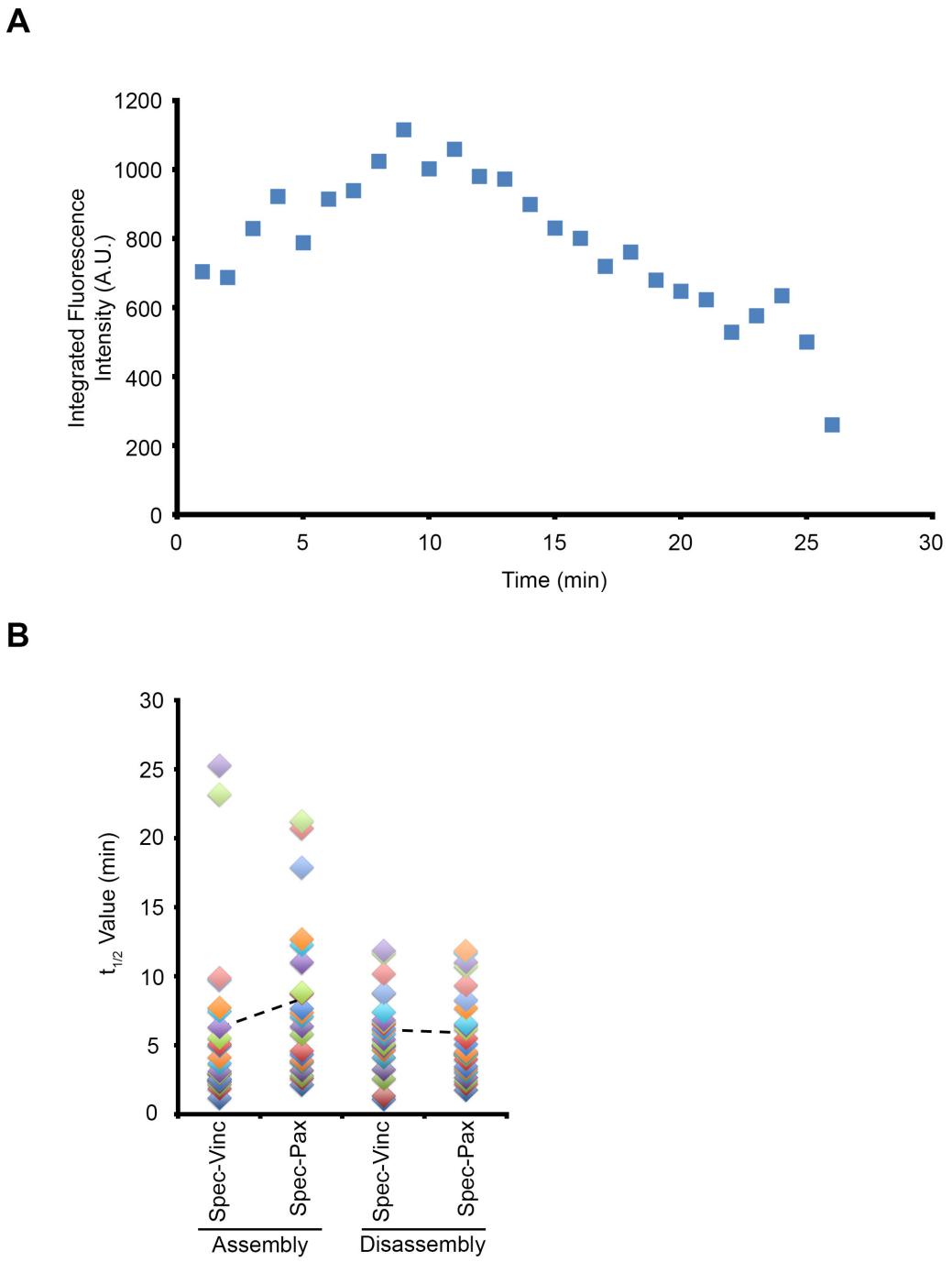

Figure A.7. PAASTA tracking and analysis of adhesion assembly and disassembly in U2OS cells embedded in 3D matrices. (A) The integrated fluorescence intensites of an individual adhesion from a Spec-Pax expressing U2OS cell, embedded in a 3D type I collagen matrix, were attained using PAASTA and plotted as a function of time. The plot shows the adhesion assembling and disassembling over time. (B) Individual $t_{1/2}$ values were obtained from imaging U2OS cells, expressing Spec-Pax or Spec-Vinc, embedded in 3D type I collagen matrices. Dashed lines correspond to the average of each category.

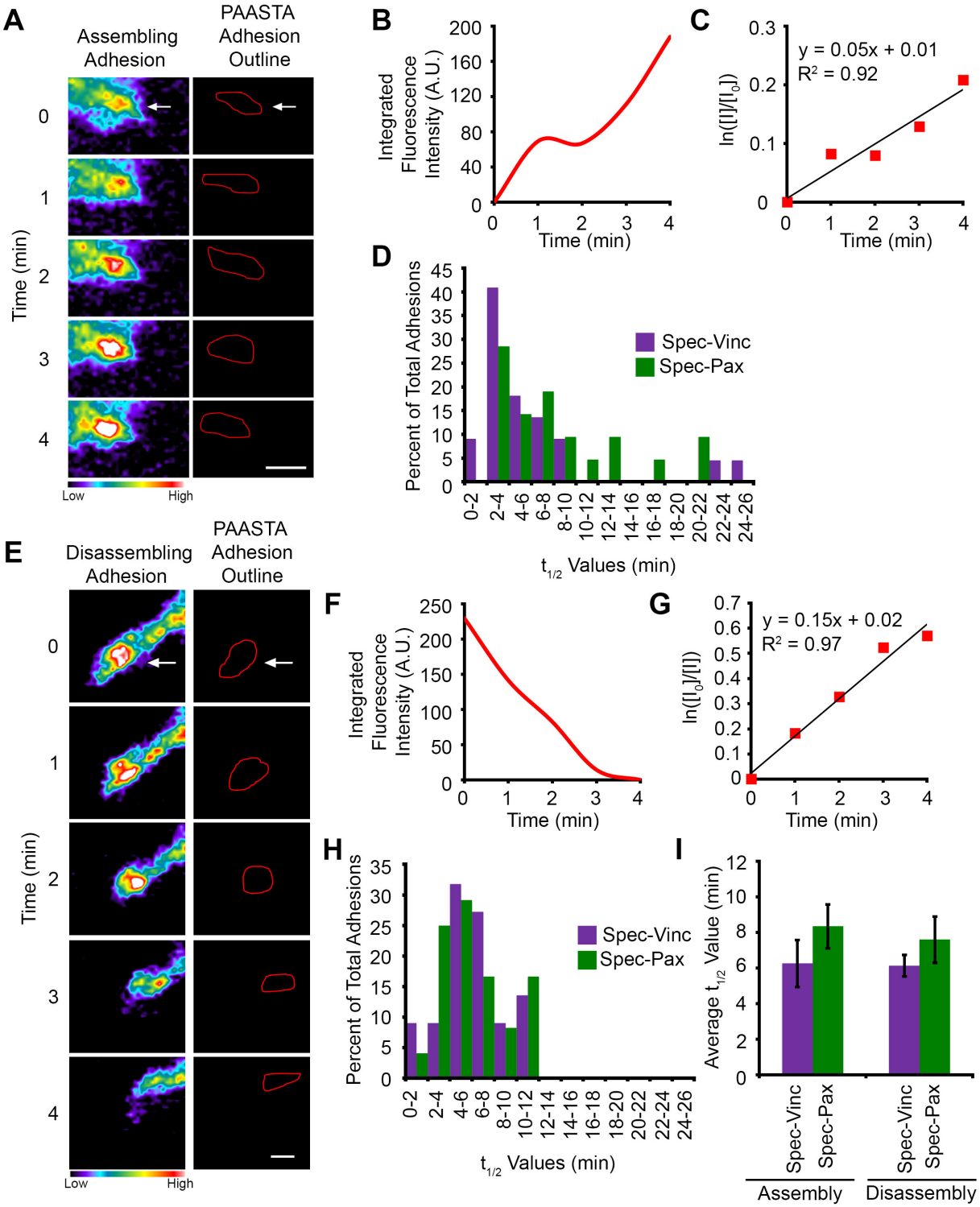

Figure A.8. Analysis of adhesion dynamics for U2OS cells migrating in 3D type I collagen matrices using PAASTA. (A) Left, Time-lapse images of an assembling adhesion (white

arrow) from a Spec-Pax expressing U2OS cell embedded in a 3D type I collagen matrix are shown. The images are shown in pseudo-color coding to indicate the range of fluorescence intensities. Warm colors represent higher fluorescence intensities while cool colors denote lower fluorescence intensities. Right, An outline of the assembling adhesion as segmented by PAASTA. (B) A graph of the fluorescence intensities that were attained with PAASTA as a function of time for the assembling adhesion is shown. (C) A graph of the natural log of the fluorescence intensity of the adhesion at a given time point (I) over the initial fluorescence intensity (I_0) is shown. (D) A histogram of the distribution of $t_{1/2}$ values for adhesion assembly is shown for U2OS cells expressing either Spec-Pax or Spec-Vinc. (E) Left, Time-lapse images are shown of a disassembling adhesion (white arrow) from a Spec-Pax expressing U2OS cell embedded in a 3D type I collagen matrix. Images are presented in pseudo-color coding. (F) A graph of fluorescence intensities, obtained with PAASTA, of the disassembling adhesion over time is shown. (G) A plot of the natural log of the initial fluorescence intensity (I_0) over the fluorescence intensity at a given time point (I) is shown. (H) A histogram of the distribution of $t_{1/2}$ values for adhesion disassembly is shown for U2OS cells expressing either Spec-Pax or Spec-Vinc. (I) The average $t_{1/2}$ values for adhesion assembly and disassembly are shown for U2OS cells expressing either Spec-Pax or Spec-Vinc. S.E.M. was calculated from 47 adhesions (21 assembly, 26 disassembly) for Spec-Pax and 44 adhesions (22 assembly, 22 disassembly) for Spec-Vinc. A total of 9 cells were used for the analysis of adhesion assembly and disassembly. A Wilcoxon rank sum test showed no statistically significant difference between Spec-Pax and Spec-Vinc for assembly ($Z= -1.269$, $p = 0.205$) or disassembly ($Z= -0.406$, $p = 0.685$). For panels A and E, Bar, 1 μm.

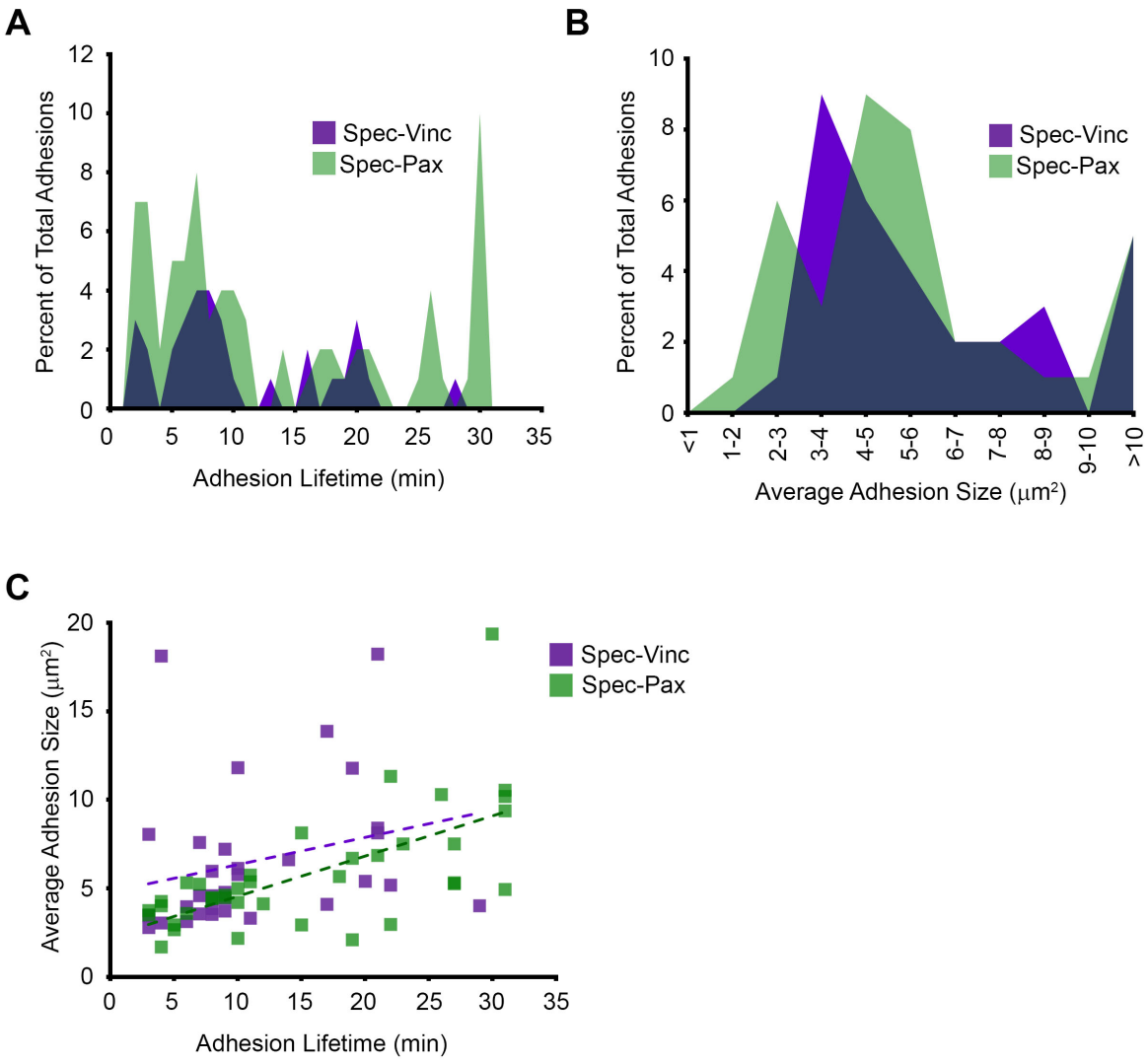

Figure A.9. PAASTA analysis of adhesion parameters in U2OS cells embedded 3D matrices. Spec-Pax or Spec-Vinc-containing adhesions in U20S cells, embedded in 3D type I collagen matrices, were tracked using PAASTA, and the adhesion lifetime and average adhesion size were calculated. (A) The percent of total adhesions with a given lifetime is shown. (B) The percent of total adhesions of a given size are shown. (C) The average adhesion size is plotted as a function of their lifetime. Dashed lines represent the trendline for cells expressing the indicated constructs.

Discussion

Since adhesions were first shown to be direct regions of contact between a cell and the substratum using interference reflection microscopy, they have been extensively studied, characterized, and analyzed on flat 2D substrates (Heath and Dunn, 1978; Horwitz, 2012; Izzard and Lochner, 1976). These studies have been extremely beneficial in understanding adhesion organization, regulation, and structure and have laid the foundation for the identification of adhesions in more complex, physiologic 3D environments (Cukierman et al., 2001; Tamariz and Grinnell, 2002; Vaughan et al., 2000; Wolf et al., 2003). Adhesions in 3D environments differ from adhesions on 2D substrates in some respects and appear to more closely resemble adhesions *in vivo* (Cukierman et al., 2001; Geraldo et al., 2012; Harunaga and Yamada, 2011). These observations warrant a more thorough analysis of adhesion organization, regulation, and dynamics in 3D environments. However, current analysis methods and systems for quantifying adhesion parameters, such as assembly, disassembly, and size, in cells plated on 2D substrates (Berginski et al., 2011; Webb et al., 2004; Wurflinger et al., 2011) have not been shown to have the capability to analyze adhesion dynamics in 3D environments. This lack of available tools to analyze adhesions in 3D environments has hindered progress toward understanding adhesions in 3D. Consequently, we have developed a reliable, powerful platform (PAASTA) for the large-scale, rapid analysis of adhesions in 3D environments. PAASTA uses multidimensional images to identify and track adhesions through z-planes over time, permitting adhesion dynamics to be quantified in 3D. Therefore, PAASTA should prove to be a useful tool for investigating adhesions in 3D environments and for deciphering the molecular mechanisms that regulate adhesion dynamics in 3D.

Using PAASTA, we examined adhesion assembly and disassembly in U2OS cells embedded in 3D type I collagen matrices. The $t_{1/2}$ values for adhesion assembly and disassembly were approximately 7 min (Figure A.8). Based on data obtained on 2D substrates (Broussard et al., 2012; Jean et al., 2013), these results suggest that adhesions in cells in 3D type I collagen matrices are relatively stable. Small adhesions in cells on 2D substrates have been reported to turn over in a few minutes (Figure A.3) (Broussard et al., 2012; Jean et al., 2013; Nayal et al., 2006). However, adhesion turnover on 2D substrates could differ among cell types, ECM proteins, and ECM concentration. Furthermore, adhesion in 3D is most likely more complex than adhesion on 2D substrates and influenced by factors, such as matrix composition, pliability, pore size, fiber alignment, as well as the immediate microenvironment of each adhesion (Harunaga and Yamada, 2011). Indeed, fiber orientation was shown to modulate adhesion size and maturation in 3D type I collagen matrices (Kubow et al., 2013). Therefore, future studies are needed to understand adhesion dynamics in 3D environments and how they compare to 2D substrates.

Investigating adhesions in 3D environments is attractive because they more closely resemble adhesions *in vivo* compared to adhesions on 2D substrates (Cukierman et al., 2001; Geraldo et al., 2012). Thus, studies characterizing adhesions in 3D matrices will provide a wealth of information on the behavior of adhesions in more physiologic environments. These studies could also serve as a foundation for examining adhesions *in vivo*, which is currently difficult with available technologies. As innovative methodologies emerge, new analytical tools will be needed to characterize adhesions in 3D environments as well as *in vivo*.

We used PAASTA to analyze adhesion turnover, lifetime, and size in 3D matrices; however, PAASTA is a versatile, automated platform for analyzing many different adhesion

characteristics in 3D environments and *in vivo*. For example, future incarnations of this platform could include features that would assess adhesion shape, distribution, and distance from the cell edge. Because PAASTA is built on the CellAnimation MATLAB platform, other modules can easily be added to the workflow. As technology advances, and adhesions can be more readily visualized *in vivo*, PAASTA should also provide a valuable platform for analyzing these structures.

REFERENCES

Abercrombie, M., Heaysman, J.E., and Pegrum, S.M. (1970). The locomotion of fibroblasts in culture. I. Movements of the leading edge. *Exp Cell Res*. **59**, 393-398.

Abercrombie, M., Heaysman, J.E., and Pegrum, S.M. (1971). The locomotion of fibroblasts in culture. IV. Electron microscopy of the leading lamella. *Exp Cell Res*. **67**, 359-367.

Alexandrova, A.Y., Arnold, K., Schaub, S., Vasiliev, J.M., Meister, J.J., Bershadsky, A.D., and Verkhovsky, A.B. (2008). Comparative dynamics of retrograde actin flow and focal adhesions: formation of nascent adhesions triggers transition from fast to slow flow. *PLoS One*. **3**, e3234.

Anthis, N.J., and Campbell, I.D. (2011). The tail of integrin activation. *Trends Biochem Sci*. **36**, 191-198.

Anthis, N.J., Wegener, K.L., Ye, F., Kim, C., Goult, B.T., Lowe, E.D., Vakonakis, I., Bate, N., Critchley, D.R., Ginsberg, M.H., and Campbell, I.D. (2009). The structure of an integrin/talin complex reveals the basis of inside-out signal transduction. *EMBO J*. **28**, 3623-3632.

Aouida, M., Kim, K., Shaikh, A.R., Pardo, J.M., Eppinger, J., Yun, D.J., Bressan, R.A., and Narasimhan, M.L. (2013). A Saccharomyces cerevisiae assay system to investigate ligand/AdipoR1 interactions that lead to cellular signaling. *PLoS One*. **8**, e65454.

Arnaout, M.A., Mahalingam, B., and Xiong, J.P. (2005). Integrin structure, allostery, and bidirectional signaling. *Annu Rev Cell Dev Biol*. **21**, 381-410.

Artemenko, Y., Lampert, T.J., and Devreotes, P.N. (2014). Moving towards a paradigm: common mechanisms of chemotactic signaling in Dictyostelium and mammalian leukocytes. *Cell Mol Life Sci*. **71**, 3711-3747.

Aschenbrenner, L., Lee, T., and Hasson, T. (2003). Myo6 facilitates the translocation of endocytic vesicles from cell peripheries. *Mol Biol Cell*. **14**, 2728-2743.

Bachir, A.I., Zareno, J., Moissoglu, K., Plow, E.F., Gratton, E., and Horwitz, A.R. (2014). Integrin-associated complexes form hierarchically with variable stoichiometry in nascent adhesions. *Curr Biol*. **24**, 1845-1853.

Bae, G.U., Lee, J.R., Kim, B.G., Han, J.W., Leem, Y.E., Lee, H.J., Ho, S.M., Hahn, M.J., and Kang, J.S. (2010). Cdo Interacts with APPL1 and Activates AKT in Myoblast Differentiation. *Mol Biol Cell*. **21**, 2399-2411.

Baker, B.M., and Chen, C.S. (2012). Deconstructing the third dimension: how 3D culture microenvironments alter cellular cues. *J Cell Sci*. **125**, 3015-3024.

Ballestrem, C., Hinz, B., Imhof, B.A., and Wehrle-Haller, B. (2001). Marching at the front and dragging behind: differential alphaVbeta3-integrin turnover regulates focal adhesion behavior. *J Cell Biol*. **155**, 1319-1332.

Banach-Orlowska, M., Pilecka, I., Torun, A., Pyrzynska, B., and Miaczynska, M. (2009). Functional characterization of the interactions between endosomal adaptor protein APPL1 and the NuRD co-repressor complex. *Biochem J*. **423**, 389-400.

Banach-Orlowska, M., Szymanska, E., and Miaczynska, M. (2015). APPL1 endocytic adaptor as a fine tuner of Dvl2-induced transcription. *FEBS Lett*. **589**, 532-539.

Bays, J.L., and DeMali, K.A. (2017). Vinculin in cell-cell and cell-matrix adhesions. *Cell Mol Life Sci*. **74**, 2999-3009.

Beauvais, D.M., and Rapraeger, A.C. (2004). Syndecans in tumor cell adhesion and signaling. *Reprod Biol Endocrinol*. **2**, 3.

Beningo, K.A., Dembo, M., Kaverina, I., Small, J.V., and Wang, Y.L. (2001). Nascent focal adhesions are responsible for the generation of strong propulsive forces in migrating fibroblasts. *J Cell Biol*. **153**, 881-888.

Beningo, K.A., Dembo, M., and Wang, Y.L. (2004). Responses of fibroblasts to anchorage of dorsal extracellular matrix receptors. *Proc Natl Acad Sci U S A*. **101**, 18024-18029.

Bergert, M., Chandradoss, S.D., Desai, R.A., and Paluch, E. (2012). Cell mechanics control rapid transitions between blebs and lamellipodia during migration. *Proc Natl Acad Sci U S A*. **109**, 14434-14439.

Berginski, M.E., Vitriol, E.A., Hahn, K.M., and Gomez, S.M. (2011). High-resolution quantification of focal adhesion spatiotemporal dynamics in living cells. *PLoS One*. **6**, e22025.

Berrier, A.L., and Yamada, K.M. (2007). Cell-matrix adhesion. *J Cell Physiol*. **213**, 565-573.

Bershadsky, A.D., Balaban, N.Q., and Geiger, B. (2003). Adhesion-dependent cell mechanosensitivity. *Annu Rev Cell Dev Biol*. **19**, 677-695.

Bhatt, A., Kaverina, I., Otey, C., and Huttenlocher, A. (2002). Regulation of focal complex composition and disassembly by the calcium-dependent protease calpain. *J Cell Sci*. **115**, 3415-3425.

Bidkhori, G., Narimani, Z., Hosseini Ashtiani, S., Moeini, A., Nowzari-Dalini, A., and Masoudi-Nejad, A. (2013). Reconstruction of an integrated genome-scale co-expression network reveals key modules involved in lung adenocarcinoma. *PLoS One*. **8**, e67552.

Bokoch, G.M. (2003). Biology of the p21-activated kinases. *Annu Rev Biochem*. **72**, 743-781.

Borisy, G.G., and Svitkina, T.M. (2000). Actin machinery: pushing the envelope. *Curr Opin Cell Biol*. **12**, 104-112.

Bottcher, R.T., Stremmel, C., Meves, A., Meyer, H., Widmaier, M., Tseng, H.Y., and Fassler, R. (2012). Sorting nexin 17 prevents lysosomal degradation of beta1 integrins by binding to the beta1-integrin tail. *Nat Cell Biol*. **14**, 584-592.

Bouvard, D., Brakebusch, C., Gustafsson, E., Aszodi, A., Bengtsson, T., Berna, A., and Fassler, R. (2001). Functional consequences of integrin gene mutations in mice. *Circ Res*. **89**, 211-223.

Bradbury, P., Fabry, B., and O'Neill, G.M. (2012). Occupy tissue: the movement in cancer metastasis. *Cell Adh Migr*. **6**, 424-432.

Bretscher, M.S. (1989). Endocytosis and recycling of the fibronectin receptor in CHO cells. *EMBO J*. **8**, 1341-1348.

Bretscher, M.S. (1992). Circulating integrins: alpha 5 beta 1, alpha 6 beta 4 and Mac-1, but not alpha 3 beta 1, alpha 4 beta 1 or LFA-1. *EMBO J*. **11**, 405-410.

Bristow, J.M., Sellers, M.H., Majumdar, D., Anderson, B., Hu, L., and Webb, D.J. (2009). The Rho-family GEF Asef2 activates Rac to modulate adhesion and actin dynamics and thereby regulate cell migration. *J Cell Sci*. **122**, 4535-4546.

Broussard, J.A., Lin, W.H., Majumdar, D., Anderson, B., Eason, B., Brown, C.M., and Webb, D.J. (2012). The endosomal adaptor protein APPL1 impairs the turnover of leading edge adhesions to regulate cell migration. *Mol Biol Cell*. **23**, 1486-1499.

Broussard, J.A., Webb, D.J., and Kaverina, I. (2008). Asymmetric focal adhesion disassembly in motile cells. *Curr Opin Cell Biol*. **20**, 85-90.

Broussard, J.A.a.D., N. L., Hummel, S., Georgescu, W., Quaranta, V., and Webb, D.J. (2015). Automated analysis of cell-matrix adhesions in 2D and 3D environments. *Sci Rep*. **5**, 8124.

Brown, M.C., Cary, L.A., Jamieson, J.S., Cooper, J.A., and Turner, C.E. (2005). Src and FAK kinases cooperate to phosphorylate paxillin kinase linker, stimulate its focal adhesion localization, and regulate cell spreading and protrusiveness. *Mol Biol Cell*. **16**, 4316-4328.

Burridge, K., and Chrzanowska-Wodnicka, M. (1996). Focal adhesions, contractility, and signaling. *Annu Rev Cell Dev Biol*. **12**, 463-518.

Burridge, K., Fath, K., Kelly, T., Nuckolls, G., and Turner, C. (1988). Focal adhesions: transmembrane junctions between the extracellular matrix and the cytoskeleton. *Annu Rev Cell Biol*. **4**, 487-525.

Byron, A., Askari, J.A., Humphries, J.D., Jacquemet, G., Koper, E.J., Warwood, S., Choi, C.K., Stroud, M.J., Chen, C.S., Knight, D., and Humphries, M.J. (2015). A proteomic approach reveals integrin activation state-dependent control of microtubule cortical targeting. *Nat Commun*. **6**, 6135.

Byron, A., Humphries, J.D., Bass, M.D., Knight, D., and Humphries, M.J. (2011). Proteomic analysis of integrin adhesion complexes. *Sci Signal*. **4**, pt2.

Cai, X., Li, M., Vrana, J., and Schaller, M.D. (2006). Glycogen synthase kinase 3- and extracellular signal-regulated kinase-dependent phosphorylation of paxillin regulates cytoskeletal rearrangement. *Mol Cell Biol*. **26**, 2857-2868.

Calderwood, D.A. (2004). Integrin activation. *J Cell Sci*. **117**, 657-666.

Calderwood, D.A., Fujioka, Y., de Pereda, J.M., Garcia-Alvarez, B., Nakamoto, T., Margolis, B., McGlade, C.J., Liddington, R.C., and Ginsberg, M.H. (2003). Integrin beta cytoplasmic domain interactions with phosphotyrosine-binding domains: a

structural prototype for diversity in integrin signaling. *Proc Natl Acad Sci U S A*. **100**, 2272-2277.

Carman, C.V., and Springer, T.A. (2003). Integrin avidity regulation: are changes in affinity and conformation underemphasized? *Curr Opin Cell Biol*. **15**, 547-556.

Casalou, C., Faustino, A., and Barral, D.C. (2016). Arf proteins in cancer cell migration. *Small GTPases*. **7**, 270-282.

Caswell, P.T., Chan, M., Lindsay, A.J., McCaffrey, M.W., Boettiger, D., and Norman, J.C. (2008). Rab-coupling protein coordinates recycling of alpha5beta1 integrin and EGFR1 to promote cell migration in 3D microenvironments. *J Cell Biol*. **183**, 143-155.

Caswell, P.T., and Norman, J.C. (2006). Integrin trafficking and the control of cell migration. *Traffic*. **7**, 14-21.

Caswell, P.T., Spence, H.J., Parsons, M., White, D.P., Clark, K., Cheng, K.W., Mills, G.B., Humphries, M.J., Messent, A.J., Anderson, K.I., McCaffrey, M.W., Ozanne, B.W., and Norman, J.C. (2007). Rab25 associates with alpha5beta1 integrin to promote invasive migration in 3D microenvironments. *Dev Cell*. **13**, 496-510.

Caswell, P.T., Vadrevu, S., and Norman, J.C. (2009). Integrins: masters and slaves of endocytic transport. *Nat Rev Mol Cell Biol*. **10**, 843-853.

Cerami, E., Gao, J., Dogrusoz, U., Gross, B.E., Sumer, S.O., Aksoy, B.A., Jacobsen, A., Byrne, C.J., Heuer, M.L., Larsson, E., Antipin, Y., Reva, B., Goldberg, A.P., Sander, C., and Schultz, N. (2012). The cBio cancer genomics portal: an open platform for exploring multidimensional cancer genomics data. *Cancer Discov*. **2**, 401-404.

Chao, W.T., Ashcroft, F., Daquinag, A.C., Vadakkan, T., Wei, Z., Zhang, P., Dickinson, M.E., and Kunz, J. (2010). Type I phosphatidylinositol phosphate kinase beta regulates

focal adhesion disassembly by promoting beta1 integrin endocytosis. *Mol Cell Biol*. **30**, 4463-4479.

Chen, P.W., Luo, R., Jian, X., and Randazzo, P.A. (2014). The Arf6 GTPase-activating proteins ARAP2 and ACAP1 define distinct endosomal compartments that regulate integrin alpha5beta1 traffic. *J Biol Chem*. **289**, 30237-30248.

Cheng, K.K., Lam, K.S., Wang, Y., Wu, D., Zhang, M., Wang, B., Li, X., Hoo, R.L., Huang, Z., Sweeney, G., and Xu, A. (2013). TRAF6-mediated ubiquitination of APPL1 enhances hepatic actions of insulin by promoting the membrane translocation of Akt. *Biochem J*. **455**, 207-216.

Cherfils, J., and Zeghouf, M. (2013). Regulation of small GTPases by GEFs, GAPs, and GDIs. *Physiol Rev*. **93**, 269-309.

Chi, C., and Trinkaus-Randall, V. (2013). New insights in wound response and repair of epithelium. *J Cell Physiol*. **228**, 925-929.

Chial, H.J., Lenart, P., and Chen, Y.Q. (2010). APPL proteins FRET at the BAR: direct observation of APPL1 and APPL2 BAR domain-mediated interactions on cell membranes using FRET microscopy. *PLoS One*. **5**, e12471.

Chial, H.J., Wu, R., Ustach, C.V., McPhail, L.C., Mobley, W.C., and Chen, Y.Q. (2008). Membrane targeting by APPL1 and APPL2: dynamic scaffolds that oligomerize and bind phosphoinositides. *Traffic*. **9**, 215-229.

Chien, F.C., Kuo, C.W., Yang, Z.H., Chueh, D.Y., and Chen, P. (2011). Exploring the formation of focal adhesions on patterned surfaces using super-resolution imaging. *Small*. **7**, 2906-2913.

Choi, C.K., Vicente-Manzanares, M., Zareno, J., Whitmore, L.A., Mogilner, A., and Horwitz, A.R. (2008). Actin and alpha-actinin orchestrate the assembly and maturation of nascent adhesions in a myosin II motor-independent manner. *Nat Cell Biol*. **10**, 1039-1050.

Christoforides, C., Rainero, E., Brown, K.K., Norman, J.C., and Toker, A. (2012). PKD controls alphavbeta3 integrin recycling and tumor cell invasive migration through its substrate Rabaptin-5. *Dev Cell*. **23**, 560-572.

Cohen, B.D., Nechamen, C.A., and Dias, J.A. (2004). Human follitropin receptor (FSHR) interacts with the adapter protein 14-3-3tau. *Mol Cell Endocrinol*. **220**, 1-7.

Cox, E.A., and Huttenlocher, A. (1998). Regulation of integrin-mediated adhesion during cell migration. *Microsc Res Tech*. **43**, 412-419.

Cukierman, E., Pankov, R., Stevens, D.R., and Yamada, K.M. (2001). Taking cell-matrix adhesions to the third dimension. *Science*. **294**, 1708-1712.

Cukierman, E., Pankov, R., and Yamada, K.M. (2002). Cell interactions with three-dimensional matrices. *Curr Opin Cell Biol*. **14**, 633-639.

Dalton, S.L., Scharf, E., Briesewitz, R., Marcantonio, E.E., and Assoian, R.K. (1995). Cell adhesion to extracellular matrix regulates the life cycle of integrins. *Mol Biol Cell*. **6**, 1781-1791.

Danen, E.H., van Rheenen, J., Franken, W., Huveneers, S., Sonneveld, P., Jalink, K., and Sonnenberg, A. (2005). Integrins control motile strategy through a Rho-cofilin pathway. *J Cell Biol*. **169**, 515-526.

Daub, H., Gevaert, K., Vandekerckhove, J., Sobel, A., and Hall, A. (2001). Rac/Cdc42 and p65PAK regulate the microtubule-destabilizing protein stathmin through phosphorylation at serine 16. *J Biol Chem*. **276**, 1677-1680.

De Franceschi, N., Hamidi, H., Alanko, J., Sahgal, P., and Ivaska, J. (2015). Integrin traffic - the update. *J Cell Sci*. **128**, 839-852.

Deakin, N.O., and Turner, C.E. (2008). Paxillin comes of age. *J Cell Sci*. **121**, 2435-2444.

Deakin, N.O., and Turner, C.E. (2011). Distinct roles for paxillin and Hic-5 in regulating breast cancer cell morphology, invasion, and metastasis. *Mol Biol Cell*. **22**, 327-341.

Deepa, S.S., and Dong, L.Q. (2009). APPL1: role in adiponectin signaling and beyond. *Am J Physiol Endocrinol Metab*. **296**, E22-36.

Del Pozo, M.A., Kiosses, W.B., Alderson, N.B., Meller, N., Hahn, K.M., and Schwartz, M.A. (2002). Integrins regulate GTP-Rac localized effector interactions through dissociation of Rho-GDI. *Nat Cell Biol*. **4**, 232-239.

del Rio, A., Perez-Jimenez, R., Liu, R., Roca-Cusachs, P., Fernandez, J.M., and Sheetz, M.P. (2009). Stretching single talin rod molecules activates vinculin binding. *Science*. **323**, 638-641.

Delorme, V., Machacek, M., DerMardirossian, C., Anderson, K.L., Wittmann, T., Hanein, D., Waterman-Storer, C., Danuser, G., and Bokoch, G.M. (2007). Cofilin activity downstream of Pak1 regulates cell protrusion efficiency by organizing lamellipodium and lamella actin networks. *Dev Cell*. **13**, 646-662.

Delorme-Walker, V.D., Peterson, J.R., Chernoff, J., Waterman, C.M., Danuser, G., DerMardirossian, C., and Bokoch, G.M. (2011). Pak1 regulates focal adhesion

strength, myosin IIA distribution, and actin dynamics to optimize cell migration. *J Cell Biol*. **193**, 1289-1303.

Dharmawardhane, S., Sanders, L.C., Martin, S.S., Daniels, R.H., and Bokoch, G.M. (1997). Localization of p21-activated kinase 1 (PAK1) to pinocytic vesicles and cortical actin structures in stimulated cells. *J Cell Biol*. **138**, 1265-1278.

Diaz, J., Mendoza, P., Ortiz, R., Diaz, N., Leyton, L., Stupack, D., Quest, A.F., and Torres, V.A. (2014a). Rab5 is required in metastatic cancer cells for Caveolin-1-enhanced Rac1 activation, migration and invasion. *J Cell Sci*. **127**, 2401-2406.

Diaz, J., Mendoza, P., Silva, P., Quest, A.F., and Torres, V.A. (2014b). A novel caveolin-1/p85alpha/Rab5/Tiam1/Rac1 signaling axis in tumor cell migration and invasion. *Commun Integr Biol*. **7**,

Diggins, N.L., and Webb, D.J. (2017). APPL1 is a multifunctional endosomal signaling adaptor protein. *Biochem Soc Trans*. **45**, 771-779.

Disanza, A., Frittoli, E., Palamidessi, A., and Scita, G. (2009). Endocytosis and spatial restriction of cell signaling. *Mol Oncol*. **3**, 280-296.

Doyle, A.D. (2016). Generation of 3D Collagen Gels with Controlled Diverse Architectures. *Curr Protoc Cell Biol*. **72**, 10 20 11-10 20 16.

Doyle, A.D., Carvajal, N., Jin, A., Matsumoto, K., and Yamada, K.M. (2015). Local 3D matrix microenvironment regulates cell migration through spatiotemporal dynamics of contractility-dependent adhesions. *Nat Commun*. **6**, 8720.

Doyle, A.D., Kutys, M.L., Conti, M.A., Matsumoto, K., Adelstein, R.S., and Yamada, K.M. (2012). Micro-environmental control of cell migration--myosin IIA is required for

efficient migration in fibrillar environments through control of cell adhesion dynamics. *J Cell Sci*. **125**, 2244-2256.

Doyle, A.D., Petrie, R.J., Kutys, M.L., and Yamada, K.M. (2013). Dimensions in cell migration. *Curr Opin Cell Biol*. **25**, 642-649.

Doyle, A.D., Wang, F.W., Matsumoto, K., and Yamada, K.M. (2009). One-dimensional topography underlies three-dimensional fibrillar cell migration. *J Cell Biol*. **184**, 481-490.

Doyle, A.D., and Yamada, K.M. (2016). Mechanosensing via cell-matrix adhesions in 3D microenvironments. *Exp Cell Res*. **343**, 60-66.

Dozynkiewicz, M.A., Jamieson, N.B., Macpherson, I., Grindlay, J., van den Berghe, P.V., von Thun, A., Morton, J.P., Gourley, C., Timpson, P., Nixon, C., McKay, C.J., Carter, R., Strachan, D., Anderson, K., Sansom, O.J., Caswell, P.T., and Norman, J.C. (2012). Rab25 and CLIC3 collaborate to promote integrin recycling from late endosomes/lysosomes and drive cancer progression. *Dev Cell*. **22**, 131-145.

Dubash, A.D., Menold, M.M., Samson, T., Boulter, E., Garcia-Mata, R., Doughman, R., and Burridge, K. (2009). Chapter 1. Focal adhesions: new angles on an old structure. *Int Rev Cell Mol Biol*. **277**, 1-65.

Dulabon, L., Olson, E.C., Taglienti, M.G., Eisenhuth, S., McGrath, B., Walsh, C.A., Kreidberg, J.A., and Anton, E.S. (2000). Reelin binds alpha3beta1 integrin and inhibits neuronal migration. *Neuron*. **27**, 33-44.

Dunphy, J.L., Moravec, R., Ly, K., Lasell, T.K., Melancon, P., and Casanova, J.E. (2006). The Arf6 GEF GEP100/BRAG2 regulates cell adhesion by controlling endocytosis of beta1 integrins. *Curr Biol*. **16**, 315-320.

Erdmann, K.S., Mao, Y., McCrea, H.J., Zoncu, R., Lee, S., Paradise, S., Modregger, J., Biemesderfer, D., Toomre, D., and De Camilli, P. (2007). A role of the Lowe syndrome protein OCRL in early steps of the endocytic pathway. *Dev Cell*. **13**, 377-390.

Erdogan, B., Ao, M., White, L.M., Means, A.L., Brewer, B.M., Yang, L., Washington, M.K., Shi, C., Franco, O.E., Weaver, A.M., Hayward, S.W., Li, D., and Webb, D.J. (2017). Cancer-associated fibroblasts promote directional cancer cell migration by aligning fibronectin. *J Cell Biol*. **216**, 3799-3816.

Evers, E.E., Zondag, G.C., Malliri, A., Price, L.S., ten Klooster, J.P., van der Kammen, R.A., and Collard, J.G. (2000). Rho family proteins in cell adhesion and cell migration. *Eur J Cancer*. **36**, 1269-1274.

Ezratty, E.J., Bertaux, C., Marcantonio, E.E., and Gundersen, G.G. (2009). Clathrin mediates integrin endocytosis for focal adhesion disassembly in migrating cells. *J Cell Biol*. **187**, 733-747.

Ezratty, E.J., Partridge, M.A., and Gundersen, G.G. (2005). Microtubule-induced focal adhesion disassembly is mediated by dynamin and focal adhesion kinase. *Nat Cell Biol*. **7**, 581-590.

Fan, S.H., Numata, Y., and Numata, M. (2016). Endosomal Na+/H+ exchanger NHE5 influences MET recycling and cell migration. *Mol Biol Cell*. **27**, 702-715.

Finney, A.C., Stokes, K.Y., Pattillo, C.B., and Orr, A.W. (2017). Integrin signaling in atherosclerosis. *Cell Mol Life Sci*. **74**, 2263-2282.

Flores-Rodriguez, N., Kenwright, D.A., Chung, P.H., Harrison, A.W., Stefani, F., Waigh, T.A., Allan, V.J., and Woodman, P.G. (2015). ESCRT-0 marks an APPL1-

independent transit route for EGFR between the cell surface and the EEA1-positive early endosome. *J Cell Sci*. **128**, 755-767.

Franco, S.J., Rodgers, M.A., Perrin, B.J., Han, J., Bennin, D.A., Critchley, D.R., and Huttenlocher, A. (2004). Calpain-mediated proteolysis of talin regulates adhesion dynamics. *Nat Cell Biol*. **6**, 977-983.

Frank, D.J., Noguchi, T., and Miller, K.G. (2004). Myosin VI: a structural role in actin organization important for protein and organelle localization and trafficking. *Curr Opin Cell Biol*. **16**, 189-194.

Friedl, P., and Alexander, S. (2011). Cancer invasion and the microenvironment: plasticity and reciprocity. *Cell*. **147**, 992-1009.

Fu, G., Wang, W., and Luo, B.H. (2012). Overview: structural biology of integrins. *Methods Mol Biol*. **757**, 81-99.

Fukui, K., Tamura, S., Wada, A., Kamada, Y., Igura, T., Kiso, S., and Hayashi, N. (2007). Expression of Rab5a in hepatocellular carcinoma: Possible involvement in epidermal growth factor signaling. *Hepatol Res*. **37**, 957-965.

Gan, Z., Ram, S., Ober, R.J., and Ward, E.S. (2013). Using multifocal plane microscopy to reveal novel trafficking processes in the recycling pathway. *J Cell Sci*. **126**, 1176-1188.

Ganguly, K.K., Pal, S., Moulik, S., and Chatterjee, A. (2013). Integrins and metastasis. *Cell Adh Migr*. **7**, 251-261.

Gant-Branum, R.L., Broussard, J.A., Mahsut, A., Webb, D.J., and McLean, J.A. (2010). Identification of phosphorylation sites within the signaling adaptor APPL1 by mass spectrometry. *J Proteome Res*. **9**, 1541-1548.

Gao, J., Aksoy, B.A., Dogrusoz, U., Dresdner, G., Gross, B., Sumer, S.O., Sun, Y., Jacobsen, A., Sinha, R., Larsson, E., Cerami, E., Sander, C., and Schultz, N. (2013). Integrative analysis of complex cancer genomics and clinical profiles using the cBioPortal. *Sci Signal*. **6**, pl1.

Gardiner, E.M., Pestonjamasp, K.N., Bohl, B.P., Chamberlain, C., Hahn, K.M., and Bokoch, G.M. (2002). Spatial and temporal analysis of Rac activation during live neutrophil chemotaxis. *Curr Biol*. **12**, 2029-2034.

Geiger, B., Bershadsky, A., Pankov, R., and Yamada, K.M. (2001). Transmembrane crosstalk between the extracellular matrix--cytoskeleton crosstalk. *Nat Rev Mol Cell Biol*. **2**, 793-805.

Geiger, B., and Yamada, K.M. (2011). Molecular architecture and function of matrix adhesions. *Cold Spring Harb Perspect Biol*. **3**,

Georgescu, W., Wikswo, J.P., and Quaranta, V. (2012). CellAnimation: an open source MATLAB framework for microscopy assays. *Bioinformatics*. **28**, 138-139.

Geraldo, S., Simon, A., Elkhatib, N., Louvard, D., Fetler, L., and Vignjevic, D.M. (2012). Do cancer cells have distinct adhesions in 3D collagen matrices and in vivo? *Eur J Cell Biol*. **91**, 930-937.

Gorelik, R., and Gautreau, A. (2014). Quantitative and unbiased analysis of directional persistence in cell migration. *Nat Protoc*. **9**, 1931-1943.

Grande-Garcia, A., Echarri, A., and Del Pozo, M.A. (2005). Integrin regulation of membrane domain trafficking and Rac targeting. *Biochem Soc Trans*. **33**, 609-613.

Grinnell, F. (2003). Fibroblast biology in three-dimensional collagen matrices. *Trends Cell Biol*. **13**, 264-269.

Haack, H., and Hynes, R.O. (2001). Integrin receptors are required for cell survival and proliferation during development of the peripheral glial lineage. *Dev Biol*. **233**, 38-55.

Habermann, B. (2004). The BAR-domain family of proteins: a case of bending and binding? *EMBO Rep*. **5**, 250-255.

Hagiwara, M., Shirai, Y., Nomura, R., Sasaki, M., Kobayashi, K., Tadokoro, T., and Yamamoto, Y. (2009). Caveolin-1 activates Rab5 and enhances endocytosis through direct interaction. *Biochem Biophys Res Commun*. **378**, 73-78.

Hakkinen, K.M., Harunaga, J.S., Doyle, A.D., and Yamada, K.M. (2011). Direct comparisons of the morphology, migration, cell adhesions, and actin cytoskeleton of fibroblasts in four different three-dimensional extracellular matrices. *Tissue Eng Part A*. **17**, 713-724.

Hanein, D., and Horwitz, A.R. (2012). The structure of cell-matrix adhesions: the new frontier. *Curr Opin Cell Biol*. **24**, 134-140.

Harshey, R.M. (2003). Bacterial motility on a surface: many ways to a common goal. *Annu Rev Microbiol*. **57**, 249-273.

Harunaga, J.S., and Yamada, K.M. (2011). Cell-matrix adhesions in 3D. *Matrix Biol*. **30**, 363-368.

Heasman, S.J., Carlin, L.M., Cox, S., Ng, T., and Ridley, A.J. (2010). Coordinated RhoA signaling at the leading edge and uropod is required for T cell transendothelial migration. *J Cell Biol*. **190**, 553-563.

Heath, J.P., and Dunn, G.A. (1978). Cell to substratum contacts of chick fibroblasts and their relation to the microfilament system. A correlated interference-reflexion and high-voltage electron-microscope study. *J Cell Sci*. **29**, 197-212.

Higgs, H.N., and Pollard, T.D. (2001). Regulation of actin filament network formation through ARP2/3 complex: activation by a diverse array of proteins. *Annu Rev Biochem*. **70**, 649-676.

Horwitz, A.R. (2012). The origins of the molecular era of adhesion research. *Nat Rev Mol Cell Biol*. **13**, 805-811.

Hu, P., and Luo, B.H. (2013). Integrin bi-directional signaling across the plasma membrane. *J Cell Physiol*. **228**, 306-312.

Humphries, J.D., Byron, A., Bass, M.D., Craig, S.E., Pinney, J.W., Knight, D., and Humphries, M.J. (2009). Proteomic analysis of integrin-associated complexes identifies RCC2 as a dual regulator of Rac1 and Arf6. *Sci Signal*. **2**, ra51.

Humphries, J.D., Byron, A., and Humphries, M.J. (2006). Integrin ligands at a glance. *J Cell Sci*. **119**, 3901-3903.

Husi, H., Ward, M.A., Choudhary, J.S., Blackstock, W.P., and Grant, S.G. (2000). Proteomic analysis of NMDA receptor-adhesion protein signaling complexes. *Nat Neurosci*. **3**, 661-669.

Hutagalung, A.H., and Novick, P.J. (2011). Role of Rab GTPases in membrane traffic and cell physiology. *Physiol Rev*. **91**, 119-149.

Huttenlocher, A., Ginsberg, M.H., and Horwitz, A.F. (1996). Modulation of cell migration by integrin-mediated cytoskeletal linkages and ligand-binding affinity. *J Cell Biol*. **134**, 1551-1562.

Huttenlocher, A., and Horwitz, A.R. (2011). Integrins in cell migration. *Cold Spring Harb Perspect Biol*. **3**, a005074.

Hynes, R.O. (2002). Integrins: bidirectional, allosteric signaling machines. *Cell*. **110**, 673-687.

Ilic, D., Furuta, Y., Kanazawa, S., Takeda, N., Sobue, K., Nakatsuji, N., Nomura, S., Fujimoto, J., Okada, M., and Yamamoto, T. (1995). Reduced cell motility and enhanced focal adhesion contact formation in cells from FAK-deficient mice. *Nature*. **377**, 539-544.

Isogai, T., van der Kammen, R., Leyton-Puig, D., Kedziora, K.M., Jalink, K., and Innocenti, M. (2015). Initiation of lamellipodia and ruffles involves cooperation between mDia1 and the Arp2/3 complex. *J Cell Sci*. **128**, 3796-3810.

Ivaska, J. (2012). Unanchoring integrins in focal adhesions. *Nat Cell Biol*. **14**, 981-983.

Izaguirre, G., Aguirre, L., Hu, Y.P., Lee, H.Y., Schlaepfer, D.D., Aneskievich, B.J., and Haimovich, B. (2001). The cytoskeletal/non-muscle isoform of alpha-actinin is phosphorylated on its actin-binding domain by the focal adhesion kinase. *J Biol Chem*. **276**, 28676-28685.

Izzard, C.S., and Lochner, L.R. (1976). Cell-to-substrate contacts in living fibroblasts: an interference reflexion study with an evaluation of the technique. *J Cell Sci*. **21**, 129-159.

Jacquemet, G., Green, D.M., Bridgewater, R.E., von Kriegsheim, A., Humphries, M.J., Norman, J.C., and Caswell, P.T. (2013a). RCP-driven alpha5beta1 recycling suppresses Rac and promotes RhoA activity via the RacGAP1-IQGAP1 complex. *J Cell Biol*. **202**, 917-935.

Jacquemet, G., Humphries, M.J., and Caswell, P.T. (2013b). Role of adhesion receptor trafficking in 3D cell migration. *Curr Opin Cell Biol*. **25**, 627-632.

Jacquemet, G., Morgan, M.R., Byron, A., Humphries, J.D., Choi, C.K., Chen, C.S., Caswell, P.T., and Humphries, M.J. (2013c). Rac1 is deactivated at integrin activation sites through an IQGAP1-filamin-A-RacGAP1 pathway. *J Cell Sci*. **126**, 4121-4135.

Jaffe, A.B., and Hall, A. (2005). Rho GTPases: biochemistry and biology. *Annu Rev Cell Dev Biol*. **21**, 247-269.

Jean, L., Majumdar, D., Shi, M., Hinkle, L.E., Diggins, N.L., Ao, M., Broussard, J.A., Evans, J.C., Choma, D.P., and Webb, D.J. (2013). Activation of Rac by Asef2 promotes myosin II-dependent contractility to inhibit cell migration on type I collagen. *J Cell Sci*. **126**, 5585-5597.

Jean, L., Yang, L., Majumdar, D., Gao, Y., Shi, M., Brewer, B.M., Li, D., and Webb, D.J. (2014). The Rho family GEF Asef2 regulates cell migration in three dimensional (3D) collagen matrices through myosin II. *Cell Adh Migr*. **8**, 460-467.

Johnson, I.R., Parkinson-Lawrence, E.J., Shandala, T., Weigert, R., Butler, L.M., and Brooks, D.A. (2014). Altered endosome biogenesis in prostate cancer has biomarker potential. *Mol Cancer Res*. **12**, 1851-1862.

Johnson, M.S., Lu, N., Denessiouk, K., Heino, J., and Gullberg, D. (2009). Integrins during evolution: evolutionary trees and model organisms. *Biochim Biophys Acta*. **1788**, 779-789.

Jones, M.C., Humphries, J.D., Byron, A., Millon-Fremillon, A., Robertson, J., Paul, N.R., Ng, D.H., Askari, J.A., and Humphries, M.J. (2015). Isolation of integrin-based adhesion complexes. *Curr Protoc Cell Biol*. **66**, 9 8 1-15.

Joshi, P., Greco, T.M., Guise, A.J., Luo, Y., Yu, F., Nesvizhskii, A.I., and Cristea, I.M. (2013). The functional interactome landscape of the human histone deacetylase family. *Mol Syst Biol*. **9**, 672.

Juliano, R.L. (2002). Signal transduction by cell adhesion receptors and the cytoskeleton: functions of integrins, cadherins, selectins, and immunoglobulin-superfamily members. *Annu Rev Pharmacol Toxicol*. **42**, 283-323.

Justus, C.R., Leffler, N., Ruiz-Echevarria, M., and Yang, L.V. (2014). In vitro cell migration and invasion assays. *J Vis Exp*.

Kalaidzidis, I., Miaczynska, M., Brewinska-Olchowik, M., Hupalowska, A., Ferguson, C., Parton, R.G., Kalaidzidis, Y., and Zerial, M. (2015). APPL endosomes are not obligatory endocytic intermediates but act as stable cargo-sorting compartments. *J Cell Biol*. **211**, 123-144.

Kanchanawong, P., Shtengel, G., Pasapera, A.M., Ramko, E.B., Davidson, M.W., Hess, H.F., and Waterman, C.M. (2010). Nanoscale architecture of integrin-based cell adhesions. *Nature*. **468**, 580-584.

Katoh, M. (2013). Functional proteomics, human genetics and cancer biology of GIPC family members. *Exp Mol Med*. **45**, e26.

Kawauchi, T. (2012). Cell adhesion and its endocytic regulation in cell migration during neural development and cancer metastasis. *Int J Mol Sci*. **13**, 4564-4590.

Kim, C., Ye, F., and Ginsberg, M.H. (2011). Regulation of integrin activation. *Annu Rev Cell Dev Biol*. **27**, 321-345.

Kim, M., Carman, C.V., and Springer, T.A. (2003). Bidirectional transmembrane signaling by cytoplasmic domain separation in integrins. *Science*. **301**, 1720-1725.

King, G.J., Stöckli, J., Hu, S.H., Winnen, B., Duprez, W.G.A., C. Meoli, C.C., Junutula, J.R., Jarrott, R.J., James, D.E., Whitten, A.E., and Martin, J.L. (2012). Membrane Curvature Protein Exhibits Interdomain Flexibility

and Binds a Small GTPase. *J Biol Chem*. **287**, 40996–41006.

Kiosses, W.B., Hood, J., Yang, S., Gerritsen, M.E., Cheresh, D.A., Alderson, N., and Schwartz, M.A. (2002). A dominant-negative p65 PAK peptide inhibits angiogenesis. *Circ Res*. **90**, 697-702.

Kok, K., Naylor, S.L., and Buys, C.H. (1997). Deletions of the short arm of chromosome 3 in solid tumors and the search for suppressor genes. *Adv Cancer Res*. **71**, 27-92.

Kramer, N., Walzl, A., Unger, C., Rosner, M., Krupitza, G., Hengstschlager, M., and Dolznig, H. (2013). In vitro cell migration and invasion assays. *Mutat Res*. **752**, 10-24.

Kubow, K.E., Conrad, S.K., and Horwitz, A.R. (2013). Matrix microarchitecture and myosin II determine adhesion in 3D matrices. *Curr Biol*. **23**, 1607-1619.

Kubow, K.E., and Horwitz, A.R. (2011). Reducing background fluorescence reveals adhesions in 3D matrices. *Nat Cell Biol*. **13**, 3-5; author reply 5-7.

Kuo, J.C., Han, X., Hsiao, C.T., Yates, J.R., 3rd, and Waterman, C.M. (2011). Analysis of the myosin-II-responsive focal adhesion proteome reveals a role for beta-Pix in negative regulation of focal adhesion maturation. *Nat Cell Biol*. **13**, 383-393.

Kutys, M.L., Doyle, A.D., and Yamada, K.M. (2013). Regulation of cell adhesion and migration by cell-derived matrices. *Exp Cell Res*. **319**, 2434-2439.

Kutys, M.L., and Yamada, K.M. (2014). An extracellular-matrix-specific GEF-GAP interaction regulates Rho GTPase crosstalk for 3D collagen migration. *Nat Cell Biol*. **16**, 909-917.

Lad, Y., Harburger, D.S., and Calderwood, D.A. (2007). Integrin cytoskeletal interactions. *Methods Enzymol*. **426**, 69-84.

LaLonde, D.P., Grubinger, M., Lamarche-Vane, N., and Turner, C.E. (2006). CdGAP associates with actopaxin to regulate integrin-dependent changes in cell morphology and motility. *Curr Biol*. **16**, 1375-1385.

Lanzetti, L., and Di Fiore, P.P. (2008). Endocytosis and cancer: an 'insider' network with dangerous liaisons. *Traffic*. **9**, 2011-2021.

Lanzetti, L., Palamidessi, A., Areces, L., Scita, G., and Di Fiore, P.P. (2004). Rab5 is a signalling GTPase involved in actin remodelling by receptor tyrosine kinases. *Nature*. **429**, 309-314.

Law, A.L., Vehlow, A., Kotini, M., Dodgson, L., Soong, D., Theveneau, E., Bodo, C., Taylor, E., Navarro, C., Perera, U., Michael, M., Dunn, G.A., Bennett, D., Mayor, R., and Krause, M. (2013). Lamellipodin and the Scar/WAVE complex cooperate to promote cell migration in vivo. *J Cell Biol*. **203**, 673-689.

Lawson, C.D., and Burridge, K. (2014). The on-off relationship of Rho and Rac during integrin-mediated adhesion and cell migration. *Small GTPases*. **5**, e27958.

Lawson, C.D., and Ridley, A.J. (2017). Rho GTPase signaling complexes in cell migration and invasion. *J Cell Biol*.

Lawson, M.A., and Maxfield, F.R. (1995). Ca(2+)- and calcineurin-dependent recycling of an integrin to the front of migrating neutrophils. *Nature*. **377**, 75-79.

Lee, J.R., Hahn, H.S., Kim, Y.H., Nguyen, H.H., Yang, J.M., Kang, J.S., and Hahn, M.J. (2011). Adaptor protein containing PH domain, PTB domain and leucine zipper (APPL1) regulates the protein level of EGFR by modulating its trafficking. *Biochem Biophys Res Commun*. **415**, 206-211.

Lefort, C.T., Rossaint, J., Moser, M., Petrich, B.G., Zarbock, A., Monkley, S.J., Critchley, D.R., Ginsberg, M.H., Fassler, R., and Ley, K. (2012). Distinct roles for talin-1 and kindlin-3 in LFA-1 extension and affinity regulation. *Blood*. **119**, 4275-4282.

Legate, K.R., Wickstrom, S.A., and Fassler, R. (2009). Genetic and cell biological analysis of integrin outside-in signaling. *Genes Dev*. **23**, 397-418.

Li, J., Ballif, B.A., Powelka, A.M., Dai, J., Gygi, S.P., and Hsu, V.W. (2005). Phosphorylation of ACAP1 by Akt regulates the stimulation-dependent recycling of integrin beta1 to control cell migration. *Dev Cell*. **9**, 663-673.

Li, J., Mao, X., Dong, L.Q., Liu, F., and Tong, L. (2007). Crystal structures of the BAR-PH and PTB domains of human APPL1. *Structure*. **15**, 525-533.

Li, S., Lao, J., Chen, B.P., Li, Y.S., Zhao, Y., Chu, J., Chen, K.D., Tsou, T.C., Peck, K., and Chien, S. (2003). Genomic analysis of smooth muscle cells in 3-dimensional collagen matrix. *FASEB J*. **17**, 97-99.

Lin, D.C., Quevedo, C., Brewer, N.E., Bell, A., Testa, J.R., Grimes, M.L., Miller, F.D., and Kaplan, D.R. (2006). APPL1 associates with TrkA and GIPC1 and is required for nerve growth factor-mediated signal transduction. *Mol Cell Biol*. **26**, 8928-8941.

Liu, J., Yao, F., Wu, R., Morgan, M., Thorburn, A., Finley, R.L., and Chen, Y.Q. (2002). Mediation of the DCC Apoptotic Signal by DIP13 *J Biol Chem*. **277**, 26281-26285.

Liu, M., Zhou, L., Wei, L., Villarreal, R., Yang, X., Hu, D., Riojas, R.A., Holmes, B.M., Langlais, P.R., Lee, H., and Dong, L.Q. (2012). Phosphorylation of adaptor protein containing pleckstrin homology domain, phosphotyrosine binding domain, and leucine zipper motif 1 (APPL1) at Ser430 mediates endoplasmic reticulum (ER) stress-induced insulin resistance in hepatocytes. *J Biol Chem*. **287**, 26087-26093.

Liu, S., Calderwood, D.A., and Ginsberg, M.H. (2000). Integrin cytoplasmic domain-binding proteins. *J Cell Sci*. **113 (Pt 20)**, 3563-3571.

Lobert, V.H., Brech, A., Pedersen, N.M., Wesche, J., Oppelt, A., Malerod, L., and Stenmark, H. (2010). Ubiquitination of alpha 5 beta 1 integrin controls fibroblast migration through lysosomal degradation of fibronectin-integrin complexes. *Dev Cell*. **19**, 148-159.

Lock, J.G., Wehrle-Haller, B., and Stromblad, S. (2008). Cell-matrix adhesion complexes: master control machinery of cell migration. *Semin Cancer Biol*. **18**, 65-76.

Lopez-Colome, A.M., Lee-Rivera, I., Benavides-Hidalgo, R., and Lopez, E. (2017). Paxillin: a crossroad in pathological cell migration. *J Hematol Oncol*. **10**, 50.

Machacek, M., Hodgson, L., Welch, C., Elliott, H., Pertz, O., Nalbant, P., Abell, A., Johnson, G.L., Hahn, K.M., and Danuser, G. (2009). Coordination of Rho GTPase activities during cell protrusion. *Nature*. **461**, 99-103.

Mao, X., Kikani, C.K., Riojas, R.A., Langlais, P., Wang, L., Ramos, F.J., Fang, Q., Christ-Roberts, C.Y., Hong, J.Y., Kim, R.Y., Liu, F., and Dong, L.Q. (2006). APPL1 binds to adiponectin receptors and mediates adiponectin signalling and function. *Nat Cell Biol*. **8**, 516-523.

Margadant, C., Kreft, M., de Groot, D.J., Norman, J.C., and Sonnenberg, A. (2012). Distinct roles of talin and kindlin in regulating integrin alpha5beta1 function and trafficking. *Curr Biol*. **22**, 1554-1563.

Margadant, C., Monsuur, H.N., Norman, J.C., and Sonnenberg, A. (2011). Mechanisms of integrin activation and trafficking. *Curr Opin Cell Biol*. **23**, 607-614.

Maritzen, T., Schachtner, H., and Legler, D.F. (2015). On the move: endocytic trafficking in cell migration. *Cell Mol Life Sci*. **72**, 2119-2134.

Mayor, R., and Etienne-Manneville, S. (2016). The front and rear of collective cell migration. *Nat Rev Mol Cell Biol*. **17**, 97-109.

Memmo, L.M., and McKeown-Longo, P. (1998). The alphavbeta5 integrin functions as an endocytic receptor for vitronectin. *J Cell Sci*. **111 (Pt 4)**, 425-433.

Menard, L., Parker, P.J., and Kermorgant, S. (2014). Receptor tyrosine kinase c-Met controls the cytoskeleton from different endosomes via different pathways. *Nat Commun*. **5**, 3907.

Mendoza, P., Diaz, J., and Torres, V.A. (2014). On the role of Rab5 in cell migration. *Curr Mol Med*. **14**, 235-245.

Mendoza, P., Ortiz, R., Diaz, J., Quest, A.F., Leyton, L., Stupack, D., and Torres, V.A. (2013). Rab5 activation promotes focal adhesion disassembly, migration and invasiveness in tumor cells. *J Cell Sci*. **126**, 3835-3847.

Meyer, A.S., Hughes-Alford, S.K., Kay, J.E., Castillo, A., Wells, A., Gertler, F.B., and Lauffenburger, D.A. (2012). 2D protrusion but not motility predicts growth factor-induced cancer cell migration in 3D collagen. *J Cell Biol*. **197**, 721-729.

Miaczynska, M., Christoforidis, S., Giner, A., Shevchenko, A., Uttenweiler-Joseph, S., Habermann, B., Wilm, M., Parton, R.G., and Zerial, M. (2004). APPL proteins link Rab5 to nuclear signal transduction via an endosomal compartment. *Cell*. **116**, 445-456.

Michael, M., Vehlow, A., Navarro, C., and Krause, M. (2010). c-Abl, Lamellipodin, and Ena/VASP proteins cooperate in dorsal ruffling of fibroblasts and axonal morphogenesis. *Curr Biol*. **20**, 783-791.

Mitra, S.K., Hanson, D.A., and Schlaepfer, D.D. (2005). Focal adhesion kinase: in command and control of cell motility. *Nat Rev Mol Cell Biol*. **6**, 56-68.

Mitsuuchi, Y., Johnson, S.W., Sonoda, G., Tanno, S., Golemis, E.A., and Testa, J.R. (1999). Identification of a chromosome 3p14.3-21.1 gene, APPL, encoding an adaptor molecule that interacts with the oncoprotein-serine/threonine kinase AKT2. *Oncogene*. **18**, 4891-4898.

Miyamoto, S., Teramoto, H., Coso, O.A., Gutkind, J.S., Burvbelo, P.D., Akiyama, S.K., and Yamada, K.M. (1995). Integrin function: molecular hierarchies of cytoskeletal and signaling molecules. *J. Cell Biol.* **131**, 791-805.

Moravec, R., Conger, K.K., D'Souza, R., Allison, A.B., and Casanova, J.E. (2012). BRAG2/GEP100/IQSec1 interacts with clathrin and regulates alpha5beta1 integrin endocytosis through activation of ADP ribosylation factor 5 (Arf5). *J Biol Chem*. **287**, 31138-31147.

Morgan, M.R., Byron, A., Humphries, M.J., and Bass, M.D. (2009). Giving off mixed signals--distinct functions of alpha5beta1 and alphavbeta3 integrins in regulating cell behaviour. *IUBMB Life*. **61**, 731-738.

Morgan, M.R., Hamidi, H., Bass, M.D., Warwood, S., Ballestrem, C., and Humphries, M.J. (2013). Syndecan-4 phosphorylation is a control point for integrin recycling. *Dev Cell*. **24**, 472-485.

Moser, M., Legate, K.R., Zent, R., and Fassler, R. (2009). The tail of integrins, talin, and kindlins. *Science*. **324**, 895-899.

Muller, P.A., Trinidad, A.G., Timpson, P., Morton, J.P., Zanivan, S., van den Berghe, P.V., Nixon, C., Karim, S.A., Caswell, P.T., Noll, J.E., Coffill, C.R., Lane, D.P.,

Sansom, O.J., Neilsen, P.M., Norman, J.C., and Vousden, K.H. (2013). Mutant p53 enhances MET trafficking and signalling to drive cell scattering and invasion. *Oncogene*. **32**, 1252-1265.

Nagano, M., Hoshino, D., Koshikawa, N., Akizawa, T., and Seiki, M. (2012). Turnover of focal adhesions and cancer cell migration. *Int J Cell Biol*. **2012**, 310616.

Nagano, M., Hoshino, D., Sakamoto, T., Kawasaki, N., Koshikawa, N., and Seiki, M. (2010). ZF21 protein regulates cell adhesion and motility. *J Biol Chem*. **285**, 21013-21022.

Nakamura, Y., Kagami, H., and Tagami, T. (2013). Development, differentiation and manipulation of chicken germ cells. *Dev Growth Differ*. **55**, 20-40.

Nayal, A., Webb, D.J., Brown, C.M., Schaefer, E.M., Vicente-Manzanares, M., and Horwitz, A.R. (2006). Paxillin phosphorylation at Ser273 localizes a GIT1-PIX-PAK complex and regulates adhesion and protrusion dynamics. *J Cell Biol*. **173**, 587-589.

Nechamen, C.A., Thomas, R.M., Cohen, B.D., Acevedo, G., Poulikakos, P.I., Testa, J.R., and Dias, J.A. (2004). Human follicle-stimulating hormone (FSH) receptor interacts with the adaptor protein APPL1 in HEK 293 cells: potential involvement of the PI3K pathway in FSH signaling. *Biol Reprod*. **71**, 629-636.

Nechamen, C.A., Thomas, R.M., and Dias, J.A. (2007). APPL1, APPL2, Akt2 and FOXO1a interact with FSHR in a potential signaling complex. *Mol Cell Endocrinol*. **260-262**, 93-99.

Ng, T., Shima, D., Squire, A., Bastiaens, P.I., Gschmeissner, S., Humphries, M.J., and Parker, P.J. (1999). PKCalpha regulates beta1 integrin-dependent cell motility through association and control of integrin traffic. *EMBO J*. **18**, 3909-3923.

Nishimura, T., and Kaibuchi, K. (2007). Numb controls integrin endocytosis for directional cell migration with aPKC and PAR-3. *Dev Cell*. **13**, 15-28.

Nobes, C.D., and Hall, A. (1995). Rho, rac, and cdc42 GTPases regulate the assembly of multimolecular focal complexes associated with actin stress fibers, lamellipodia, and filopodia. *Cell*. **81**, 53-62.

Palamidessi, A., Frittoli, E., Garre, M., Faretta, M., Mione, M., Testa, I., Diaspro, A., Lanzetti, L., Scita, G., and Di Fiore, P.P. (2008). Endocytic trafficking of Rac is required for the spatial restriction of signaling in cell migration. *Cell*. **134**, 135-147.

Palfy, M., Remenyi, A., and Korcsmaros, T. (2012). Endosomal crosstalk: meeting points for signaling pathways. *Trends Cell Biol*. **22**, 447-456.

Pankov, R., Endo, Y., Even-Ram, S., Araki, M., Clark, K., Cukierman, E., Matsumoto, K., and Yamada, K.M. (2005). A Rac switch regulates random versus directionally persistent cell migration. *J Cell Biol*. **170**, 793-802.

Parsons, J.T., Horwitz, A.R., and Schwartz, M.A. (2010). Cell adhesion: integrating cytoskeletal dynamics and cellular tension. *Nat Rev Mol Cell Biol*. **11**, 633-643.

Pasapera, A.M., Schneider, I.C., Rericha, E., Schlaepfer, D.D., and Waterman, C.M. (2010). Myosin II activity regulates vinculin recruitment to focal adhesions through FAK-mediated paxillin phosphorylation. *J Cell Biol*. **188**, 877-890.

Paul, N.R., Allen, J.L., Chapman, A., Morlan-Mairal, M., Zindy, E., Jacquemet, G., Fernandez del Ama, L., Ferizovic, N., Green, D.M., Howe, J.D., Ehler, E., Hurlstone, A., and Caswell, P.T. (2015a). alpha5beta1 integrin recycling promotes Arp2/3-independent cancer cell invasion via the formin FHOD3. *J Cell Biol*. **210**, 1013-1031.

Paul, N.R., Jacquemet, G., and Caswell, P.T. (2015b). Endocytic Trafficking of Integrins in Cell Migration. *Curr Biol*. **25**, R1092-1105.

Peacock, J.G., Miller, A.L., Bradley, W.D., Rodriguez, O.C., Webb, D.J., and Koleske, A.J. (2007). The Abl-related gene tyrosine kinase acts through p190RhoGAP to inhibit actomyosin contractility and regulate focal adhesion dynamics upon adhesion to fibronectin. *Mol Biol Cell*. **18**, 3860-3872.

Pellinen, T., Arjonen, A., Vuoriluoto, K., Kallio, K., Fransen, J.A., and Ivaska, J. (2006). Small GTPase Rab21 regulates cell adhesion and controls endosomal traffic of beta1-integrins. *J Cell Biol*. **173**, 767-780.

Pellinen, T., and Ivaska, J. (2006). Integrin traffic. *J Cell Sci*. **119**, 3723-3731.

Pereira-Leal, J.B., and Seabra, M.C. (2000). The mammalian Rab family of small GTPases: definition of family and subfamily sequence motifs suggests a mechanism for functional specificity in the Ras superfamily. *J Mol Biol*. **301**, 1077-1087.

Pereira-Leal, J.B., and Seabra, M.C. (2001). Evolution of the Rab family of small GTP-binding proteins. *J Mol Biol*. **313**, 889-901.

Petrie, R.J., Doyle, A.D., and Yamada, K.M. (2009). Random versus directionally persistent cell migration. *Nat Rev Mol Cell Biol*. **10**, 538-549.

Petrie, R.J., Harlin, H.M., Korsak, L.I., and Yamada, K.M. (2017). Activating the nuclear piston mechanism of 3D migration in tumor cells. *J Cell Biol*. **216**, 93-100.

Petrie, R.J., Koo, H., and Yamada, K.M. (2014). Generation of compartmentalized pressure by a nuclear piston governs cell motility in a 3D matrix. *Science*. **345**, 1062-1065.

Petrie, R.J., and Yamada, K.M. (2016). Multiple mechanisms of 3D migration: the origins of plasticity. *Curr Opin Cell Biol*. **42**, 7-12.

Petroll, W.M., and Ma, L. (2003). Direct, dynamic assessment of cell-matrix interactions inside fibrillar collagen lattices. *Cell Motil Cytoskeleton*. **55**, 254-264.

Pick, R., Brechtefeld, D., and Walzog, B. (2013). Intraluminal crawling versus interstitial neutrophil migration during inflammation. *Mol Immunol*. **55**, 70-75.

Pollard, T.D., and Borisy, G.G. (2003). Cellular motility driven by assembly and disassembly of actin filaments. *Cell*. **112**, 453-465.

Powelka, A.M., Sun, J., Li, J., Gao, M., Shaw, L.M., Sonnenberg, A., and Hsu, V.W. (2004). Stimulation-dependent recycling of integrin beta1 regulated by ARF6 and Rab11. *Traffic*. **5**, 20-36.

Pyrzynska, B., Banach-Orlowska, M., Teperek-Tkacz, M., Miekus, K., Drabik, G., Majka, M., and Miaczynska, M. (2013). Multifunctional protein APPL2 contributes to survival of human glioma cells. *Mol Oncol*. **7**, 67-84.

Rashid, S., Pilecka, I., Torun, A., Olchowik, M., Bielinska, B., and Miaczynska, M. (2009). Endosomal adaptor proteins APPL1 and APPL2 are novel activators of beta-catenin/TCF-mediated transcription. *J Biol Chem*. **284**, 18115-18128.

Reddig, P.J., and Juliano, R.L. (2005). Clinging to life: cell to matrix adhesion and cell survival. *Cancer Metastasis Rev*. **24**, 425-439.

Reig, G., Pulgar, E., and Concha, M.L. (2014). Cell migration: from tissue culture to embryos. *Development*. **141**, 1999-2013.

Ren, X.D., Kiosses, W.B., and Schwartz, M.A. (1999). Regulation of the small GTP-binding protein Rho by cell adhesion and the cytoskeleton. *EMBO J*. **18**, 578-585.

Ridley, A.J. (2001). Rho GTPases and cell migration. *J Cell Sci*. **114**, 2713-2722.

Ridley, A.J. (2011). Life at the leading edge. *Cell*. **145**, 1012-1022.

Ridley, A.J. (2015). Rho GTPase signalling in cell migration. *Curr Opin Cell Biol*. **36**, 103-112.

Ridley, A.J., Schwartz, M.A., Burridge, K., Firtel, R.A., Ginsberg, M.H., Borisy, G., Parsons, J.T., and Horwitz, A.R. (2003). Cell migration: integrating signals from front to back. *Science*. **302**, 1704-1709.

Roca-Cusachs, P., del Rio, A., Puklin-Faucher, E., Gauthier, N.C., Biais, N., and Sheetz, M.P. (2013). Integrin-dependent force transmission to the extracellular matrix by alpha-actinin triggers adhesion maturation. *Proc Natl Acad Sci U S A*. **110**, E1361-1370.

Ross, T.D., Coon, B.G., Yun, S., Baeyens, N., Tanaka, K., Ouyang, M., and Schwartz, M.A. (2013). Integrins in mechanotransduction. *Curr Opin Cell Biol*. **25**, 613-618.

Rossier, O., Octeau, V., Sibarita, J.B., Leduc, C., Tessier, B., Nair, D., Gatterdam, V., Destaing, O., Albiges-Rizo, C., Tampe, R., Cognet, L., Choquet, D., Lounis, B., and Giannone, G. (2012). Integrins beta1 and beta3 exhibit distinct dynamic nanoscale organizations inside focal adhesions. *Nat Cell Biol*. **14**, 1057-1067.

Ryu, J., Galan, A.K., Xin, X., Dong, F., Abdul-Ghani, M.A., Zhou, L., Wang, C., Li, C., Holmes, B.M., Sloane, L.B., Austad, S.N., Guo, S., Musi, N., DeFronzo, R.A., Deng, C., White, M.F., Liu, F., and Dong, L.Q. (2014). APPL1 potentiates insulin sensitivity by facilitating the binding of IRS1/2 to the insulin receptor. *Cell Rep*. **7**, 1227-1238.

Sackmann, E. (2015). How actin/myosin crosstalks guide the adhesion, locomotion and polarization of cells. *Biochim Biophys Acta*. **1853**, 3132-3142.

Sadok, A., and Marshall, C.J. (2014). Rho GTPases: masters of cell migration. *Small GTPases*. **5**, e29710.

Sakurai, A., Gavard, J., Annas-Linhares, Y., Basile, J.R., Amornphimoltham, P., Palmby, T.R., Yagi, H., Zhang, F., Randazzo, P.A., Li, X., Weigert, R., and Gutkind, J.S.

(2010). Semaphorin 3E initiates antiangiogenic signaling through plexin D1 by regulating Arf6 and R-Ras. *Mol Cell Biol*. **30**, 3086-3098.

Saleh, A.J., Soltani, B.M., Dokanehiifard, S., Medlej, A., Tavalaei, M., and Mowla, S.J. (2016). Experimental verification of a predicted novel microRNA located in human PIK3CA gene with a potential oncogenic function in colorectal cancer. *Tumour Biol*. **37**, 14089-14101.

Sander, E.E., ten Klooster, J.P., van Delft, S., van der Kammen, R.A., and Collard, J.G. (1999). Rac downregulates Rho activity: reciprocal balance between both GTPases determines cellular morphology and migratory behavior. *J Cell Biol*. **147**, 1009-1022.

Sandri, C., Caccavari, F., Valdembri, D., Camillo, C., Veltel, S., Santambrogio, M., Lanzetti, L., Bussolino, F., Ivaska, J., and Serini, G. (2012). The R-Ras/RIN2/Rab5 complex controls endothelial cell adhesion and morphogenesis via active integrin endocytosis and Rac signaling. *Cell Res*. **22**, 1479-1501.

Santiago-Medina, M., Gregus, K.A., and Gomez, T.M. (2013). PAK-PIX interactions regulate adhesion dynamics and membrane protrusion to control neurite outgrowth. *J Cell Sci*. **126**, 1122-1133.

Sanz-Moreno, V., Gadea, G., Ahn, J., Paterson, H., Marra, P., Pinner, S., Sahai, E., and Marshall, C.J. (2008). Rac activation and inactivation control plasticity of tumor cell movement. *Cell*. **135**, 510-523.

Sanz-Moreno, V., Gaggioli, C., Yeo, M., Albrengues, J., Wallberg, F., Viros, A., Hooper, S., Mitter, R., Feral, C.C., Cook, M., Larkin, J., Marais, R., Meneguzzi, G., Sahai, E., and Marshall, C.J. (2011). ROCK and JAK1 signaling cooperate to control actomyosin contractility in tumor cells and stroma. *Cancer Cell*. **20**, 229-245.

Scales, T.M., Jayo, A., Obara, B., Holt, M.R., Hotchin, N.A., Berditchevski, F., and Parsons, M. (2013). alpha3beta1 integrins regulate CD151 complex assembly and membrane dynamics in carcinoma cells within 3D environments. *Oncogene*. **32**, 3965-3979.

Schaller, M.D. (2001). Paxillin: a focal adhesion-associated adaptor protein. *Oncogene*. **20**, 6459-6472.

Schenck, A., Goto-Silva, L., Collinet, C., Rhinn, M., Giner, A., Habermann, B., Brand, M., and Zerial, M. (2008). The endosomal protein Appl1 mediates Akt substrate specificity and cell survival in vertebrate development. *Cell*. **133**, 486-497.

Schiller, H.B., Friedel, C.C., Boulegue, C., and Fassler, R. (2011). Quantitative proteomics of the integrin adhesome show a myosin II-dependent recruitment of LIM domain proteins. *EMBO Rep*. **12**, 259-266.

Schiller, H.B., Hermann, M.R., Polleux, J., Vignaud, T., Zanivan, S., Friedel, C.C., Sun, Z., Raducanu, A., Gottschalk, K.E., Thery, M., Mann, M., and Fassler, R. (2013). beta1- and alphav-class integrins cooperate to regulate myosin II during rigidity sensing of fibronectin-based microenvironments. *Nat Cell Biol*. **15**, 625-636.

Schlessinger, J., and Lemmon, M.A. (2003). SH2 and PTB domains in tyrosine kinase signaling. *Sci STKE*. **2003**, RE12.

Schmidt, A., and Hall, A. (2002). Guanine nucleotide exchange factors for Rho GTPases: turning on the switch. *Genes Dev*. **16**, 1587-1609.

Schober, M., Raghavan, S., Nikolova, M., Polak, L., Pasolli, H.A., Beggs, H.E., Reichardt, L.F., and Fuchs, E. (2007). Focal adhesion kinase modulates tension signaling to control actin and focal adhesion dynamics. *J Cell Biol*. **176**, 667-680.

Schwartz, M. (2004). Rho signalling at a glance. *J Cell Sci*. **117**, 5457-5458.

Sczekan, M.M., and Juliano, R.L. (1990). Internalization of the fibronectin receptor is a constitutive process. *J Cell Physiol*. **142**, 574-580.

Seyfried, T.N., and Huysentruyt, L.C. (2013). On the origin of cancer metastasis. *Crit Rev Oncog*. **18**, 43-73.

Shi, F., and Sottile, J. (2008). Caveolin-1-dependent beta1 integrin endocytosis is a critical regulator of fibronectin turnover. *J Cell Sci*. **121**, 2360-2371.

Soldati, T., and Schliwa, M. (2006). Powering membrane traffic in endocytosis and recycling. *Nat Rev Mol Cell Biol*. **7**, 897-908.

Song, J., Mu, Y., Li, C., Bergh, A., Miaczynska, M., Heldin, C.H., and Landström, M. (2015). APPL proteins promote TGFβ-induced nuclear transport of the
TGFβ type I receptor intracellular domain. *Oncotarget*. **7**, 279-292.

Stark, C., Breitkreutz, B.J., Reguly, T., Boucher, L., Breitkreutz, A., and Tyers, M. (2006a). BioGRID: a general repository for interaction datasets. *Nucleic Acids Res*. **34**, D535-539.

Stark, C., Breitkreutz, B.J., Reguly, T., Boucher, L., Breitkreutz, A., and Tyers, M. (2006b). Biogrid: A General Repository for Interaction Datasets. . *Nucleic Acids Res*. **34**, D535-539

Stehbens, S.J., Paszek, M., Pemble, H., Ettinger, A., Gierke, S., and Wittmann, T. (2014). CLASPs link focal-adhesion-associated microtubule capture to localized exocytosis and adhesion site turnover. *Nat Cell Biol*. **16**, 561-573.

Steinberg, F., Heesom, K.J., Bass, M.D., and Cullen, P.J. (2012). SNX17 protects integrins from degradation by sorting between lysosomal and recycling pathways. *J Cell Biol*. **197**, 219-230.

Sun, Z., Lambacher, A., and Fassler, R. (2014). Nascent adhesions: from fluctuations to a hierarchical organization. *Curr Biol*. **24**, R801-803.

Svitkina, T.M., Bulanova, E.A., Chaga, O.Y., Vignjevic, D.M., Kojima, S., Vasiliev, J.M., and Borisy, G.G. (2003). Mechanism of filopodia initiation by reorganization of a dendritic network. *J Cell Biol*. **160**, 409-421.

Szczepanowska, J. (2009). Involvement of Rac/Cdc42/PAK pathway in cytoskeletal rearrangements. *Acta Biochim Pol*. **56**, 225-234.

Takei, K., Slepnev, V.I., Haucke, V., and De Camilli, P. (1999). Functional partnership between amphiphysin and dynamin in clathrin-mediated endocytosis. *Nat Cell Biol*. **1**, 33-39.

Tamariz, E., and Grinnell, F. (2002). Modulation of fibroblast morphology and adhesion during collagen matrix remodeling. *Mol Biol Cell*. **13**, 3915-3929.

Tan, Y., Xin, X., Coffey, F.J., Wiest, D.L., Dong, L.Q., and Testa, J.R. (2016). Appl1 and Appl2 are Expendable for Mouse Development But Are Essential for HGF-Induced Akt Activation and Migration in Mouse Embryonic Fibroblasts. *J Cell Physiol*. **231**, 1142-1150.

Tan, Y., You, H., Wu, C., Altomare, D.A., and Testa, J.R. (2010). Appl1 is dispensable for mouse development, and loss of Appl1 has growth factor-selective effects on Akt signaling in murine embryonic fibroblasts. *J Biol Chem*. **285**, 6377-6389.

Tanentzapf, G., and Brown, N.H. (2006). An interaction between integrin and the talin FERM domain mediates integrin activation but not linkage to the cytoskeleton. *Nat Cell Biol*. **8**, 601-606.

Tani, T.T., and Mercurio, A.M. (2001). PDZ interaction sites in integrin alpha subunits. T14853, TIP/GIPC binds to a type I recognition sequence in alpha 6A/alpha 5 and a novel sequence in alpha 6B. *J Biol Chem*. **276**, 36535-36542.

Teckchandani, A., Mulkearns, E.E., Randolph, T.W., Toida, N., and Cooper, J.A. (2012). The clathrin adaptor Dab2 recruits EH domain scaffold proteins to regulate integrin beta1 endocytosis. *Mol Biol Cell*. **23**, 2905-2916.

Teckchandani, A., Toida, N., Goodchild, J., Henderson, C., Watts, J., Wollscheid, B., and Cooper, J.A. (2009). Quantitative proteomics identifies a Dab2/integrin module regulating cell migration. *J Cell Biol*. **186**, 99-111.

Tiwari, A., Jung, J.J., Inamdar, S.M., Brown, C.O., Goel, A., and Choudhury, A. (2011). Endothelial cell migration on fibronectin is regulated by syntaxin 6-mediated alpha5beta1 integrin recycling. *J Biol Chem*. **286**, 36749-36761.

Torres, V.A., Mielgo, A., Barbero, S., Hsiao, R., Wilkins, J.A., and Stupack, D.G. (2010). Rab5 mediates caspase-8-promoted cell motility and metastasis. *Mol Biol Cell*. **21**, 369-376.

Torres, V.A., and Stupack, D.G. (2011). Rab5 in the regulation of cell motility and invasion. *Curr Protein Pept Sci*. **12**, 43-51.

Turner, C.E. (2000). Paxillin and focal adhesion signalling. *Nat Cell Biol*. **2**, E231-236.

Urban, E., Jacob, S., Nemethova, M., Resch, G.P., and Small, J.V. (2010). Electron tomography reveals unbranched networks of actin filaments in lamellipodia. *Nat Cell Biol*. **12**, 429-435.

Urbanska, A., Sadowski, L., Kalaidzidis, Y., and Miaczynska, M. (2011). Biochemical characterization of APPL endosomes: the role of annexin A2 in APPL membrane recruitment. *Traffic*. **12**, 1227-1241.

Valdembri, D., Caswell, P.T., Anderson, K.I., Schwarz, J.P., Konig, I., Astanina, E., Caccavari, F., Norman, J.C., Humphries, M.J., Bussolino, F., and Serini, G. (2009). Neuropilin-1/GIPC1 signaling regulates alpha5beta1 integrin traffic and function in endothelial cells. *PLoS Biol*. **7**, e25.

Valdembri, D., Sandri, C., Santambrogio, M., and Serini, G. (2011). Regulation of integrins by conformation and traffic: it takes two to tango. *Mol Biosyst*. **7**, 2539-2546.

Valdembri, D., and Serini, G. (2012). Regulation of adhesion site dynamics by integrin traffic. *Curr Opin Cell Biol*. **24**, 582-591.

van der Bliek, A.M. (2005). A sixth sense for Rab5. *Nat Cell Biol*. **7**, 548-550.

Varsano, T., Dong, M.Q., Niesman, I., Gacula, H., Lou, X., Ma, T., Testa, J.R., Yates, J.R., 3rd, and Farquhar, M.G. (2006). GIPC is recruited by APPL to peripheral TrkA endosomes and regulates TrkA trafficking and signaling. *Mol Cell Biol*. **26**, 8942-8952.

Varsano, T., Taupin, V., Guo, L., Baterina, O.Y., Jr., and Farquhar, M.G. (2012). The PDZ protein GIPC regulates trafficking of the LPA1 receptor from APPL signaling endosomes and attenuates the cell's response to LPA. *PLoS One*. **7**, e49227.

Vaughan, M.B., Howard, E.W., and Tomasek, J.J. (2000). Transforming growth factor-beta1 promotes the morphological and functional differentiation of the myofibroblast. *Exp Cell Res*. **257**, 180-189.

Vicente-Manzanares, M., and Horwitz, A.R. (2011). Adhesion dynamics at a glance. *J Cell Sci*. **124**, 3923-3927.

Vicente-Manzanares, M., Ma, X., Adelstein, R.S., and Horwitz, A.R. (2009). Non-muscle myosin II takes centre stage in cell adhesion and migration. *Nat Rev Mol Cell Biol*. **10**, 778-790.

Vicente-Manzanares, M., Webb, D.J., and Horwitz, A.R. (2005). Cell migration at a glance. *J Cell Sci*. **118**, 4917-4919.

Vignjevic, D., Yarar, D., Welch, M.D., Peloquin, J., Svitkina, T., and Borisy, G.G. (2003). Formation of filopodia-like bundles in vitro from a dendritic network. *J Cell Biol*. **160**, 951-962.

von Wichert, G., Haimovich, B., Feng, G.S., and Sheetz, M.P. (2003). Force-dependent integrin-cytoskeleton linkage formation requires downregulation of focal complex dynamics by Shp2. *EMBO J*. **22**, 5023-5035.

Wang, C., Xin, X., Xiang, R., Ramos, F.J., Liu, M., Lee, H.J., Chen, H., Mao, X., Kikani, C.K., Liu, F., and Dong, L.Q. (2009). Yin-Yang regulation of adiponectin signaling by APPL isoforms in muscle cells. *J Biol Chem*. **284**, 31608-31615.

Webb, D.J., Donais, K., Whitmore, L.A., Thomas, S.M., Turner, C.E., Parsons, J.T., and Horwitz, A.F. (2004). FAK-Src signalling through paxillin, ERK and MLCK regulates adhesion disassembly. *Nat Cell Biol*. **6**, 154-161.

Webb, D.J., Parsons, J.T., and Horwitz, A.F. (2002). Adhesion assembly, disassembly and turnover in migrating cells -- over and over and over again. *Nat Cell Biol*. **4**, E97-100.

Wegener, K.L., and Campbell, I.D. (2008). Transmembrane and cytoplasmic domains in integrin activation and protein-protein interactions (review). *Mol Membr Biol*. **25**, 376-387.

Wegener, K.L., Partridge, A.W., Han, J., Pickford, A.R., Liddington, R.C., Ginsberg, M.H., and Campbell, I.D. (2007). Structural basis of integrin activation by talin. *Cell*. **128**, 171-182.

Wehrle-Haller, B. (2012). Assembly and disassembly of cell matrix adhesions. *Curr Opin Cell Biol*. **24**, 569-581.

Welf, E.S., Naik, U.P., and Ogunnaike, B.A. (2011). Probabilistic modeling and analysis of the effects of extra-cellular matrix density on the sizes, shapes, and locations of integrin clusters in adherent cells. *BMC Biophys*. **4**, 15.

Welf, E.S., Ogunnaike, B.A., and Naik, U.P. (2009). Quantitative statistical description of integrin clusters in adherent cells. *IET Syst Biol*. **3**, 307-316.

Wennerberg, K., Forget, M.A., Ellerbroek, S.M., Arthur, W.T., Burridge, K., Settleman, J., Der, C.J., and Hansen, S.H. (2003). Rnd proteins function as RhoA antagonists by activating p190 RhoGAP. *Curr Biol*. **13**, 1106-1115.

White, D.P., Caswell, P.T., and Norman, J.C. (2007). alpha v beta3 and alpha5beta1 integrin recycling pathways dictate downstream Rho kinase signaling to regulate persistent cell migration. *J Cell Biol*. **177**, 515-525.

Winograd-Katz, S.E., Fassler, R., Geiger, B., and Legate, K.R. (2014). The integrin adhesome: from genes and proteins to human disease. *Nat Rev Mol Cell Biol*. **15**, 273-288.

Wittmann, T., Bokoch, G.M., and Waterman-Storer, C.M. (2003). Regulation of leading edge microtubule and actin dynamics downstream of Rac1. *J Cell Biol*. **161**, 845-851.

Wolf, K., Mazo, I., Leung, H., Engelke, K., von Andrian, U.H., Deryugina, E.I., Strongin, A.Y., Brocker, E.B., and Friedl, P. (2003). Compensation mechanism in tumor cell migration: mesenchymal-amoeboid transition after blocking of pericellular proteolysis. *J Cell Biol*. **160**, 267-277.

Wolfenson, H., Lavelin, I., and Geiger, B. (2013). Dynamic regulation of the structure and functions of integrin adhesions. *Dev Cell*. **24**, 447-458.

Wurflinger, T., Gamper, I., Aach, T., and Sechi, A.S. (2011). Automated segmentation and tracking for large-scale analysis of focal adhesion dynamics. *J Microsc*. **241**, 37-53.

Xiang, C., Chen, J., and Fu, P. (2017). HGF/Met Signaling in Cancer Invasion: The Impact on Cytoskeleton Remodeling. *Cancers (Basel)*. **9**,

Xue, G., and Hemmings, B.A. (2013). PKB/Akt-dependent regulation of cell motility. *J Natl Cancer Inst*. **105**, 393-404.

Yang, L., Lin, H.K., Altuwaijri, S., Xie, S., Wang, L., and Chang, C. (2003). APPL suppresses androgen receptor transactivation via potentiating Akt activity. *J Biol Chem*. **278**, 16820-16827.

Ye, F., Kim, C., and Ginsberg, M.H. (2011). Molecular mechanism of inside-out integrin regulation. *J Thromb Haemost*. **9 Suppl 1**, 20-25.

Yuan, L., Fairchild, M.J., Perkins, A.D., and Tanentzapf, G. (2010). Analysis of integrin turnover in fly myotendinous junctions. *J Cell Sci*. **123**, 939-946.

Zaidel-Bar, R., Ballestrem, C., Kam, Z., and Geiger, B. (2003). Early molecular events in the assembly of matrix adhesions at the leading edge of migrating cells. *J. Cell Sci.* **116**, 4605-4613.

Zaidel-Bar, R., Itzkovitz, S., Ma'ayan, A., Iyengar, R., and Geiger, B. (2007a). Functional atlas of the integrin adhesome. *Nat Cell Biol*. **9**, 858-867.

Zaidel-Bar, R., Milo, R., Kam, Z., and Geiger, B. (2007b). A paxillin tyrosine phosphorylation switch regulates the assembly and form of cell-matrix adhesions. *J Cell Sci*. **120**, 137-148.

Zaoui, K., Honore, S., Isnardon, D., Braguer, D., and Badache, A. (2008). Memo-RhoA-mDia1 signaling controls microtubules, the actin network, and adhesion site formation in migrating cells. *J Cell Biol*. **183**, 401-408.

Zenke, F.T., King, C.C., Bohl, B.P., and Bokoch, G.M. (1999). Identification of a central phosphorylation site in p21-activated kinase regulating autoinhibition and kinase activity. *J Biol Chem*. **274**, 32565-32573.

Zerial, M., and McBride, H. (2001). Rab proteins as membrane organizers. *Nat Rev Mol Cell Biol*. **2**, 107-117.

Zhai, J.S., Song, J.G., Zhu, C.H., Wu, K., Yao, Y., and Li, N. (2016). Expression of APPL1 is correlated with clinicopathologic characteristics and poor prognosis in patients with gastric cancer. *Curr Oncol*. **23**, e95-e101.

Zhang, G., Chen, L., Sun, K., Khan, A.A., Yan, J., Liu, H., Lu, A., and Gu, N. (2016). Neuropilin-1 (NRP-1)/GIPC1 pathway mediates glioma progression. *Tumour Biol*. **37**, 13777-13788.

Zheng, D.Q., Woodard, A.S., Tallini, G., and Languino, L.R. (2000). Substrate specificity of alpha(v)beta(3) integrin-mediated cell migration and phosphatidylinositol 3-kinase/AKT pathway activation. *J Biol Chem*. **275**, 24565-24574.

Zhu, G., Chen, J., Liu, J., Brunzelle, J.S., Huang, B., Wakeham, N., Terzyan, S., Li, X., Rao, Z., Li, G., and Zhang, X.C. (2007). Structure of the APPL1 BAR-PH domain and characterization of its interaction with Rab5. *EMBO J*. **26**, 3484-3493.

Zoncu, R., Perera, R.M., Balkin, D.M., Pirruccello, M., Toomre, D., and De Camilli, P. (2009). A phosphoinositide switch controls the maturation and signaling properties of APPL endosomes. *Cell*. **136**, 1110-1121.